An Electrophysiological and Morphometric Study of the Effect of Different Methods of Surgical Repair in Motor and Mixed Nerve - A Comparison of the Repair of the Facial Nerve and the Median Nerve in a Large Animal Model.

By Nicola E Starritt

Submitted for the degree of Doctor of Medicine

University of Edinburgh, 2005

STATEMENT OF ORIGINALITY

I, Nicola Elizabeth Starritt, declare that this thesis has been composed totally by myself and that the work presented here is my own. Any technical assistance has been acknowledged.

ACKNOWLEDGEMENTS

I would like to thank the following people for their help with this project; Gail Valler for ensuring the general smooth-running of things and for her (very much appreciated) expert advice and help with cutting nerve sections; the staff at Roslin Institute (Joan Docherty, Marjorie Thomson, Dennis Doogan and John Hogg) for the day-to-day care of the animals and in particular Joan and Marion for providing an anaesthetic service; Tom Gilchrist and David Healy at Giltech for providing the biodegradable glass material; David Perry for his technical advice regarding computer problems and Action Research for their financial assistance. I would also like to thank my fellow research fellow, Sarah Kettle, for her friendship and practical support during this time. Finally, I would like to thank my supervisor, Michael Glasby, for his guidance throughout this work. His knowledge and experience of research, expectation of high standards (both technical and intellectual) and fondness of lively debate, has enabled me to complete this work and provided me with a sound basis on which to approach future research.

ABSTRACT

The outcome of peripheral nerve injuries has been poorly documented. This is due to the heterogeneity of the injuries, the variety of surgeons from different surgical specialtities performing the repairs and a lack of objective follow up. Anecdotal reports have suggested that injuries to purely motor nerves have a better outcome than those affecting mixed nerves.

This aims of this work were to document the natural history of nerve injuries and their repair under controlled conditions in order to ascertain the outcome of different types of nerve injury and to compare the outcome of the same injuries in motor nerves and mixed nerves. A further objective was to determine which investigations would be useful in the assessment and follow up of peripheral nerve injuries both as predictors of outcome and in clinical practice.

The sheep model was selected as its peripheral nerves are a similar size, and behave in a similar manner to, human peripheral nerves. A set of six standardised nerve injuries (normal control, neurapraxia, axonotmesis, neurotmesis and suture repair, neurotmesis and entubulation, and nerve graft) was created in both the facial (motor) nerve and the median (mixed) nerve. The function of the nerves and their target muscles was assessed using nerve conduction studies (maximum conduction velocity, distribution of conduction velocities, refractory period), single-fibre electromyography (jitter), target muscle tension and mass, and nerve fibre morphometry.

In the carefully controlled conditions of the experiments, for both nerves the transection injuries had a poorer outcome than the non-transection injuries. This effect was more marked in the median nerve than in the facial nerve suggesting that the type of nerve affected the outcome of injury. Maximum conduction velocity was determined to be the most useful test for use in the clinical management of nerve injuries. Distribution of conduction velocities, a nerve conduction test based on collision theory, may be too sensitive to be of use in the management of mechanical nerve injury but may have a valuable role in the assessment of more subtle conditions such as neuropathies and Bell's palsy. Nerve fibre morphometry discriminated between the different injuries and remains a useful tool in a research setting.

TABLES & FIGURES

ABBREVIATIONS

Ach	acetyl choline
AP	action potential
ARP_{max}	maximum absolute refractory period
ARP_{min}	minimum absolute refractory period
ARP_{range}	range of absolute refractory period
ATP	adenine triphosphate
CAP	compound action potential
CMAP	compound muscle action potential
CNAP	compound nerve action potential
CMRR	common mode rejection ratio
CRG	controlled release glass
CV_{max}	maximum conduction velocity
DCV	distribution of conduction velocities
EDL	extensor digitorum longus
EMG	electromyography
FCR	flexor carpi radialis
FCU	flexor carpi ulnaris
FDL	flexor digitorum longus
FDP	flexor digitorum profundus
FDS	flexor digitorum superficialis
fsd	full scale deflection
IPI	interpotential interval
ISI	interstimulus interval
LLM	levator labii maxillaris

MCD	mean consecutive difference
MUAP	motor unit action potential
NMJ	neuromuscular junction
PD	potential difference
PNS	peripheral nervous system
RRP	relative refractory period
SFAP	single fibre action potential
SFEMG	single fibre electromyography
VRF	velocity recovery function
SUAP	single unit action potential

System international units were used throughout the work presented here.

TABLE OF CONTENTS

1 GENERAL INTRODUCTION

Nerve conduction studies and electromyography allow an objective assessment of the peripheral neuromuscular system. These tests are useful both in the diagnosis of nerve injuries and other conditions affecting the peripheral neuromuscular system and also in monitoring disease progression and/or recovery of function after peripheral nerve injury and repair.

1.1 HISTORY OF ELECTRODIAGNOSIS

In 1797 Galvani described the generation of electricity by nervous tissue (Kimura 1983). During the same period Volta established the basic concepts of electricity. However, there remained scepticism over 'bioelectricity' until an experiment by Matteucci in 1838. He placed the sciatic nerve of a frog still innervating its target leg muscles on the dissected thigh muscles of the contralateral leg and demonstrated movement of the leg on contraction of the thigh muscles. Further experiments in the latter half of the 19th century established the relationship between both current strength and the duration of stimulation in exciting muscle contraction and the characteristic responses seen in different diseases. This formed the basis of classical electrodiagnosis.

Modern clinical electrodiagnosis began with the advent of the cathode-ray oscilloscope invented by Gasser and Erlanger in 1922. In 1929 Adrian and Bronk introduced the concentric needle electrode and further advances were made in 1934 with the development of the differential amplifier by Matthews.

The two world wars resulted in a large number of peripheral nerve injuries, and in conjunction with the concurrent polio epidemics, this generated an increased demand

for electrophysiological testing. Consequently, this led to further technical advances and the first studies of nerve conduction velocity in experimental animals.

In 1937, Eichler reported percutaneous recording of nerve action potentials by electrical stimulation of the median and ulnar nerves and in 1947 Dawson described signal averaging (using photographic superimposition) to record from sensory nerves. By the 1960s nerve conduction velocity was a standard electrodiagnostic test and the first International Congress of Electromyography was held in Pavia, Italy in 1961.

1.2 CLASSIFICATION OF NERVE INJURY

Nerve injuries have been classified by many different clinical and anatomical systems. Two of the more commonly used clinical grading systems are the House-Brackman classification for the facial nerve and the Medical Research Council grading for peripheral nerve injuries of the limb. These are shown in Table 1.1 and Table 1.2.

House-Brackman grading system for facial nerve injuries.		
Grade	**Description**	**Characteristics**
I	Normal	Normal facial function in all areas
II	Mild dysfunction	**Gross:** slight weakness noticeable on close inspection; may have very slight synkinesis. **At rest:** normal symmetry and tone **Motion:** Forehead: moderate-to-good function. Eye: complete closure with effort. Mouth: slightly weak with maximum effort.
III	Moderate dysfunction	**Gross:** obvious, but not disfiguring difference between two sides; noticeable but not severe synkinesis, contracture or hemifacial spasm. **At rest:** normal symmetry and tone **Motion:** Forehead: slight-to-moderate movement. Eye: complete closure with effort. Mouth: slightly weak with maximum effort.
IV	Moderately severe dysfunction	**Gross:** obvious weakness and / or disfiguring asymmetry **At rest:** normal symmetry and tone **Motion:** Forehead: none.Eye: incomplete closure.Mouth: asymmetric with maximum effort.
V	Severe dysfunction	**Gross:** only barely perceptible motion. **At rest:** asymmetry **Motion:** Forehead: none. Eye:incomplete closure.Mouth: slight movement
VI	Total paralysis	No movement

Table 1.1 House-Brackman grading system.

	Medical Researh Council grading
Grade	**Description**
0	No active muscle contraction.
1	Visible or palpable muscle contraction without active movement
2	Movement which is possible with gravity eliminated.
3	Movement which is possible against gravity.
4	Movement which is possible against gravity plus resistance but which is weaker than normal.
5	Normal power.

Table 1.2 shows the Medical Research Council grading system for assessment of power in limbs.

The most popular of the anatomical grading systems were described by Seddon and Sunderland. In 1943 Seddon described three types of nerve injury, neurapraxia, axonotmesis and neurotmesis.

Neurapraxia is the most minor type of nerve injury. The usual mechanism of injury is compression or ischaemia. This results in local demyelination at the site of injury with an associated conduction block. However, there is no axonal damage and the nerve conducts normally both proximal and distal to the site of the lesion. The nerve does not undergo Wallerian degeneration and full recovery is expected within a few days or weeks. Axonotmesis, as the name suggests, involves axonal disruption which results in Wallerian degeneration distal to the site of injury. However, both the endoneurium and the perineurium remain intact. Recovery is by axonal sprouting proximal to the site of injury and, because the endoneurium is intact there is no 'miswiring'. Regenerating axons should therefore reach their original destinations and successfully reinnervate the appropriate target organs.

Neurotmesis involves transection of the nerve and is usually easy to diagnose because there is an associated penetrating injury. It always requires surgical repair.

In 1978 Sunderland expanded Seddon's classification and described five different degrees of nerve injury (Sunderland 1978). This classification was based entirely in terms of anatomy whereas Seddon's scheme was based on clinical / pathological findings. In Sunderland's classification, Ist degree injuries are equivalent to neurapraxia, IInd degree to axonotmesis and Vth degree to neurotmesis, however, Sunderland also included IIIrd and IVth degree injuries.

IIIrd degree injuries involve a hidden fascicular lesion in which the perineurium is intact and the fascicles are in continuity but the endoneurial sheaths are disrupted. Within the fascicle the axons undergo Wallerian degeneration and because the endoneurial sheath is disrupted the axonal sprouts may be misdirected into a foreign tube. There is associated haemorrhage, oedema, inflammation and latterly fibrosis. Fibrous tissue may block axonal growth or constrict those axons that do regenerate. The outcome of this injury ranges from minimal function to almost complete recovery (Mackinnon & Dellon 1988).

In IVth degree injuries the fascicular structure of the nerve is destroyed, the perineurium is breached and continuity is maintained only by the epineurium. Although on inspection the nerve appears intact regeneration of axons is blocked by intraneural scar tissue. These injuries require surgical reconstruction often with the use of nerve grafts (Flores, Lavernia, & Owens 2000).

1.3 PATHOPHYSIOLOGY OF NERVE INJURY AND RECOVERY

Injury of a peripheral nerve initiates a complex chain of events not only at the site of injury but also in the adjacent proximal and distal nerve segments, in neuronal cell bodies, in target organs and in the brain grey matter.

In the cell bodies (situated in the dorsal root ganglia in the case of sensory neurons and in the anterior horns of the spinal cord in the case of motor neurons) changes are observed a few hours after injury (Flores, Lavernia, & Owens 2000). Morphological changes include cell body and nucleolar swelling, nuclear eccentricity and disappearance of basophilic material from the cytoplasm (Sunderland 1978). This is collectively known as chromatolysis. Chromatolysis is thought to be due to a reorganisation of the rough endoplasmic reticulum, initiated by altered levels of neurotrophic growth factors, secondary to changes in the retrograde axonal transport system (Lundborg 2000).

Neurotrophic growth factors are classified into three main groups: neurotrophins, neuropoietic cytokines and fibroblast growth factors (Lundborg 2000). They may be specific for different types of nerve. For example, nerve growth factor, which is upregulated in the distal segment of damaged nerves, plays an important role in the survival of sensory neurons but has little effect on motor neurons. However, the converse is true for brain-derived neurotrophic factor. These altered concentrations of neurotrophic factors result in significant changes in cell metabolism as the cell body alters its primary function from neuronal transport to synthesis of structural components for axonal regeneration (Seckel 1990). The metabolic changes are demonstrated by increased synthesis of RNA, protein and lipids as well as glucose-6-

phosphate dehydrogenase and hydrolytic enzymes. Between 20% to 50% of cells do not survive chromatolysis (Lundborg 2000).

Proximal to the site of injury the nerve dies back to the next node of Ranvier. This process is known as 'traumatic degeneration'. However, it has been suggested that the extent of retrograde degeneration is related to the type of injury sustained, and that injuries of a more disruptive nature *e.g.* gunshot wounds, result in more extensive loss of neurons (Seddon 1972). Changes at the site of nerve injury occur quickly and axonal sprouting has been observed six hours after injury (Cajal 1928; Miller 1987). Each parent axon sends out a large number of thin sprouts, each of which terminates in a growth cone that plays an important role in the direction of neuronal growth (Young 1942).

Distal to the site of injury the nerve undergoes a process called Wallerian degeneration. This starts immediately after injury with myelin and axonal degeneration, proliferation of Schwann cells and invasion of macrophages. Macrophages and Schwann cells are important in the process of nerve regeneration. Macrophages phagocytose myelin and cellular debris and also stimulate synthesis of neurotrophic factors in the injured nerve (Nathan 1987). Undifferentiated daughter Schwann cells line up within basement membrane tubes to form *bands of Büngner* that serve as a guide for regenerating axonal sprouts (Young 1942). It has been shown that without Schwann cells few axons will regenerate even in the presence of an appropriate basement membrane scaffold (Enver & Hall 1994). Axonal injury induces a change in Schwann cell gene-expression and protein production and switches the cells to a reactive 'axon-responsive state'. This involves increased production of neurotrophins and upregulation of receptors for axon-derived and Schwann-cell-derived ligands, as well as the increased expression of molecules onto the cell surface

or into the extracellular matrix, which facilitate axonal growth(Hall 2001). As these changes take two to six days, this explains the shorter lag-time for axonal re-growth in 'pre-degenerate' grafts as compared to freshly prepared ones (McQuarrie & Grafstein 1973). Upon successful re-innervation Schwann cells revert to their original phenotype, however, if this fails to occur the cells lose their capacity to support axonal regeneration (Terenghi et al. 1998). The chronically denervated distal nerve stump undergoes fibrosis and collagen deposition (Thomas 1964; Young 1942). There is a gradual decrease in the number of Schwann cells although shrunken bands of Büngner may still be found eighteen months after injury (Sunderland 1978). At the neuromuscular junction (NMJ), failure of neuromuscular transmission occurs before the process of Wallerian degeneration is complete. Initial conduction block is due to decreased acetylcholine (ACh) synthesis because of decreased amounts of cholinacetyltransferase, reduced release of ACh because of destruction of active zones and decreased excitability of nerve terminals (Stålberg 1990). Failure of the NMJ leads to hypersensitivity of the muscle membrane to ACh and the development of extra-junctional receptors (Wiechers 1990). This is associated with an increase in membrane resistance and a decrease in the resting membrane potential of muscle fibres (Sunderland 1978). These changes are thought to arise from a lack of neurotrophic factors from the injured nerve (Sunderland 1978).

The proximal nerve stump sends out large numbers of thin, pioneering axons which invade the endoneurial tubes. Initially each tube, particularly the larger ones, contains many of these thin axons. To survive, axons must enter a suitable endoneurial tube and reinnervate an appropriate target organ. Axons which make inappropriate distal connections or fail to reach the target organ will die. Therefore, the number of axons within each endoneurial tube decreases over time (Young 1942).

In 1928 Cajal observed that axons from the proximal stump of a severed nerve preferentially grow toward a nerve graft or distal nerve stump (Cajal 1928). He proposed that the distal nerve exerts an attractive force on the regenerating axons and introduced the term neurotropism. However, when a nerve has been surgically repaired the more pertinent question (given that the nerve ends are coapted) is how a particular axon ends up in a particular band of Büngner. Once an axon enters a band of Büngner it is physically committed to that band and will either continue to grow and re-innervate a target organ or will degenerate. It has yet to be established whether this axon-band selection is a controlled or 'chance' phenomenon. Gillespie *et al* transected the common nerve to the rat gastrocnemius (fast twitch) and soleus (slow twitch) muscles, to study whether there was any selective reinnervation of the muscles (Gillespie, Gordon, & Murphy 1985). The results were consistent with random reinnervation. However, Hoh found that the denervated rat extensor digitorum muscle was preferentially reinnervated by its own nerve as opposed to the nerve to soleus (Hoh 1975). Brushart suggested that specificity of fibre-endoneurial tube pairing arose by 'pruning' of inappropriate fibres within the tube rather than by selection of a particular endoneurial tube by an axon (Brushart 1993). He postulated that this was because Schwann cells in 'motor' bands of Bungner had a carbohydrate epitope which was recognised by motor axons but not sensory axons.

Reinnervation of muscle results from outgrowth of new motor axons or sprouting of axons from adjacent intact fibres. When pioneering axons make contact with muscle this results in a decrease in ACh sensitivity, closure of extra-junctional receptors and formation of new end-plates (Sunderland 1978). If an axon successfully reinnervates a target organ the fibres then increase in diameter and in the case of motor fibres become medullated (Gutmann & Sanders 1943). This increase in fibre diameter and

myelin sheath thickness may be necessary before the axons can conduct impulses which produce effective function (Young 1942).

1.4 PERIPHERAL NERVE REPAIR

The first attempts at peripheral nerve repair were made in the 19th century. Since then surgical techniques have progressed, the biggest advance being the introduction of the operating microscope, which allowed visualisation of nerve structures. It is now widely accepted that these surgical techniques of nerve repair have been optimised and new advances in nerve repair lie in other directions. The ideal nerve repair is tension-free, end-to-end coaptation (Gutmann & Sanders 1943). There are two types of primary nerve suture repair: epineurial repair and fascicular or perineurial repair. Epineurial repair is the technique most commonly employed and involves repair of the epineurial sheath after the lining-up of anatomical landmarks in the nerve trunk such as fascicles and blood vessels. In fascicular repair sutures are placed in the perineurium to reconstruct individual fascicles or groups of fascicles. Theoretically the latter type of repair should be more accurate and therefore more effective however, this is not reflected in clinical results (Lundborg 2000). This may be because of erroneous matching of fibres and increased intraneural scarring in the fascicular repair whilst epineurial repair allows neurotrophic and neurotropic factors to support and direct nerve regeneration.

Tension at a nerve repair site leads to decreased blood flow to the nerve as well as increased scarring and adhesion formation (Clark et al. 1992). If it is not possible to perform a tension-free end-to-end coaptation then nerve grafting should be performed. A requirement for nerve grafting may arise because of loss of a segment of nerve after traumatic injury or tumour resection, or retraction of nerve ends in a delayed repair. Nerve grafts are inferior to primary repair (Gutmann & Sanders 1943). After grafting the injured nerve must regenerate across two suture lines which has been shown to

slow the rate of axonal regeneration as well as providing two potential sites for mismatching of axons and endoneurial tubes (Gutmann et al. 1942; Gutmann & Sanders 1943). Nerve grafts are also relatively poor providers of neurotropic and neurotrophic substances.

At present autogenous nerve grafts are used in clinical practice. The most commonly utilised nerves are the sural nerve from the leg and the medial antebrachial cutaneous nerve and the lateral antebrachial cutaneous nerve from the arm. Use of autogenous grafts causes morbidity at the donor site *e.g.* numbness. Furthermore, there is also likely to be mismatching of fibre size between the injured and donor nerves, with the donor nerves having smaller endoneurial tubes. The size of endoneurial tubes has been shown to affect the fibre diameter of the regenerating nerve (Holmes & Young 1942; Sanders & Young 1944; Young 1942).

An alternative to nerve grafting which avoids the problems of donor site morbidity and mismatching of fibre size is the use of conduits. This technique, known as entubulation, is not a new one. It provides a tubular guide for the regenerating nerve between the two nerve stumps. Many different materials have been used as conduits. Naturally occurring substances used for this purpose include artery, vein, collagen and freeze-thawed muscle (Glasby, Fullarton, & Lawson 1997; Glasby, Fullarton, & Lawson 1998; Kelleher et al. 2001). A wide variety of synthetic conduits have also been tried including non-resorbable substances such as silicone and biodegradable materials such as polyglycolic acid and controlled release glass(Gilchrist et al. 1998;Lundborg, Dahlin, & Danielson 1991). Unfortunately the synthetic materials used to-date have been found to cause chronic irritation, inflammation and nerve compression (Lundborg, Dahlin, & Danielson 1991). The ideal conduit would be inert and resorbable over a suitable period of time after the nerve had regenerated.

Entubulation is postulated to allow the nerve ends to be immersed in neurotrophic and neurotropic substances whilst decreasing peripheral sprouting (Gilchrist, Glasby, Healy, Kelly, Lenihan, McDowall, Miller, & Myles 1998). There is also interest in further enhancement of the microenvironment surrounding the nerve by the provision of neurotrophic factors either by embedding Schwann cells or fibroblasts along the conduit or by delivery via mini-pumps. The former is preferable, as it does not require a second surgical procedure to remove the pump.

1.5 THE FACIAL NERVE

The facial nerve is the seventh cranial nerve. It has both a motor root and a sensory root. The motor root supplies the muscles of facial expression. The sensory root, also known as the nervus intermedius consists of taste fibres, parasympathetic efferents to salivary and lacrimal glands and a minor sensory cutaneous branch. The motor nucleus is situated in the lower third of the pons whilst the sensory root has a more complex arrangement. Both roots emerge from the brainstem between the olive and the inferior cerebellar peduncle and together enter the petrous temporal bone through the internal auditory meatus. The nerve then lies in the facial canal and turns in a dorsolateral direction at the geniculate ganglion to lie close to the tympanic cavity. After a further dorsal turn it gives off the nerve to stapedius and is joined by the chorda tympani. It then finishes its bony course by exiting through the stylomastoid foramen. Here it gives off fibres to stylohyoid, the posterior belly of digastric and platysma before entering the parotid gland to divide into its terminal branches.

Damage to the facial nerve results in ipsilateral facial palsy. This has sequalae such as impairment of oral, nasal and ocular sphincter control, which can result in drooling, lacrimation and corneal irritation and ulceration. However, the most devastating consequence is the ensuing facial disfigurement that can lead to loss of self-confidence and depression. Women, the young and those with previously low self-esteem are at higher risk of developing psychological complications (Cross et al. 2000). Another study has showed that specific impairment of the ability to smile as compared to the loss of other facial expressions was associated with an increased risk of depression (VanSwearingen, Cohn, & Bajaj-Luthra 1999).

Upper motor neuron lesions of the facial nerve may be differentiated from lower motor neuron lesions by the preservation of forehead wrinkling and the blink reflex. Hyperacusis indicates involvement of the nerve to stapedius and altered taste indicates involvement of the chorda tympani therefore, localising the lesion to the intratemporal portion of the facial nerve (Coles 2001).

The intracranial segment of the facial nerve is predominantly at risk from posterior fossa tumours both within the substance of the brainstem *e.g.* glioma and at the cerebellopontine angle *e.g.* acoustic neuroma. As with all tumours in the vicinity of the facial nerve, the nerve may be damaged by the tumour itself or the surgery required to excise. In the temporal bone the nerve is susceptible to injury from temporal bone fracture, tumour, infection (most commonly herpes zoster), cholesteatoma and middle ear and mastoid surgery. As the nerve emerges from the stylomastoid foramen it loses its bony protective covering and is at risk from penetrating traumatic injury. It may be invaded by malignant tumours of the parotid gland or damaged by surgery in this region.

Idiopathic peripheral facial palsy, 'Bell's palsy', is one of the commonest mononeuropathies. The cause of Bell's palsy is by definition unknown, however, a viral origin, with particular reference to herpes, has been postulated. Swelling and constriction of the nerve is observed at the level of the geniculate ganglion as the nerve passes from the internal acoustic meatus into the facial canal. The condition affects all age groups and has an equal sex distribution. Facial weakness develops over three to seventy-two hours and is preceded by otalgia in fifty percent of patients (Binnie et al. 1995). Around a fifth of those affected will be left with permanent facial weakness and others will develop synkinesis and 'crocodile tears' (crying during mastication) due to aberrant regeneration of nerve fibres. Complete paralysis within

the first week and age above fifty are commonly regarded as bad prognostic indicators. Studies on facial nerve lesions have demonstrated that the amplitude of the compound muscle action potential (CMAP) on the affected side compared with that on the intact contralateral side can indicate likelihood of recovery. CMAP amplitudes of 30% or more of the intact side indicate excellent prognosis whereas those of less than 10% have a poor outcome (Sillman et al. 1992).

The treatment of Bell's palsy remains controversial. A meta-analysis showed a benefit from steroids in complete facial palsy but the situation is less clear with incomplete paralysis (Ramsey et al. 2000). Studies have also shown a synergistic effect of steroids with acyclovir (Adour et al. 1996;Sittel et al. 2000). Surgical decompression of the facial nerve following failure of medical therapy in profound facial nerve palsy has also been attempted with some success (Yanagihara et al. 2001). However, a report published in 2001 from the Quality Standards Subcommittee of the American Academy of Neurology stated that there was insufficient evidence to recommend any definitive treatment of Bell's palsy and highlighted the need for further well-designed studies (Grogan & Gronseth 2001)

1.6 THE MEDIAN NERVE

The median nerve is formed in the axilla from the medial and lateral cords of the brachial plexus. It runs down the arm alongside the brachial artery (first lateral then medial to it). In the cubital fossa it gives off motor branches to pronator teres, flexor carpi radialis, palmaris longus and flexor digitorum superficialis (FDS), as well as articular branches to the elbow joint. It exits the cubital fossa between the two heads of pronator teres, where it gives off the anterior interosseous nerve (which supplies flexor pollicis longus, pronator quadratus, the lateral half of flexor digitorum profundus (FDP) and articular branches to the wrist and inferior radio-ulnar joint) and continues distally between FDS and FDP. A palmar cutaneous branch arises from the median nerve in the distal half of the forearm. This branch crosses anterior to the flexor retinaculum and supplies the lateral half of the palm. At the wrist the median nerve emerges from behind the lateral border of FDS and passes underneath the flexor retinaculum to enter the palm. Here it divides into a medial branch (which supplies the second lumbrical and sensation to the index, middle and ring fingers) and a lateral branch (which supplies abductor pollicis brevis, flexor pollicis brevis, opponens pollicis and the first lumbrical).

The median nerve is most commonly injured in the distal forearm owing to incised wounds. However, it may also be damaged in the arm by supracondylar fractures of the humerus. Complete lesions of the median nerve at the elbow result in paralysis of the pronator muscles of the forearm and the long flexor muscles of the wrist and fingers. Flexor carpi ulnaris and the medial half of FDP are spared as they are supplied by the ulnar nerve. Together these muscles can effect weak flexion (with adduction) of the wrist. There is loss of flexion of the interphalangeal joints of the

index and middle fingers, but some weak flexion of the metacarpophalangeal joints of these fingers owing to the action of the interrossei muscles. Flexion of the terminal phalanx of the thumb is also lost and the thenar eminence becomes wasted. Sensation is lost over the lateral half of the palm, and of the palmar aspect and fingertips of the thumb, index and middle fingers as well as the lateral border of the ring finger. Loss of the sympathetic nerve supply results in warm, dry skin and longstanding injuries lead to dry, scaly skin with cracked nails and atrophy of finger pulp.

Injury of the median nerve at the wrist results in paralysis of the thenar eminence, with the thumb laterally rotated and adducted. The hand is described as 'ape-like' and there is loss of opposition of the thumb to the fingers. The index and middle fingers lag behind the ring and little fingers when the hand is made into a fist. The sensory, vasomotor and trophic changes are the same as those arising from injury at the elbow. The most serious consequences of median nerve injury are loss of opposition of the thumb to the other fingers, and loss of sensation from the lateral fingers. The functional outcome of median nerve repair is poor (Platt & Bristow 1924).

The median nerve may also be compressed in carpal tunnel syndrome. The carpal tunnel is formed below by the concave anterior aspect of the carpal bones and above by the flexor retinaculum. It contains the long flexor tendons of the fingers and the median nerve. Compression of the nerve results in pins and needles in the hand in the distribution of the median nerve as well as weakness of the thenar eminence. Carpal tunnel syndrome most commonly affects women in the fifth decade. It may be caused by thickening of the synovial sheaths of the flexor tendons or by arthritic changes of the carpal bones. It has also been associated with pregnancy, gout, diabetes mellitus, hypothyroidism, acromegaly and multiple myeloma. The patient may be wakened by discomfort in the hand and relief is often obtained by shaking or elevating the hand.

The symptoms may be reproduced by exaggerated flexion of the wrist (Phalen's sign) or percussion over the median nerve (Tinel's sign). Nerve conduction studies are useful in the diagnosis of carpal tunnel syndrome and show increased latency of impulse conduction of the median nerve. Symptomatic relief from this condition may be obtained by splinting the wrist in a neutral position but definitive treatment is by surgical division of the flexor retinaculum.

1.7 AIMS OF PRESENT STUDY

The 'natural history' of peripheral nerve injuries has been poorly documented. This is due to a number of factors including the heterogeneity of the injuries themselves, the large number of different surgeons from different surgical specialties performing the repairs and a lack of follow up in the out-patient department. The latter is due to a lack of money and time and also the low attendance rates of this particular group of patients. Furthermore, the appropriate equipment and expertise to perform objective testing of the peripheral neuromuscular system is not available in a routine outpatient clinic and there are long waiting times for outpatient neurophysiology appointments.

To address this lack of knowledge of peripheral nerve injuries, six different standardised models of nerve injury (control, neurapraxia, axonotmesis, neurotmesis with suture repair, neurotmesis and entubulation, nerve graft) were created in the peripheral nerves of sheep. The sheep was selected as previous work had demonstrated that its peripheral nerves are of a similar size and behave in a similar manner to, human peripheral nerves. The nerves were assessed using nerve conduction tests (maximum conduction velocity, distribution of conduction velocities), measurement of refractory period, jitter (single fibre electromyographic technique), target muscle tensions and mass and morphometric analysis.

A report of the outcome of a large number of nerve repairs (from injuries sustained during WWI) showed that repair of the radial nerve (motor) was much more successful than repair of the median nerve or the ulnar nerve (both mixed) (Platt & Bristow 1924). Therefore, it was decided to use the standardised models of nerve injury to compare the outcome of the facial nerve (motor) with that of the median nerve (mixed). The facial nerve and the median nerve were selected because they

were surgically easily accessible and data on both theses nerves were available from previous workers in the group. Furthermore, both theses nerves are commonly injured (due to trauma or surgery) and/or affected by other conditions (Bell's palsy, carpal tunnel syndrome).

The sophistication of microsurgery is now such that new surgical techniques are unlikely greatly to improve the functional outcome of nerve repair. Other approaches such as chemical enhancement of nerve regeneration *e.g.* the use of growth factors, may be the next step for the treatment of peripheral nerve injuries. However, improvements using these techniques are likely to be subtle, therefore it is important to document the outcome of different nerve injuries using the current methods of repair and also to determine which electrophysiological tests provide the most information to both discriminate between injuries and to provide information on the progress of nerve regeneration and reinnervation of target organs. Ideally these tests would be non-invasive and quick to perform. They should also be simple enough that they could be used by surgeons in a general outpatient clinic. Electrophysiological testing could therefore become part of the routine assessment of nerve injuries rather than a specialist referral with an associated waiting time which, in the context of nerve injuries, may render the test irrelevant.

The aims of this work were

(i) To document the outcome of different models of nerve injuries, using nerve conduction studies, electromyography, target muscle tension and nerve fibre morphometry.

(ii) To compare the outcome of the same nerve injuries between a motor nerve and a mixed nerve.

(iii) To determine which investigations are useful in the assessment of peripheral nerves in a research setting.

(iv) To decide which electrophysiological tests would be useful in the clinical assessment of nerve injuries.

2 GENERAL ANIMAL CARE AND ANAESTHESIA

2.1 EXPERIMENTAL GROUPS

Historically, many different animal models have been used in the study of peripheral nerve injury and regeneration. These include rats, rabbits, dogs and cats (Boyd 1964; Cragg & Thomas 1964; Erlanger & Schoepfle 1946; Hursh 1939). The sheep was selected for this study for two reasons. First, the sizes of peripheral nerves in the sheep are close to those in the human. Therefore, the surgical repair of peripheral nerves in the sheep approximates to that encountered in clinical practice.

Secondly, previous work on the sheep has revealed that the behaviour of regenerating nerves is similar to that observed in humans (Drew et al. 1995; Glasby, Fullarton, & Lawson 1997; Gilchrist et al. 1998; Glasby, Fullarton, & Lawson 1998). Nerve regeneration in other animal models used in the study of peripheral nerves, has been shown to occur in conditions and over distances which would not occur in the human or sheep. Kline *et al* compared peripheral nerve regeneration across a gap of 2cm to 3cm, after excision of a 1cm length of nerve (retraction of the nerve stumps accounts for the resultant gap being longer than the nerve excised), in the dog, Rhesus monkey, baboon and chimpanzee (Kline, Hayes, & Morse 1964a). This procedure resulted in neuroma formation in the baboon and the chimpanzee. However, peripheral nerves in the canine model and some of the monkeys were seen to regenerate across the gap with longitudinally orientated axons and to restore conduction. In a companion paper, these workers assessed regeneration, in the same animal models, after crush injuries in the peroneal and radial nerves and after nerve transection and suture repair in the peroneal and ulnar nerves (Kline, Hayes, & Morse 1964b). The chimpanzee showed significantly slower remyelination of axons in the distal stump than the other animal

models after both types of injury and slower recovery of function after the transection injury with suture repair.

As one of the aims of this study was to gather information to enable prediction, in clinical practice, of the outcome of peripheral nerve injuries it was important to choose an animal model with a peripheral nervous system (PNS) which resembled the human PNS as closely as possible. The sheep was selected as such a model. The animals used were young adults, between one and two years old. The majority of the animals were ewes. Several rams were used in the study and these were distributed between the groups to minimise any sex bias. The weight of the sheep ranged from 50kg to 80kg.

The facial nerve and the median nerve were selected for this study for several reasons. In the human, both these nerves are commonly damaged through trauma and iatrogenous damage. Experience had been gained in investigating both these nerves by previous workers within the research group (Drew et al. 1995; Glasby, Fullarton, & Lawson 1997; Gilchrist et al. 1998; Glasby, Fullarton & Lawson 1998). Both nerves were surgically accessible and the length of nerve which could be exposed was found to be suitable for electrophysiological assessment. Target muscles solely supplied by the nerve in question could be identified and both nerves innervated muscles with tendinous insertions which could be dissected free and used for the measurement of twitch and tetanic muscle tensions.

Transection (or other injury) of the median nerve or the facial nerve in the sheep results in a low level of morbidity. Previous work by Mountain and Glasby involving concurrent damage to ipsilateral facial and hypogastric nerves in the sheep had resulted in 'cud-dropping' and consequent weight loss (Drew et al.1995). (Sheep are ruminant animals which regurgitate swallowed food for further mastication in order to

aid digestion. The term cud-dropping refers to the sheep's dropping food onto the ground.) No similar problems have been observed after isolated injury to the facial nerve. Previous experiments on the median nerve had not resulted in lameness or problems in mobilisation. This is thought to be because the intact ulnar nerve allows flexion of the ankle and elbow joints and the radial nerve is active in extension.

For the facial nerve and the median nerve the following models of injury were assessed: *neurapraxia; axonotmesis; neurotmesis with epineurial sutured repair; neurotmesis with repair by entubulation* and finally *nerve autografting*. The models of injury are described in the next chapter.

2.2 GROUP SIZE

Home Office regulations state that minimum numbers of animals that will allow a statistically significant result should be used (Home Office 1986). One of the drawbacks of using a large animal model such as the sheep is that these animals are expensive to buy and maintain. Power studies, based on results from previous workers, enabled estimation of the required sample size (Fullarton, Myles, et al. 2001).

Of the large number of tests and investigations which have been performed during the investigation of peripheral nerves the measurement of maximum conduction velocity (*CVmax*) has been shown to be the most discriminatory. Power calculations were performed using data from previous work which had been performed on measurement of maximum conduction velocity (Fullarton, Myles, et al. 2001). These workers took 15m s^{-1} to be an appreciable difference in *CVmax* between groups, with a standard deviation of 7m s^{-1}. A sample size calculation was performed, for these values, using a

statistical computer program 'Statistica' (StatSoft Inc, Tulsa, Oklahoma, USA). The estimated required group size, for a power goal of 0.9, was six. Therefore, each experimental group comprised six animals.

2.3 ANIMAL HOUSING

The experiments described in this work were performed at the Marshall Building at Roslin Institute for Bioresearch, near Roslin. This is a Home Office approved site. It also had the advantage that the animals were housed in surrounding fields, therefore, they did not have to undergo transportation or a 'settling-in' period to become accustomed to new surroundings. The animals were transferred to a barn the day before surgery and were fasted overnight. For routine daily care the animals were looked after by experienced personnel at Roslin Institute, one of whom also acted as the anaesthetist for the surgical procedures.

2.4 ANAESTHESIA

The animals were transferred from the barn to an anaesthetic room adjacent to the operating theatre. The area overlying the left internal jugular vein was shaved using clippers. General anaesthesia was induced with an intra-venous injection of thiopentone (1ml / 5kg) into the left jugular vein. The animal was then placed supine on a trolley and its trachea intubated, under direct vision, with a cuffed endotracheal tube. Correct positioning of the tube was confirmed by bilateral auscultation of the chest wall listening for breath sounds.

The sheep was then transferred to the operating theatre and placed on the operating table in a supine position for median nerve experiments or in a right lateral position for facial nerve experiments. The endotracheal tube was connected to a pressure-

controlled ventilator (BOC-Manley Promovent) and general anaesthesia was maintained with a mixture of 1% to 2% halothane, 2l min^{-1} nitrous oxide and 6l to 8l min^{-1} oxygen. The animal was monitored throughout the procedure using pulse oximetry, three limb lead ECG and a temperature probe placed in the oesophagus. Depth of anaesthesia was determined by loss of the corneal reflex and observation of the pulse rate, looking for the development of a tachycardia.

In the recovering animals an intramuscular injection of 50mg flunixin (Schering Plough, Animal Health), a non-steroidal anti-inflammatory agent, was administered at the end of the procedure for postoperative analgesia. For the animals with neurapraxia injuries or transection injuries repaired by entubulation, of which both procedures involved insertion of a foreign body, an intramuscular injection of 750mg of cefuroxime (Zinacef, Glaxo, UK) was administered to minimise the risk of infection.

At the end of the procedure the delivery of halothane and nitrous oxide was stopped and the delivery of oxygen increased. The animal was extubated once it was breathing spontaneously and coughing on the endotracheal tube. For those animals undergoing a second procedure general anaesthesia was not reversed and a lethal injection of pentobarbitone (140mg kg^{-1}) was administered in keeping with Home Office regulations.

2.5 POST-OPERATIVE CARE

After surgery the animals were transferred to a recovery pen. They were positioned upright against a wall of the recovery pen with one bale of straw along the opposite flank and a smaller bale of straw to support the head. The animals were closely monitored in the immediate postoperative period until they had fully regained

consciousness and were standing unaided. They were kept in the recovery pen overnight and transferred the following day to the barn or outside to a field. Those animals who had foreign bodies as a result of their procedure (the neurapraxia groups and the neurotmesis with entubulation groups) received a further two intramuscular doses of 750mg cefuroxime.

In the facial nerve experiments, the animals had an obvious left-sided facial weakness in the immediate post-operative period. However, in all cases, this had resolved by the time of the second procedure. The animals were observed to be eating normally the day after surgery. One of the sheep developed a small wound effusion, however, this did not become infected and resolved spontaneously. Two of the sheep that underwent facial nerve procedures died from illnesses unrelated to the surgery.

In the median nerve experiments all the animals made a good post-operative recovery and were seen to be mobilising well the day after surgery. There were no incidences of lameness and the animals were able to bear weight on the operated limb without difficulty. One of the sheep developed a wound infection but this responded to treatment with antibiotics. Another of the sheep, which underwent a median nerve procedure, died from an illness unrelated to the surgery.

3 SURGERY AND MODELS OF NERVE INJURY

3.1 SURGICAL APPROACH TO THE FACIAL NERVE

The animal was placed in the right lateral position thereby exposing the left side of its face, which was shaved using electric clippers. The facial nerve and vein could be palpated through the skin. This enabled the course of the nerve to be marked using indelible ink. In the second procedure the scar from the first operation acted as a marker of the position of the facial nerve.

Some of the animals with bigger horns required removal of the tip of the left horn to allow access to the facial nerve and to allow correct positioning of the microscope. This was achieved using a small saw. The skin below the horn and the left eye were protected during this procedure using a metal plate. The amount of horn removed was minimised to avoid bleeding from blood vessels present in the more proximal region of the horn.

3.1.1 First Facial Nerve Procedure

This procedure was carried out under sterile operative conditions. The left side of the face, which had previously been shaved, was prepared with povidone-iodine solution (Betadine, Seton Healthcare, England). The surrounding area was covered with sterile surgical drapes. These were secured in position with towel clips. The skin was incised along the previously marked course of the nerve. Bleeding points were coagulated using bipolar diathermy. Small skin flaps were raised. These were reflected and secured in position with 4/0 polyamide sutures (Ethilon, Ethicon, UK) Connective tissue was divided using sharp dissection to expose the underlying facial nerve

approximately 3cm from the parotid gland and before it passed deep to the masseter muscle. The nerve was carefully dissected from the adjacent facial vein. A nerve stimulator was used in some cases to aid location of the nerve.

The appropriate procedure was then carried out for the particular model of nerve injury to be investigated. Each model of nerve injury is described in detail in Section 2. After ensuring haemostasis the incision was closed. Interrupted sutures were placed in the subcutaneous tissue using 4/0 polyglactin (Vicryl, Ethicon, UK). The skin was closed with a continuous subcuticular suture also using 4/0 polyglactin. An antiseptic dressing spray was applied to the wound (Opsite, Smith and Nephew, England). No other dressings were used.

3.1.2 Second Facial Nerve Procedure

The second facial nerve procedure was performed six months after the initial one. This period had been demonstrated by previous workers within the research group to be adequate for facial nerve injuries to recover. In accordance with the Home Office licence for these experiments the second procedure was a terminal one. Therefore, clean but not sterile instruments and drapes were used. This procedure lasted several hours. The temperature of the animal was monitored throughout the procedure and 500mls of intravenous saline was administered to offset increased insensible fluid losses from the site of dissection.

The animal was placed in the right lateral position exposing the left side of its face as in the previous procedure. The left side of its face and the nasal bridge were shaved using electric clippers. The skin was cleaned with alcohol to remove lanolin present on the skin as this can hinder the attachment of surface recording electrodes.

A unipolar ground electrode was positioned on the skin over the bony nasal bridge. Efficacy of conduction was improved with a small amount of electrode paste (Ten 20,

Weaver & Co., Aurora, USA). Surface recording electrodes were placed over the zygomaticus muscle. The zygomaticus muscle was located near the snout of the animal. The muscle bulk was easily located by palpation. This muscle is solely supplied by the facial nerve. The cathode was positioned over the motor point of the muscle and the reference electrode 1cm distally.

The motor point is defined as the area of muscle where contraction of that muscle may be elicited with minimal-intensity, short duration electrical stimulation (Kimura 1983). Anatomically it corresponds to the location of the terminal portion of the motor nerve fibres. The motor point is usually found in the proximal third of the muscle. In these experiments the motor point was located by altering the position of the cathode to obtain the CMAP with the sharpest take-off point.

The facial neurovascular bundle was more difficult to palpate at the second procedure. This difficulty was thought to be due to scar tissue resulting from the first operation. A skin incision was made parallel and slightly rostral to the pre-existing scar. This approach was found to avoid the worst of the scar tissue whilst still being close to the previously located facial nerve. At this point no attempt was made to dissect around the area of the nerve where the previous surgery had been performed. The nerve here was surrounded by a dense mass of scar tissue and therefore more difficult to dissect and hence more susceptible to damage.

The nerve was dissected proximal and distal to the site of injury. A nerve stimulator was used in those cases where location of the nerve proved difficult. The least amount of dissection required to expose adequate amounts of nerve to allow electrode placement was performed. This was to minimise disruption of the blood supply, avoid the nerve's drying out and to keep the nerve warm. The maximum conduction velocity of a nerve has been shown to decrease with decreasing temperature (de Jesus,

Hausmanowa-Petrusewicz & Barchi 1973; Johnson & Olsen 1960). The areas of exposed nerve were kept moist with saline-soaked gauze swabs.

Proximally, the facial nerve was dissected approximately 1cm from its exit from the parotid gland. Extreme care was taken to avoid breaching the parotid gland. Parotid gland secretions contain high concentrations of potassium which can cause hyperpolarisation of nerves and render nerve conduction studies impossible. A bipolar stimulating electrode (proximal anode and distal cathode), held in position by means of a plastic casing, was placed under the nerve at this site and connected to stimulator B on the Medelec machine. This electrode was termed S1.

Distally, the facial nerve was located by dividing the masseter muscle to reveal the nerve lying underneath. The nerve was dissected free from surrounding structures and a bipolar stimulating electrode, S2, was positioned under the nerve. This electrode was connected to stimulator A on the Medelec machine. The maximum possible distance between the stimulating electrodes was achieved as nerve conduction studies are more accurate over longer distances (Kimura 1983).

3.2 SURGICAL APPROACH TO THE MEDIAN NERVE

The animal was placed in a supine position. Supports were placed on both sides of the chest wall. The right side of the chest wall and the right foreleg were shaved using electric clippers. Padding was placed under the right side of the thorax and the operating table was rotated to the left. The animal's right foreleg was abducted and secured in position on an arm-rest using adhesive tape. This positioning was found to create the most obtuse angle between the chest wall and the right foreleg allowing access to the region where the median nerve was located.

3.2.1 First Median Nerve Procedure

This procedure was performed under sterile operative conditions. The skin was prepared with povidone-iodine solution (Betadine, Seton Health Care, England) and the surrounding area covered with sterile surgical drapes. These were secured with towel clips. The extension of the right foreleg as previously described caused visible taughtening of the right pectoralis major muscle. This muscle was used as a guide for the position of the skin incision. The skin was incised transversely along the right lateral chest wall. The incision was then extended to run longitudinally along the right foreleg, just superior to the pectoralis major muscle. Bipolar diathermy was used to achieve haemostasis.

The incision revealed loose connective tissue which could be easily dissected with fingers to reveal the neurovascular bundle of the median nerve, the brachial artery and the ulnar nerve (lying in that order in a cranial to caudal direction). The neurovascular bundle lay on a flat bed of muscle and had an overlying layer of connective tissue. This connective tissue was divided and the median nerve carefully dissected free from the adjacent artery. The appropriate procedure was then carried out for the particular

model of nerve injury to be investigated. Each model of nerve injury is described in detail in Section 3.3.

After ensuring haemostasis the wound was closed. Interrupted sutures were placed in the subcuticular tissue using 4/0 polyglactin (Vicryl, Ethilon, UK) and the skin was closed with a 3/0 polyglactin (Vicryl, Ethilon, UK) continuous subcuticular suture. An antiseptic spray dressing was applied to the wound (Opsite, Smith and Nephew, England). No other dressings were used.

3.2.2 Second Median Nerve Procedure

The second median nerve procedure was performed nine months after the initial one. This period had been demonstrated by previous workers within the research group to be adequate for facial nerve injuries to recover. In accordance with the Home Office licence for these experiments the second procedure was a terminal one. Therefore, clean but not sterile instruments and drapes were used. As the procedure lasted several hours, the temperature of the animal was monitored throughout the procedure and 500mls of intravenous saline was administered to offset increased insensible fluid losses from the dissection site.

The animal was positioned as described for the first median nerve procedure. The skin overlying the lateral wall of the right side of the chest and the right foreleg was shaved using electric clippers and cleaned with alcohol to remove lanolin. A ground electrode was positioned on the lateral wall of the right side of the chest. Efficacy of conduction was improved using a small amount of electrode paste. Surface recording electrodes were placed over the flexor carpi radialis (FCR) muscle which is solely supplied by the median nerve. The muscle was easily located and palpated, lying adjacent to the bigger flexor carpi ulnaris (FCU). The cathode was positioned over the

motor point of the muscle (located as described in Section 3.1.2) and the reference electrode over the distal tendon.

The skin was incised half a centimetre cranial and parallel to the scar from the previous procedure. Haemostasis was obtained using bipolar diathermy. Sharp and blunt dissection was required to locate the neurovascular bundle. The dissection was more difficult than in the first procedure as a consequence of scar tissue. A nerve stimulator was used in those cases where location of the median nerve proved difficult. The median nerve was dissected proximal and distal to the site of injury. As with the facial nerve the least amount of dissection required to expose adequate amounts of nerve to allow electrode placement was performed, for the reasons stated above.

Proximally, the median nerve was dissected out as close as possible to its emergence from the brachial plexus, to maximise the distance between the stimulating electrodes. A bipolar stimulating electrode (proximal anode and distal cathode), held in position by means of a plastic casing, was placed under the nerve at this site and connected to stimulator B on the Medelec machine. This electrode was designated S1.

The adjacent ulnar nerve was also identified and a 2cm section of this nerve was excised. This was to prevent unwanted stimulation of the ulnar nerve by antidromic impulses in the median nerve activating anterior horn cells resulting in orthodromic impulses in the ulnar nerve (analogous to F waves).

Distally, the median nerve was identified by the division of a thick condensation of fibrous tissue 1cm proximal to the origin of FCR. A stimulating electrode, identical to that used proximally, was positioned under the nerve at this site. This electrode was designated S2 and was connected to stimulator A on the Medelec machine.

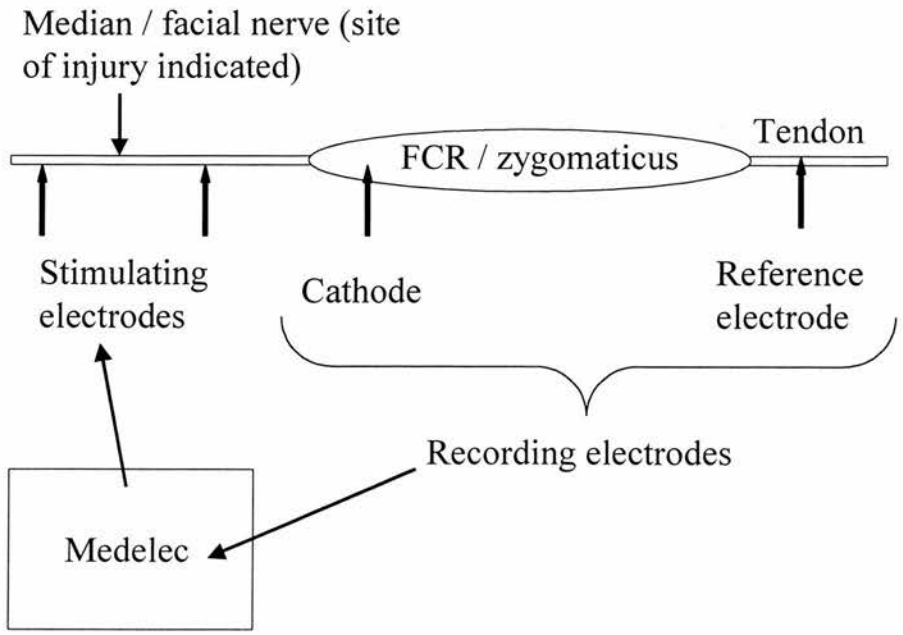

Figure 3.1 This figure is a diagram showing the positioning of the stimulating and recording electrodes in relation to the facial/median nerve and the related muscle.

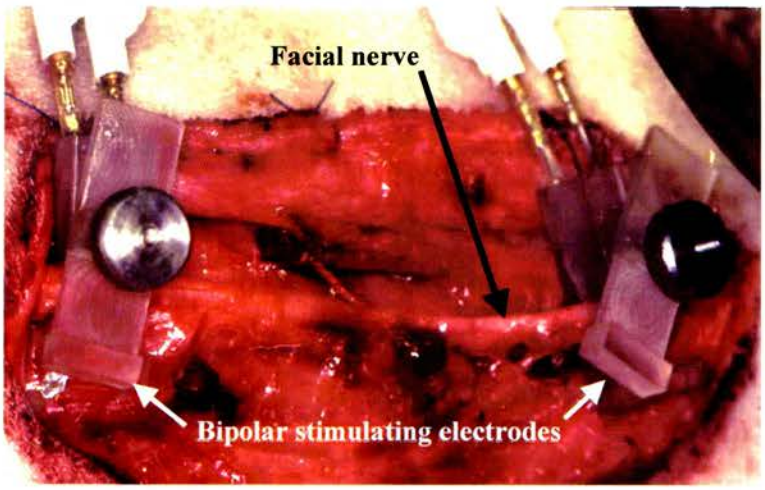

Figure 3.2 shows bipolar stimulating electrodes (held in a plastic casing) positioned on the facial nerve.

3.3 MODELS OF NERVE INJURY

3.3.1 Neurapraxia Model

Neurapraxia involves localised demyelination of a nerve with an associated conduction block (Cajal 1928). Neurapraxia does not result in Wallerian degeneration distal to the site of injury whereas more severe injuries, including axonotmesis, do. In motor nerve conduction studies, neurapraxia is characterised by a decrease in amplitude of the target muscle compound muscle action potential (CMAP) and an increase in latency (Kimura 1983).

Neurapraxia is caused by ischaemia and/or compression. Several previous workers have described models of chronic nerve compression. Weisl and Osborne encased the sciatic nerve in rats with polythene tubing, 'gently' compressing it (Weisl & Osborne 1964). They demonstrated an increase in latency of impulse conduction (as compared to the opposite control side) between two and five weeks after the initial injury. Bennet and Xie developed a different method of nerve compression whereby they used four chromic catgut ligatures tied around the sciatic nerve in the rat at 1mm intervals (Bennett & Xie 1988). The ligatures were tightened until the blood flow through the epineurial vasculature 'was retarded but not arrested' and there was minimal compression of the nerve. Histological examination demonstrated 'extensive demyelination' by the first post-operative day, however, no nerve conduction studies were performed. Histological examination of the distal nerve, two weeks after the injury, demonstrated extensive axonal loss. Furthermore, sequential examination of the injury site revealed that the ligatures were in continuity until between ten and fourteen days after the original procedure.

Both these models of nerve injury produced a chronic compression of the nerve with Wallerian degeneration of the distal nerve. In this work, a new model of injury was developed to produce a neurapractic lesion (with minimal Wallerian degeneration) using a short period of nerve compression.

A ligature, composed of biodegradable glass (Giltech, Ayr, Scotland), was tied around a nerve to cause localised compression. The biodegradable ligature was of a composition such that it lost tensile strength over twenty-four hours. This resulted in a transient insult to the nerve as is commonly associated with this type of nerve injury. It was postulated that this procedure would result in localised demyelination of the nerve without distal Wallerian degeneration. Experiments testing the validity of the models of injury for neurapraxia and axonotmesis are described in Section 3.3.3.

A stimulating electrode was placed on the nerve proximal to the intended site of injury. This was connected to stimulator A on the Medelec machine. In the case of the facial nerve surface recording electrodes were placed over the zygomaticus muscle. The cathode was positioned over the motor point of the muscle and the reference electrode 1cm distally (as described in Section 3.1.2). For the median nerve surface recording electrodes were placed over the flexor carpi radialis muscle. The cathode was positioned over the motor point of the muscle and the reference electrode over the distal tendon (as described in Section 3.3.2).

The ligature was positioned under the nerve (see Figure 3.1 for the facial nerve and Figure 3.4 for the median nerve). One throw of a surgical knot was performed and the ends of the ligature pulled so that it tightened around the nerve (see Figure 3.2 for the facial nerve and Figure 3.5 for the median nerve). The ligature was held in this position and, using a hand-held stimulator, the nerve was stimulated proximal to the site of injury. (The same stimulator was also used for the axonotmesis models. The

stimulator is shown in Figure 3.11, which shows the axonotmesis model for the facial nerve.) The ligature was progressively tightened around the nerve until a decrease in CMAP amplitude (1mV-5mV) and/or an increase in latency (0ms-1.5ms) was observed. The second throw of a surgical knot was then placed to secure the ligature in this position and the ends of the ligature trimmed (see Figure 3.3 for the facial nerve and Figure 3.6 for the median nerve). The skin was closed as previously described in Section 3.1.1.

The values for latency and CMAP amplitude before and after the ligature was applied are shown in Table 3.1. The values for the second median nerve neurapraxia experiment were not recorded.

	Latency (ms)		Amplitude (mV)	
Nerve	**Before**	**After**	**Before**	**After**
Facial	2.40	3.00	1.9	0.5
	2.15	2.80	3.3	0.6
	2.10	2.80	4.6	0.5
	1.55	3.05	2.9	1.2
	2.75	2.85	5.2	1.8
	2.45	3.75	5.3	0.3
Median	2.40	2.80	7.6	3.3
	2.45	2.60	5.5	4.5
	2.80	2.80	6.6	2.3
	2.00	2.95	8.1	6.3
	2.70	2.90	4.3	3.2

Table 3.1 This table shows the values for latency and amplitude of the CMAP for the facial and median nerves before and after tightening of the ligature to produce a neurapractic lesion.

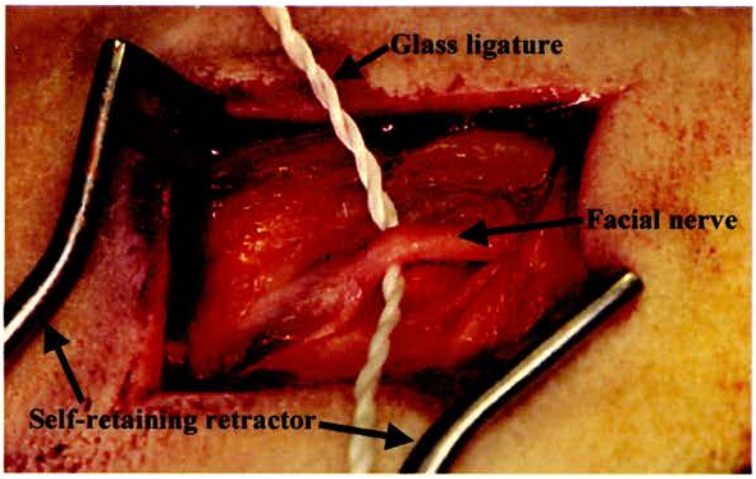

Figure 3.3 Facial nerve neurapraxia model. Glass ligature positioned under facial nerve.

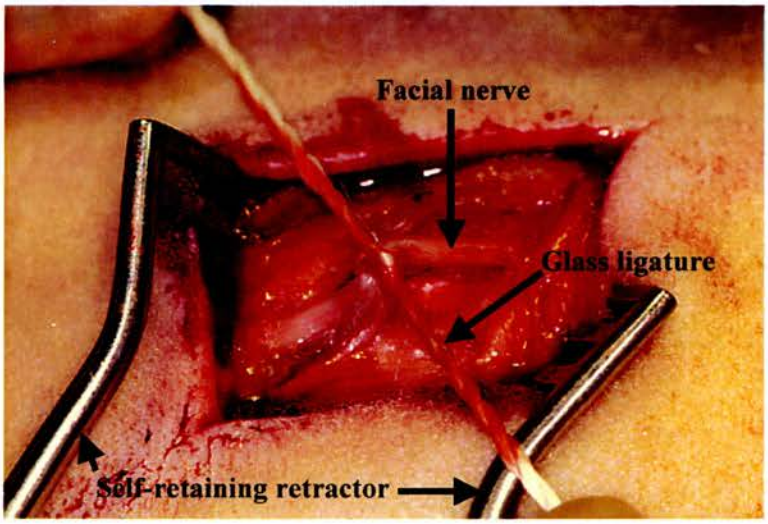

Figure 3.4 Facial nerve neurapraxia model. Photograph showing glass ligature tied and tightened around facial nerve.

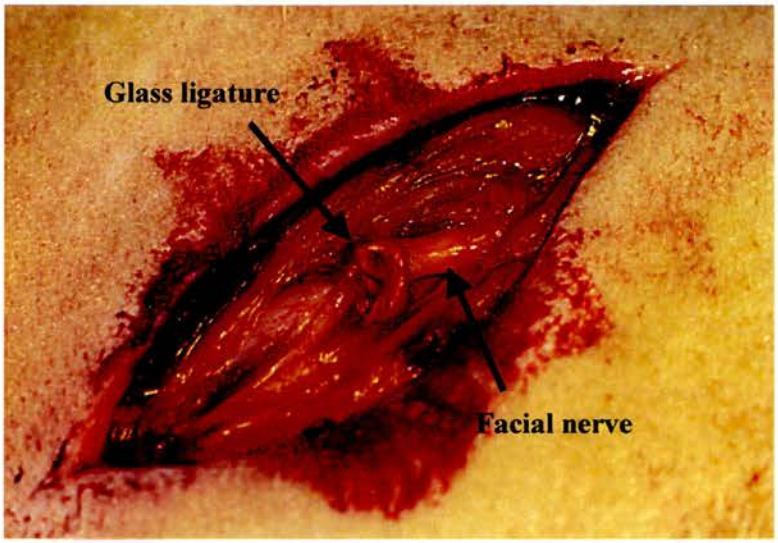

Figure 3.5 Facial nerve neurapraxia model. Photograph showing final appearance of trimmed glass ligature around facial nerve.

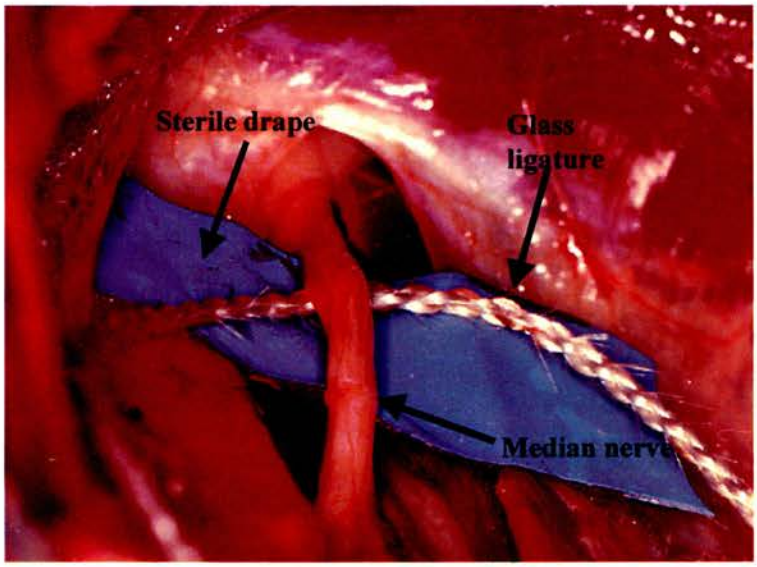

Figure 3.6 Median nerve neurapraxia model. Photograph of glass ligature positioned under median nerve.

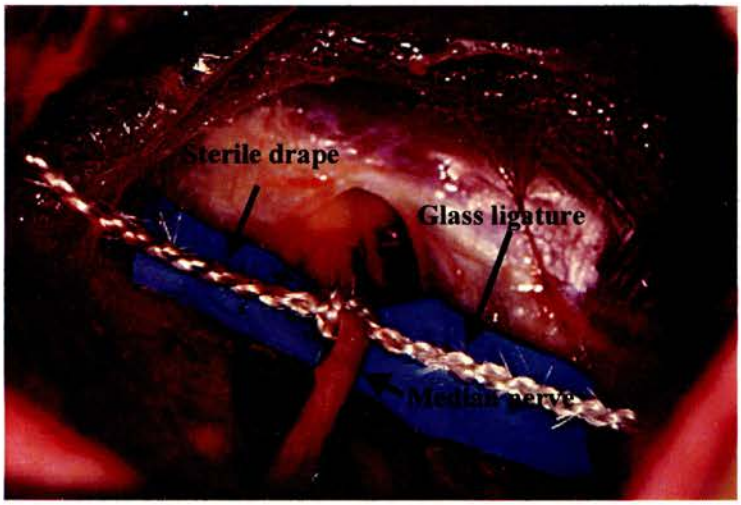

Figure 3.7 Median nerve neurapraxia model. Photograph showing glass ligature tied and tightened around median nerve.

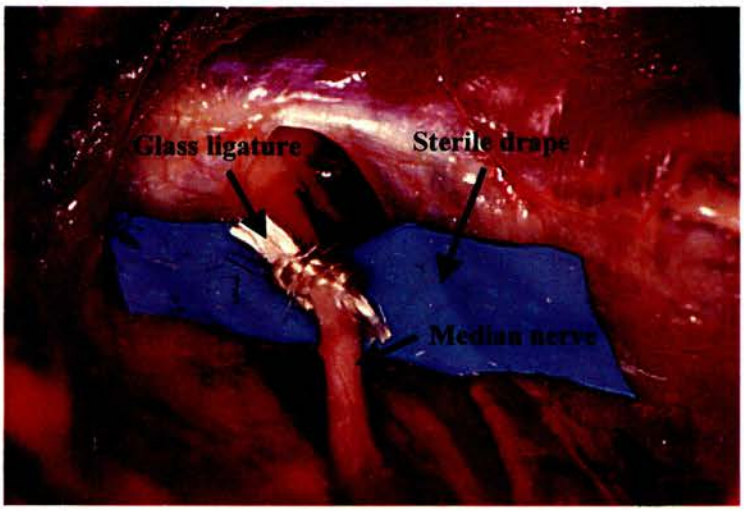

Figure 3.8 Median nerve neurapraxia model. Photograph showing final appearance of trimmed glass ligature around median nerve.

3.3.2 Axonotmesis Model

Axonotmesis involves axonal disruption resulting in Wallerian degeneration distal to the site of injury (Cajal 1928). The endoneurial tubes remain intact therefore axons should regenerate along their original path. Gutmann *et al* described a method for producing an axonotmesis-type injury in the tibial and peroneal nerves in the rabbit (Gutmann, Guttmann, Medawar, & Young 1942). These workers used 'fine, sharp, smoothed-faced watchmakers' forceps' to crush the nerve several times at the same spot producing a 'transparent thread over 1mm to 2mm'. They confirmed that all fibres had been disrupted by the fact that the distance from the site of injury at which reflexes could be elicited increased with time, in a similar manner to that after neurotmesis and suture repair. They postulated that smooth-faced forceps were better than toothed forceps as the latter was more likely to disrupt endoneurial tubes, effectively creating a Sunderland Type III or Type IV injury (Sunderland 1978). A similar method was used by Sanders and Whitteridge (Sanders & Whitteridge 1946). These workers crushed the peroneal nerve of rabbits for ten seconds using smooth-tipped watchmakers' forceps.

In the work presented here axonotmesis was produced by crushing the nerve for ten seconds using a ratcheted-non-toothed micro-needleholder (Codman, Randolph, Massachussettes, USA). This was tightened to the second ratchet allowing a reproducible injury for each nerve. A photograph of the needleholder is shown in Figure 3.7. This method of producing axonotmesis had been developed by previous workers within the group (Fullarton 1994).

Figure 3.8 is a photograph of the median nerve being crushed and Figure 3.9 shows the resulting indentation in the nerve. Figure 3.10 shows the equivalent indentation in the facial nerve. After being crushed the nerve was stimulated proximal to the site of

injury with a hand held stimulator, in an identical manner to that used for the neurapraxia model, to confirm a conduction block. A photograph of this is shown for the facial nerve in Figure 3.11.

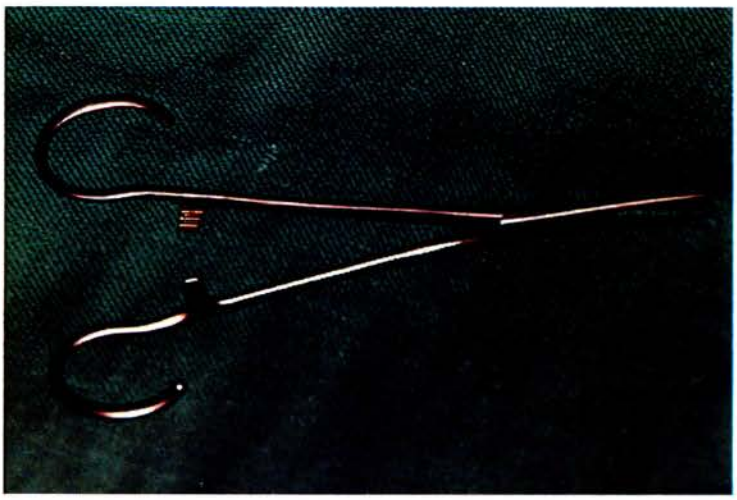

Figure 3.9 Photograph showing non-toothed crushing clamp.

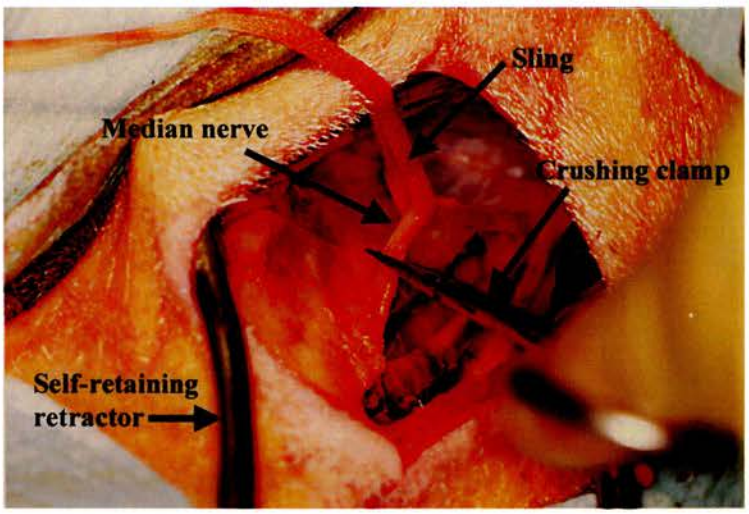

Figure 3.10 Median nerve axonotmesis model. Photograph showing the median nerve being crushed using a non-toothed clamp.

Figure 3.11 Median nerve axonotmesis model. Photograph showing indentation in median nerve after being crushed with non-toothed clamp.

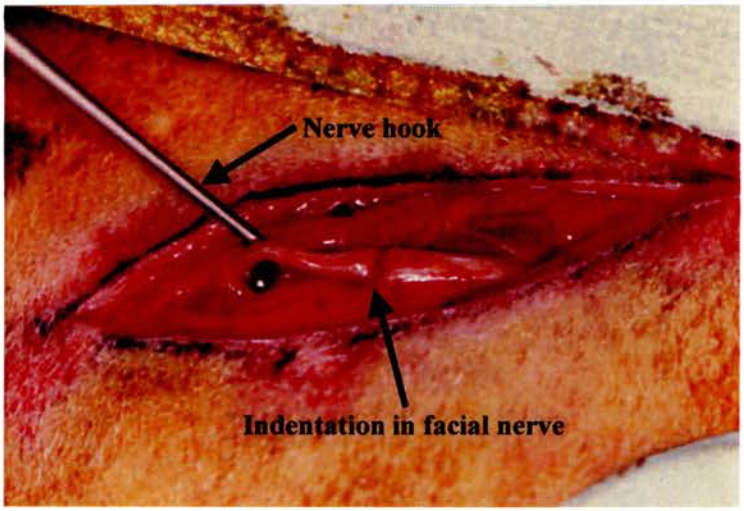

Figure 3.12 Facial nerve axonotmesis model. Photograph of facial nerve, elevated using nerve hook. Indentation in nerve from crushing with non-toothed clamp.

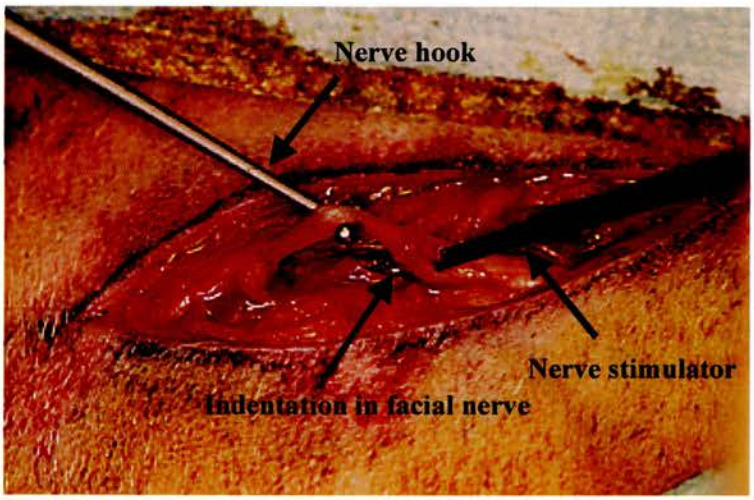

Figure 3.13 Facial nerve axonotmesis model. Photograph of facial nerve elevated using nerve hook. Indentation in nerve from being crushed. Nerve stimulator positioned proximal to crush site.

3.3.3 Testing the Neurapraxia and Axonotmesis Models

Axonotmesis results in Wallerian degeneration distal to the site of nerve injury whereas neurapraxia lesions only result in localised demyelination (Cajal 1928). In axonotmesis, conduction in the distal nerve segment will initially be normal as the axons remain excitable. At this time nerve conduction studies are unable to distinguish between neurapraxia and axonotmesis. However, three days after axonotmesis axons and myelin fragment (Robinson 2000). This is associated with a fall in amplitude of the CMAP. By day nine no CMAP can be elicited, usually due to both failure of neuromuscular transmission and Wallerian degeneration. However, the process of Wallerian degeneration can take up to two weeks.

This illustrates the importance of timing of investigations. If nerve conduction tests are performed too early they may underestimate the severity of the injury, as the distal segments of nerves with axonotmesis (and transection) injuries are still excitable. At two weeks however, nerve conduction studies can differentiate between neurapraxia and axonotmesis (and transection) injuries as the distal segments have undergone Wallerian degeneration. In neurapraxia, stimulating distal to the lesion results in a CMAP whereas, in axonotmesis stimulating distal to the lesion does not elicit a response.

The aim of the work described in this section was to determine whether the models of nerve injury for neurapraxia and axonotmesis (described in the previous two sections) were valid. A neurapraxia model of injury and an axonotmesis model of injury were performed on the left facial nerves of two sheep, using the methods described in Section 3.3.1 and Section 3.3.2. The sheep were brought back for electrophysiological assessment of these nerves two weeks later. This allowed adequate time for Wallerian degeneration to take place.

General anaesthesia was induced and maintained as described in Section 2.4. Surface recording electrodes were placed over the zygomaticus muscle and a ground electrode positioned on the nasal bridge as described in Section 3.1.2. The left facial nerve was exposed and dissected proximal and distal to the site of injury also as described in Section 3.1.2. Although the second procedure was performed only two weeks after the initial one there was already an increased amount of fibrous tissue around the site of injury which was easily identifiable. For each of the two models of injury the nerve was stimulated proximal and distal to the site of injury using the hand-held stimulator previously shown in Figure 3.11.

In the neurapraxia model a CMAP was elicited by stimulating distal but not proximal to the site of injury indicating there was a localised conduction block but no Wallerian degeneration. In the axonotmesis model no response was elicited by stimulating proximal or distal to the site of injury indicating that this nerve had undergone Wallerian degeneration. These findings support the validity of the models of nerve injury for neurapraxia and axonotmesis.

3.3.4 Neurotmesis Model with Epineurial Sutured Repair

The nerve was transected using a scalpel. A rectangle of green contrast material (cut from a sterile disposable surgical drape) was placed under the nerve and the cut ends of the nerve were apposed. An operating microscope, with a sterile cover, was positioned over the nerve (Wild, Heerbrugg M690, Switzerland). Sterile handle covers allowed positioning of the microscope by the surgeon so that the nerve was in the field of vision. Foot pedals allowed alteration of focus and the degree of magnification. The nerve was viewed through the microscope and checked for the presence of bleeding intraneural vessels. If present these were coagulated with bipolar diathermy. Visible anatomical structures such as fascicles and surface vessels were aligned in an attempt to restore the nerve to its original configuration. The nerve was coapted using interrupted 9-0 polyamide (Ethilon, Ethicon, UK) epineurial sutures, placed using microsurgical instruments. The sutures were placed in the epineurium at high magnification taking care to avoid the fascicles. Surgical knots were tied using a lower magnification as this made location of the end of the suture easier. The minimum number of sutures required were used, usually six.

3.3.5 Neurotmesis Model with Entubulation Repair

Entubulation has both practical (*e.g.* no need for microsurgical technique and expensive equipment) and theoretical (*e.g.* less surgical trauma to nerve ends, a reservoir for growth factors in the chemical manipulation of nerve regeneration) advantages over conventional sutured nerve repair. Its possible disadvantages include the retraction of nerve stumps from the conduit, inflammation and scarring due to foreign-body reaction and requirement for a second procedure because of this.

Conduits may be biological (artery, vein, freeze-thawed muscle) or non-biological (silicone, polyglycolic acid, biodegradable glass) (Glasby, Fullarton, & Lawson 1998; Gilchrist et al.1998; Kelleher et al. 2001).

In the experiments described here, a flexible cloth was used made from a substance known as 'controlled release glass' (CRG) (Giltech, Ayr, Scotland). CRG is a biodegradable polymer of phosphates of sodium and calcium. The glass dissolves to form salts of its constituent ions. The rate of solubility is determined by the relative proportions of these constituent ions. Controlled release glass has been demonstrated to be non-toxic and is already in clinical use for example as an antimicrobial dressing for burns.

Previous work using rigid CRG tubes to repair peripheral nerves yielded results comparable with standard epineurial sutured repair (Gilchrist et al.1998). However, these rigid tubes had to be manufactured in predetermined sizes whereas the cloth version is more versatile as it can be adapted to any size of nerve.

The nerve was transected using a scalpel, in an identical manner to that used for the neurotmesis and suture repair group. The glass material for each procedure was sealed in an individual packet, sterilised by irradiation. The initial size of the glass was 4cm by 5cm however, this was trimmed to approximately 3cm by 4cm to make it easier to position and manipulate. The glass was brittle and non-toothed forceps were found to be the best instruments to handle it, as toothed forceps tended to fracture pieces from the edge. Care was taken to ensure the surgical field was dry as the glass tended to disintegrate when wet.

A rectangle of glass material was placed under the cut ends of the nerve which were then apposed. An operating microscope was not used at any point throughout this procedure. However, those anatomical structures of the nerve which were visible with

the naked eye were aligned, in an attempt to restore the nerve to its original configuration. Drops of fibrin sealant (Tisseel, Immuno AG, Vienna, Austria) were used to secure the edges of the material to the nerve as shown in Figure 3.12. The fibrin sealant was produced by simultaneous application of a solution of fibrinogen and aprotinin with a solution of thrombin. This was achieved using two syringes with a common plunger. The setting process commenced immediately the two solutions came into contact. Care was taken to ensure that glue did not contaminate the cut ends of the nerve. The material was then wrapped once over the nerve and the free ends opposed and secured to each other using a gel polymer (polycaprolactone) of the glass. Figure 3.13 shows a photograph of the facial nerve after the glass has been wrapped over it. The polycaprolactone gel was applied where indicated by the black arrow. A further application of fibrin glue was made at either end of the material and excess material was trimmed as shown in Figure 3.14. The wound was closed as previously described.

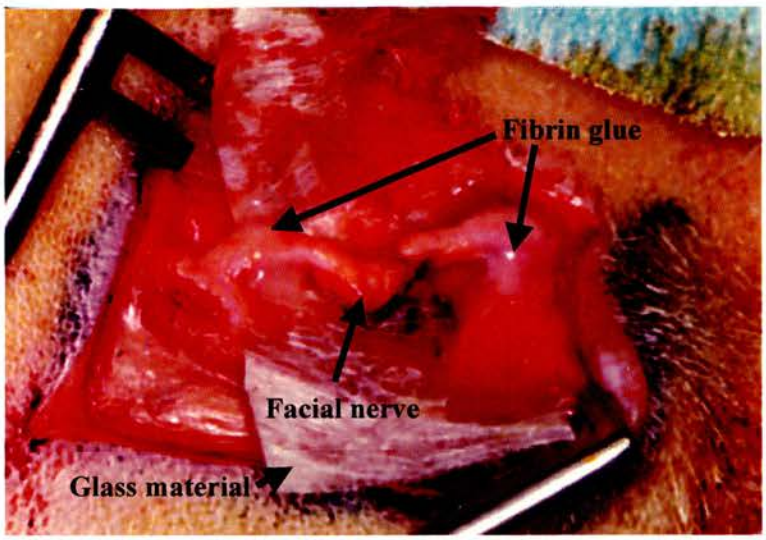

Figure 3.14 Facial nerve neurotmesis and wrap repair model. This photograph shows a transected facial nerve lying on glass material. Fibrin glue has been applied to attach the nerve to the material.

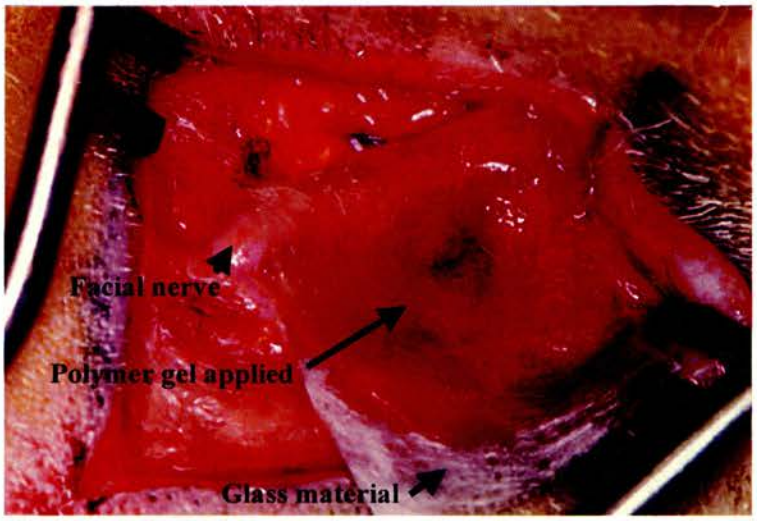

Figure 3.15 Facial nerve neurotmesis and wrap repair model. This photograph shows glass material wrapped around a facial nerve. Polymer gel has been applied to the free ends of The material.

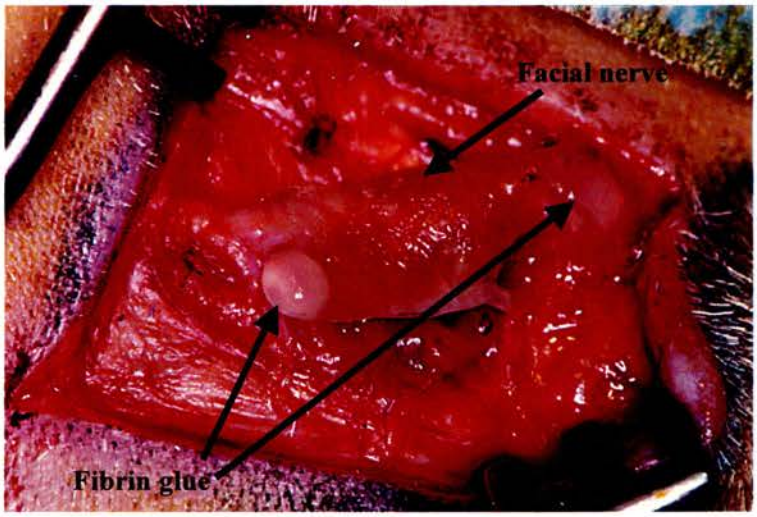

Figure 3.16 Facial nerve neurotmesis and wrap repair model. This photograph shows the final appearance of the trimmed glass material around facial nerve, with more fibrin glue on the ends of the material.

3.3.6 Nerve Graft Model

A 1cm portion of nerve was excised with a scalpel. The excised portion was rotated 180° through its long access, there by reversing it. The graft was rotated as described to decrease the likelihood of matching of original fibres, which could potentially give this procedure an advantage over grafts used in clinical practice which are harvested from other nerves.

An operating microscope (Wild, Heerbrugg M690, Switzerland) was positioned and used for the rest of the procedure as described in Section 3.3.6. Using the microsurgical technique described in Section 3.3.6, the graft was sutured into position between the cut nerve ends using interrupted 9-0 polyamide (Ethilon, Ethicon, UK) epineurial sutures. The wound was closed as previously described.

4 GENERAL ELECTROPHYSIOLOGY

4.1 THE 'MEDELEC'

The Medelec Synergy machine (Oxford Instruments, Surrey, UK) used in these experiments was a mobile digital two-channel electromyograph. It was designed to allow reliable recording, display and documentation of electrophysiological information, in a clinical setting. The Medelec was comprised of the following components:

(1) Personal computer (Windows 95 Operating System, Intel Pentium Processor, 64MB RAM), zip and floppy disc drives.

(2) 17" monitor (0.01μV to 100mV per division).

(3) User interface: Control panel (adjacent to monitor screen), keyboard, mouse, and foot pedals.

(4) Connector unit (connection point for EMG loudspeaker, electrical stimulator probes, trigger in and trigger out).

(5) Two-channel pre-amplifier (see Section 4.2).

(6) Two external stimulators (see Section 4.4).

(7) Trolley with power supply unit, a mains isolating transformer (designed to meet specified safety requirements) and a mobile arm which houses a pre-amplifier and one of the electrical stimulators.

4.2 AMPLIFIERS

Neurophysiological signals are small therefore they need to be amplified so they can be displayed. However, the signal may be contaminated by other sources *e.g.* diathermy, power cables, dirty electrodes. These erroneous signals may also be

amplified and result in interference in the output trace. There are two types of contamination, electrostatic and electromagnetic. Electrostatic interference arises from potential differences in the environment whilst electromagnetic interference is caused by current flow. Differential amplifiers allow electrophysiological recording in the presence of electrostatic and electromagnetic fields.

In simple amplifiers, one electrode is used as the signal input and the other is connected to earth. This means the potential difference (PD) between the electrodes cannot be displayed and both the signal and the PD between the electrodes are amplified. This can result in large interference signals.

In differential amplifiers there are two active input signals and the PD *between* the inputs is amplified. Signals common to both inputs (in phase and of the same amplitude), as in seen with interference, are cancelled out. These signals are referred to as 'common mode potentials'. Signals which differ between the two inputs are referred to as 'differential potentials' and are amplified. The differential amplifier may be regarded as two separate amplifiers recording with respect to a third electrode, usually earth. The combined output of the two amplifiers, is the amplified potential difference between the two input signals, when compared to a common earth. This may be expressed as

$$(V_A + V_C) - (V_B + V_C) = V_A - V_B$$

where V_A and V_B are electrophysiological signals and V_C is the common mode potential.

The ratio of amplification between differential and common-mode signals is known as the discrimination or common mode rejection ratio (CMRR) of the amplifier. This is a method of stating the ability of the amplifier to record electrophysiological signals in

the presence of interference. For electrophysiological recording the CMRR should be at least 100000:1 (100dB). The CMRR of the amplifier on the Medelec is >110dB. Interference commonly arises in connections between the patient, the electrodes and the input to the amplifier. PD is induced between the electrodes by current flow. This PD is interpreted as a differential signal and is amplified. This source of interference can be minimised by using amplifiers with high impedance to decrease the induced current. Preamplifiers are located close to the patient. They perform little amplification but decrease the impedance of the signal so there is less interference during transmission. Amplifiers used for electrophysiological recording should have an impedance of >5MΩ. The amplifier on the Medelec had an impedance of > 1000MΩ. Interference can also be minimised by using recording electrodes with low impedance to minimise the resulting potential difference and wires should be as short as possible. The Medelec pre-amplifier had an integral two-channel impedance check indicator (<2, 4, 8, 16, 32 and >32KΩ). Before any electrophysiological tests were performed, this was used to check that the impedance of the recording electrodes was <4KΩ. Every sensitive electrical system has a small fluctuating output even when there is no input. This is called noise. Sources of noise include switch contacts and thermal noise (caused by random movement of electrons). The noise of the amplifier used here was <0.7μV r.m.s. (0.1-10kHz bandwidth).

4.3 FILTERS

As discussed earlier neurophysiological signals are small and therefore must be amplified to generate a recordable output. However, amplification can cause distortion of the signal. Filters are used to allow equal amplification of the relevant

range of frequencies. They also block unwanted or irrelevant signals thereby reducing interference.

High frequency (low pass) filters attenuate high frequency signals whilst low frequency (high pass) filters attenuate low frequency signals. Simple filters consist of a resistor and a capacitor. The input PD of the filter must equal the output PD. In high frequency filters the resistor is connected in series and the capacitor is connected in parallel. At high frequencies the capacitor does not have time to charge therefore there is minimal output however at lower frequencies it has time to do so resulting in an increased PD across it and a bigger output. In low frequency filters the resistor is connected in parallel and the capacitor is connected in series. The PD across the resistor equals the PD of the input minus the PD across the capacitor. At low frequencies the capacitor has time to charge thus decreasing the PD across the resistor and hence decreasing the output. At high frequencies the capacitor is uncharged and most of the PD is across the resistor therefore there is a large output.

The range of frequencies over which an amplifier is active is known as the *bandwidth*. Different bandwidths are required for different investigations *e.g.* the bandwidth for single-fibre EMG is 500Hz to 10kHz whereas the bandwidth for clinical EEG is 0.5Hz to 70Hz.

The frequency characteristic of an amplifier can be expressed as a *frequency response curve*. This is a graph of the amplitude of the signal, after it has been filtered, against different frequencies. The x-axis is logarithmic (compressed at higher frequencies) to allow a wide range of frequencies to be displayed. The amplitudes of the signals between the filter values are not all 100%. This is because filters do not abruptly cut-off a signal at a specified frequency. This results in a degree of filtering within the bandwidth. The *pass band* of an amplifier is determined by its *turnover points*. The

turnover points are the upper and lower frequencies at which 3dB attenuation of the signal takes place. The relationship between decibels and amplitude can be expressed as

$$\text{decibels} = 20 \log_{10} \frac{\text{amplitude signal out of filter}}{\text{amplitude signal into filter}}$$

Therefore, 3dB corresponds to a reduction in amplitude to 70.7%. The rate of attenuation of a filter is expressed in decibels per octave (the range over which the frequency doubles). Theoretically the greater the attenuation rate the better the filter as it results in sharper 'drop-off'. However, filters with high rates of attenuation can result in phase distortion and erroneous signals.

Another method of expressing the characteristics of a low frequency amplifier is the *'time constant'*. If a voltage is applied to an amplifier with a low frequency filter this will generate an output which will return to the base-line in an exponential manner even though the voltage is still applied to the amplifier. The time taken for the output to decay to 37.7% of its initial deflection is defined as the time constant. The turnover point of a low frequency filter in an amplifier is related to the time constant by the following equation.

$$TC = 1 / (2\pi F)$$

Where TC = time constant

F= turnover frequency

Filters used for neurophysiological recording usually have an attenuation rate of 6dB per octave. The low frequency filter in the Medelec had an attenuation rate of 6dB per octave. The frequency of this filter could be chosen from the following values, 0.01Hz, 0.1Hz, 0.3Hz, 1Hz, 3Hz, 10Hz, 20Hz, 30Hz, 50Hz, 100Hz, 200Hz, 300Hz, 500Hz, 1000Hz, 2000Hz. The high frequency filter in the Medelec had an attenuation

rate of 12dB per octave. The frequency of this filter could be chosen from the following values, 30Hz, 50Hz, 100Hz, 200Hz, 300Hz, 500Hz, 1kHz, 1.5kHz, 2kHz, 3kHz, 5kHz, 10kHz, 20kHz. There was also a notch filter which could be set at 50Hz or 60Hz. A notch filter is designed to block mains frequency. It should only be if other methods of minimising interference have failed as it can cause distortion of the signal.

4.4 EXTERNAL STIMULATORS

The Medelec had two external stimulators. These could provide a constant current or constant voltage output. Constant current was selected because a constant current stimulator passes the selected current through the electrodes even if they are in poor contact with the tissue(Kimura 1983). A constant voltage stimulator will apply the same voltage to the electrodes regardless of their impedance. If the impedance is high this could result in submaximal stimulation of the nerve. Therefore, constant current provides a more consistent stimulus than constant voltage.

The pattern of delivery of the stimulus could be selected using the stimulus mode (single, double, refractory, collision and train). The rate of delivery could be chosen from 0.05pps to 200pps and the duration of the stimulus from 0.05ms to 1.0ms. There was a high output range (0-100mA, 0-300V) and low output range (0-25mA, 0-75V) and a delay setting of 0 to 9 screen divisions.

The two external stimulators were designated A and B. Stimulator A was always positioned distal to stimulator B on the nerve. In the models of nerve injury this was distal and proximal to the site of injury.

4.5 DATA ACQUISITION

In an electrical circuit which is used for analogue purposes the current (or voltage) is proportional to a measurement which varies in a continuous fashion. For example, action potentials are analogue electrical fluctuations. An electrical circuit used for digital purposes has a discrete number of states. Therefore, an analogue circuit provides more information but a digital circuit is more accurate and reliable. The most commonly used digital circuits have only two states. The number of states can be increased but this reduces reliability. Instead, more circuits are used to increase the quantity of information transmitted.

Computer systems use the binary system because of the reliability of 'two state' digital circuits. The binary system has only two characters, 0 and 1. Therefore, more digits are required to express a number than in the ten character digital system. Each digit place of a binary representation is termed a *bit* (an abbreviation of binary digit). The number of bits is equivalent to two to the power of that number *e.g.* 8 bits is equivalent to 2^8 which equals 256.

Converting an analogue voltage into digital form requires an arrangement of analogue and digital circuits termed an A-to-D converter. The digital representation has a finite number of discrete values, the number (and accuracy) of which depends on the number of bits used. The digitising error of the process is determined by dividing the maximum analogue input range by the number of digital combinations. This gives the 1 bit resolution of the converter. A-D converters used in electrophysiology usually have at least 8 bit or 10 bit converters. The Medelec used here a 16 bit A-D converter.

4.6 SOFTWARE & TEST OPTIONS

Standard software provided with the Medelec includes a patient database, Protocol Wizard and on-line report generation. The patient database contains the patient demographics and links to the tests catalogues which contain test results and reports. Protocol Wizard allows configuration of new tests not available from the standard test options. The on line report facility allows compilation of a report (Microsoft Word compatible) as the tests are performed. Optional Synergy Reader software allows analysis of data and recompilation of reports on a personal computer, away from the Medelec machine. The standard test options include

(1) Motor nerve conduction

(2) Sensory nerve conduction

(3) Combined motor and sensory nerve conduction

(4) F wave

(5) H reflex

(6) Blink reflex

(7) Repetitive stimulation (decrement)

(8) Sympathetic skin response

(9) Needle EMG

(10) MUAP analysis

(11) Jitter

(12) Somatosensory evoked potential

(14) Brainstem auditory evoked response

(15) Cortical evoked response

(16) Visual evoked potential

(17) Intraoperative monitoring

5 STATISTICAL METHODS

All statistical calculations on these experiments were performed using the statistics programme Statistica (Version 6- Statsoft Inc, 2300 East 14th Street, Tulsa, O.K., 71404, U.S.A.). In these experiments the independent or grouping variables were the type of nerve and the type of nerve injury and the dependent variables were the electrophysiological and morphometric measurements.

5.1 ELIMINATION OF OUTLIERS

Before commencing statistical analysis of the data derived from the experiments it was necessary to identify and reject outliers. For each dependent variable, a half-normal probability plot was constructed, with an ellipse representing 95% confidence limits. Outliers were identified as those data points lying outside this ellipse. The half-normal probability plot was constructed in the same way as the standard normal probability plot (see below), except that all values were taken to be positive. A small number of outliers was found and rejected. An example of a half normal probability plot is shown for facial nerve for the variable CV_{max} in Figure 5.1.

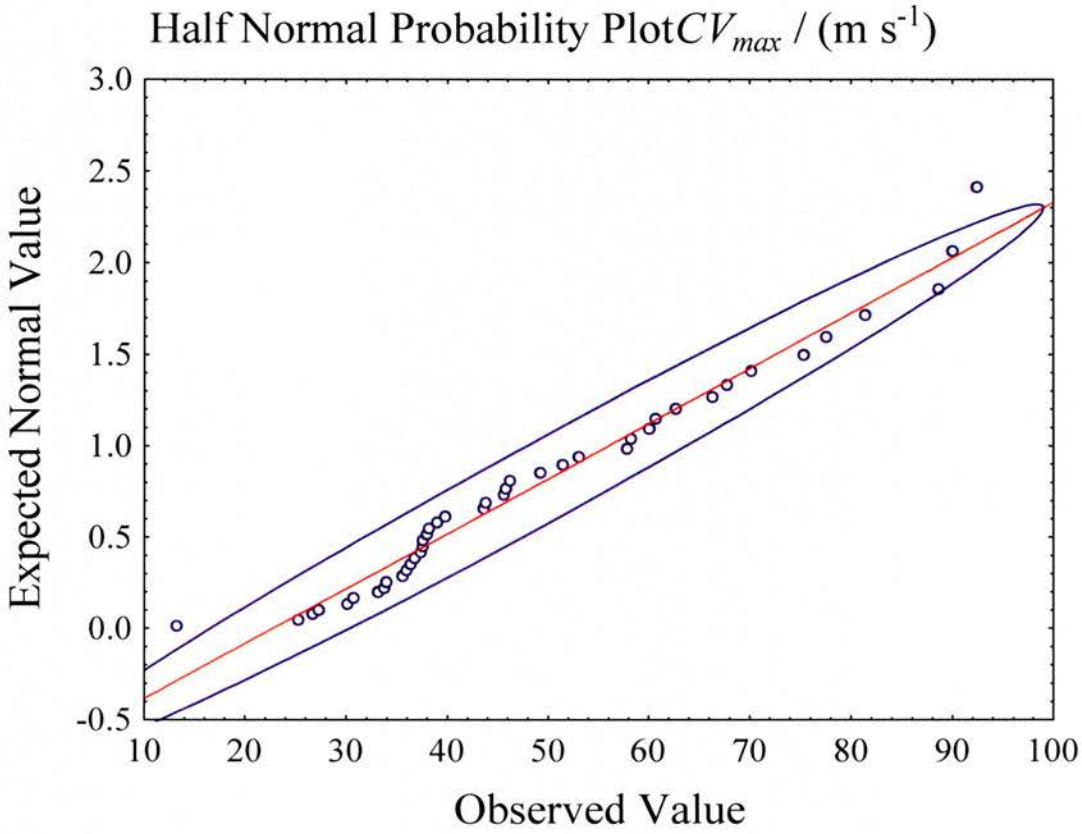

Figure 5.1 shows an example of a half normal probability plot for facial nerve for the variable CV_{max}. Two points lie outwith the ellipse and are therefore regarded as outliers.

5.2 NORMALITY OF DATA

All groups of measurements have an underlying mathematical distribution. It is essential that this distribution be identified to enable the correct statistical test to be selected. If a frequency histogram is plotted for normally distributed data a classic bell-shaped (Gaussian) curve is produced which is symmetrical around its mid-point. However, in non-parametrically distributed data the curve is asymmetrical being positively or negatively skewed.

In these experiments the distribution of the data was identified using normal probability plots. These plots were constructed for each variable as follows. The values for each variable were placed in order of rank. From this Z values were then calculated (standardised values of the normal distribution) based on the assumption that the values were normally distributed. The Z values were plotted on the y-axis and the observed values on the x-axis. If the observed values were normally distributed then all values would lie on a straight line. The Shapiro–Wilk W test was used to compare the scatter of raw data to the computed line. If the W statistic was significant *i.e.* there was a significant difference between the scatter of the raw data and the computed line, then the hypothesis that the data were normally distributed was rejected.

An example of normally distributed results is shown for the facial nerve for the variable *jitter* in Figure 5.2 and an example of non-parametrically distributed data is shown for the facial nerve for the variable CV_{max} in Figure 5.3. Table 5.1 shows the distribution of data for the facial nerve and Table 5.2 shows the distribution of data for the median nerve.

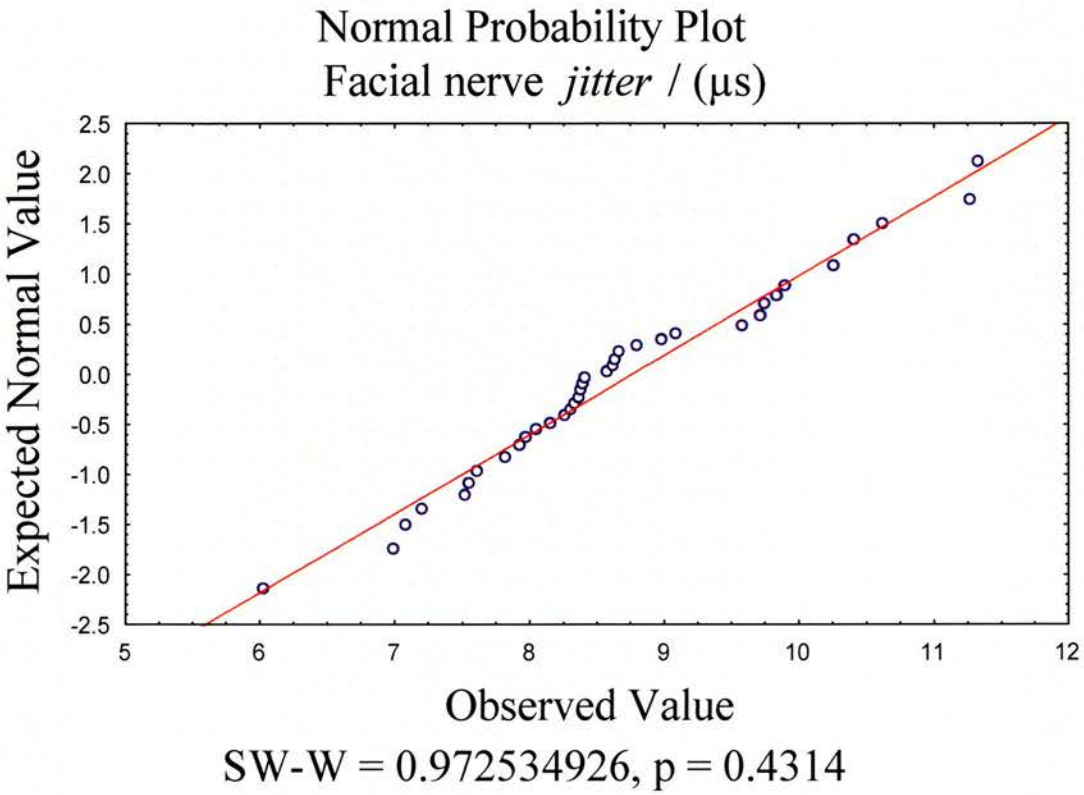

Figure 5.2 This shows a normal probability plot for *jitter* for the facial nerve. The p value is not significant therefore the data are normally distributed.

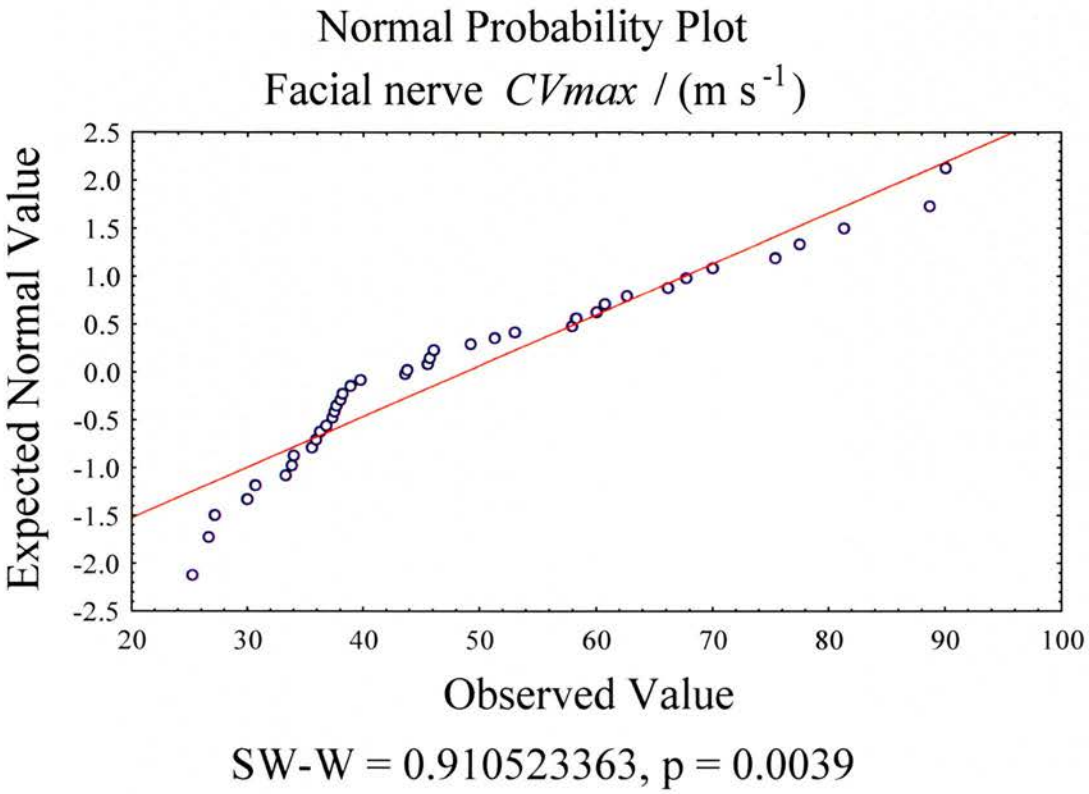

Figure 5.3 This shows a normal probability plot for CV_{max} for the facial nerve. The p- value is significant and a sigmoid curve is seen therefore the data are non-parametrically distributed.

Distribution of Facial Nerve Results	
Normal Distribution	**Non-parametric Distribution**
Maximum tetanic force	*Absolute refractory period (min)*
Jitter	*Absolute refractory period (max)*
Muscle mass	*Maximum conduction velocity*
Axon diameter	*Time to peak twitch*
Fibre diameter	*Amplitude peak twitch*
Myelin sheath thickness	*Time twitch-tension integral*
g ratio	*Time twitch-tension index*
Time to ½ relaxation twitch	*Time to ½ fatigue tetanus*
Time tetanic- tension index	*Time tetanic- tension integral*

Table 5.1 This table shows the distribution of data for the facial nerve experiments.

Distribution of Median Nerve Results	
Normal Distribution	**Non-parametric Distribution**
Jitter	*Absolute refractory period (min)*
Maximum conduction velocity	*Absolute refractory period (max)*
Time to peak twitch	*Amplitude peak twitch*
Time to ½ fatigue tetanus	*Time to ½ relaxation twitch*
Time- titanic tension integral	*Time twitch- tension integral*
Muscle mass	*Time twitch- tension indexl*
	Maximum tetanic force
	Time tetanic- tension index
	Axon diameter
	Fibre diameter
	Myelin sheath thickness
	g ratio

Table 5.2 This table shows the distribution of data for the median nerve experiments.

5.3 STATISTICAL TESTS

Statistical tests were then performed to identify the presence of significant differences between groups (variations of the F test), then subsequently to identify where those differences lay.

Different tests were required for normally distributed and non-parametric data. Statistical tests are based on comparisons of the central tendency of each group of data. Tests on normal data are based on mean values whereas tests on non-parametric data are based on median values or rank order. Non-parametric tests may be applied to normally distributed data but are generally less sensitive than parametric tests. However, parametric tests may not be applied to non-parametrically distributed data.

5.3.1 F Tests

The F test is a test of variance which is applied, simultaneously, to multiple groups. It identifies the presence of significant between-groups variation but does not identify which groups are statistically different. For normally distributed groups the F test was applied in the form of a one-way ANOVA test and for non-parametrically distributed groups the Kruskal-Wallis test was used.

In these experiments the one-way ANOVA test revealed differences for four of the normally distributed median nerve groups and one of the normally distributed facial nerve groups. The Kruskal-Wallis test revealed differences for two of the non-parametrically distributed groups for the facial nerve and five of the non-parametrically distributed groups for the median nerve. The results are shown in Table 5.3.

Variables with between-groups variation		
	Normally distributed variables	**Non-parametrically distributed variables**
Facial Nerve	*Fibre diameter*	CV_{max} ARP_{max}
Median Nerve	CV_{max} *Jitter* *Area under tetanus curve to ½ fatigue* *Muscle mass*	*Time tension index* *Axon diameter* *Fibre diameter* *Myelin thickness* *g ratio*

Table 5.3 shows the variables which had between groups variation when an F test was applied.

5.3.2 Post Hoc Tests

Post hoc tests were used to identify where these between-group differences lay. The most commonly used *post hoc* test for normally distributed data is the Student's t test which compares the means of two independent samples. However, if multiple t tests are performed, as would be required for these experiments since there were multiple differences, the likelihood of Type 1 errors increases. A Type 1 error occurs if the null hypothesis is incorrectly rejected, effectively a 'false positive'. The probability of a Type I error is the significance level of the test and is defined as p (Type I) = α (α is usually taken to be 0.05). To minimise the possibility of Type I errors a variation of the t test, called Scheffé's test, was used. This test was designed as a *post hoc* test to follow on from analysis of variance involving multiple groups.

For the facial nerve Scheffé's test found significant differences between individual groups for fibre diameter. For the median nerve significant differences were found between individual groups for CV_{max} and *muscle mass*. The results are discussed in further detail in the relevant chapters.

For non-parametrically distributed groups the Mann-Whitney-U test was used. This test is similar to the unpaired t test except it is calculated from rank sums as opposed to mean values. There is therefore the possibility of creating Type I errors however, there is no equivalent to Scheffé's test for non-parametric data.

For the facial nerve the Mann-Whitney U test found significant differences between individual groups for CV_{max} and ARP_{max}. For the median nerve the Mann-Whitney U test found significant differences between individual groups for *time tension index, axon diameter, fibre diameter, myelin sheath thickness* and *g ratio*. The results are discussed in further detail in the relevant chapters.

5.3.3 Power Calculations

The power of a statistical test is the probability of rejecting a false null hypothesis. A Type II error is the failure to reject a false null hypothesis, effectively a 'false negative'. The probability of detecting a Type II error is defined as p (Type II) = β. The power of a test is therefore 1-β. Power calculations were used in this work to assess the accuracy of the tests applied *i.e.* 1-β was calculated for the required value of α. Power studies were performed on each of those variables which showed significant differences ($p<0.05$) when tested with Scheffé's test or the Mann-Whitney-U test. The results are shown in Table 5.4.

Power calculations are also used to help calculate the sample size required to allow a statistically valid result. Sample size is affected by statistical significance (α. or Type I error), power (1- β), effect size and the variability of the data. Sample size is generally increased if a highly significant effect or a high power is desired, and/or, a small-sized effect or high population variability is present. Data from previous studies can be used to calculate the required sample size. Sample size calculation for these experiments was performed as described in Section 2.2.

Power Studies		
Nerve	**Variable**	**Power**
Facial	CV_{max}	1
	ARP_{max}	0.4
Median	CV_{max}	1
	Time tension index	1
	Muscle mass	0.9
	Axon diameter	1
	Fibre diameter	1
	Myelin sheath thickness	1
	g ratio	0.9

Table 5.4 This table shows the power calculations for those variables which showed significant differences between individual groups when tested with Scheffé's test or the Mann-Whitney-U test.

6 JITTER

6.1 INTRODUCTION

Single fibre electromyography (SFEMG) was developed to enable assessment of the microphysiology of individual motor units (Stålberg & Trontelj 1994b). If a nerve fibre is stimulated supramaximally and single fibre action potentials (SFAPs) recorded from a muscle fibre there is variability in the latency of the SFAP. This variability is termed *jitter*. *Jitter* may be due to variation in impulse transmission-time along the nerve fibre, variation in transmission-time across the neuromuscular junction (NMJ) and/or variation in impulse transmission-time along the muscle fibre.

6.1.1 Types of Jitter

Jitter may be voluntary or stimulated. In the former, *jitter* is measured in voluntarily activated muscle whilst in *stimulated jitter* a single motor axon is electrically stimulated. In *voluntary jitter* SFAPs are recorded from *two* muscle fibres innervated by the same motor axon. One of the SFAPs is used as a time reference *i.e.* to trigger recording and *jitter* is determined from the variability in the time (interpotential interval) between the two SFAPs. In *stimulated jitter* a single terminal motor axon is stimulated and a SFAP recorded from a *single* muscle fibre. In this case *jitter* is calculated from the variability between successive APs as described in Section 6.2. In a normal setting *stimulated jitter* is $\sqrt{2}$ lower than *voluntary jitter* (Stålberg 1990).

In *voluntary jitter* voluntary contraction results in low strength activation of muscle. This results in recruitment of low threshold small motor units, consisting mainly of Type I fibres (Trontelj, Stålberg, & Mihelin 1990). This can be used to assess the order of physiological recruitment of motor units, their dependence on afferent input

and their relation to fatigue (Trontelj & Stålberg 1992). Larger axons have lower thresholds for activation than smaller ones (Borg 1980). However, because of the high resistance of muscle, the distance of the axon from the stimulating electrode is thought to be more important in determining which fibres are activated. Therefore, *stimulated jitter* recruits low and high threshold motor units but predominantly Type II fibres (Trontelj, Stålberg, & Mihelin 1990).

Voluntary jitter requires the co-operation of the patient whereas *stimulated jitter* does not require active participation of the patient, and can be useful for young children, the unconscious and those with profound muscle weakness. Jerky muscle contractions can result in superimposition of APs from different motor units and result in erroneously high jitter levels (Trontelj, Stålberg, & Mihelin 1990). *Stimulated jitter* also enables *jitter* studies to be performed on animal models. *Stimulated jitter* was used in the work presented in this chapter.

In *voluntary jitter* variability may arise owing to the velocity recovery function of muscle (VRF). VRF is a phenomenon whereby the conduction velocity of muscle fibres is affected by a conditioning impulse (Mihelin, Trontelj, & Stålberg 1991). After an impulse there is an initial period of subnormal conduction velocity followed by a period of supernormal conduction velocity. The amplitude of the muscle fibre SFAP may also be reduced after a discharge. In a normal muscle fibre the conduction velocity may vary by 0.5% to 1% for consecutive discharges (Stålberg & Trontelj 1994b). In a pathological setting the effect of VRF may be much higher, partly because of the increased variability of the stimulation rate as a result of poorly controlled or jerky muscle contractions and also because of the increased VRF in abnormal muscle fibres (Trontelj, Stålberg, & Mihelin 1990). In a normal setting the variability of the interstimulus interval is minimised by providing patients with

auditory and visual feedback and asking them to maintain the rate of stimulation at a constant level. Trontelj *et al* investigated the effect of the rate of stimulation using different patterns (constant, 'physiological' and random) of direct muscle stimulation in normal human volunteers (Trontelj, Stålberg, & Mihelin 1990). They found that *jitter* was increased with the random pattern but not with the stimulation pattern designed to imitate the amount of variability seen in normal physiological activation of muscle fibres. They did not find a correlation with muscle fibre conduction velocity and the level of *jitter*.

VRF has no overall effect in the calculation of *stimulated jitter* because the same muscle fibre is stimulated at a constant rate (Trontelj et al. 1986). *Stimulated jitter* may therefore have an advantage over *voluntary jitter* in those situations where there may be a large VRF effect.

6.1.2 Levels of Jitter

It has been demonstrated that there is little variability in the conduction time of normal nerve and muscle fibres (Stålberg & Trontelj 1994a). Therefore, in a normal setting the main source of *jitter* is the NMJ. This variability is thought to arise from electrical membrane noise causing fluctuating thresholds for depolarisation of the muscle membrane and variation in the amplitude and gradient of the end-plate potential.

Abnormally low levels of *jitter* may be observed in *voluntary jitter* because of a branching muscle fibre (Stålberg & Trontelj 1994b). This means that no end-plate transmission is involved between the triggering impulse and the second AP. This phenomenon is occasionally seen in normal muscle but more commonly in association with muscular dystrophies. In *stimulated jitter*, direct stimulation of muscle fibres may result in abnormally low *jitter* values (Stålberg 1990). This is recognised by *jitter*

values less than 4μs as this is the amount of *jitter* associated with the normal NMJ. Summation of two or more single fibre potentials may result in a lower *jitter* level in the compound potential at least than in the higher of the two single APs. Stålberg *et al* ascribed this to the partial cancellation of variation in latency which changes in randomly alternating directions for each AP (Stålberg, Trontelj, & Mihelin 1992).

Stimulated jitter may be over-estimated by using threshold rather than supramaximal stimulation. Threshold stimulation can result in a variable stimulation rate introducing 'myogenic' *jitter* caused by VRF in muscle fibres (Trontelj, Stålberg, & Mihelin 1990). The selected rate of stimulation can also affect the level of *jitter*. Transmission at the NMJ is reduced at stimulation rates less than 2Hz whereas the amplitude of muscle fibre APs may decrease at stimulation rates above 20Hz (Trontelj & Stålberg 1992). Superimposition of two APs can result in erroneously high *jitter* measurements if the interfering peak has an innately higher *jitter* value or is not stimulated supramaximally (Stålberg, Trontelj, & Mihelin 1992).

Abnormally high levels of *jitter* are associated with pathological processes involving nerve conduction, NMJ transmission and muscle fibre conduction. *Stimulated jitter* studies have found abnormally high levels of *jitter* after peripheral nerve injuries (Lenihan et al. 1997); (Lenihan, Sojitra, & Glasby 1998). Several processes at the NMJ may result in increased *jitter* including a low mean amplitude of the end-plate potential (*e.g.* due to post-synaptic receptor resistance in myasthenia gravis), variation in the amplitude of the end-plate potential due to impaired acetylcholine release (*e.g.* botulism) and abnormal variation in the depolarisation threshold of the muscle fibre membrane (*e.g.* electrolyte abnormalities). As discussed previously pathological processes affecting muscle also cause increased *jitter* because abnormal conduction exacerbates the effect of VRF (Mihelin, Trontelj, & Stålberg 1991).

6.1.3 Calculation of Stimulated Jitter

S*timulated jitter* is a single fibre electromyographic technique: in *stimulated jitter* a single terminal motor axon is stimulated and action potentials recorded from a single muscle fibre using a single-fibre (SFEMG) needle. This single-fibre needle consists of an inner thin platinum or silver wire and an outer steel cannula, separated by a layer of insulation. The inner wire is the recording electrode and the outer steel cannula is the reference electrode. The recording electrode is exposed, through a window in the casing, 1mm to 5mm from the needle tip, opposite the side of the bevel, to avoid recording from muscle fibres which may be damaged by insertion of the needle.

Two monopolar needle electrodes are used to stimulate a terminal motor axon one hundred times using constant current rectangular pulses of 10Hz frequency and 50μs duration. The latencies of the resulting action potentials from an associated muscle fibre are recorded using a single fibre needle. The rising edge of the stimulus pulse is used to trigger recording. Each latency period is termed an interpotential interval (IPI). The variability between these IPIs is the *jitter* value or mean consecutive difference (MCD) and is calculated using the following equation:

$$MCD = \sum \left(\frac{(IPI_n) - (IPI_{n-1})}{n} \right)$$

Where:

MCD = mean consecutive difference (μs)

IPI = interpotential interval (ms)

n = number of stimulations

This process is repeated twenty times, with different sitings of the recording electrode in the muscle, as it has been shown that at least twenty fibres from a

particular muscle must be tested in this way to give a reliable result(Stålberg & Trontelj 1994b). These twenty results are then averaged to give a mean *jitter* value for a particular muscle.

6.2 EXPERIMENTAL SET-UP

A Medelec Synergy machine (Oxford Instruments, Surrey, UK) was used for all stimulating and recording procedures in the measurement of *jitter*.

6.2.1 Jitter Set-up in the Facial Nerve

The animal was positioned in the right lateral position, the tip of the left horn removed and the skin prepared as described in Section 3.1.1. A ground electrode was placed on the skin over the bony nasal bridge of the animal and connected to the preamplifier on the Medelec. Two monopolar stimulating needle electrodes were inserted into the zygomaticus muscle which is supplied by the facial nerve. The cathode was inserted into the motor point (previously defined in Section 3.1.2) and the anode (reference) electrode was placed 0.5cm proximal and superior to the cathode. The stimulating electrodes were connected to external stimulator A on the Medelec. It has been shown that the selectivity of stimulation is as important in the assessment of *stimulated jitter* as the selectivity of recording (Trontelj & Stålberg 1992). The use of intramuscular stimulating electrodes has an inherent advantage over direct stimulation of the nerve trunk because motor axons are more dispersed at this point and therefore, they are easier to stimulate in isolation.

The zygomaticus muscle was stimulated with constant current rectangular pulses of 10Hz frequency and 50μs duration. A frequency of 10Hz was selected as studies have shown that at very low frequencies (<2Hz) NMJ transmission may be reduced whereas at high frequencies (>20Hz) the amplitude of the AP of some muscle fibres decreases whilst the latency increases (Stålberg & Trontelj 1994a). A frequency of 10Hz is within the normal physiological rate of stimulation (6Hz - 20Hz) (Trontelj & Stålberg 1992). A stimulus duration of 50μs was used because the depolarisation

thresholds of axons in the vicinity of the stimulating cathode are more dispersed with short pulses (Trontelj, Mihelin, Fernandez, & Stålberg 1986). Therefore, it was easier to stimulate supramaximally a single axon using a short stimulus. Also it has been shown that this pulse-width does not generate additional *jitter* at the point of stimulation on the motor axon (Trontelj & Stålberg 1992).

The stimulus amplitude was gradually increased until the zygomaticus muscle was seen to be twitching. A single-fibre recording needle electrode was inserted into the area of muscle seen to be maximally contracting. The electrode was withdrawn slightly so the muscle 'gripped' the needle. This is thought to minimise movement artefact by steadying the needle.

The recording electrode was connected to the preamplifier on the Medelec. Muscle fibre action potentials were displayed on the monitor screen. The output of the preamplifier was also connected to a loudspeaker.

Studies have demonstrated the importance of supramaximal stimulation as lower levels of stimulation result in longer latencies of the APs and high levels of jitter (Stålberg & Trontelj 1994b). The stimulus amplitude was therefore increased until the there was no further reduction in latency or *jitter* values. This was between 2mA and 3mA.

Filters were used to improve the selectivity of the recorded signal. Muscle acts as a high frequency filter so that those signals from more distant fibres are of lower frequency (Kimura 1983). A low frequency filter of 500Hz was used to block these signals (Trontelj, Mihelin, Fernandez, & Stålberg 1986). The high frequency filter was set at 10kHz to minimise noise but maintain the higher frequency signals of those APs in close vicinity to the recording electrode (Stålberg 1990).

The position of the recording electrode was manipulated (by rotating it through 90 degrees) at a time until a sharp muscle fibre action potential, '*jitter* peak', was observed on the monitor screen. Isolation of an action potential was helped by listening to the output from the loudspeaker. When the recording electrode was near a contracting muscle fibre the rate and quality of the noise became more constant. The recording electrode was then maintained, as still as possible, in this position and one hundred consecutive APs were recorded. The peak for which a *jitter* value was to be calculated was selected by placement of a cursor, using a mouse control, across both the upslope and the downslope of the peak. The corresponding *jitter* value was calculated by the Medelec for each set of APs using the formula described in Section 6.1.3.

In some cases more than one *jitter* peak was seen on the screen. The *jitter* values for these peaks could be calculated be choosing 'New pair' from the control panel and repositioning the cursor across the next selected peak.

A study measuring stimulated *jitter* in normal human subjects found that *jitter* values had a bimodal distribution (Trontelj, Mihelin, Fernandez, & Stålberg 1986). The first peak of lower jitter values (<5μs) was thought to arise from direct stimulation of muscle fibres and the second peak (>5μs) from indirect stimulation of muscle fibres via terminal motor axons. Therefore, in this study, APs with latencies less than 5μs were rejected.

The electrode was withdrawn and reinserted into the muscle in a different position after three recordings. This was to decrease the chance of recording from the same muscle fibre. The *jitter* values of twenty muscle fibres were calculated. These were averaged to give a mean *jitter* value for the muscle.

6.2.2 Jitter set-up in the Median Nerve

The animal was positioned and the skin prepared as described in Section 3.2.2. The ground electrode was placed on the lateral wall of the right side of the chest of the animal and connected to the preamplifier on the Medelec. Two monopolar stimulating electrodes were inserted into flexor carpi radialis (FCR) which is supplied by the median nerve. The cathode needle-electrode was inserted into the motor point of FCR (located as described in Section 3.1.2) and the anode (reference) electrode 0.5cm proximal to this. The electrodes were connected to external stimulator A on the Medelec. The muscle was stimulated with constant current pulses of 10Hz frequency and 50μs duration as described for the facial nerve procedure. The same filters were also selected (low frequency filter of 500Hz, high frequency filter of 10kHz).

The stimulus amplitude was gradually increased until the muscle was seen to be twitching. A single-fibre recording needle electrode, connected to the preamplifier on the Medelec, was inserted into the area of the FCR muscle seen to be maximally contracting. The stimulus amplitude was increased until the there was no further reduction in latency or *jitter* values. As for the facial nerve experiments, this was between 2mA and 3mA. The recording electrode was manipulated by rotating it to obtain sharp muscle fibre APs or *jitter peaks* on the monitor screen. It was then held still in this position and one hundred APs were recorded. The *jitter* value was calculated by the Medelec using the equation described in Section 6.1.3. The electrode was repositioned after every three sets of recordings. Twenty sets of recordings were made and a mean *jitter* value for the muscle was calculated.

6.3 FACIAL NERVE RESULTS FOR JITTER

The raw data for *jitter* results are shown in Appendix 2. *Jitter* values for the facial nerve were normally distributed. A one-way ANOVA test did not reveal between-groups variation therefore *post hoc* tests were not performed. The mean *jitter* values for each experimental group are shown in Table 6.1.

Despite the fact that there were no significant differences between the mean *jitter* values of the groups there was an obvious difference in the pattern, on the monitor screen, of muscle fibre APs between the normal control group and the experimental groups with the exception of the neurapraxia group. More jitter peaks were observed for those nerves which had undergone Wallerian degeneration. No blocking (failure of impulse transmission) was seen for any of the experimental groups. Another phenomenon which was occasionally observed was the gradual decrease in amplitude of a *jitter* peak. There was no obvious difference in the occurrence of this phenomenon between the control groups and the nerve injury groups.

6.4 MEDIAN NERVE RESULTS FOR JITTER

The raw data for the *jitter* results are shoen in Appendix 2. *Jitter* values for the median nerve were normally distributed. A one-way ANOVA test revealed between groups variation. However, when pairs of experimental groups were compared using the Scheffé test no significant differences were found. Although not of statistical significance the nerve graft group had the highest mean *jitter* value (10.45) and the normal control group had the lowest mean *jitter* value (8.52). The mean *jitter* values for each experimental group are shown in Table 6.1.

The pattern of the muscle fibre APs for the median nerve experiments was similar to that observed for the facial nerve experiments. Again, more spikes were seen on the screen for the nerve injury models (except the neurapraxia group) than the normal control group. Particular difficulty was experienced in obtaining discrete *jitter* peaks in the nerve graft group. Occasionally a decrease in amplitude of a jitter peak was seen but there were no incidences of blocking in those peaks which were measured.

Mean *jitter* values (μs)						
	Normal	Neura	Axono	Neurotmesis & suture	Neurotmesis & wrap	Graft
Facial nerve [SD]	8.6 [1.5]	9.7 [0.7]	8.5 [0.7]	8.5 [0.8]	8.7 [1.3]	9.1 [1.5]
Median nerve [SD]	8.5 [1.0]	10.2 [1.5]	10.1 [0.6]	10.2 [0.7]	9.6 [1.3]	10.4 [1.2]

Table 6.1 This table shows the mean *jitter* values for each experimental group for the facial nerve and the median nerve.

6.5 COMPARISON OF FACIAL NERVE & MEDIAN NERVE RESULTS FOR JITTER

Jitter values for the facial nerve experimental groups and the median nerve experimental groups were compared. A normal probability plot was constructed of the raw residual values for both nerves. The data were shown to be normally distributed as they lay along a straight line. Factorial ANOVA was performed to detect the presence of between groups variation. Factorial ANOVA was used as there were two independent grouping variables (type of nerve and experimental group). No significant differences were found when both the nerve and the experimental group were considered.

6.6 DISCUSSION

Peripheral nerve injury, more severe than neurapraxia, results in Wallerian degeneration, failure of the NMJ and muscle fibre denervation. Initial conduction block is due to decreased acetylcholine (ACh) synthesis because of decreased amounts of cholinacetyltransferase, reduced release of ACh because of destruction of active zones and decreased excitability of nerve terminals (Stålberg 1990). Failure of the NMJ leads to hypersensitivity of the muscle membrane to ACh and the development of extra-junctional receptors (Wiechers 1990). This is associated with an increase in membrane resistance and a decrease in the resting membrane potential of muscle fibres (Sunderland 1978). These changes are thought to arise from a lack of neurotrophic factors from the injured nerve (Sunderland 1978).

EMG studies on denervated muscle are characterised by positive sharp waves, fibrillation potentials and complex repetitive discharges (Kimura 1983). Fibrillation is the spontaneous activity which arises in denervated muscle. It continues whilst the contractile elements are still active. Complex repetitive discharges may be caused by ephaptic activation of muscle fibres by the action potential of an adjacent fibre (Stålberg, Trontelj, & Mihelin 1992). SFEMG can detect fibrillation potentials and spontaneous depolarisation of single muscle fibres of denervated muscle. In *stimulated jitter* studies on denervated muscle, a gradual increase of the stimulus strength results in a shortening of the latency of the APs (Stålberg, Trontelj, & Mihelin 1992). This is attributed to the presence of low-threshold stimulation sites, as mentioned previously, along the muscle fibre membrane.

Reinnervation of muscle results from outgrowth of new motor axons or sprouting of axons from adjacent intact fibres. When pioneering axons make contact with muscle

this results in a decrease in ACh sensitivity, closure of extra-junctional receptors and formation of new end-plates (Sunderland 1978). These immature NMJs are inherently unstable resulting in increased variability in the time of impulse transmission (Stålberg & Trontelj 1994b). The end-plates mature over a period of six months (Wiechers 1990).

In normal muscle, fibres supplied by a single motor unit are not adjacent to each other. This facilitates smooth muscle contraction and less intense areas of depolarisation. As a result of this, in normal muscle, single-fibre needles record between one to three muscle fibre Aps (Kimura 1983). This was the pattern seen in the normal control group and the neurapraxia group. However, in more severe nerve injuries which result in Wallerian degeneration and subsequent muscle reinnervation, there is a change in the distribution of the motor unit (Wiechers 1990). In this case adjacent muscle fibres may be part of the same motor unit. The overall size of the motor unit is relatively unchanged but the density of fibres is increased. Fibre density increases as reinnervation of muscle progresses and stops when this process is complete. This is the first process of reinnervation which can be detected with SFEMG. The single-fibre needle electrode may record a higher number of muscle fibre APs as adjacent fibres are supplied by the same terminal motor axon. In the measurement of *jitter* this as seen as multiple *jitter* peaks on the monitor screen.

Fibre density was not formally assessed in this work as these experiments were designed to investigate the final outcome of nerve injuries rather than the process of muscle reinnervation. Furthermore, a general anaesthetic would have been required to allow measurement of fibre density and according to the Home Office licence for these experiments would therefore have had to be a terminal procedure. However, as mentioned in the previous section, it was clear from the increased number of *jitter*

peaks observed on the monitor screen, during the examination of those animals with the models of nerve injury (other than neurapraxia), that reconfiguration of motor units had occurred.

The nerve graft group in particular had a large number of smaller peaks some of which may have resulted from extradischarges. Extradischarges are additional muscle fibre discharges occurring after the primary AP (Stålberg, Trontelj, & Mihelin 1992). They arise from ectopic sites on axons or muscle fibres and are more dispersed and of lower amplitude than the primary AP.

Another phenomenon seen early in the process of reinnervation is 'blocking'. This commonly arises from failure of impulse transmission at the branching point of an immature axonal sprout from its parent axon (Stålberg & Trontelj 1994b). If the axonal sprout divides distal to this, this can result in concomitant blocking. Concomitant blocking is rarely seen in normal muscle and is an indication of intermittent impulse transmission in the terminal motor axon (Stålberg 1990). With maturation of the terminal axons and the NMJs blocking disappears. Blocking was not observed in any of the measured *jitter* peaks in any of the experimental groups for the facial nerve or the median nerve. This would suggest that the process of reinnervation in the nerve injury groups was mature.

Another phenomenon which was occasionally observed was the gradual decrease in amplitude of a *jitter* peak. Trontelj *et al* observed a similar occurrence in a *stimulated jitter* study on the extensor digitorum muscle in normal human volunteers (Trontelj, Mihelin, Fernandez, & Stålberg 1986). They found this process happened gradually with prolonged stimulation at 10Hz (the frequency used in the present experiments) and more quickly at higher stimulation rates. They attributed it to activation of muscle fibres by ephaptic transmission from other fibres. In the work presented here there

was no obvious difference in the frequency of this phenomenon among the control groups and the nerve injury groups.

Jitter levels are increased after nerve injury (Lenihan, Sojitra, & Glasby 1998; Wiechers 1990). As discussed previously, this may arise from variable axon and muscle fibre conduction velocity and instability of immature NMJs. In the early stages of reinnervation, *jitter* may be stimulation-rate dependent, usually increasing with increasing frequency of stimulation (Stålberg 1990). Concomitant jitter and blocking may also occur. This may be due to ephaptic activation of a muscle fibre or by recording from two branches of a split muscle fibre (Stålberg, Trontelj & Mihelin 1992). Ephaptic activation is suspected when the jitter and blocking are unaffected by increasing the stimulus strength but disappear on increasing the stimulation frequency. *Jitter* levels decrease as reinnervation progresses. Several isolated cases of peripheral nerve injuries in humans are described in the literature which report increased levels of *jitter* in the early period after injury which later return to normal (Wiechers 1990). Lenihan *et al* transected the sciatic nerve in the rat model and performed an epineurial end-to-end suture repair (Lenihan et al. 1997). They measured stimulated *jitter* levels 14, 30, 60, and 90 days after surgery. Initial *jitter* values were high but progressively declined with time from surgery to lie within normal limits. These workers proposed that *jitter* was a useful tool to monitor progress after peripheral nerve injury and/or surgery.

The distance over which the nerve must regenerate, the extent of the nerve injury and the number of suture lines which the pioneering axons must cross, have all been shown to affect the timing of muscle reinnervation (Sunderland 1978). The site of injury (and hence the distance of axonal regeneration) was the same for all the facial nerve cases and similarly for all the median nerve cases. However, the extent of the

injury obviously varied among the different models as did the number of suture lines. Therefore, it might be expected that the nerve graft models would take longer to regenerate and mature than the other injuries. If the process of reinnervation were incomplete in one (or more) of the experimental groups it would be invalid to compare them with those groups where the process was complete.

Lenihan *et al* performed further experiments on *stimulated jitter* assessing levels of jitter after different types of nerve repair (Lenihan, Sojitra, & Glasby 1998). As before they transected the sciatic nerve of the rat. In the first group they performed a direct end-to-end epineurial suture repair, in the second they used a nerve autograft and in the third they used a freeze-thawed muscle graft. *Stimulated jitter* was measured ninety days after surgery. The results were compared to a normal control group. There was no significant difference between the normal control group, the end-to-end sutured repair group and the nerve graft group. However, the muscle-graft group had a statistically significant, higher jitter result than the other groups. The authors concluded that this group had not formed mature NMJs and attributed this to a slower rate of nerve regeneration.

Based on the results of the experiments of Lenihan *et al*, *stimulated jitter* was used in this work to assess first whether the process of nerve regeneration and muscle reinnervation had been successful and secondly whether the process was finished. In this work there were no significant differences in the *stimulated jitter* values between the facial nerve groups or between the median nerve groups. This was taken as evidence that the process of reinnervation had been successful *and* was complete in all cases. Therefore, it was valid to compare measurement of different nerve and target muscle function between the different experimental groups.

7 MAXIMUM CONDUCTION VELOCITY

7.1 THEORY

Conventional measurement of the maximum conduction velocity (CV_{max}) of a nerve reflects the velocity of the fastest conducting axons. In a motor nerve this is only 5% of the total population of motor neurons (Dorfman, Cummins, & Abraham 1982). Despite this, measurement of CV_{max}, in clinical practice, provides an objective, non-invasive and reliable test of nerve function. This is partly because many disease processes affect all nerve fibres uniformly or predominantly affect the faster fibres. CV_{max} is used both as a diagnostic tool and to monitor progress after surgical repair.

Conduction velocity is affected by many different factors both anatomical (fibre diameter, myelin sheath thickness, internodal length and nodal properties) and physiological (temperature, age and the surrounding environment of the nerve). These factors will be considered below.

In general, there are two types of study to investigate the factors affecting nerve conduction velocity. The first is the experimental study. This approach has the advantage of providing experimental data directly derived from nerve fibres. The disadvantage of this type of study is the covariance of some of the variables investigated, for example fibre diameter and myelin sheath thickness. The second type of study is theoretical. This uses computer programme simulations based on mathematical models and has the advantage that it permits a consideration of the different parameters affecting the variables which might be measured. The disadvantage of this type of study is that it is based on a set of assumptions, often from submammalian studies, regarding the properties of the nerve.

7.1.1 Fibre Diameter

Several experimental studies have shown that for 'geometrically similar' myelinated fibres, CV_{max} is almost proportional to fibre diameter (Waxman 1980). Hursh demonstrated in a variety of kitten and adult cat nerves that the maximum conduction velocity of a nerve could be predicted by multiplying the diameter of the largest fibre (in microns) by six (Hursh 1939). In other experiments on nerves from the hind limbs of cats, Boyd found that the ratio between fibre diameter and conduction velocity was lower for γ fibres than for α fibres. He also distinguished two sets of γ fibres, histologically (thickly and thinly myelinated fibres) and electrophysiologically (fast and slow fibres). The multiplication factors he derived for conversion of fibre diameter (μ) to conduction velocity (m s^{-1}) were 5.6 for α fibres, 4.4 for fast γ fibres and 4.5 for slow γ fibres (Boyd 1964). Although these are different from these determined by Boyd they support the argument that for geometrically similar fibres CV_{max} is proportional to fibre diameter. Computer simulated studies have also confirmed the proportional relationship between fibre diameter and conduction velocity (Goldman & Albus 1968; Rushton 1951).

7.1.2 Myelin Sheath Thickness

The ratio of axon diameter to the overall fibre diameter is termed the 'g ratio'. The g ratio may therefore be regarded as an expression of myelin sheath thickness for a given axon diameter. Conduction velocity is affected by myelin sheath thickness (Smith & Koles 1970). Many studies have been carried out on this area and there is general agreement that conduction velocity is optimised at a g ratio between 0.6 and 0.7 (Goldman & Albus 1968; Moore et al. 1978; Rushton 1951; Smith & Koles 1970).

This value is generally observed in normal peripheral nerves (Goldman & Albus 1968). Brill *et al* found that myelin sheath capacitance as well as thickness affected conduction velocity (Brill et al. 1977).

7.1.3 Internodal Length

Early studies on internodal length and conduction velocity did not demonstrate an obvious relationship between the two variables. In experiments on the nerve to semitendinosus in the cat Coppin and Jack demonstrated a non-linear relationship between internodal length and conduction velocity (Coppin & Jack 1971). The relationship was linear on a semi-logarithmic plot.

Goldman and Albus suggested there was an optimal internodal length for a given fibre diameter and that this length was usually observed in normal peripheral nerves (Goldman & Albus 1968). Using computer simulation techniques Brill *et al* showed the optimal internodal length to be a ratio of internodal length to axon diameter of between 100 and 200 (or an internodal length between 1000μm to 2000 μm in normal peripheral nerves) (Brill, Waxman, Moore, & Joyner 1977). Fibres with internodal lengths around this range were shown to be relatively insensitive to changes in internodal length as there was optimal conduction over a broad range of values. Internodal length did not impinge on conduction velocity until it was less than half its normal value. This may explain why earlier workers failed to find a correlation between these two parameters. Those fibres with a small internodal length to axon diameter ratio were more sensitive to changes in internodal length (Koles & Rasminsky 1972). In these experiments internodal lengths of less than 1000μm correlated with a significant decrease in conduction velocity. Conversely if the internodal length was too long, failure of propagation of the action potential was observed.

7.1.4 Nodal Properties

In a simulated model Moore *et al* found conduction velocity to be relatively insensitive to changes in nodal capacitance, conductance and area (Moore et al. 1978). They suggested that this explained why internodal properties as oppose to nodal properties were altered (as compared to normal fibres) in those central axons which function as delay systems. In another simulated study, Koles and Rasminsky found that conduction velocity was more sensitive to 'paranodal' demyelination than uniform internodal demyelination (Koles & Rasminsky 1972).

7.1.5 Age

In newborn infants motor conduction velocity is around 27m s^{-1} (Johnson & Olsen 1960). A study on human ulnar nerves showed the highest conduction velocities in young adults but these values could be achieved at the age of four to five years (Wagman & Lesse 1952). This correlates with the histological studies which showed that fibres in the ventral roots of the lumbar and sacral regions reach adult size between the ages of two to five years (Waxman 1980). As discussed previously conduction velocity is proportional to fibre diameter.

Conduction velocity has been shown to decrease after the age of sixty (Waxman 1980). This may be as a consequence of selective degeneration of the fastest fibres, decreased oxygen supply with consequent slower metabolism in neurons or lower temperature of the nerves in the forearm. Norris *et al* performed another motor nerve conduction study on human ulnar nerves (Norris & Wagman 1953). They also found that conduction velocity decreases with age. However, they proposed that this was more likely to be due to vascular changes in the nerve trunk and altered metabolism

which resulted in changes in membrane properties such as permeability rather than to selective degeneration of fibres or to an altered temperature gradient.

7.1.6 Surrounding Environment

Several experimental studies have shown a linear relationship between conduction velocity and temperature. Johnson and Olsen described a change in conduction velocity of 5% per degree centigrade (Johnson & Olsen 1960). Other studies have shown a decrease in motor conduction velocity of 2.4m s-1 per degree between 38°C and 29°C (de Jesus, Hausmanowa-Petrusewicz, & Barchi 1973). de Jesus *et al* looked at the relationship between human limb temperature and conduction velocity. They found a Q_{10} of 1.51 for both sensory and motor fibres (de Jesus, Hausmanowa-Petrusewicz, & Barchi 1973). Computer simulations also confirm an increase in conduction velocity with an increase in temperature (Moore et al. 1978). Other factors in the environment surrounding a nerve can also affect conduction velocity. For example, phenytoin therapy and haemodialysis can transiently affect conduction velocity (Waxman 1980).

7.2 MEASUREMENT OF MAXIMUM CONDUCTION VELOCITY

The latency measured when a motor nerve is stimulated and its corresponding CMAP recorded consists of three components; the time for nerve conduction from the stimulus point to the nerve terminal, the time for transmission across the neuromuscular junction (NMJ) and the time for muscle excitation. Stimulating the nerve at two different points and subtracting the resulting latencies effectively cancels out the time for transmission across the NMJ and the time for muscle excitation, as these are the same in both cases. By measuring the distance between the two points of stimulation the maximum conduction velocity for that segment of the nerve can be calculated.

7.2.1 Facial Nerve Experimental Set-up

The unipolar ground electrode was positioned on the bony nasal bridge. Surface recording electrodes were placed over the zygomaticus muscle. The cathode was positioned over the motor point and the reference electrode 1cm distally. The motor point is the area of muscle where contraction of that muscle may be elicited with minimal-intensity, short duration electrical stimulation. Anatomically it corresponds to the location of the terminal portion of the motor nerve fibres (Kimura 1983). Efficacy of conduction was improved with a small amount of electrode cream.

The facial nerve was exposed as previously described in Section 3.1.2. Bipolar stimulating electrodes (proximal anode and distal cathode) held in position by means of a plastic casing. The casing also served to isolate thenerve from the underlying tissue. The electrodes were positioned on the nerve so that one electrode, S1, lay proximal to the site of nerve injury and the other electrode, S2, lay distal to the site of nerve injury. S1 was connected to 'stimulator B' on the Medelec machine and S2 was connected to 'stimulator A'.

7.2.2 Median Nerve Experimental Set-up

In the median nerve experiments the unipolar ground electrode was positioned on the right lateral chest wall. The surface recording electrodes were placed over flexor carpi radialis (FCR), the cathode over the motor point and the reference electrode distally over the tendon. The median nerve was exposed and the ulnar nerve divided as described in Section 3.2.2. Stimulating electrodes were positioned in relation to the site of injury and connected to the Medelec machine as described for the facial nerve.

7.2.3 Calculation of Maximum Conduction Velocity

The stimulating and recording electrodes were set up as described in the previous section. The sweep speed of the Medelec screen was set at 20ms fsd, with a gain of 2mV per division. These settings were altered if necessary to obtain an optimal trace.

The nerve was initially stimulated at S1 by means of stimulator B using square wave impulses of 50μs at a frequency of one pulse per second. Constant-current stimulation was used, as oppose to constant-voltage stimulation, as it provides a more consistent stimulus (Kimura 1983).

The amplitude of the current was gradually increased until the zygomaticus muscle in the case of the facial nerve or the FCR muscle in the case of the median nerve was noted to be twitching and a CMAP, termed M1, was observed on the Medelec screen. The intensity of the current was increased further until the amplitude of M1 no longer increased. This current is known as the maximal stimulation current. Further stimulation was carried out with a supramaximal current, 30% greater than this level, to ensure activation of all axons innervating the muscle (Kimura 1983). It has been shown that fast fibres with a large diameter have a lower threshold for excitation than thinner, slower fibres (Borg 1980). Other studies have shown that slower fibres are only recruited at relatively high stimulus levels (Cummins & Dorfman 1981). The same procedure was carried out for the distal stimulus, S2, and its resultant CMAP, M2. The latency from the upstroke of the stimulus artefact to the take-off point from the baseline was measured for M1 and M2. The distance between S1 and S2 was measured and the segment velocity of the nerve calculated using the following formula:

$$CV_{max} = \text{distance S1 to S2} / (\text{latency M1} - \text{latency M2})$$

7.3 FACIAL NERVE RESULTS FOR MAXIMUM CONDUCTION VELOCITY

In the measurement of CV_{max} care was taken to ensure both stimuli were supramaximal. Lower levels of stimulation can result in partial activation of the nerve, an altered profile of the resultant CMAP and inaccurate measurement of CV_{max}. In most of the experimental groups the proximal site (S1) required a slightly higher stimulus than the distal site (S2). In the graft group, especially high levels of current were required (100mA) and this resulted in problems with direct stimulation of muscle surrounding the electrode. Particular care was therefore taken in these cases to isolate the proximal electrode from surrounding structures. The parotid gland was avoided when dissecting the proximal portion of the facial nerve and no problems were encountered with parotid gland secretions causing hyperpolarisation of the nerve.

The raw data for these experiments are shown in Appendix 2. The results for maximum conduction velocity were found to be non-parametrically distributed. The Kruskal-Wallis test showed that there was significant between-groups variation. Mann-Whitney U tests were performed for pairs of experimental groups to calculate where those differences lay. The results are shown in Table 7.1. The significant results ($p<0.05$) are highlighted in red.

For the variable CV_{max} the normal control group had a significantly faster maximum conduction velocity than any of the groups containing models of nerve injury. The neurapraxia group had a faster mean conduction velocity than any of the other models of nerve injury. This difference was significant for the neurotmesis and suture-repair group ($p=0.037$) and the nerve-graft group ($p=0.045$) and just outwith statistical

significance for the axonotmesis group (p=0.054). There was no statistical difference between the two methods of nerve repair (i.e. the epineurial suture and entubulation) after transection of the nerve.

Power analysis (one way ANOVA) revealed CV_{max} to have a power of one. Figure 7.1 is a box and whisker plot of CV_{max} showing the median, the box indicates the 25^{th} to the 75^{th} percentiles and the whiskers the non-outlier range.

Facial Nerve: Mann Whitney U test CV_{max} / (m s^{-1})						
	Normal	Neurapraxia	Axonotmesis	Neurotmesis (suture)	Neurotmesis (wrap)	Graft
Normal		0.012	0.001	0.001	0.001	0.002
Neurapraxia			0.054	0.037	0.078	0.045
Axonotmesis				0.63	0.873	0.855
Neurotmesis (suture)					0.202	0.715
Neurotmesis (wrap)						0.465
Graft						
Mean [SEM]	71.31 [3.72]	51.53 [4.96]	38.28 [3.11]	35.43 [1.67]	38.00 [2.92]	36.54 [4.10]

Table 7.1 shows the results of the Mann-Whitney U test for *CVmax* for the facial nerve. The results are shown in Table 7.1. The significant results ($p<0.05$) are highlighted in red.

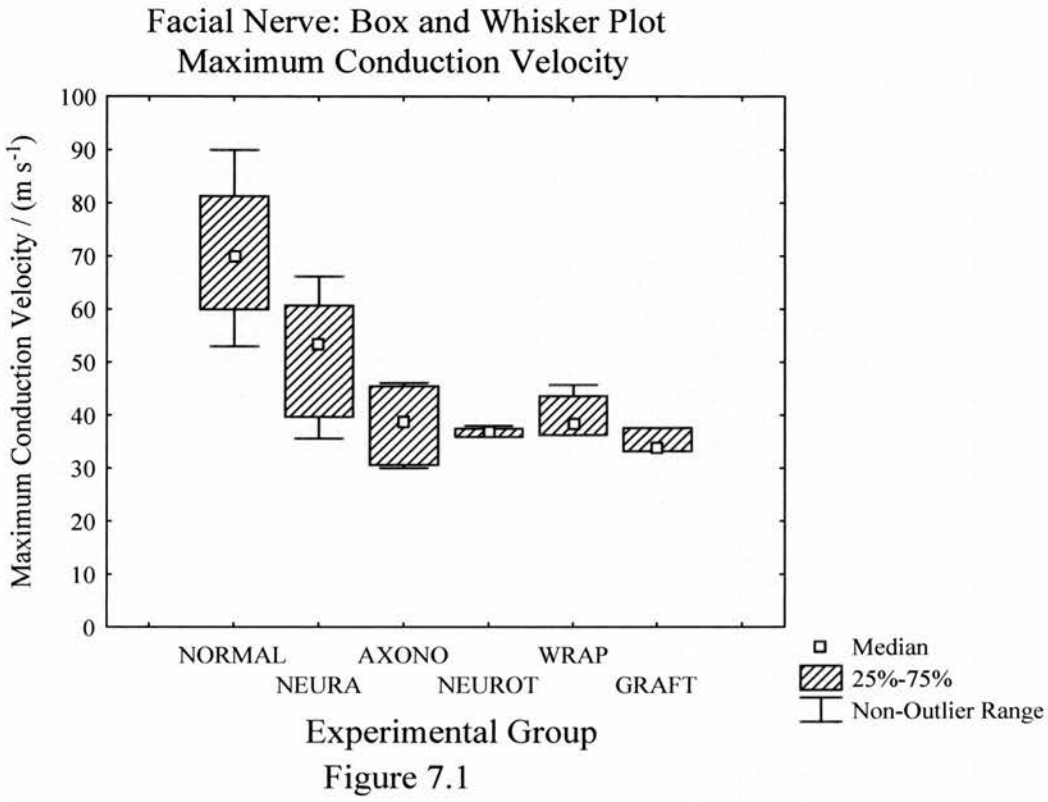

Figure 7.1

Figure 7.1 is a box and whisker plot of CV_{max} for the facial nerve showing the median value, the box indicates the 25th to the 75th percentiles and the whiskers the non-outlier range.

7.4 MEDIAN NERVE RESULTS FOR MAXIMUM CONDUCTION VELOCITY

Before measurement of CV_{max} was attempted in the median nerve the adjacent ulnar nerve was identified and divided. This was to avoid possible activation of the ulnar nerve by antidromic impulses from the median nerve activating motor neurons, in the spinal cord, destined for the ulnar nerve. In some cases a small branch of the median nerve was found proximally and this was also divided as it resulted in an aberrant CMAP trace.

Care was taken to ensure both proximal and distal stimuli were supramaximal. Again it was found that the normal control nerves and the more minor models of injury required lower levels of stimulation whereas the nerve-graft group required higher levels. Also the proximal electrode required higher levels of stimulation than the distal one.

Time was taken manipulating the cathode to locate the motor-point in order to achieve the optimal CMAP This was particularly difficult for the nerve graft group, especially for the proximal electrode trace.

The raw data for these experiments are shown in Appendix 2. The results for CV_{max} in the median nerve were normally distributed. One-way ANOVA revealed between-groups variation. Scheffé tests were performed for pairs of experimental groups to identify where those differences lay. The results are shown in Table 7.2. For the variable CV_{max} the normal control group exhibited faster conduction velocities than in all the other experimental groups. This difference was significant for all but the neurapraxia group. The nerves in the neurapraxia group conducted faster than those in the other models of nerve injury, that is, the axonotmesis model (p=0.177), the

neurotmesis and suture-repair model (p=0.001), the neurotmesis and wrap-repair (p=0.003) and the nerve-graft model (p=0.000). This difference was significant except for the axonotmesis group. There was no statistical difference between the two methods of nerve repair (i.e. the epineurial suture and entubulation) after transection of the median nerve. The nerve-graft group had the lowest mean CV_{max}.

Power analysis (one way ANOVA) revealed CV_{max} to have a power of one. Figure 7.2 is a box and whisker plot of CV_{max} showing the median, the box indicates the 25^{th} to the 75^{th} percentiles and the whiskers the non-outlier range.

Median Nerve: Scheffé test CV_{max} / (m s^{-1})						
	Normal	Neurapraxia	Axonotmesis	Neurotmesis (suture)	Neurotmesis (wrap)	Graft
Normal		0.993	0.033	0.000	0.000	0.000
Neurapraxia			0.177	0.001	0.003	0.000
Axonotmesis				0.446	0.602	0.206
Neurotmesis (suture)					0.999	0.992
Neurotmesis (wrap)						0.962
Graft						
Mean [SEM]	82.44 [4.99]	77.80 [5.24]	56.26 [3.38]	40.40 [2.99]	42.52 [2.52]	35.44 [9.01]

Table 7.2 shows the results of the Scheffé test for *CVmax* for the median nerve. The significant results ($p<0.05$) are highlighted in red.

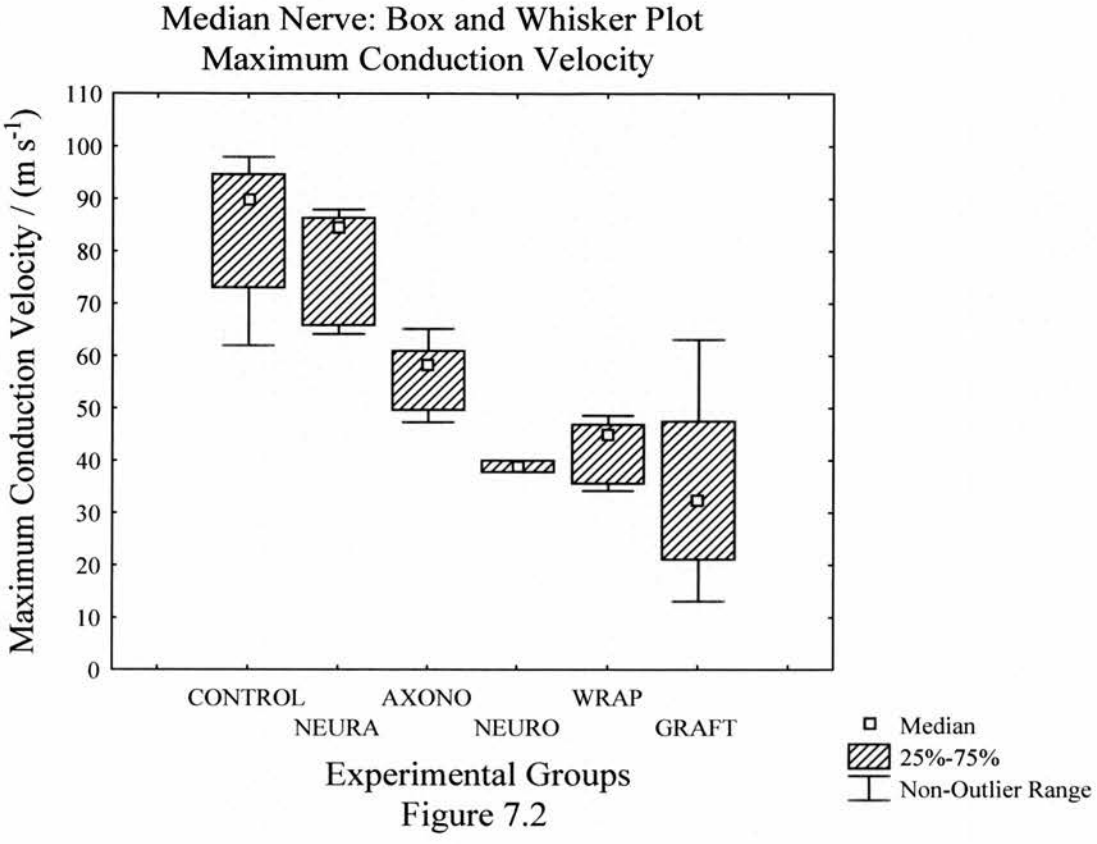

Figure 7.2

Figure 7.2 is a box and whisker plot of CV_{max} for the nerve showing the median value, the box indicates the 25th to the 75th percentiles and the whiskers the non-outlier range.

7.5 Comparison of Facial Nerve and Median Nerve Results

The CV_{max} results for the facial nerve experimental groups and the median nerve experimental groups were compared. A normal probability plot was constructed of the raw residual values for both nerves. This is shown in Figure 7.3. The data were shown to be normally distributed as they lay along a straight line. Factorial ANOVA was performed to detect the presence of between groups variation. Factorial ANOVA was used as there were two independent grouping variables (type of nerve and experimental group). No significant differences were found when both the nerve and the experimental group were considered (p=0.65). Figure 7.4 is a box and whisker plot which shows the mean values for each experimental group for both the facial nerve and the median nerve. Lines were drawn between the mean values (boxes) for each experimental group. It can be seen that the gradient of the line decrease with increasing severity of nerve injury, this is particularly the case for the transection injuries. Therefore, although not of statistical significance, the outcome after transection injuries is worse for the median nerve than the facial nerve.

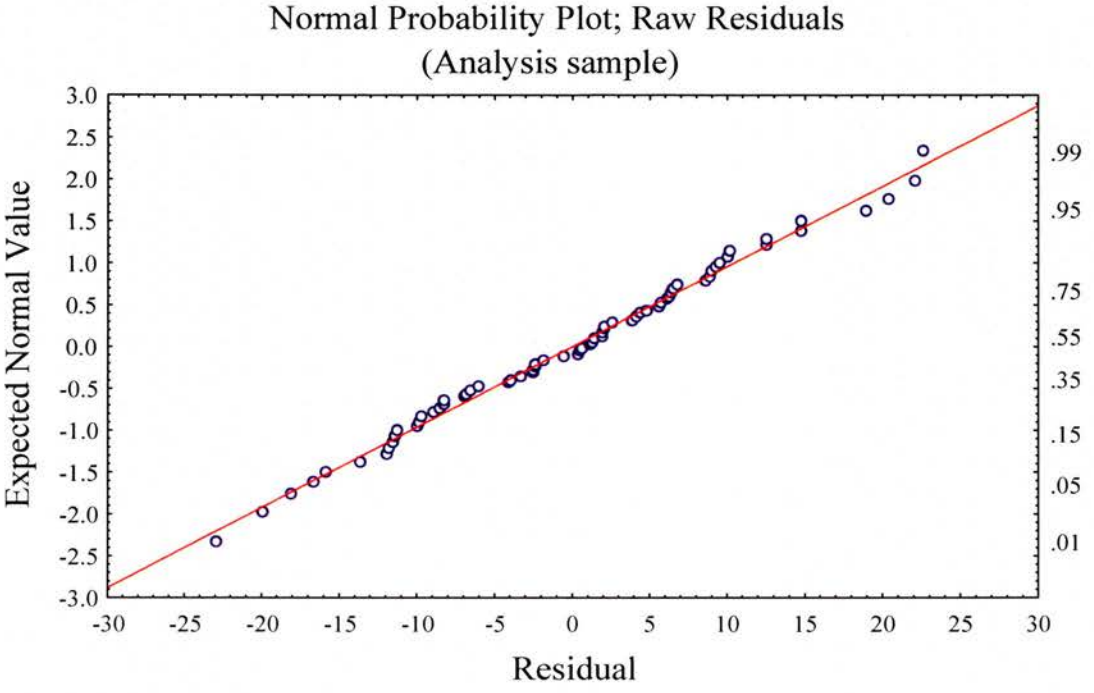

Figure 7.3

Figure 7.3 shows a normal probability plot constructed from the raw residual values for *CVmax* for both the facial nerve and the median nerve.

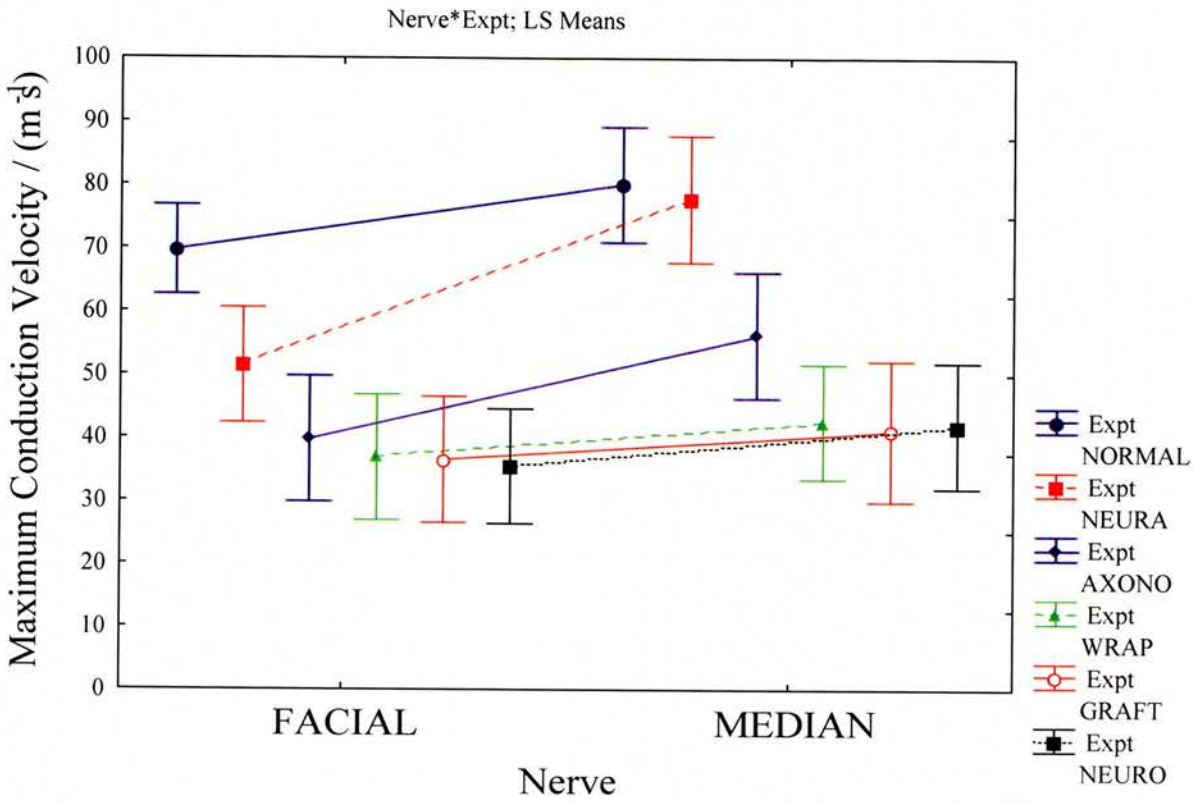

Vertical bars denote 0.95 confidence intervals

Figure 7.4

Figure 7.4 is a box and whisker plot which shows the mean values for each experimental group for both the facial nerve and the median nerve. Lines were drawn between the mean values (boxes) for each experimental group.

7.6 DISCUSSION

It has been demonstrated, and is now well accepted, that after peripheral nerve injury CV_{max} does not return to normal. Erlanger and Schoepfle crushed the VIth root of the phrenic nerve in the dog (the phrenic nerve in the dog is composed of the Vth, VIth and VIIth cervical nerves). They measured a reduction in CV_{max} of 40% compared with normal controls (Erlanger & Schoepfle 1946). Cragg and Thomas crushed the peroneal nerve in adult rabbits. In the regenerated nerves they observed a reduction in CV_{max} of 25% compared with normal controls (Cragg & Thomas 1964). In the distal nerve segment they measured a small reduction in fibre diameter, a normal g ratio and a reduction in internodal length of more than 50%. These workers did not think that the measured reduction in CV_{max} could be completely accounted for by the small decrease in fibre diameter but neither did they attribute it to the decrease in internodal length. However, as discussed above, computer simulations by Brill *et al* demonstrated that more than 50% shortening of the internode will affect conduction velocity (Brill et al. 1977).

In contrast to the findings of Erlanger and Schoepfle, and, Cragg and Thomas, Sanders and Whitteridge did not find a reduction in nerve conduction velocity after crush injuries to the peroneal nerve of the rabbit (Sanders & Whitteridge 1946). Cragg and Thomas pointed out that the conduction velocity in the control models in these experiments was relatively low (68m s^{-1} as oppose to 87.4m s^{-1} in their own series) and postulated that these measurements may have been taken in immature animals.

Berry *et al* transected the tibial, peroneal and saphenous nerves of cats and performed immediate epineurial suture repair. In these experiments CV_{max} was reduced by more

than 20% of the normal value (Berry, Grundfest, & Hinsy 1944). These authors also measured a reduction in diameter in the regenerated fibres of 20%.

The reduction in conduction velocity observed after nerve injury is due to a combination of factors including, a reduction in fibre diameter, reduced myelin sheath thickness and shortened internodal length (Waxman 1980). As discussed above, all these factors are related to conduction velocity. Gutman and Sanders looked at the effects on fibre number and diameter, in the peroneal nerve in rabbits, after crushing, nerve transection and immediate epineurial suture repair and nerve autografting. In the crush model there was restitution of normal numbers of fibres and fibre diameters. There was also a return of the normal toe-spreading reflex. However, in both the end-to-end-suture group and the nerve-autograft group both fibre numbers and diameters were reduced and the normal toe-spreading reflex was not regained. Furthermore in both these groups there was loss of the bimodal distribution in the fibre-diameter histogram although the authors did comment that all the distal stumps did contain some large diameter fibres (Gutmann & Sanders 1943).

In these series of experiments the velocities of the normal control groups for both the facial nerve and the median nerve were significantly faster than those of all the other experimental groups with the exception of the median nerve neurapraxia group. These findings are in agreement with the above studies of Erlanger and Schoepfle, Cragg and Thomas and Berry *et al.* Table 7.3 shows the mean CV_{max} for each experimental group expressed as a percentage of the mean CV_{max} of the normal control group for both the facial and the median nerve.

	Neurapraxia	Axonotmesis	Neurotmesis (Suture)	Neurotmesis (Entubulation)	Graft
Facial nerve: % of normal CV_{max}	72%	54%	50%	53%	51%
Median nerve: % of normal CV_{max}	94%	68%	49%	52%	43%

Table 7.3 shows the mean CV_{max} for each experimental group expressed as a percentage of the mean CV_{max} of the normal control group for both the facial and the median nerve.

The distinction between the neurapraxia group and the axonotmesis group as compared to the other experimental groups is that the endoneurial tubes remain intact. The neurapraxia group does not undergo Wallerian degeneration and after axonotmesis, pioneering axons should grow down the original endoneurial tubes and reinnervate the original target organs. Transection injuries inevitably result in more disruption of the endoneurial tubes. The probability of mismatching at the site of injury will depend on the ratio of the number of pioneering axons as compared to the number of endoneurial tubes. However, in a mixed nerve the probability of reaching the wrong sort of target organ will be increased.

When the velocities of the neurapraxia group and the axonotmesis group were compared there were no significant differences between the groups for either nerve although the mean values were higher for the neurapraxia group. However, the neurapraxia group conducted significantly faster than all of those groups which had

undergone transection injuries with the exception of the median nerve wrap group. There was no significant difference between the axonotmesis group and the transection injury groups although, the mean conduction velocities were higher in the axonotmesis groups for both nerves. These findings suggest that the integrity, or otherwise, of endoneurial tubes influences outcome after nerve regeneration. Unfortunately most nerve injuries encountered in clinical practice are transection injuries.

When the transection injuries were compared, there were no significant differences in conduction velocities between the three groups for either nerve. Interestingly there was no difference in outcome between standard epineurial-suture repair and entubulation after simple transection of the nerve. There were no incidences of 'pull-out' of the repair, increased wound infection or 'foreign-body' reaction with the glass wrap model.

In the facial nerve the models of transection injury regained about 50% of the conduction velocity in the normal control group (neurotmesis and suture group 50%, neurotmesis and wrap repair group 51%, nerve graft group 51%). Similar results were obtained for the median nerve neurotmesis and suture-repair group (49%) and the wrap-repair group (52%) but the result for the graft group was worse (43%). Thus it would appear that the presence of two suture lines has a relatively more detrimental effect on the median nerve as opposed to the facial nerve.

Table 7.4 shows the mean conduction velocity for each of the facial nerve experimental groups expressed as a percentage of the corresponding median nerve group.

	Normal	Neura	Axono	Suture	Wrap	Graft
Facial nerve vs median nerve (%)	86%	66%	68%	88%	89%	100%

Table 7.4 shows the mean conduction velocity for each of the facial nerve experimental groups expressed as a percentage of the corresponding median nerve group.

From these results it can be seen that the normal median nerve conducts faster than the normal facial nerve. The facial nerve does relatively poorer in the neurapraxia and axonotmesis groups. This may be a function of the models of injury. The facial nerve is thinner than the median nerve and may have been more damaged. For the transection injuries both nerves only regain around 50% of the normal conduction velocity. The outcome for the median nerve graft group is worse. It only regains 43% of normal conduction velocity. By comparison the facial nerve has regenerated better and has the same mean conduction velocity as the median nerve. Therefore it would appear that the median nerve is more disrupted by the second suture line involved in the nerve graft than the facial nerve. This is shown in Figure 7.4. This figure shows the mean value and data range for CV_{max} for the facial and median nerves. Lines have been drawn between the mean values for corresponding experimental groups. There is an obvious decrease in the gradient of the line for the transection injuries.

All nerve injuries, with the exception of neurapraxia, resulted in decreased nerve conduction velocity. The conduction velocity in regenerated nerves after transection injuries was reduced by 50%. There was no difference in outcome between the two methods of repair (endoneurial suture and entubulation with glass wrap) after transection of both the facial and the median nerves. In the transection injuries, the

median nerve groups had a poorer outcome than the equivalent facial nerve groups. These results demonstrate that the integrity of the endoneurial tubes has a strong influence over the outcome of nerve injury and repair, and that this effect is more marked for the median nerve the facial nerve.

8 DISTRIBUTION OF MOTOR CONDUCTION VELOCITIES (DCV)

8.1 INTRODUCTION

Measurement of the distribution of conduction velocities (*DCV*) in a peripheral nerve is a technique whereby the individual conduction velocities of a range of fibres within a nerve are calculated. DCV can be measured for motor, sensory and mixed nerves. It may be regarded as the electrophysiological counterpart of the morphological fibre-diameter histogram which historically has been regarded as the 'gold-standard' investigation in the study of peripheral nerve injury and regeneration.

Conventional measurement of maximum conduction velocity (*CVmax*) is an assessment of only the faster fibres within a nerve. In motor studies these constitute only 5% of the total number of fibres (Dorfman, Cummins, & Abraham 1982). Despite the small proportion of fibres which *CVmax* assesses, the test is remarkably useful in a clinical setting. This is because many conditions affect nerve fibres uniformly or predominantly affect the fastest fibres. However, some disease processes affect fibres non-uniformly (diabetes mellitus, amyloid polyneuropathy, hereditary sensory neuropathy) and studies have demonstrated an abnormal *DCV* profile when *CVmax* remains within normal limits (Brown, Martin, & Asbury 1974; Dorfman 1984). Therefore, study of alterations in the DCV profile may provide a more sensitive and specific alternative investigation to simple nerve conduction studies.

To date much of the published literature in this area has concentrated on the different methods to calculate DCV and the effect of various neuropathies and environmental factors (age, temperature, lead poisoning) on the DCV profile. Most studies have been performed on human volunteers or used computer simulations.

The work presented in this chapter was an investigation of the effect of different types of injury (neurapraxia, axonotmesis, neurotmesis with suture-repair, neurotmesis with entubulation-repair and nerve-grafting) on the motor DCV profile of the median nerve and the facial nerve.

8.2 TECHNIQUES FOR THE MEASUREMENT OF DCV

There are several approaches to the calculation of *DCV*. Three of these methods are discussed below.

8.2.1 Deconstruction of Compound Action Potentials

A compound muscle action potential (CMAP) may be considered to be the weighted sum of its component motor unit action potentials (MUAPs) (Dorfman 1984). The size and shape of the CMAP is determined by the amplitude and duration of the MUAPs, the number of motor units, the conduction velocities of the nerve fibres and the distance the impulse travels along the nerve.

A CMAP may be reconstructed using a nominal MUAP and histological data regarding the diameters of the relevant nerve fibres. This method depends on assumptions regarding the relationship between conduction velocity and fibre diameter and conduction velocity and MUAP spike duration and amplitude. These relationships are referred to as weighting functions.

Conduction velocity is (almost) linearly related to fibre diameter (Boyd 1964); (Hursh 1939). Large nerve fibres generate short MUAPs with short latencies whereas smaller fibres generate more dispersed MUAPs with longer latencies. The amount of dispersion of the CMAP will increase with a longer conduction distance as the slower fibres progressively lag behind the faster ones. The amplitude of the action potential is dependant on both the conduction velocity and number of fibres contributing to it.

The first reconstruction experiments were performed by Gasser and Erlanger in 1927 and by Gasser and Grundfest in 1939 (Gasser & Erlanger 1927; Gasser & Grundfest 1939). Gasser and Grundfest performed sensory studies on the cat saphenous nerve

and demonstrated that a compound nerve action potential (CNAP), almost identical to the recorded CNAP, could be constructed using a nominal sensory unit action potential (defined as the action potential recorded from a single nerve fibre, SUAP) and a fibre-diameter histogram of the nerve. They reconstructed a CNAP as follows. A conduction velocity was assigned to fibres of a given size. For larger fibres, a variation of 1μm in the diameter of the fibres in each group was allowed because the amount of dispersion of their SUAPs was small. For smaller fibres each group had variations in fibre diameter of only 0.1μm to 0.25μm because of the greater dispersion of the SUAPs. The conduction time was calculated for each assigned conduction velocity using the conduction distance which had been used in the generation of the recorded CNAP. A triangle was drawn for each group imitating the dimensions of a SUAP. The height of each triangle was calculated by multiplying the mean diameter of the fibres in a particular group by the number of fibres in that group. The vertex corresponded to the maximum voltage. The front of each triangle touched the abscissa at a point corresponding to the conduction time. Once all the triangles were drawn they were summated and the resulting curve compared with the recorded CNAP. This was found to be an accurate method of reconstructing a CNAP.

The opposite process may be performed to generate a DCV profile. If the amplitude and waveform of a nominal SUAP are known along with the relative weighting functions then a CNAP can be deconstructed to enable calculation of its component SUAP latencies and hence conduction velocity(Cummins, Perkel, & Dorfman 1978).

One of the problems of this technique is disagreement regarding the values of weighting functions. For example, Gasser and Erlanger (Gasser & Erlanger 1927) assumed that the amplitude of the SUAP was proportional to the cross-sectional area of the fibre whereas Gasser and Grundfest (Gasser & Grundfest 1939) assumed it to

be proportional to the fibre diameter. In the same work Gasser and Grundfest assumed the duration of the spike to be constant (0.4ms) whereas other workers demonstrated that spike duration in mammalian medullated fibres is inversely related to conduction velocity (Dorfman 1984). Most workers accept that conduction velocity is proportional to fibre diameter but different values for the ratio for this relationship have been suggested. For example, in the cat model Hursh found a conduction velocity to fibre diameter ratio of 6:1, Boyd (also in the cat) found a ratio of 5.6:1 whilst in the peroneal nerve in the rabbit Cragg and Thomas found a ratio of 4.4:1(Boyd 1964; Cragg & Thomas 1964; Hursh 1939). These differences may be due to variations in recording technique or inherent differences between specific nerves or between animal models. Cummins *et al* developed a mathematical model to allow different weighting functions to be used depending on the physiological data available (Cummins, Perkel, & Dorfman 1978).

In human sensory DCV studies there may be difficulty determining a nominal SUAP as this requires single-fibre recordings; futhermore, CNAPs may be distorted by a low signal to noise ratio (Morita et al. 2002). Conversely, in motor studies the action potentials which are generated are of much higher amplitude and MUAPs are easily recorded using intramuscular electrodes. However, MUAPs vary in amplitude, duration and shape and will change in response to disease processes. This makes determination of a nominal MUAP difficult. Lee *et al* attempted to circumvent this problem by deriving a "mean" MUAP for a particular muscle (Lee et al. 1975). An intramuscular bipolar needle electrode was introduced into the thenar eminence of human volunteers. This electrode was used to identify a spike from a single motor unit and trigger recording from two surface electrodes. The signal from the surface electrodes was averaged. This process was repeated for between 100 to 500

discharges of the motor unit and enabled determination of a single MUAP from the surface electrode. This process was repeated for 20 to 30 motor units. The results were then averaged to give a representative MUAP for that muscle. Using computer simulations these workers studied the effect of different distributions of conduction velocity on the CMAP shape and were able to determine ranges of conduction velocities associated with particular pathological CMAPs.

8.2.2 Comparison of Two CMAPs.

In this method of deriving *DCV* the shapes of two compound action potentials (CAPs), resulting from different conduction lengths, are compared. For motor studies the nerve is stimulated in a manner identical to that for the measurement of *CVmax* (Dorfman 1984). Differences in amplitude and temporal dispersion of the CAPs are assessed. As the conduction distance lengthens the amplitude of the associated CAP decreases and its duration increases. *DCV* is derived as a function of the difference in conduction distance.

This approach has the advantage over the previous method that it does not require knowledge of a nominal SUAP or MUAP. However, the two CAP method may be inapplicable over short conduction distances because of a high noise to signal ratio (Cummins, Dorfman, & Perkel 1979). Distortion of the signal can result from activation of different nerve fibres at the two stimulation points (despite supramaximal stimulation), branching of nerve fibres (especially if longer distances are used) and differences in nerve-to-electrode-transfer function (NETF). NETF is determined by the geometry of the nerve with respect to the size and position of the electrode. Wells and Gozani developed a method to normalise NETF using an array of stimulating and recording electrodes positioned along the course of the nerve (Wells

& Gozani 1999). This allowed them to minimise the level of noise so that the dominant influence on the CAP shape was temporal dispersion. This allowed shorter segments of nerve to be used.

This method of calculating DCV assumes uniform conduction velocity throughout the nerve segment under investigation making it unsuitable for the assessment of localised conduction blocks or discontinuous pathologies.

8.2.3 Collision Technique.

The first collision experiments were carried out by Hopf (Dorfman 1984). These experiments were based on individual MUAPs. Leifer *et al* developed this technique to allow estimation of the distribution of conduction velocities of a population of motor axons within a peripheral nerve (Dorfman 1984). Using this method two supramaximal stimuli are applied to the nerve under investigation and the resultant CMAPs recorded from a target muscle. Both stimuli cause orthodromic and antidromic impulses. If S1 (distal stimulus) and S2 (proximal stimulus) are fired simultaneously the orthodromic stimulus from S1 will reaches the target muscle generating a CMAP (M1). However, the antidromic stimulus from S1 will collide with the orthodromic stimulus from S2 preventing it from reaching the target muscle and generating a second CMAP (M2). Therefore, only one CMAP will be observed.

If the interstimulus interval (ISI) is increased, that is, the time between stimulating at S1 (fired first) and S2, the S1 antidromic impulse in the fastest fibres will have passed S2 by the time it is stimulated and provided the refractory period is over in these fibres they will conduct an orthodromic impulse to the target muscle and generate a second CMAP, M2. As the ISI is further increased fibres with lower conduction velocities will be unblocked and will contribute to M2. M2 will initially be of low

amplitude as only a small number of fibres are contributing to it but will increase in size as slower fibres are recruited progressively.

Another collision technique was developed by Ingram (1987) using three supramaximal stimuli: a proximal stimulus (p1) fired first, a distal stimulus (d) fired second and a further proximal stimulus (p2) fired last (Ingram, Davis, & Swash 1987). The ISI between the first and second stimuli is variable (ISI_{p1-d}) whilst the ISI between the second and third stimuli is constant (ISI_{d-p2}). ISI_{d-p2} is short to ensure collision of all fibres if these stimuli are fired in isolation of the first proximal stimulus. The orthodromic impulse from distal stimulus always reaches the target muscle generating a CMAP, Md. When ISI_{p1-d} is short, orthodromic impulses from p1 collide with antidromic impulses from d. This allows impulses from p2 to reach the target muscle creating a second late CMAP, Mp2. As ISI_{p1-d} is increased orthodromic impulses from p1 will pass the distal stimulation site before d is delivered. These impulses will generate a small early MUAP, Mp1. In these fibres the antidromic impulse from the distal stimulus, d, will then collide with the orthodromic impulse from p2 thereby blocking these fibres from contributing to the late CMAP, Mp2. The ISI_{p1-d} which cancels the late second CMAP (Mp2) is the conduction time and the refractory period for these fibres at the distal site. As ISI_{p1-d} is incremented the early CMAP, Mp1, increases in size and the late CMAP, Mp2, decreases in size as more fibres pass the distal stimulus before it is fired. The elimination of the Mp2 CMAP corresponds to the conduction time of the slowest fibres.

Ruijten *et al* compared the methods of Hopf/Leifer and Ingram in the calculation of motor DCV in the peroneal nerves of healthy human volunteers (Ruijten, Sallé et al. 1993). They found no preference for either technique in their study but did suggest that Ingram's technique may be superior over shorter distances.

Harayama *et al* proposed another three stimuli technique (Harayama et al. 1990). The stimuli are fired in the same order as in Ingram's method (proximal, distal, proximal). In this instance however, the interval between the first proximal stimulus and the distal stimulus is fixed and the interval between the distal stimulus and the second proximal stimulus is varied. The fixed interval is short to ensure collision of all fibres. The two CMAPs generated correspond to those in Hopf's technique but these workers suggest that the second proximal stimulus which generates the second CMAP (M2) is less affected by the subnormal period of the nerve because the antidromic impulse from the distal stimulus is cancelled by the orthodromic impulse from the first proximal stimulus. Therefore, the nerve has longer to recover before it is stimulated again.

A variation of the double-stimulus collision technique was used for the calculation of DCV in this work.

8.3 CALCULATION OF DCV BY THE DOUBLE-STIMULUS METHOD

In the series of experiments performed on each nerve, DCV was measured after *CVmax*. For the calculation of DCV the positions of the stimulating and recording electrodes, and their connections to the Medelec machine, were identical to those used for *CVmax*, as described in Chapter 3. Therefore the distal stimulus, S1, was connected to stimulator A and the proximal stimulus, S2, was connected to stimulator B.

The motor point of the target muscle and the supramaximal current required at both points of stimulation had previously been identified during the determination of *CVmax*. However, both S1 and S2 were stimulated in isolation to ensure this was still the case. Constant current, square-wave impulses of 50μs duration were used. Supramaximal stimulation was particularly important in DCV as this test looks at the conduction velocities of a range of fibres and slower fibres have higher thresholds for excitation (Borg 1980; Cummins & Dorfman 1981).

The recording electrodes were manipulated to achieve the optimum CMAPs. Again this was important in DCV as the shape of the CMAP affects the pattern of collision. Furthermore the calculation of the area of M2 relies on the accurate placement of markers on the points of take-off, maximum deflection and return to baseline.

Initially the same sweep speed and gain selected for the measurement of *CVmax* were used. These were altered later if necessary so that both CMAPs could be visualised

on the monitor screen. It was also useful as an aid in visualising M2 CMAPs of low amplitude (associated with short ISIs).

The range of ISIs with which the nerve was to be stimulated was then calculated as follows. *CVmax,* which had been measured previously, was used as a guide to the range of conduction velocities to be expected. This range was set from a minimum conduction velocity of $10ms^{-1}$ to a maximum conduction velocity of (measured *CVmax* + $10ms^{-1}$). These values along with the interstimulus distance, between S1 and S2, were entered into an Excel Microsoft spreadsheet. The spreadsheet had been previously configured to divide this range into forty equal divisions and calculate the corresponding ISI using the following formula:

$$ISI = \frac{d}{CV}$$

Where:

ISI = interstimulus interval (ms)

d = distance between stimulating electrodes (cm)

CV = selected conduction velocity ($m\ s^{-1}$)

These values for ISI were then entered individually into the Medelec machine. An initial ISI of 0ms was selected to generate an M1 reference trace (all impulses from S2 were blocked). The ISI was then increased to the maximum of the previously calculated values and decremented. At higher ISI values M1 and M2 were observed as discrete traces. As the ISI was decreased M2 was seen to collide with M1, decreasing

in size until it finally disappeared. The initial reference trace was then digitally subtracted from the subsequent traces to isolate the test trace M2.

An example of the traces from one of the median nerve control experiments is shown in Figure 8.1 and Figure 8.2. In the collision program only twenty traces were allocated for each investigation therefore the 'opposite side' (left then right or vice versa) was used to allow all forty ISIs to be tested. Thus Figure 8.1 shows the traces obtained using the first twenty (longer) ISIs and Figure 8.2 shows the traces for the second twenty (shorter) ISIs. In each figure the first twenty traces show M1 and M2. M2 can be seen to collide progressively with M1. The second twenty traces in each figure show an isolated M2 trace after the digital subtraction of M1.

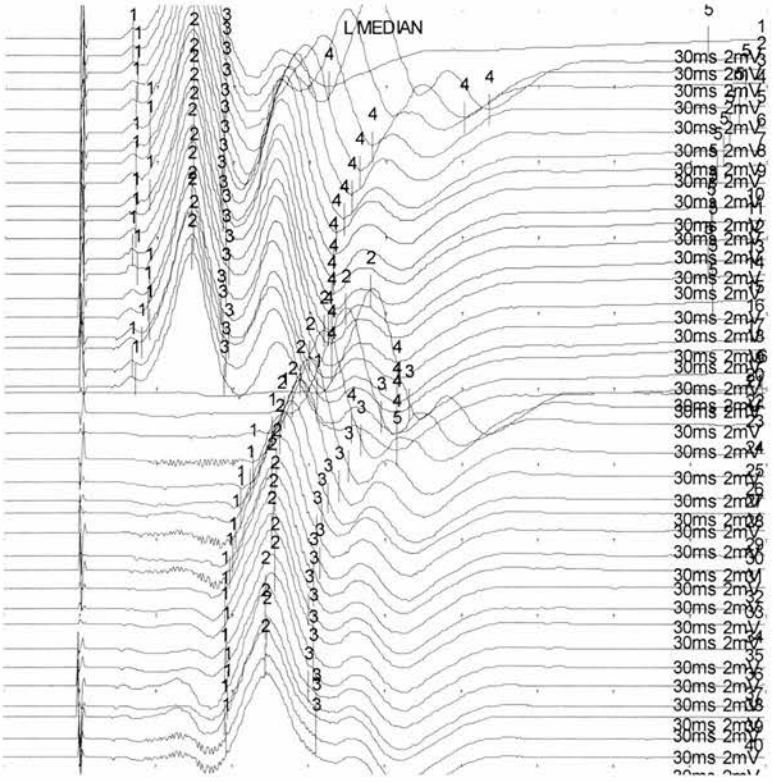

Figure 8.1

Figure 8.1 is an example of the traces obtained from one of the median nerve control experiments, using the first twenty longer ISIs. The first twenty traces show M1 and M2. The second twenty traces in each figure show an isolated M2 trace after the digital subtraction of M1.

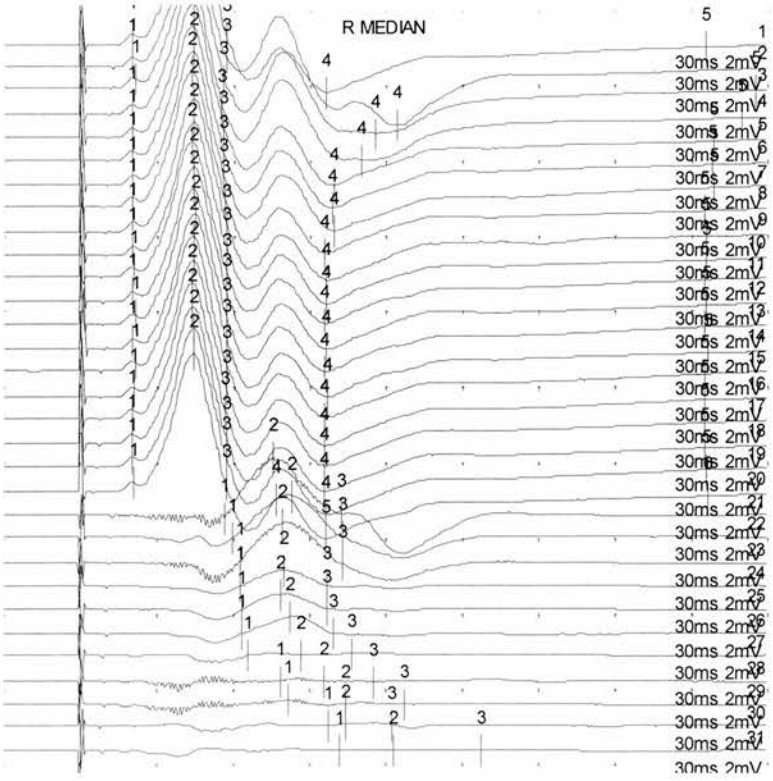

Figure 8.2

Figure 8.2 is an example of the traces obtained from one of the median nerve control experiments, using the second twenty shorter ISIs. The first twenty traces show M1 and M2. The second twenty traces in each figure show an isolated M2 trace after the digital subtraction of M1.

Markers were then manually positioned on M2 at the points of take-off, maximum amplitude and return to baseline. This enabled the area of each M2 wave to be calculated, using the collision program on the Medelec machine. The values of these areas were then entered into an Excel spreadsheet beside the corresponding conduction velocity. Both sets of data were then exported into a mathematical modelling program (Datafit, Version 7.1, Oakfield Engineering) where the values for the area of M2 were plotted against the range of conduction velocities. A fifth order polynomial function was found to provide the best fit for the scatter of points. An example of this is shown in Figure 8.3. The dark blue points represent the individual areas of M2 for a particular conduction velocity bin and the black line is derived from the closest-fitting function.

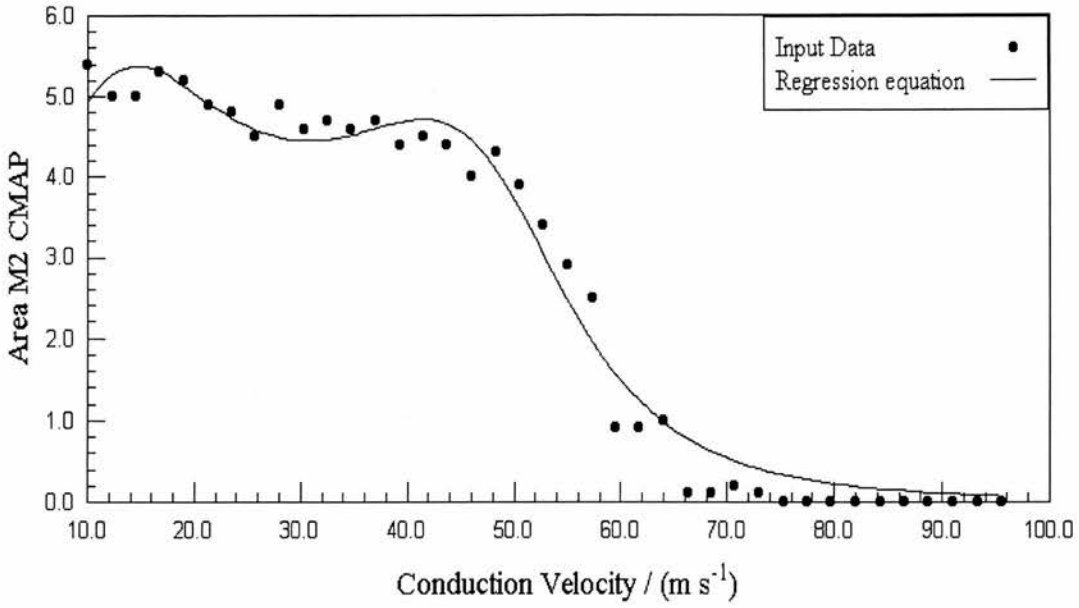

Figure 8.3

Figure 8.3 is an example of one of the graphs plotted in Datafit. The dark blue points represent the individual areas of M2 for a particular conduction velocity bin and the black line is derived from the closest-fitting function.

The function of the best-fitting line was exported into an Excel spreadsheet and differentiated. This allowed the gradient or rate of change at each point along the line to be calculated. The gradient of the line at a particular point corresponded to the change in the proportion of active fibres at a particular conduction velocity. These values were plotted to give a graphical representation of the distribution of conduction velocities for the nerve under investigation. These graphs are shown in Figure 8.4 to Figure 8.14.

Care was taken to ensure supramaximal stimulation of the nerve and optimal CMAPs. The collision method of calculating DCV depends on accurate calculation of the area of M2. The two-stimuli technique used in this work requires the digital subtraction of M1 to isolate M2. This was achieved by generating a reference trace by simultaneously stimulating at S1 and S2 then subtracting this reference trace from the subsequent test traces using the digital subtraction function in the collision program on the Medelec. However, if the profile of M1 changed during the investigation then subtraction of the reference trace did not isolate M2. Furthermore because only twenty traces could be stored at one time a second reference trace had to be generated. Variation between the two reference traces was another possible source of error in the isolation of M2.

Higher levels of current were required to achieve supramaximal stimulation in the nerve-graft models in both nerves. This resulted in direct activation of surrounding muscle and in the case of the median nerve gross movement of the forelimb. The shape of the CMAPs in the nerve graft group was variable and M2 in particular was distorted. It was not possible to obtain DCV graphs on the median nerve nerve-graft group. DCV profiles were generated for the facial nerve. This took much longer than

usual to accomplish as the nerve required time to recover between successive stimulations and stimulations had to be repeated several times because of CMAP variability.

8.4 FACIAL NERVE RESULTS FOR DISTRIBUTION OF CONDUCTION VELOCITIES (DCV)

Each experimental group contained six animals, the corresponding six DCV graphs were displayed on one page. The percentage of fibres conducting impulses was represented on the y-axis whilst the range of conduction velocities across which the nerve was conducting was represented on the x-axis.

Figure 8.4 shows the six DCV graphs for the normal control group for the facial nerve. All six graphs have a bimodal distribution.

Figure 8.5 shows the six DCV graphs for the neurapraxia model for the facial nerve. Again all six graphs have a bimodal distribution. The graphs are shifted to the left as compared to the normal control model.

Figure 8.6 shows the six DCV graphs for the axonotmesis model for the facial nerve. Again all six graphs have a bimodal distribution. The graphs are shifted to the left as compared to the normal control model and graphs two, three and five are shifted to the left compared to the neurapraxia model.

Figure 8.7 shows the six DCV graphs for the neurotmesis and suture repair model for the facial nerve. Graphs one to five have a bimodal distribution but in graph six there is only the suggestion of a second peak. The graphs are shifted to the left as compared to the normal control model, neurapraxia model and axonotmesis model.

Figure 8.8 shows the six DCV graphs for the neurotmesis and wrap repair model for the facial nerve. The bimodal distribution is preserved in all six graphs. The graphs are shifted to the left as compared to the normal control model, the neurapraxia model

and axonotmesis model. There is no obvious difference between the neurotmesis and suture repair model and the neurotmesis and wrap repair model.

Figure 8.9 shows five DCV graphs for the nerve graft model for the facial nerve. Graph 2 is missing as this animal died. All five graphs have a bimodal distribution. The graphs are shifted to the left as compared to the other models of nerve injury.

Facial Nerve DCV
Normal Control Model

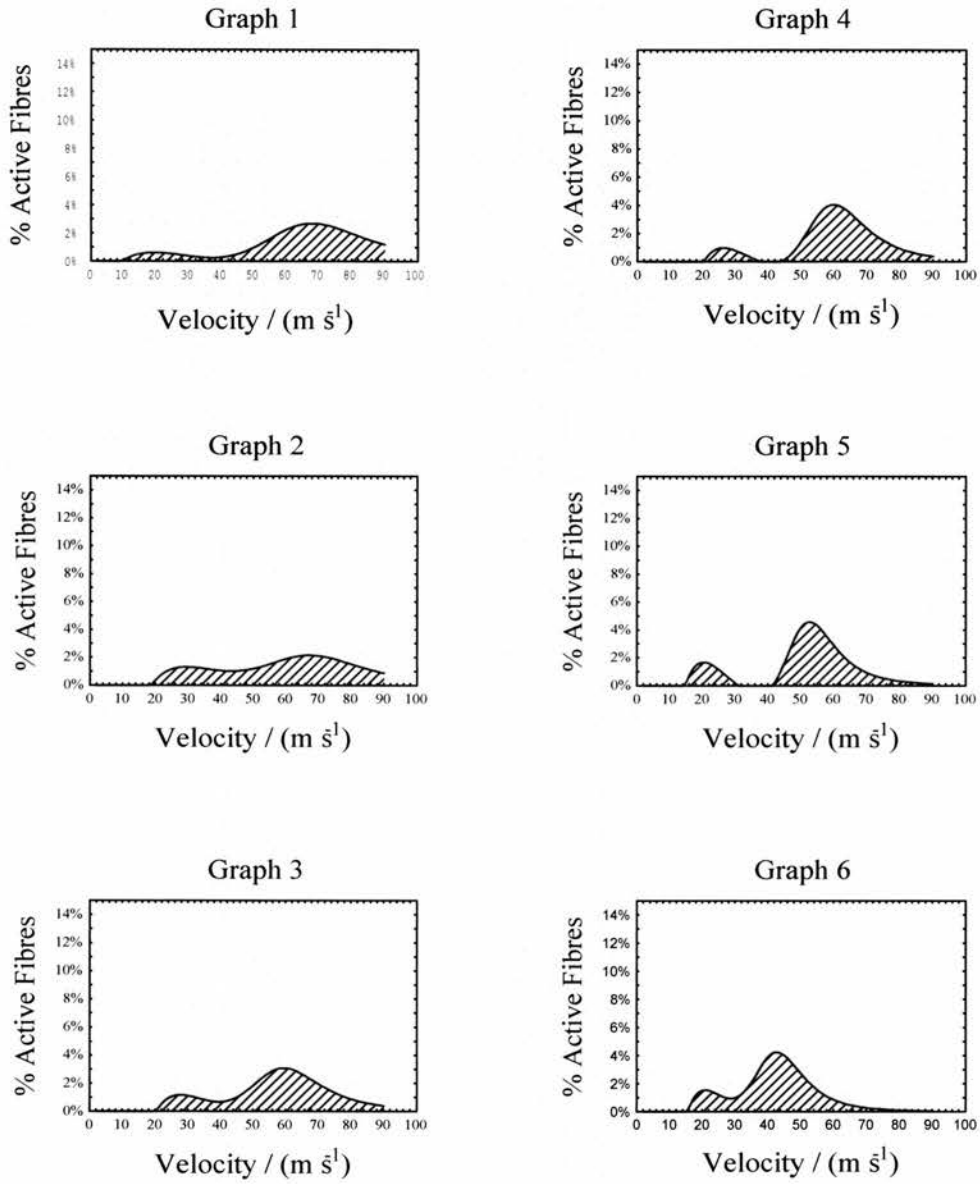

Figure 8.4

Facial Nerve DCV
Neurapraxia Model

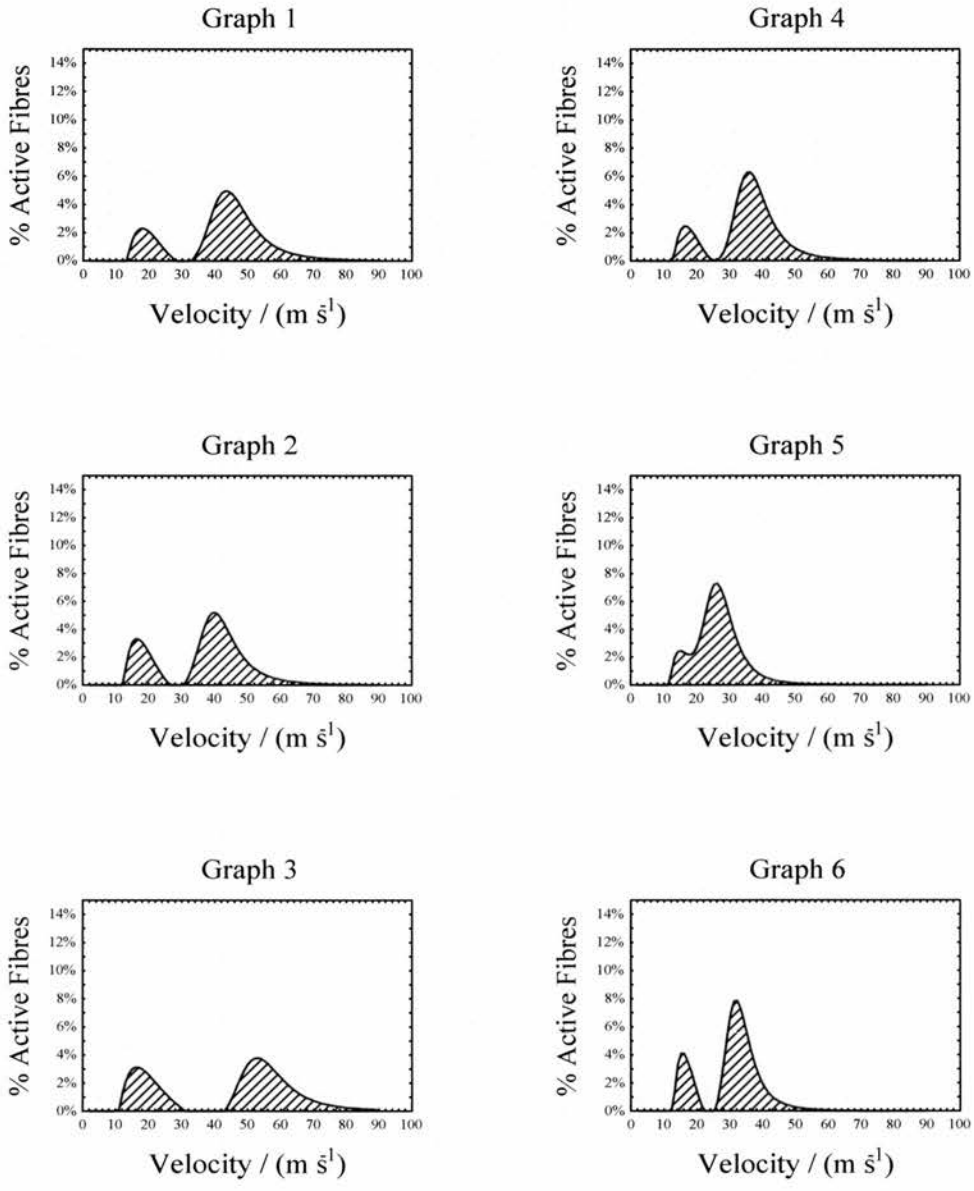

Figure 8.5

Facial Nerve DCV
Axonotmesis Model

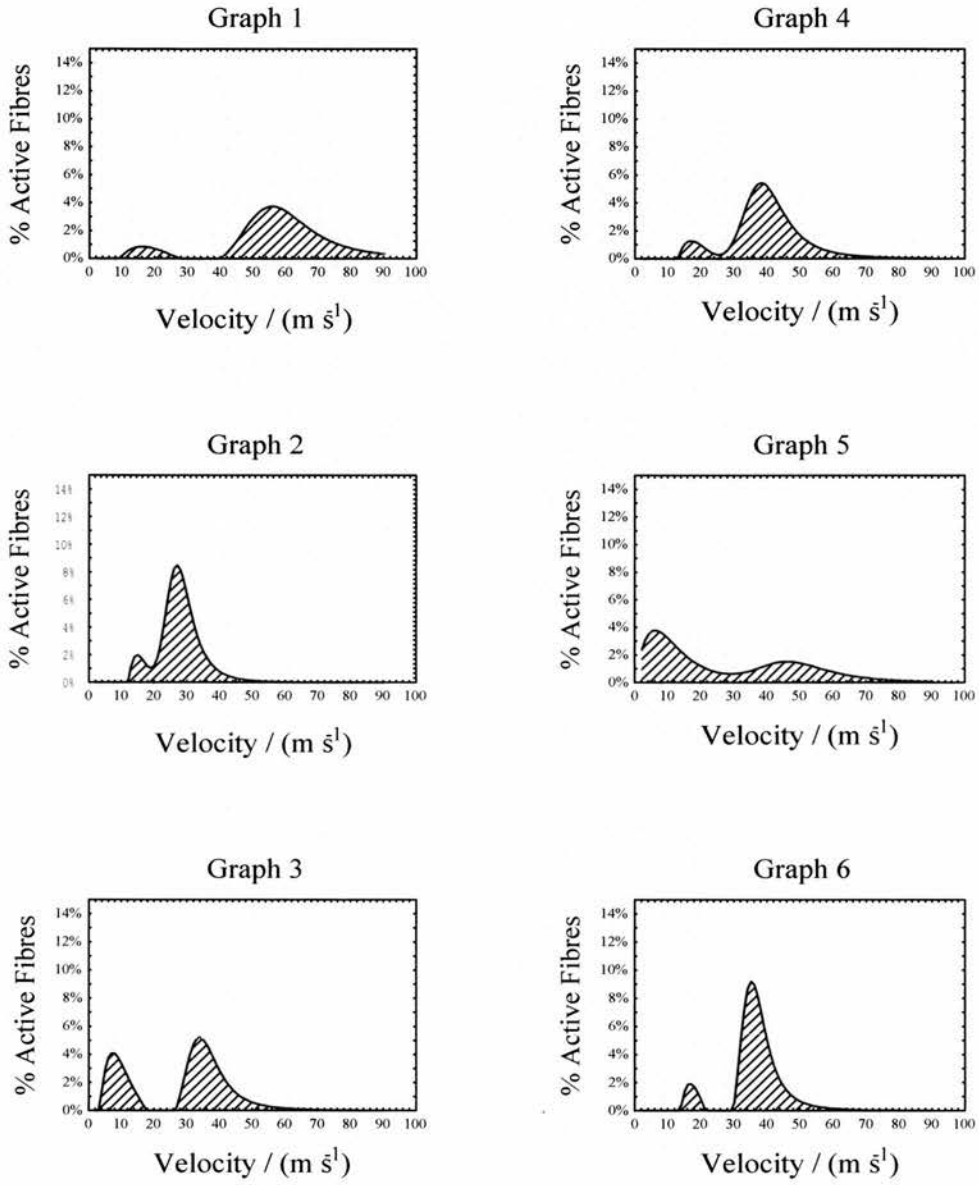

Figure 8.6

Facial Nerve DCV
Neurotmesis Model (Sutured Repair)

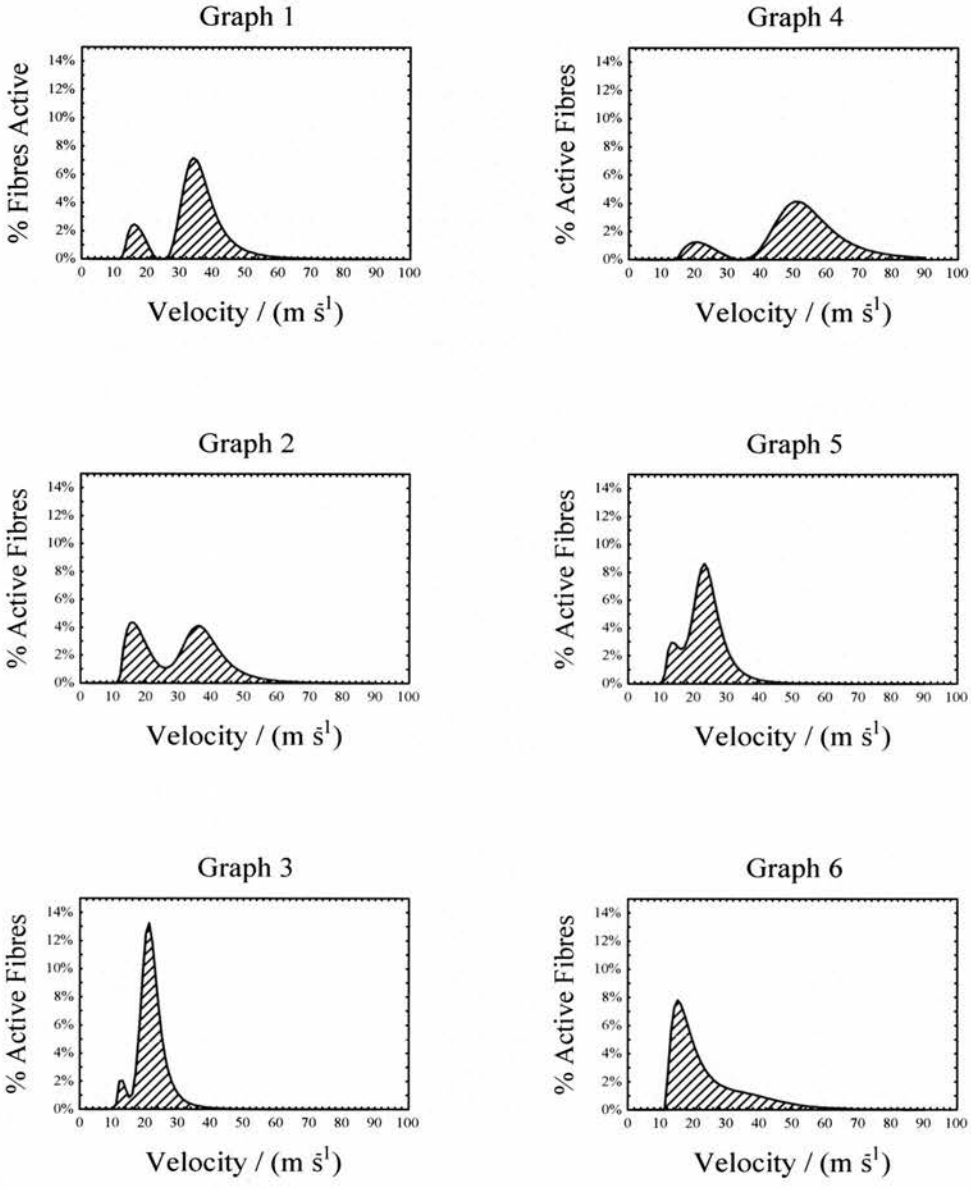

Figure 8.7

Facial Nerve DCV
Neurotmesis Model (Wrap Repair)

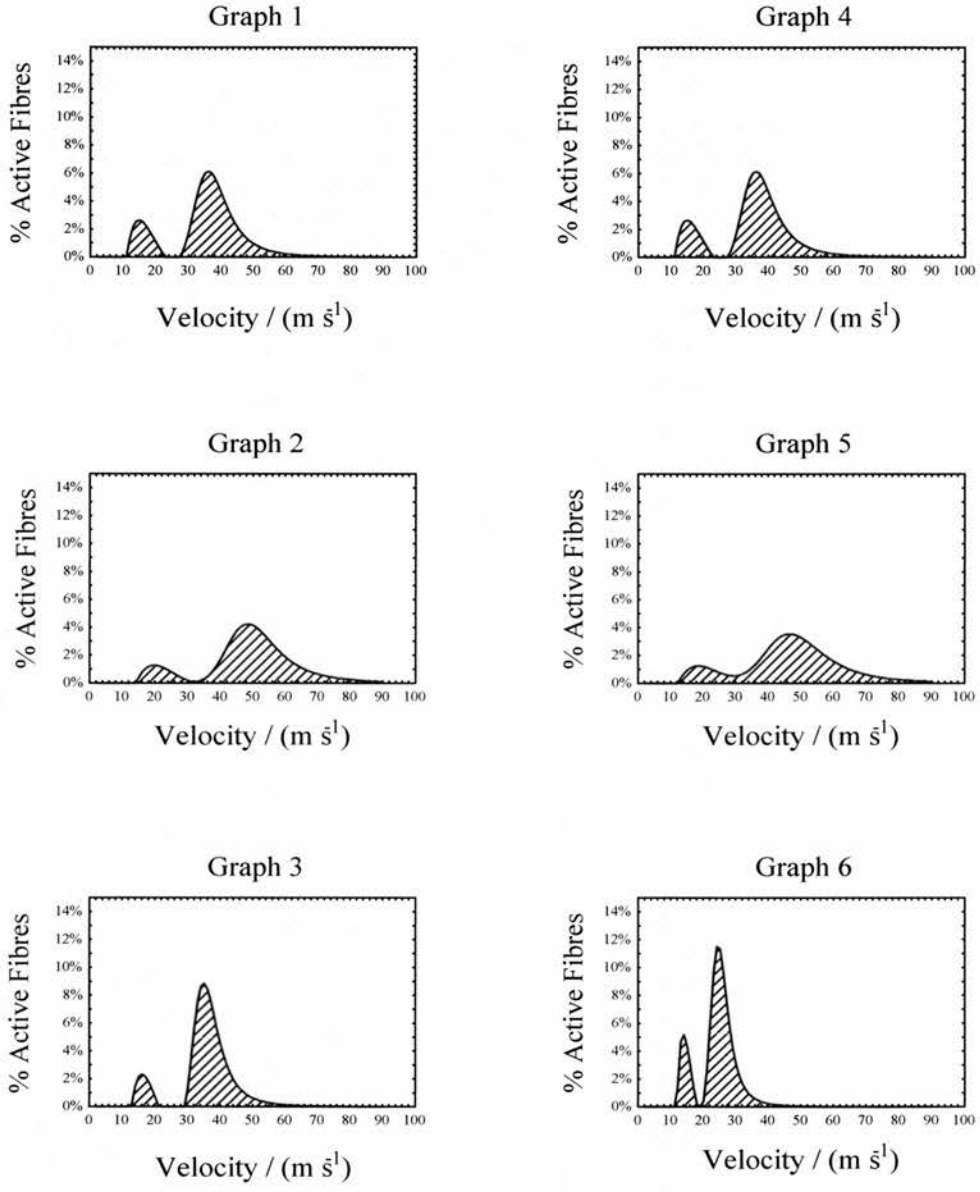

Figure 8.8

Facial Nerve DCV
Nerve Graft Model

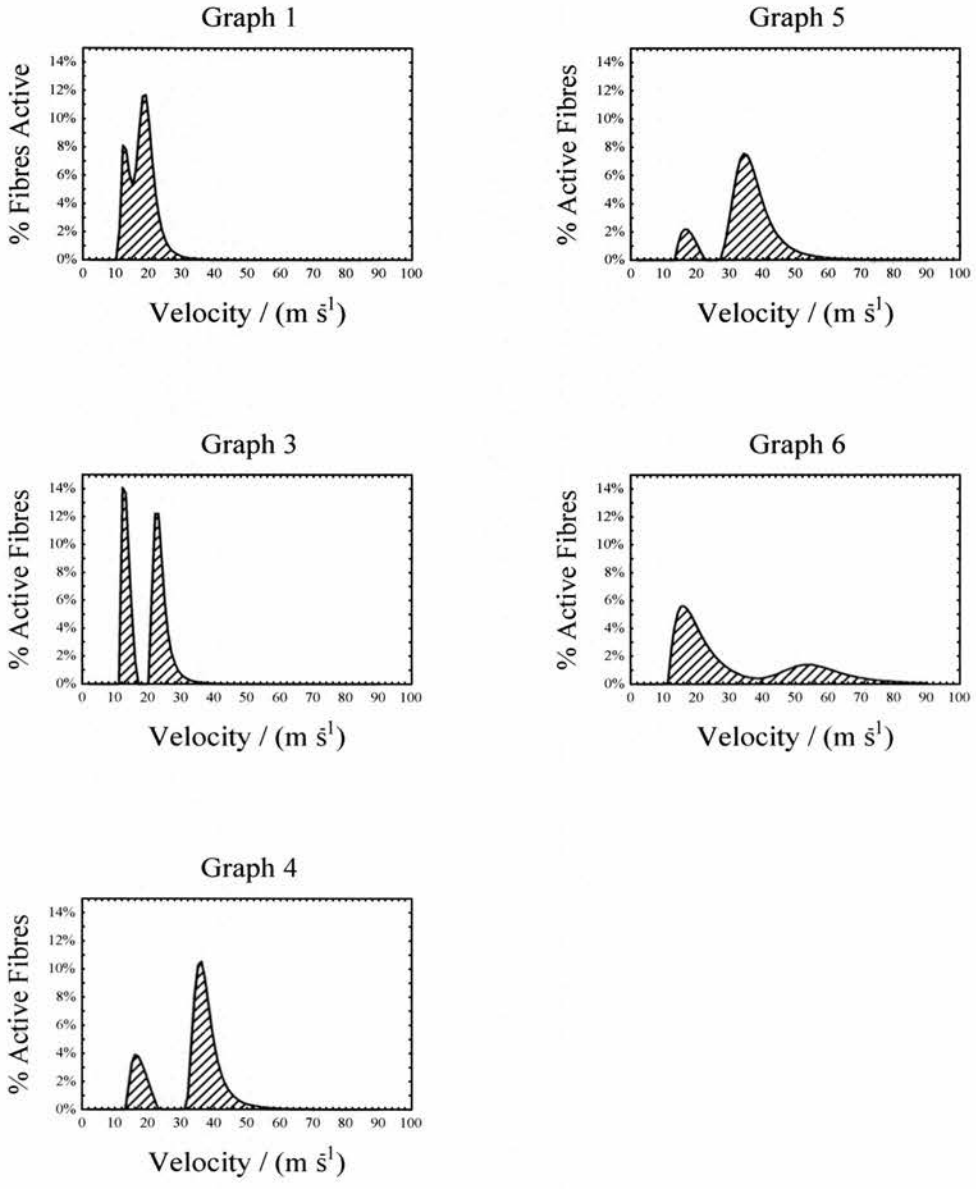

Figure 8.9

8.5 MEDIAN NERVE RESULTS FOR DISTRIBUTION OF CONDUCTION VELOCITIES (DCV)

Each experimental group contained six animals, the corresponding six DCV graphs were displayed on one page. The percentage of fibres conducting impulses was represented on the y-axis whilst the range of conduction velocities across which the nerve was conducting was represented on the x-axis.

Figure 8.10 shows the six DCV graphs for the normal control group for the median nerve. All six graphs have a bimodal distribution.

Figure 8.11 shows five DCV graphs for the neurapraxia model for the median nerve. Graph four is missing as this animal died. All five graphs have a bimodal distribution. There is no marked difference between the neurapraxia model and the normal control group.

Figure 8.12 shows five DCV graphs for the axonotmesis model for the median nerve. Graph six is missing as this animal died. All the graphs have a bimodal distribution. There is a general shift of the graphs to the left as compared to the normal control model and the neurapraxia model.

Figure 8.13 shows the six DCV graphs for the neurotmesis and suture repair model for the median nerve. Graphs one to four and graph six have a bimodal distribution but in graph five has only one peak. The graphs are shifted to the left as compared to the normal control model, neurapraxia model and axonotmesis model.

Figure 8.14 shows the six DCV graphs for the neurotmesis and wrap repair model for the median nerve. A bimodal distribution is preserved in all six graphs. The graphs are shifted to the left as compared to the normal control model, the neurapraxia model and axonotmesis model. There is no obvious difference between the neurotmesis and suture repair model and the neurotmesis and wrap repair model.

It was not possible to obtain DCV graphs for the nerve graft model in the median nerve.

Median Nerve DCV
Normal Control Model

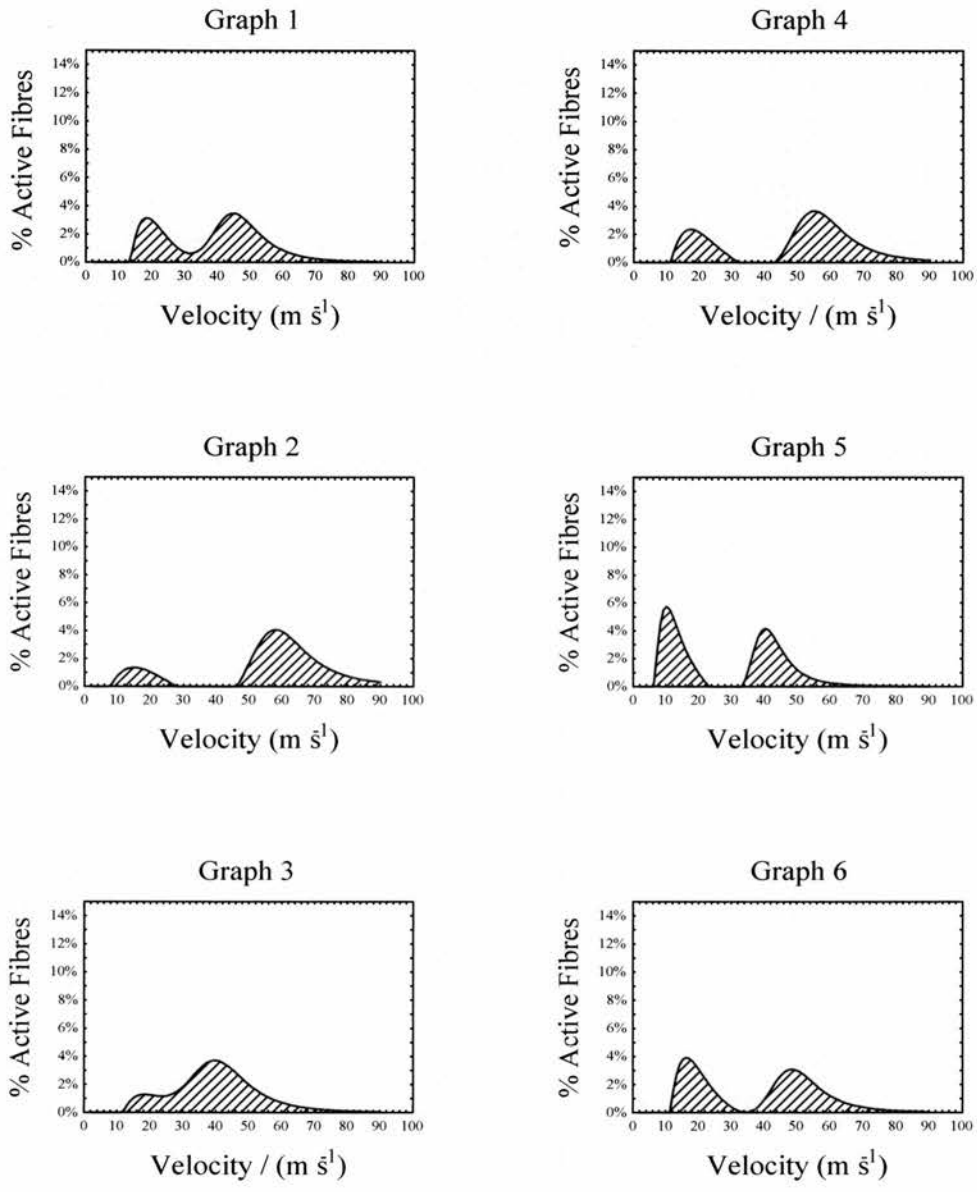

Figure 8.10

Median Nerve DCV
Neurapraxia Model

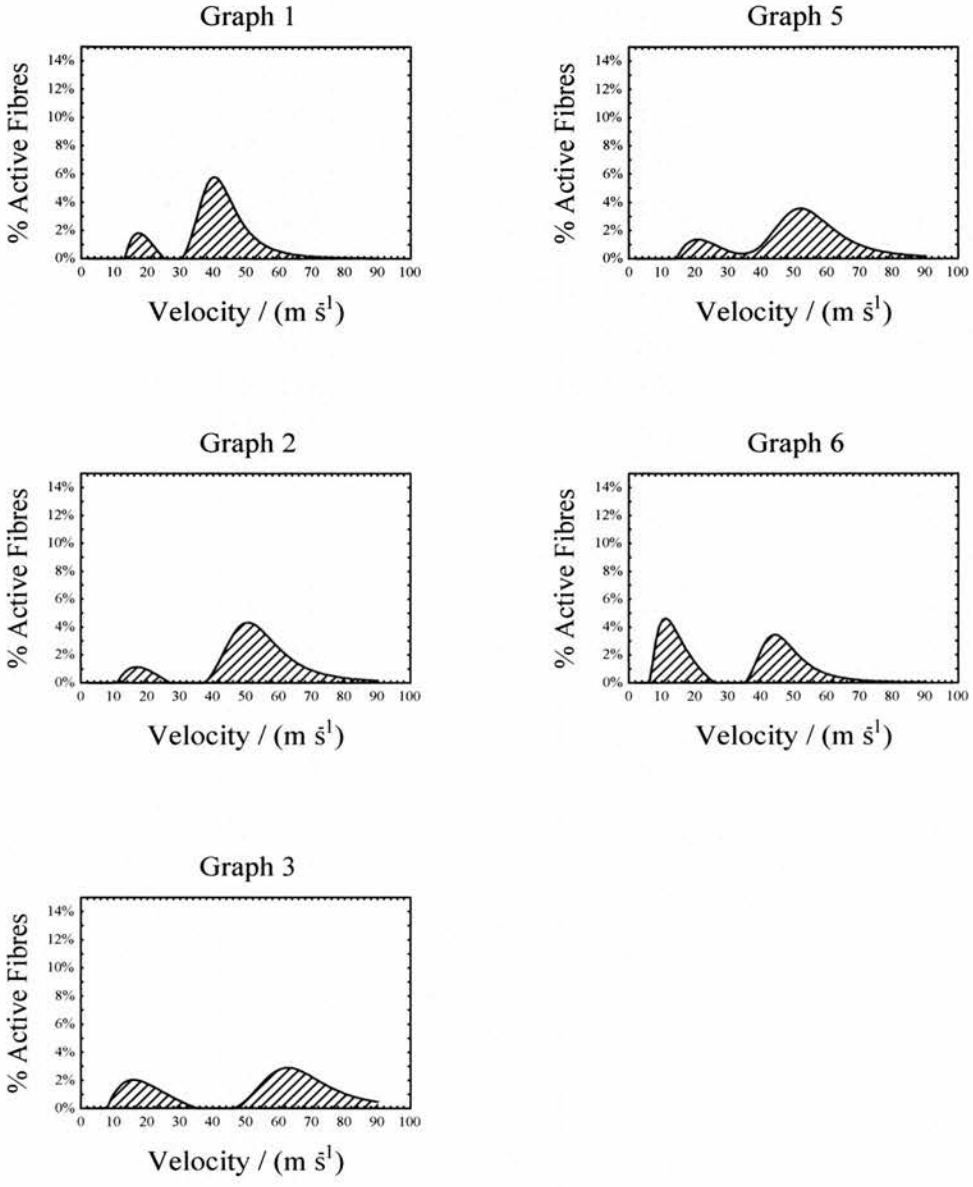

Figure 8.11

Median Nerve DCV
Axonotmesis Model

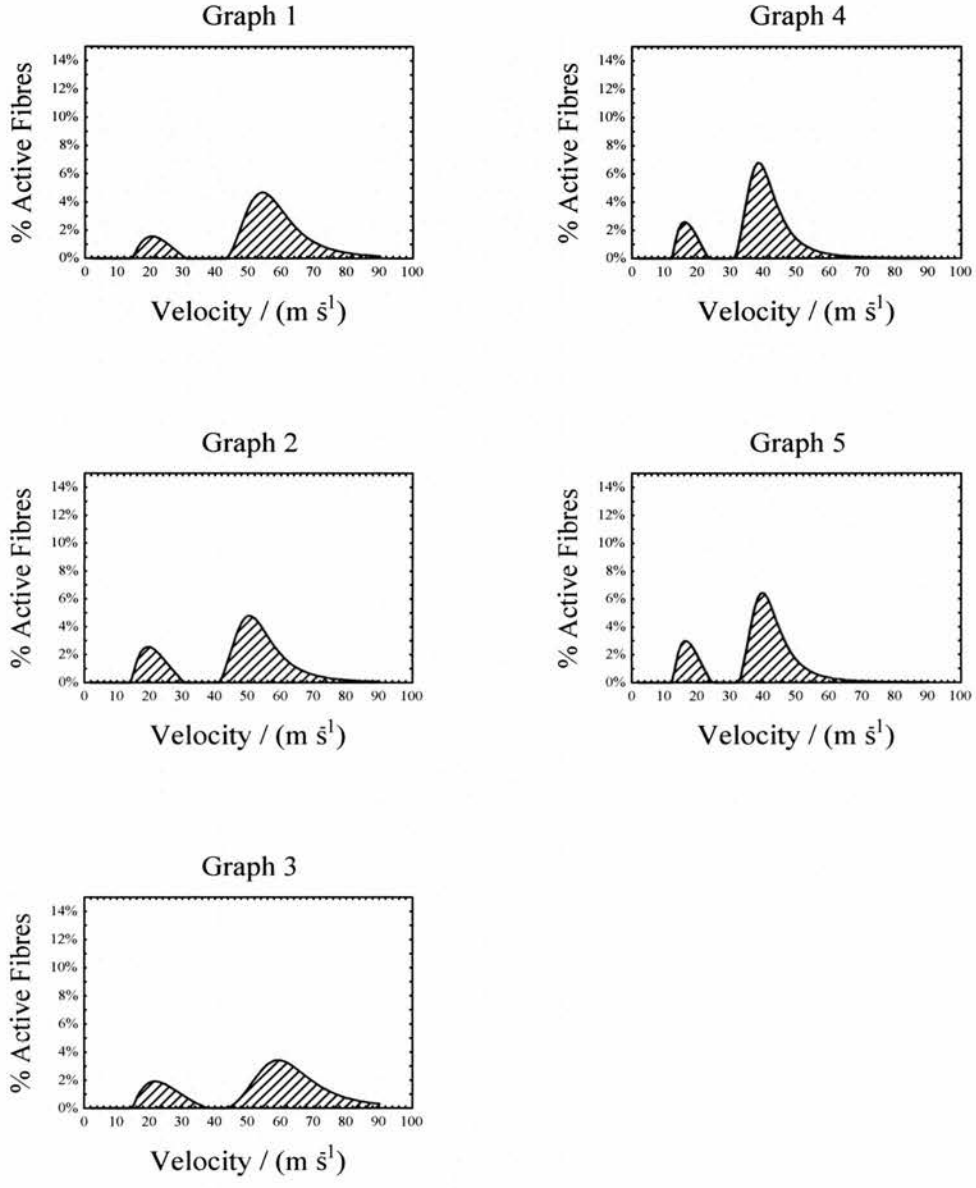

Figure 8.12

Median Nerve DCV
Neurotmesis Model (Sutured Repair)

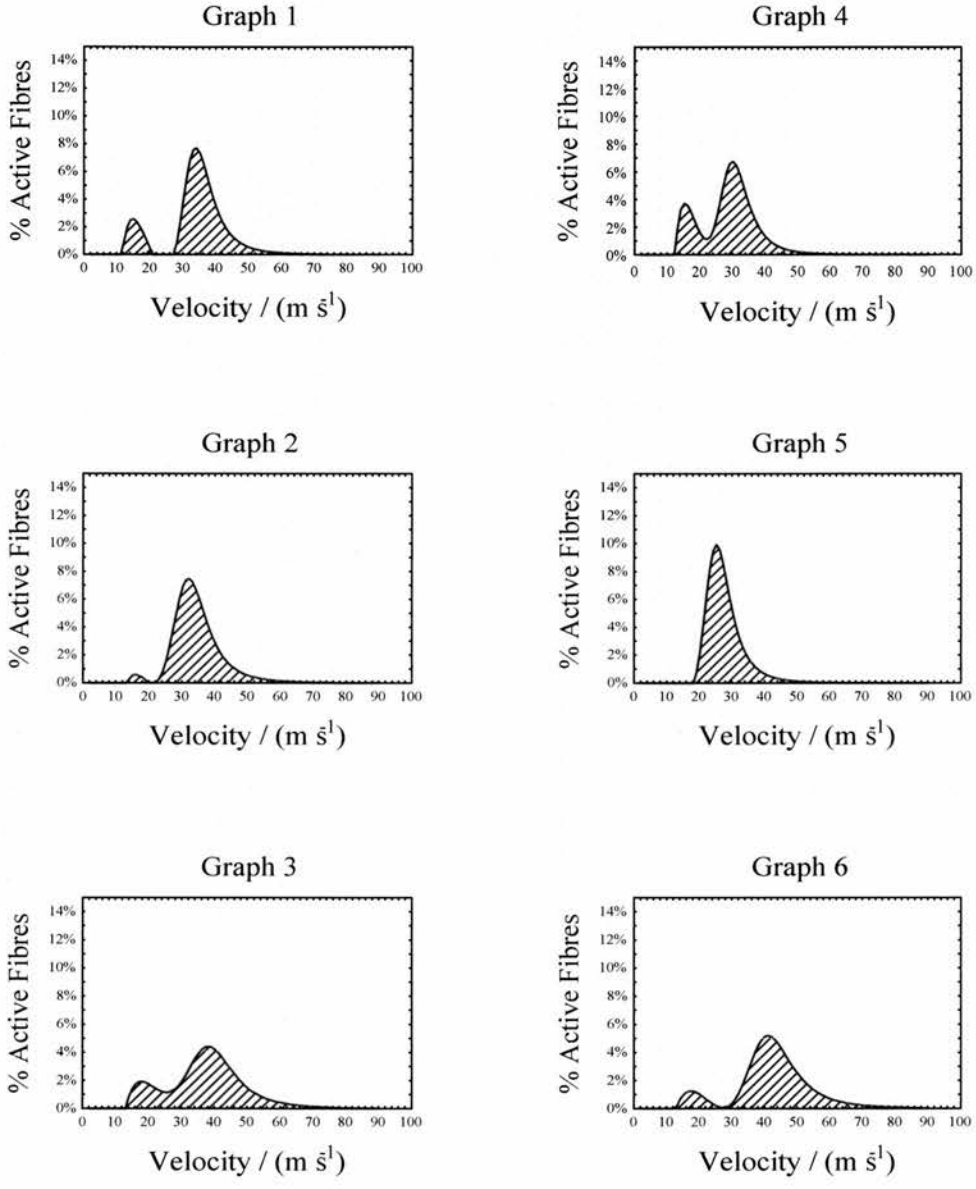

Figure 8.13

Median Nerve DCV
Neurotmesis Model (Wrap Repair)

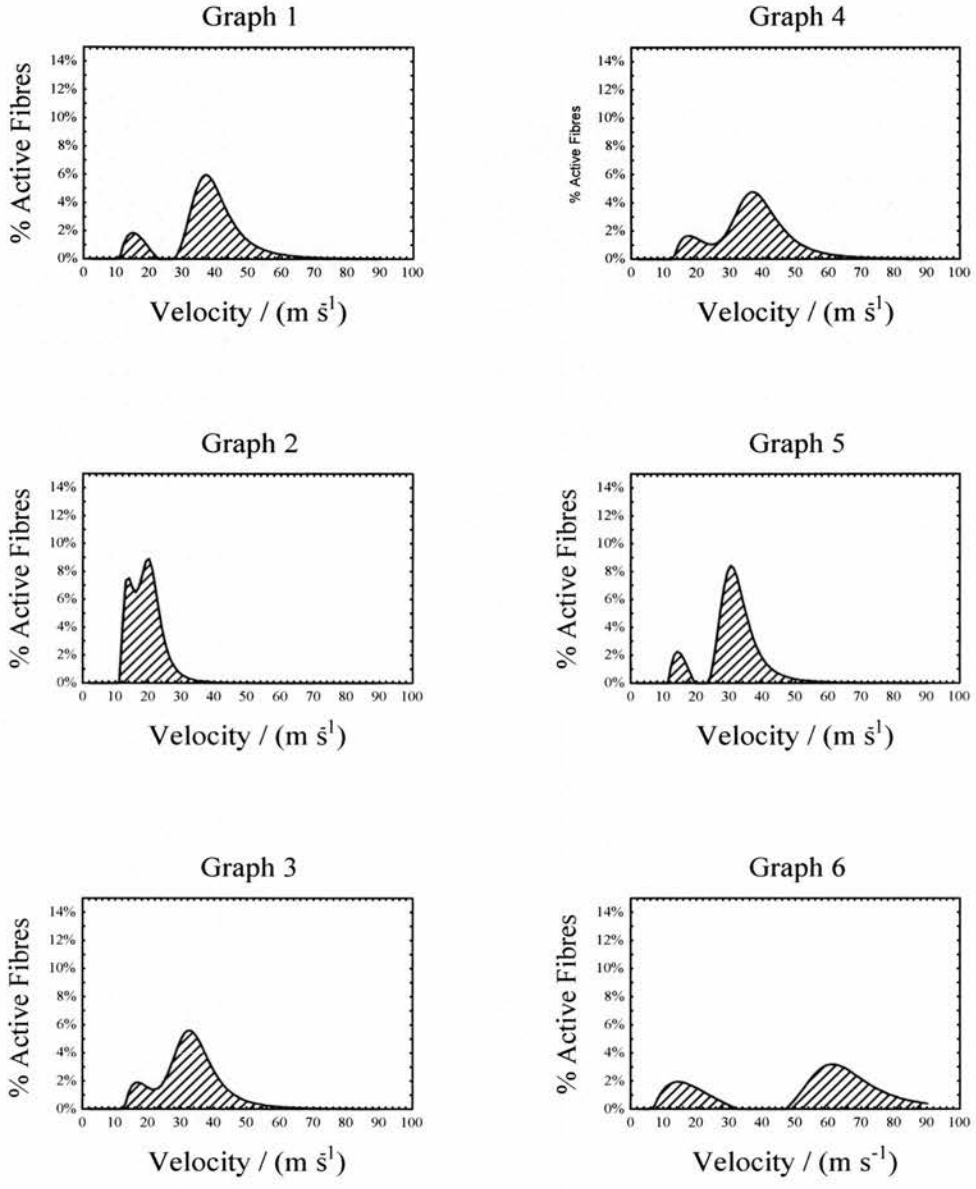

Figure 8.14

8.6 DISCUSSION

All the DCV profiles (except for one of the facial nerve neurotmesis and suture repair group and one of the median nerve neurotmesis and suture repair group) had a bimodal distribution. This was a purely motor study therefore only motor fibres contributed to the DCV profile. Based on Erlanger and Gasser classification of nerve fibres the left peak was thought to represent γ-motor efferent fibres and the right peak faster α-motor efferent fibres.

The DCV curves showed a progressive shift to the left *i.e.* slower conduction velocities, with increasing severity of nerve injury. This reflected the results for *CVmax*. Quantitative comparison between nerves was not possible as the total number of active fibres for each nerve was unknown *e.g.* 8% of fibres in a graft model may be a significantly smaller number of fibres than 8% of fibres in a normal control model.

The fact that it was impossible to obtain DCV profiles for the nerve-graft injuries in the median nerve supports the suggestion of increased fibre-mismatching resulting in a mixed nerve (median) as opposed to a purely motor nerve (facial) as previously discussed in Chapter 7, regarding *CVmax*.

One of the difficulties in determining DCV in the graft models was the variability of the CMAPs. Ingram's three-stimuli technique has the advantage that it does not require the digital subtraction of the CMAP generated from the distal stimulus to isolate the test CMAP. In Ingram's method the test CMAP, Mp2, is a separate entity as it occurs later therefore no subtraction is required.

All collision techniques designed to measure motor distribution of conduction velocities are based on a number of assumptions. One of these is the linear summation

of MUAPs to generate a CMAP which assumes that all MUAPs, regardless of their position within the muscle or the conduction velocity of the associated axon, contribute equally to the CMAP. However, Henneman et al showed that the contractile properties of a motor unit are related to the size of its motor axon (Henneman et al. 1974). This relationship is referred to as the size principle and proposes that faster axons innervate larger motor units.

Failure to take account of this principle results in over-estimation of the proportion of faster fibres and under-estimation of the proportion of slower fibres. Theoretically, correcting for the size principle would increase the height of the first DCV peak whilst diminishing the height of the second. This phenomenon may be exacerbated in the models of nerve injury studied here as after injury, motor-units undergo remodelling to form a smaller number of larger units (Dorfman, Cummins, & Abraham 1982).

Comparison of the DCV profiles obtained here reveal that the transection-injury groups (neurotmesis and suture-repair, neurotmesis and entubulation-repair and nerve-graft) for both nerves generally have higher DCV peaks than the other less severe models of injury. This suggests there may be more remodelling of the motor-units in these groups.

The double-stimulus collision technique based on Hopf's method was used for the calculation of DCV in this work. Ingram *et al* who developed a three-stimuli technique described earlier criticised this method on the following points:

(i) It takes no account of variation in refractory period between different sizes of fibres.

(ii) The test CMAP (that is M2) is distorted because of slowing of the orthodromic impulse from the proximal stimulus as the nerve would still

be in its subnormal period (or relative refractory period) because of recent activation by the antidromic impulse from the distal stimulus.

(iii) The test CMAP is further affected by the velocity-recovery effect in muscle fibres.

It is generally accepted that for medullated fibres refractory period is inversely related to conduction velocity (Harayama, Shinozawa, Kondo, & Miyatake 1990). Therefore, refractory period should be taken into account when calculating DCV by the collision technique as the ISIs used to calculate conduction velocity consist of the conduction time and the refractory period (Dorfman 1984). Several methods have been described which use a collision technique to estimate the distribution of refractory period in motor fibres (Betts, Johnston, & Brown 1976; Ingram, Davis, & Swash 1986; Kimura 1983).

In these experiments refractory period was not taken into account. Previous workers in the group had attempted to incorporate a calculation for refractory period based on an inverse relationship between conduction velocity and refractory period. However, it then proved impossible to fit the spread of points generated from calculating the areas of the test CMAP, M2, to a polynomial equation. It may be that for the models of nerve injury studied the inverse relationship between conduction velocity and refractory period does not apply.

Betts *et al* in a study on the distribution of refractory period and conduction velocity in the human median nerve found that for group A fibres the random scatter of refractory period values was far greater than variation due to conduction velocity (Betts, Johnston, & Brown 1976). They suggested a single median value for refractory period was more appropriate when calculating DCV by the collision technique.

However, it is more commonly believed that failure to incorporate an inverse relationship between conduction velocity and refractory period in the calculation of DCV results in a relative over-estimation of conduction time for the slower fibres. Therefore, the points on the DCV curves corresponding to the slower fibres were artificially shifted to the left. This effect will have had more impact on the facial-nerve-graft DCV profiles which are conducting at slower velocities. However, the differences in the DCV profiles assessed in this work were of a magnitude that failure to account for refractory period was unlikely to obscure the changes of profile resulting from the injuries themselves. Consideration of refractory period is more important in DCV experiments which are looking for more subtle changes in conduction velocity in slower fibres.

After conducting an impulse a nerve becomes inexcitable (absolute refractory period) then progressively recovers (relative refractory period). During the relative refractory period, also referred to as the subnormal period, conduction velocity is reduced. An impulse elicited during this period will lag progressively behind the conditioning impulse until it reaches normal nerve at which point it will conduct at normal velocity. As the two stimuli in Hopf's technique are fired in close succession Ingram stated that the orthodromic impulse from the proximal stimulus would therefore be delayed as it would be propagating in this subnormal period (Ingram, Davis, & Swash 1987). However, Ruijten *et al*, who compared Hopf's and Ingram's methods, observed that in Hopf's collision technique the conditioning impulse (that is the antidromic impulse from the distal stimulus) is travelling in the opposite direction from the test impulse which is travelling orthodromically (Ruijten, Sallé, et al. 1993). These workers suggested that the effect of the subnormal period would be less than that suggested by Ingram as more distally the fibres would have time to recover.

Conduction velocity in muscle fibres is also affected by a conditioning impulse (Mihelin, Trontelj, & Stålberg 1991). This is termed the velocity recovery function. After an impulse there is an initial period of subnormal conduction velocity followed by a period of supernormal conduction velocity. The amplitude of the MUAP may also be reduced after a discharge. Mihelin *et al* studied the recovery functions of muscle by direct stimulation of the muscle. This approach eliminated any influence of the recovery functions of the associated motor axons and motor end-plates. These workers investigated normal, denervated and dystrophic muscle. No detailed descriptions of the nerve injuries were supplied other than the injuries had occurred one to four months previously and the muscles tested were completely denervated. Normal muscle fibres had a subnormal conduction velocity for ISIs less than 6ms and a supernormal conduction velocity for ISIs greater than 10ms. The values for the ISIs were lower for the dystrophic muscle, less than 4ms and greater than 7.5ms respectively. These workers proposed that this was due to exaggerated excitability of this muscle. Conversely, the values of the ISIs for the denervated muscle were increased. The period of subnormal conduction for denervated muscle extended up to an ISI of 11.5ms. Furthermore, the subnormal conduction velocity was more reduced compared with that of normal and dystrophic muscle and also associated with a marked reduction in MUAP amplitude. A period of supernormal conduction was reached for ISIs greater than 15ms although this was less pronounced than for the other muscle fibres.

The nerve injuries reported by Mihelin *et al* were relatively recent injuries, with the associated muscle described as denervated. These injuries differ from the nerve injuries described in this work in that the nerves in these experiments have been repaired (if necessary) and allowed time to regenerate and reinnervate the target

muscle. Maturation of this process was confirmed by an electromyographic technique, stimulated jitter, which is used to assess the stablility of the neuromuscular junction (see Chapter 6). The VRF of the muscle may therefore have returned to normal or may lie somewhere between the values quoted in Mihelin's experiments for normal and deinnervated muscle.

It should be noted that using the collision technique the ISI for the muscle is longer than the corresponding ISI with which the nerve is stimulated as it also includes the latency between the two points of stimulation. A longer interstimulus length increases the muscle ISI and may move the test CMAP from the subnormal period to the normal period. For example for the conduction velocity range 10m s^{-1} to 100m s^{-1} an interstimulus length of 5cm gives resultant latencies of 0.5ms-5ms whereas a conduction length of 10cm increases this to 1ms-10ms. In these experiments the maximum conduction length possible was used. For the facial nerve this ranged from 6cm to 9cm and for the median nerve from 7.5cm to 10cm. However despite maximising the conduction lengths there is no doubt that the second CMAP, M2, was affected by VRF.

Ingram's three-stimuli technique has an advantage over the two-stimuli technique in that the ISI between the conditioning impulse and the test impulse is always constant (ISI_{d-p2}) whereas in double-stimulus technique the ISI is variable. However, in the three-stimuli technique the ISI is generally shorter. Thus Ingram's technique has a constant but larger VRF effect whereas the double-stimuli method has a variable but smaller VRF effect.

The work presented in this chapter was an investigation of the effect of different types of nerve injury on the DCV profile of the facial nerve and the median nerve. As mentioned previously much of the published work to data has concentrated on

different methods of calculating DCV and the effect of various neuropathies and environmental factors. This work is the first attempt to methodically investigate the effect of standardised models of nerve injuries on the pattern of DCV and to compare the DCV profiles of a motor nerve and a mixed nerve. Despite the short-comings of the double-stimulus technique used, which have been discussed above, this study revealed the progressive leftward shift of the DCV profile seen with the increasing severity of nerve injury. These results reflect the decreasing value of *CVmax* seen with increasing severity of nerve injury. As such DCV probably has little advantage over *CVmax* in the clinical investigation of nerve injuries. However, it may have a more useful role to play in the investigation of more subtle nerve dysfunction such as that associated with neuropathies.

8.7 CONCLUSIONS

(i) DCV provides more comprehensive information regarding the conduction velocities of fibres within a peripheral nerve than conventional *CVmax*.

(ii) In the case of the models of nerve injury investigated here DCV does not provide any more clinically useful information than conventional *CVmax*. This is because of the extent of these nerve injuries and the fact that most of the fibres are conducting at slower velocities.

(iii) Future work on DCV should attempt to account for refractory period.

(iv) Three-stimuli techniques have advantages over two-stimuli techniques in regard to the subnormal period of the nerve and the velocity response function of muscle.

(v) Ingram's technique has the further advantage it does not require digital subtraction of the conditioning CMAP to isolate the test CMAP. This is of particular benefit when only twenty traces can be recorded at a time and also in situations with increased variability of the CMAPs in this case the nerve-graft models.

(vi) DCV may have a more clinically useful role in the investigation of more subtle conditions affecting nerves perhaps at a subclinical level. It would be particularly useful in the detection of conditions affecting slower fibres where measurement of *CVmax* remains within normal limits.

9 REFRACTORY PERIOD

9.1 INTRODUCTION

Immediately after depolarisation an axon becomes inexcitable. This is called the absolute refractory period (*ARP*) and lasts between 0.5ms to 1.0ms in a normal nerve (Kimura 1983). The *ARP* is a result of closure of sodium channels, to allow repolaristion of the axon. Initially these channels are unable to reopen regardless of the magnitude of the stimulus. However, during the subsequent few milliseconds an extremely large stimulus, beyond physiological levels, can trigger depolarisation. This time is known as the relative refractory period (*RRP*). During the *RRP* impulses propagate more slowly than normally because of the increased time required for each cell to generate an action potential (AP) (Kimura 1983). Using normal human volunteers, Gilliatt and Williams demonstrated the slower conduction velocity associated with the *RRP* (Gilliatt & Willison 1963). They applied two maximal stimuli to the median nerve at the wrist and recorded APs from the nerve at the elbow. With interstimulus intervals (ISIs) of 5ms and 3ms the interval between the APs at the elbow was the same as the ISI. However, for ISIs less than 3ms the interval between the APs was greater than the ISI as the second impulse was propagated during the *RRP* of the nerve and was therefore conducted more slowly. For example with an ISI of 0.7ms the interval between the resulting APs was 1.6ms.

Different methods have been developed to measure refractory period. Initial attempts were made by applying paired stimuli to the same point on a nerve and altering the ISI. Most of these studies were on sensory or mixed nerves. Wagman and Flick applied a similar technique to measure refractory period in motor fibres. However, at

short ISIs the conditioning (first) and test (second) responses overlapped and this resulted in distortion of the test response (Wagman & Flick 1951).

In 1976 Kimura described a collision technique to measure refractory period in motor nerves. In doing so he addressed the problem of distortion of the test impulse (Kimura 1976). This method entailed the use of two proximal stimuli and a single distal stimulus and compound muscle action potentials (CMAPs) were recorded from a target muscle. The first proximal stimulus and the distal stimulus were delivered simultaneously. An early CMAP was produced by the orthodromic impulse from the distal stimulus, whilst the antidromic impulse from the distal stimulus collided with the orthodromic stimulus from the first proximal stimulus, so that it did not produce a CMAP. The interstimulus interval (ISI) between the proximal impulses was gradually increased. As the orthodromic impulse from the first proximal stimulus was blocked there was no distortion of the CMAP associated with the second proximal impulse, as had been encountered with earlier methods using only two stimuli.

With very short ISIs between the proximal stimuli only those fibres with a short refractory period had recovered from the conditioning impulse and therefore were able to conduct a second impulse and generate a late (test) CMAP. As the ISI was increased, successive populations of fibres were recruited and the test CMAP increased in amplitude. Therefore, the fastest-recovering fibres generated the first increase in the test CMAP and the slowest-recovering fibres contributed the final increment.

Kimura *et al* proposed that this method could be used to define the range of absolute refractory periods. They ascribed a decrease in amplitude of the test CMAP to failure of activation of fibres at the site of the second proximal stimulus because these fibres were still refractory. They stated that the amplitude of the test CMAP was

proportional to the number of fibres no longer refractory and that if the amplitude of the test CMAP was compared to the amplitude of the proximal stimulus fired in isolation (where all the fibres would be active) this would give the proportion of the fibres recovered from the refractory period.

In a further series of experiments by the Kimura *et al* two different ISIs were used between the distal stimulus and the first proximal stimulus to assess the effect of altering the length of the refractory segment of nerve (Kimura, Yamada, & Rodnitzky 1978). Using a shorter ISI of 0.5ms the refractory segment was 3cm and with a longer ISI of 1.5ms it was 9cm (this was based on an assumption of a conduction velocity of 60m s^{-1}). The increase in amplitude of the test CMAP with increasing ISI between the distal impulse and the second proximal (test) impulse was the same for both lengths of the refractory segment. However, the latency of the test CMAP was increased with the longer refractory segment of nerve but not in proportion to the length of the refractory segment. This change in latency was attributed to a faster average conduction velocity of the test impulse in the longer refractory segment of nerve than the shorter refractory segment. As the test impulse reached the refractory segment it was slowed by those fibres still in the *RRP* and lagged progressively further behind the conditioning impulse. However, as this distance increased, the test impulse was conducted by more recovered (and therefore faster) fibres. Therefore, the conduction velocity of the test impulse increased in the distal part of the refractory segment. This process took place to a greater extent in the longer refractory segment therefore, the average conduction velocity of the test impulse was faster.

Kimura *et al* proposed that an increase in amplitude of the test CMAP was attributable to the ARP as once a fibre was activated the impulse would be propagated to the muscle regardless of the length of the refractory segment. They also proposed that

changes in latency of the test CMAP were a result of the recovery of conduction velocity of the fastest fibres and hence a measure of the relative refractory period of those fibres.

Ingram *et al* criticised Kimura's methods on three points (Ingram, Davis, & Swash 1986). They stated that the orthodromic impulse from the second proximal stimulus was conducted in the subnormal period of the nerve and was therefore conducted more slowly resulting in over-estimation of the refractory period. They also proposed that the test impulse would be affected by the relative refractory zone associated with the antidromic colliding impulse and the velocity recovery function (VRF) effect in muscle from the conditioning CMAP. VRF is equivalent to the subnormal period of conduction in nerves and has previously been discussed in Chapter 6, in the context of *jitter.*

Ingram *et al* described an alternative technique to measure the range of refractory period in motor fibres using two proximal shocks and two distal shocks (Ingram, Davis, & Swash 1986). The ISI between the proximal stimuli was kept the same and was longer than the refractory period of the whole nerve. This meant that the second proximal stimulus was always conducted. The ISI between the distal stimuli was varied. The first proximal shock and the first distal shock were fired simultaneously. Therefore, the orthodromic impulse from the proximal stimulus was always blocked. When the ISI between the distal stimuli was less than the shortest refractory period the second distal stimulus did not elicit a response. This allowed all the fibres contributing to the orthodromic impulse from the second proximal impulse to generate a late CMAP. This CMAP was therefore of maximum size. As the distal ISI was increased, successive populations of fibres were recruited. These recruited impulses collided with the second proximal impulse and blocked some of the APs. This

collision resulted in a reduction in size of the late CMAP. As the distal ISI was increased, progressively more of the second proximal orthodromic impulse was blocked until the second distal impulse completely blocked the second proximal impulse so that no late CMAP was generated. Disappearance of the late CMAP indicated the end of the range of the refractory periods. Ingram *et al* stated that their method was better than Kimura's because as the ISI between the proximal stimuli was constant, the effect of the subnormal period of nerve conduction and the VRF effect of muscle was the same in all cases. They also stated that indication of the end-point of the range of refractory period by the disappearance of the late CMAP was easier to identify than the final increments in amplitude (indicating unblocking of all fibres) of the test CMAP used in Kimura's method.

In 1976 Betts *et al* described a method to measure refractory period using double stimulation with an "automatic subtraction technique" (Betts, Johnston, & Brown 1976). These authors applied two supramaximal stimuli, with varying ISIs, to a single point on the median or ulnar nerves of normal human volunteers. They recorded APs from a proximal position on the nerve. These APs were passed through an eight-bit analogue-to-digital converter and stored in the memory. A single supramaximal stimulus was then applied and the resulting AP recorded and fed to an analogue subtractor, synchronously, with the two APs previously stored in the memory, which had been passed through a digital-to-analogue converter. The single response effectively cancelled the conditioning response, thus isolating the test response. This process was repeated for a range of ISIs. With long ISIs none of the test response was blocked. The amplitude of this response was assumed to represent 100% of the fibres. As the ISI was shortened, the amplitude of the test response decreased. This decrease in amplitude was thought to be due to blockage of fibres (*i.e.* that these fibres were in

the refractory period) rather than temporal dispersion as there was no measurable change in the dispersion or the latency of the second waveform. The amplitude of successive test responses was expressed as a percentage of the maximum test response allowing calculation of the percentage of fibres which were refractory.

Kopec *et al* described a similar technique to that of Betts *et al* but recorded APs from muscle (Kopec, Delbecke, & McComas 1978). Using normal human volunteers they stimulated the median nerve at the elbow or at the wrist and recorded CMAPs from the thenar eminence. The CMAP (reference trace) generated by a single supramaximal stimulus was stored in the first quarter of the memory in a signal analyser. Paired stimuli were then applied with a range of ISIs. The CMAPs (conditioning and test traces) were stored in the second quarter of the memory of the signal analyser. A programmable calculator was used to subtract the first quarter of the memory from the second quarter of the memory. Since the CMAP from the single stimulus was the same as the conditioning CMAP this isolated the test CMAP. The amplitude of this CMAP was then measured and used to calculate the proportion of fibres in the refractory period. The absolute refractory period was determined from the shortest ISI which allowed generation of a test CMAP.

In the work presented here the *minimum absolute refractory period* (ARP_{min}) and the *maximum absolute refractory period* (ARP_{max}) were calculated using the paired shock technique described by Kopec *et al* (Kopec, Delbecke, & McComas 1978). A reference trace was generated using an ISI of 0ms. Paired stimuli were then applied to the nerve over a range of ISIs from 0ms to 10ms. In the experiments described here test traces were isolated by digitally subtracting the reference trace from the subsequent traces using this function on the Medelc machine whereas Kopec *et al* used a programmable calculator.

ARP_{max} was defined as the ISI associated with the first decrease in amplitude of the test CMAP. Previous workers have interpreted the first decrease in the amplitude of the test CMAP to represent the *RRP* however, in the *RRP* there is slowing of impulse conduction but no blocking therefore a decrease in amplitude of the test CMAP must result from fibres in the *ARP*. ARP_{min} was defined as the smallest ISI before the disappearance of the test CMAP. The *RRP* was not assessed in this work.

Changes in refractory period have been described in association with a variety of systemic conditions and neuropathies. These are discussed in more detail in the discussion. It has also been shown that refractory period is longer in smaller, slower fibres (Blair & Erlanger 1933). Therefore, after nerve injury and regeneration it might be expected that refractory period would be increased.

9.2 MEASUREMENT OF REFRACTORY PERIOD

The positioning of the stimulating and recording electrodes on the nerve and muscle was identical to that used in the measurement of *CVmax* and *DCV* (see Chapter 7, Section 7.2.1 for the facial nerve and Chapter 7, Section 7.2.2 for the median nerve). However, in the calculation of refractory period only the distal stimulating electrode, S1, was required. S1 was connected to stimulator A on the Medelec machine, which provided constant current stimulation using square wave pulses of 50μs duration.

The size of the current required to ensure supramaximal stimulation was determined using a single stimulus. The amplitude of the current was gradually increased until the resulting CMAP no longer increased in size. The stimulus was then increased by a further 30% to ensure activation of all axons. This was designated the supramaximal current and was used for all subsequent stimulation of the nerve.

A reference trace was generated by setting the interstimulus interval (ISI) to 0ms. Using an ISI of 0ms all impulses from the second stimulation were blocked and therefore only one CMAP was generated. This reference trace was digitally subtracted from the subsequent traces to isolate the test trace.

The ISI was then increased to 10ms to obtain two discrete CMAPs. With this ISI the amplitude of the second (test) CMAP was the same as the first (conditioning) CMAP. This indicated that no fibres were blocked and therefore no fibres were refractory.

The ISI was then decreased in steps of 0.5ms until the amplitude of the second CMAP was observed to decrease. The ISI associated with the first decrement in amplitude of the test CMAP was designated ARP_{max}. The decrease in the test CMAP was ascribed to the slowest recovering fibres still being in the absolute refractory period. With the longer ISIs associated with ARP_{max}, the conditioning CMAP did not distort the test CMAP. Therefore it was not necessary to isolate the test CMAP by digitally

subtracting the reference trace. However, in those cases where it was difficult to determine if there was a decrease in the amplitude of the test CMAP, consecutive traces were superimposed on top of each other, using a function on the refractory period program on the Medelec machine, to compare the amplitudes of the traces.

After determination of ARP_{max} the ISI was then further decreased in steps of 0.5ms. This resulted in a decrease in size of the test CMAP and collision of the test CMAP with the conditioning CMAP. As the collision point was approached the ISI was decreased in smaller decrements of 0.1ms. The reference trace was digitally subtracted from these traces to isolate the test CMAP. As defined by Adrian, the ISI preceeding the ISI which resulted in complete blocking of the test trace, was accepted as the absolute refractory period of the nerve (Adrian 1921). In this work this was designated ARP_{min}.

9.3 FACIAL NERVE RESULTS FOR REFRACTORY PERIOD

The raw data for the results of these experiments are shown in Appendix 2. There were no technical difficulties in the measurement of refractory period. The mean values for ARP_{min}, ARP_{max} and ARP_{range} are shown in Table 9.1. The combined results of all the groups are presented graphically in Figure 9.1 using a box and whisker plot.

Facial nerve **Mean values for ARP_{min}, ARP_{max} and ARP_{range} (ms)**						
	Control	**Neurapraxia**	**Axonotmesis**	**Neurotmesis (suture)**	**Neurotmesis (wrap)**	**Graft**
ARP_{min}	0.9	1.0	1.2	1.2	1.1	0.9
ARP_{max}	5.7	6.4	6.4	5.8	6.0	5.1
ARP_{range}	4.7	5.4	5.2	4.6	4.9	4.2

Table 9.1 This table shows mean values of the minimum absolute refractory period, the maximum absolute refractory period and the range of the absolute refractory period for the facial nerve.

Using the normal plot method the measurements of the both ARP_{min} and ARP_{max} were found to be non-parametrically distributed. Kruskal-Wallis tests were then applied to detect the presence of between groups variation. There were no significant differences in ARP_{min} between any of the groups. ARP_{max} showed a significant difference between the normal control group and the neurapraxia group (p=0.025) and between the graft group and both the neurapraxia group (p=0.014) and the axonotmesis group (p=0.039). The results are shown in Table 9.2. When the mean results of the groups were compared it was noted that the graft group had the shortest mean ARP_{max} (5.1ms), whilst the neurapraxia group had the longest mean ARP_{max} (6.4ms). Power

analysis on ARP_{max} revealed it to have a power of 0.4. Figure 9.2 is a box and whisker plot of ARP_{max} showing the median, the box indicates the 25^{th} to the 75^{th} percentiles and the whiskers the minimum and maximum non-outlier range.

ARP_{min} and ARP_{max} were then compared with each other. The combined sets of data were non-parametrically distributed. The Kruskal-Wallis test revealed the presence of significant differences and the Mann-Whitney U test showed that for every experimental group ARP_{max} was significantly longer than $ARP_{min.}$ The range of the absolute refractory period (ARP_{range}) was calculated for each nerve by subtracting ARP_{min} from $ARP_{max.}$ These data were found to be non-parametrically distributed and the Kruskal-Wallis test revealed the presence of significant between groups variation. The Mann-Whitney U test showed that this difference was between the neurapraxia group and all the other experimental groups, including the control group. The neurapraxia group had the highest mean value for $ARP_{range.}$

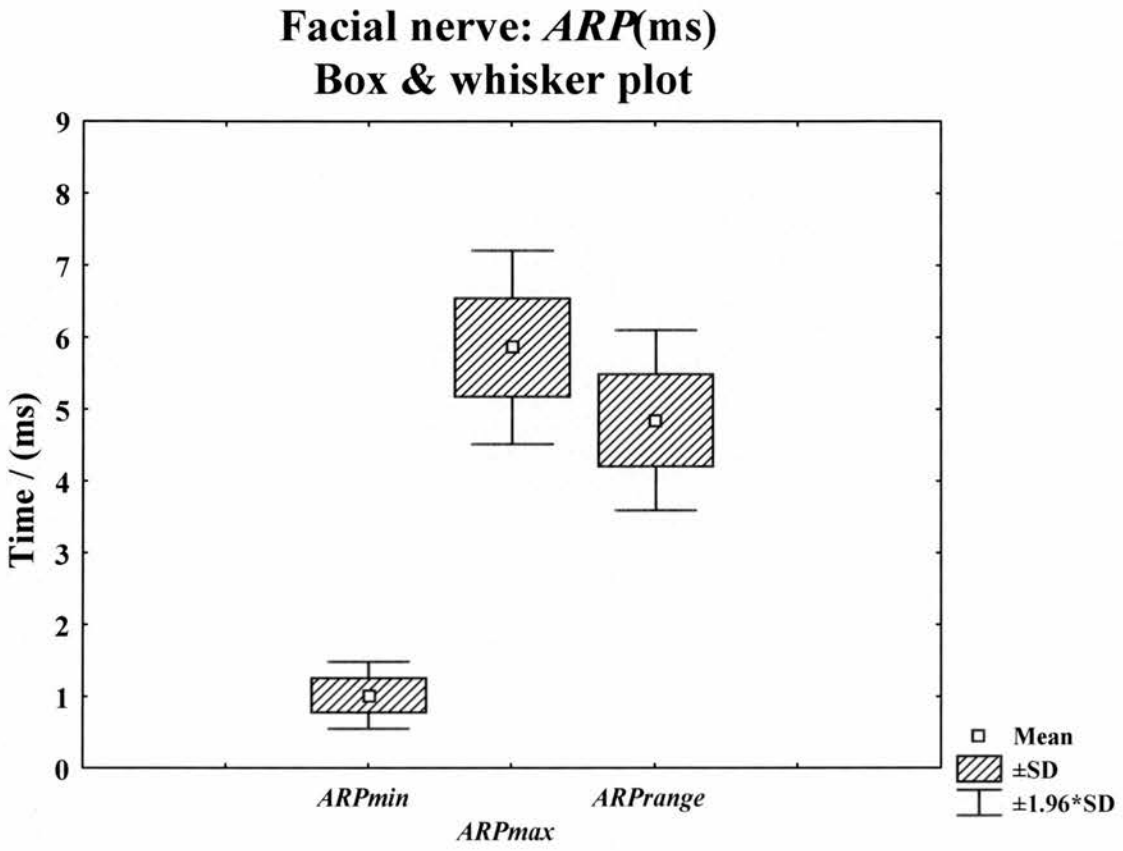

Figure 9.1 This is a box and whisker plot showing the minimum absolute refractory period, the maximum absolute refractory period and the range of the absolute refractory period for the facial nerve. It shows the median value, the box indicates the 25th to the 75th percentiles and the whiskers the minimum and maximum non-outlier range.

Facial Nerve: Mann Whitney U test ARP_{max} / (ms)						
	Normal	Neurapraxia	Axonotmesis	Neurotmesis (suture)	Neurotmesis (wrap)	Graft
Normal		0.025	0.095	0.778	0.304	0.233
Neurapraxia			0.498	0.051	0.067	0.014
Axonotmesis				0.180	0.342	0.039
Neurotmesis (suture)					0.530	0.176
Neurotmesis (wrap)						0.073
Graft						
Mean [SEM]	5.7 [0.21]	6.4 [0.15]	6.4 [0.19]	5.8 [0.25]	6.0 [0.13]	5.1 [0.40]

Table 9.2 This table shows the p values for the Mann–Whitney U test for the maximum absolute refractory period for the facial nerve. Significant differences $p<0.05$ and are highlighted in red. The table also shows the mean values of maximum absolute refractory period for the different experimental groups.

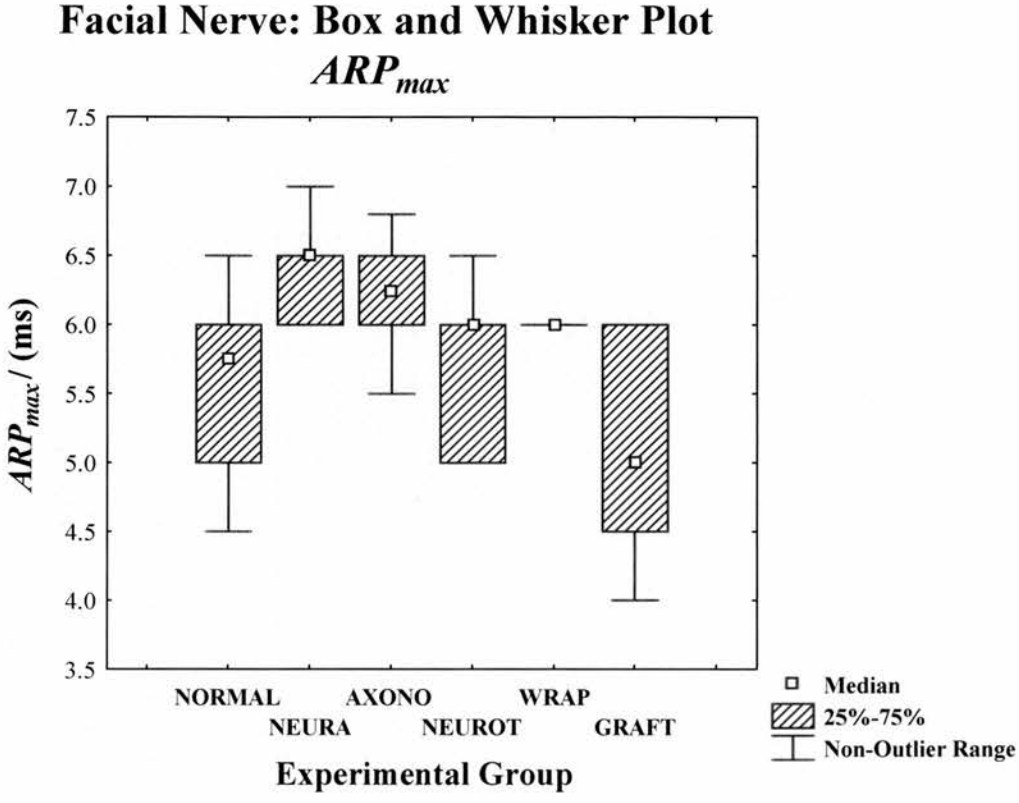

Figure 9.2 This figure is a box and whisker plot which shows the maximum absolute refractory periods for the experimental groups for the facial nerve. It shows the median value, the box indicates the 25th to the 75th percentiles and the whiskers the minimum and maximum non-outlier range.

9.4 MEDIAN NERVE RESULTS FOR REFRACTORY PERIOD

The raw data for the results of these experiments are shown in Appendix 2. There were no technical difficulties in the measurement of refractory period. The mean values for ARP_{min}, ARP_{max} and ARP_{range} are shown in Table 9.3. The combined results for all the groups are presented graphically in Figure 9.3 using a box and whisker plot.

Median nerve **Mean values for ARP_{min}, ARP_{max} and ARP_{range} (ms)**						
	Control	**Neurapraxia**	**Axonotmesis**	**Neurotmesis (suture)**	**Neurotmesis (wrap)**	**Graft**
ARP_{min}	1.0	1.0	0.9	0.9	0.7	0.8
ARP_{max}	6.2	6.6	6.3	6.4	6.3	6.7
ARP_{range}	5.2	5.6	5.4	5.6	5.6	5.9

Table 9.3 This table shows mean values of the minimum absolute refractory period, the maximum absolute refractory period and the range of the absolute refractory period for the median nerve.

Using the normal plot method the measurements of the both ARP_{min} and ARP_{max} were found to be non-parametrically distributed. Kruskal-Wallis tests were then applied to detect the presence of between-groups variation. There were no significant differences in ARP_{min} and ARP_{max} among any of the experimental groups.

As for the facial nerve experiments, ARP_{min} and ARP_{max} were compared with each other. The combined sets of data were non-parametrically distributed. The Kruskal-Wallis test revealed the presence of significant between groups variation and the Mann-Whitney U test showed that for every experimental group ARP_{max} was significantly longer than ARP_{min}. The range of the absolute refractory period (ARP_{range})

was calculated for each nerve by subtracting ARP_{min} from $ARP_{max.}$ These data were found to be non-parametrically distributed. The Kruskal-Wallis test revealed there were no significant differences between any of the experimental groups.

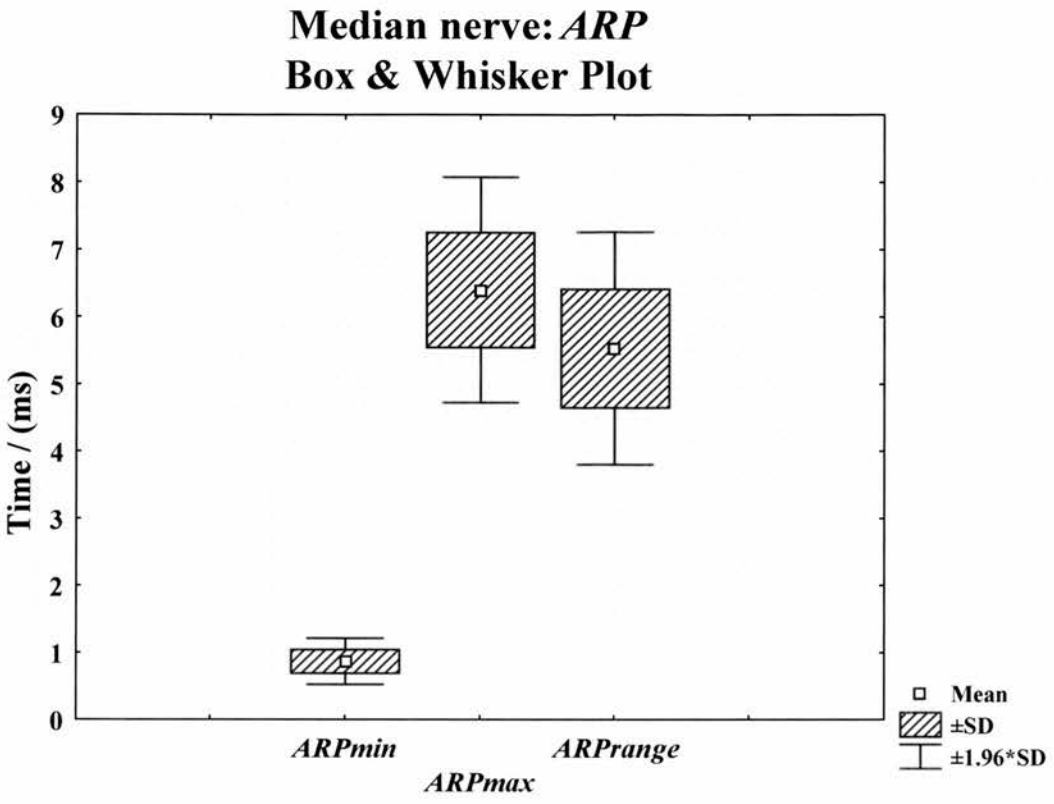

Figure 9.3 This is a box and whisker plot showing the minimum absolute refractory period, the maximum absolute refractory period and the range of the absolute refractory period for the median nerve. It shows the median value, the box indicates the 25th to the 75th percentiles and the whiskers the minimum and maximum non-outlier range.

9.5 Comparison of Facial Nerve & Median Nerve Results for Absolute Refractory Period

The results of ARP_{min} *and* ARP_{max} for the facial nerve experimental groups and the median nerve experimental groups were compared. The data sets were combined and normality of the data was determined by constructing normal probability plots of the raw residual values. Both sets of data were shown to be normally distributed as they lay along a straight line. Factorial ANOVA was performed to detect the presence of between groups variation. Factorial ANOVA was used as there were two independent grouping variables (nerve and experimental group). No significant differences were found when both the specific nerve and the experimental group were considered together.

9.6 DISCUSSION

ARP_{min} varied between 0.9ms and 1.1ms for the facial nerve and 0.7ms and 0.1ms for the median nerve. ARP_{max} varied between 5.1ms and 6.4ms for the facial nerve and 6.2ms and 6.7ms for the median nerve. There were no significant differences for ARP_{min} among any of the experimental groups for both the facial nerve and the median nerve. There were no significant differences for ARP_{max} among the experimental groups for the median nerve. Significant differences were found for ARP_{max} for the facial nerve experimental groups but on scrutiny of the results it was noted that the neurapraxia group had the longest mean ARP_{max} whilst the nerve graft group had the shortest mean ARP_{max}. Therefore, there was no correlation of ARP_{max} with the severity of nerve injury. Power analysis revealed ARP_{max} to have a power of only 0.4 and these findings may therefore be attributed to small group size.

It should also be noted that the measurement of ARP_{min} was more precise than that of ARP_{max}. ARP_{min} was determined by the disappearance of the test CMAP after subtraction of the conditioning CMAP whereas ARP_{max} was determined by judging that the amplitude of the test CMAP had decreased. Although the traces were superimposed to help compare amplitudes this was still a more subjective test. Furthermore, the ISI was altered by decrements of 0.5ms in the measurement of ARP_{max} and decrements of 0.1ms in the measurement of ARP_{min}.

When ARP_{min} was compared to ARP_{max} for each experimental group, there was a significant difference between these two variables for both the facial nerve and the median nerve. When ARP_{range} was compared, the facial nerve neurapraxia group had a significantly higher value than the other experimental groups. This can be explained by the high mean value for ARP_{max} for this group. There were no significant

differences between any of the other facial nerve experimental groups for ARP_{range} and there were no differences in ARP_{range} between any of the experimental groups for the median nerve.

The above results show that the severity of the nerve injury had no significant effect on *ARP*. However, there was a significant difference between ARP_{min} (fastest recovering fibres) and ARP_{max} (slowest recovering fibres) for each experimental group for both nerves. There was no difference in the size of the range of *ARP* (ARP_{range}) between the experimental groups. ARP_{range} was between 4.2ms and 5.4ms for the facial nerve and between 5.2ms and 5.9ms for the median nerve. These results suggest there was more variation in *ARP* within each nerve than between experimental groups.

It is generally accepted that smaller slower fibres have longer refractory periods than larger faster fibres (Blair & Erlanger 1933). However, there has been some debate regarding the relationship between refractory period and conduction velocity and consequently how this relationship should be incorporated into nerve conduction studies in particular collision studies such as *DCV*.

Betts *et al* measured the range of *ARP* and the range of conduction velocities in the motor fibres of ulnar nerves of normal human volunteers using a double stimulus technique (Betts, Johnston, & Brown 1976). They measured a range of *ARP* from 0.65ms to 3.6ms and plotted the amplitude of the test CMAP as a fraction of the maximum amplitude of the test CMAP (100% of fibres active) against ISI. They then differentiated this to derive the proportion of fibres which had recovered from the *ARP* for each ISI and found that the distribution of refractory period was skewed to the left, with the majority of fibres having a short absolute refractory period.

Betts *et al* concluded that for Group A fibres the random scatter of refractory periods was greater than any variation due to a correlation between conduction velocity and

refractory period. They suggested that if refractory period was to be considered in the calculation of conduction velocity a median value should be used (given that the range of refractory period had a non-parametric distribution). When these authors used an inverse relationship to correlate the range of refractory periods with conduction velocity they generated negative conduction velocities. However, using a single median value they calculated a velocity range of 15m s^{-1} to 20m s^{-1}. For the fast conduction velocities this correction factor gave results similar to those derived from direct measurement. However, in their calculations of *DCV* Harayama *et al* used an inverse relationship between conduction velocity and refractory period and found that this generated appropriate values of conduction velocity (Harayama, Shinozawa, Kondo, & Miyatake 1990).

Kimura *et al* found that by increasing the ISIs, the test CMAP reached its maximum amplitude before the latency returned to its minimum value (Kimura, Yamada, & Rodnitzky 1978). They proposed that this was because the most excitable (fastest) fibres were still in the relative refractory period when the least excitable (slowest) fibres were no longer in the absolute refractory period. These results may suggest that the relative refractory periods of different fibres have a close distribution.

In investigations on human single short toe extensor motor units Borg demonstrated that increasing the strength of the stimulus resulted in shorter refractory periods (Borg 1980). Using a stimulus 10% above threshold the mean refractory period of twenty-five motor units was 1.72ms±0.29 whereas using a stimulus 50% above threshold, the mean refractory period was 0.64ms±0.22. The difference of the refractory period between these two stimulation levels was a mean of 1.08ms ($p<0.001$). There was a small decrease in latency using the 50% supramaximal stimulus. This indicated some stimulus spread but not enough to account for the decrease in refractory period. Borg

commented that there may be as much as a hundred-fold difference between high-threshold and low-threshold axons and advocated a stimulus strength for measurement of refractory period 50% above that which produced a percutaneously recorded maximal muscle response. Using supramaximal stimulation, 10% above threshold, there was an inverse relationship between conduction velocity and *ARP* however, with stimulation 50% above threshold this relationship disappeared.

There was a significant difference in *ARP* between the fastest recovering fibres and the slowest recovering fibres for each experimental group. This suggests that *ARP* should be taken into account in the determination of *DCV*. Failure to consider refractory period will lead to an underestimation of the conduction velocity of the slower fibres as these fibres have a longer refractory period which is therefore a bigger proportion of the latency of an impulse. However, in the work presented here there were no significant differences in *ARP* between the different experimental groups. Therefore, failure to consider *ARP* in the determination of *DCV* may have had a similar effect on each group.

The proportion of time which the refractory period contributes to the latency of an impulse is also determined by the length of nerve examined and with regard to *RRP* to the length of the refractory segment. The length of the refractory segment of the nerve is important because the average conduction velocity of a test impulse is faster in a longer refractory segment of nerve than a shorter refractory segment. This is because the test impulse is slowed in the refractory segment and progressively lags behind the conditioning impulse. However, as the distance between the impulses increases the test impulse is conducted by progressively more recovered fibres until it eventually reaches normal nerve. Therefore, the conduction velocity of the test impulse increases in the distal part of the refractory segment (Kimura, Yamada, & Rodnitzky 1978).

The refractory period is a bigger proportion of the conduction time in short segments of nerve as compared to longer segments (Betts, Johnston, & Brown 1976). Kopec *et al* measured refractory period in the median nerve of normal human volunteers (Kopec, Delbecke, & McComas 1978). They used paired stimulation of the nerve at the elbow or at the wrist and recorded CMAPs from the thenar eminence. With paired stimulation at the wrist the shortest ISI which elicited a test CMAP was 1.1ms whereas at the elbow a response was elicited with an ISI of 0.8ms. They noted that the test impulse was more delayed with stimulation at the elbow and ascribed this to slowing of the impulse during the relative refractory period in the additional length of nerve available for conduction from the elbow to the wrist. Therefore, as described before, the test impulse, with stimulation at the elbow, is conducted in progressively more recovered nerve therefore allowing a response to be elicited at lower ISIs.

In the work presented here, *ARP* was measured by stimulation of the nerve distal to the site of the injury. It would be interesting to repeat the experiments using stimulation proximal to the site of injury. This could affect the results obtained on two counts; first because the length of nerve investigated would be longer and secondly because the impulse would be propagated across the site of injury. From *DCV* experiments, which involved repeated stimulation of the nerve proximal to the site of injury, it was observed that the facial nerve graft group required time to recover between pairs of stimulations and it was not possible to obtain *DCV* profiles on the median nerve graft models. Therefore, if *ARP* was measured by stimulation proximal to the site of injury these groups may have had longer *ARP*s than the less severely injured groups.

Shefner and Dawson investigated the use of refractory period in the diagnosis of peripheral nerve disease (Shefner & Dawson 1990). They measured *CVmax* and *RRP*

in the sural nerves of diabetic patients with and without symptoms of neuropathy. In symptomatic patients they found that *CVmax* was decreased in 53% of cases and *RRP* was increased in 77% of cases. In asymptomatic patients *CVmax* was decreased in only 11% of cases whereas *RRP* was increased in 46% of patients. Similarly they found that *RRP* was increased in multiple sclerosis whilst *CVmax* remained within normal limits. They also found that *RRP* was increased in alcoholism, schizophrenics on lithium (*RRP* returned to normal on cessation of lithium) and carpal tunnel syndrome. These authors concluded that *RRP* was a sensitive indicator of nerve pathology.

Delbecke *et al* found that refractory period was normal in patients with myotonic dystrophy, motor neurone disease and spinal muscular atrophy (Kopec, Delbecke, & McComas 1978). They suggested that the measurement of refractory period remained normal in these patients because the abnormal fibres were not activated and therefore not assessed. They also found that refractory period was normal in patients with renal failure undergoing haemodialysis. It is known that uraemic nerves undergo axonal degeneration and secondary demyelination (Lowitzsch et al. 1981). The resting cell membrane potential is also decreased which may be a result of hyperkalaemia associated with renal failure. Lowitzsch *et al* investigated the refractory period of sural nerves, using supramaximal double shocks of varying ISI, in eighteen renal dialysis patients before and after they underwent dialysis (Lowitzsch, Gohring, Hecking, & Kohler 1981). Prior to dialysis half the patients had increased refractory periods but after dialysis all but one returned to normal. These results are in keeping with Delbecke's findings.

Borg showed that refractory period was increased with skin temperatures 4°C below normal and more than doubled with temperatures 10°C below normal (Borg 1980).

Delbecke also demonstrated an increase in *ARP* and *RRP* with decreasing temperature (Kopec, Delbecke, & McComas 1978). This increase in refractory period was thought to be secondary to prolongation of sodium channel inactivation and potassium channel opening.

There is no clear consensus on the relationship between refractory period and different disease processes. There is some suggestion from the literature that *RRP* is a more sensitive indicator of nerve pathology than *ARP*, therefore in future work it would be interesting to measure *RRP* as well as *ARP* (Shefner & Dawson 1990).

In summary, there were no significant differences in *ARP* among the experimental groups. However, stimulation of the nerve proximal to the site of injury may have revealed differences with those groups with more severe injuries having longer refractory periods. There were significant differences in *ARP* among the fibres within each experimental group. Therefore, in the determination of *DCV* refractory period should be considered. It would be useful to determine the range of refractory period using the double stimulation technique described by Betts *et al*(Betts, Johnston, & Brown 1976). This would elucidate whether nerve injuries have any effect on the distribution of refractory period and help to determine how refractory period should be incorporated into the calculation of *DCV*.

10 MUSCLE PHYSIOLOGY

10.1 INTRODUCTION

Measurements of the properties of muscles are useful in the study of nerve injury and regeneration because it provides information on end-organ function. When an axonal impulse reaches the neuromuscular junction (NMJ) it results in release of acetylcholine (ACh) into the synaptic cleft (the region between the nerve terminal and the muscle fibre). ACh binds to receptors on the muscle membrane resulting in end-plate action potentials. This initiates opening of sodium channels an action potential of the muscle membrane, which is conducted to myofibrils within the fibre, by a system of T-tubules. The T-tubule APs result in release of Ca^{2+} ions from the sarcoplasmic reticulum which leads to muscle contraction. This is termed excitation-contraction coupling (Guyton 1991).

The contractile machinery of muscle consists of the proteins actin (thin filament) and myosin (thick filament). Actin is bound to the inhibitory troponin-tropomysin complex. When Ca^{2+} ions are released from the sarcoplasmic reticulum they bind to troponin C. This is thought to induce a conformational change in tropomysin which exposes active sites on the actin protein allowing muscle contraction to proceed. Actin and myosin produce muscle contraction by sliding along each other by making and breaking cross-bridges. Energy for this process is supplied by adenosine triphosphate (ATP) binding to myosin. ATP is supplied from three sources; creatine phosphate, the glycolysis-lactic acid system (anaerobic metabolism) and oxidative phosphorylation (aerobic metabolism).

Mammalian skeletal muscle contains three types of fibre, Type I/red/slow-twitch, Type IIb/white/fast-twitch and Type IIa/red/fast-twitch. Red/slow-twitch fibres

contain high levels of myoglobin and mitochondria which facilitate oxidative phosphorylation. They are resistant to fatigue and predominate in tonic, postural muscles. White/fast-twitch fibres have a well-developed glycolytic enzyme system and demonstrate high myosin-ATPase activity. They fatigue rapidly and are predominantly found in phasic muscles. Red/fast-twitch fibres are intermediate between red/slow fibres and white/fast fibres.

A motorneurone and the muscle fibres which it innervates are termed a motor unit. The number of fibres in each motor unit varies from two to three fibres, for those muscles which require fine control, to several hundred fibres, for those muscles involved in more gross movement. For example, laryngeal and extrinsic eye muscle motor units have only a few muscle fibres whereas those in gastrocnemius have several hundred (Kimura 1983). Muscle fibres of a single motor unit do not lie adjacent to each other but interdigitate with other motor units (Borg 1980). The fibres are spread out through the muscle in microbundles of three to fifteen fibres. Muscle fibres of a single motor unit are the same type (Kugelberg, Edström, & Abbruzzese 1970).

Denervation of muscle results in flaccidity and paralysis. After denervation the blood supply to muscle is decreased owing to loss of the pumping action on blood vessels caused by muscle contraction. Forty-eight hours after denervation the resting membrane potential decreases and over the next three days the muscle becomes more sensitive to ACh (Kimura 1983). Changes in action potentials and altered excitability result in spontaneous muscle activity called fibrillation. Fibrillation persists as long as the contractile elements within muscle survive.

Denervated muscle becomes paler and decreases in both size and weight. Weight loss is most marked in the first two months after denervation then stabilises (Sunderland

1978). 10% to 25% of normal muscle consists of connective tissue. Weiss and Eds transected the sciatic nerves of rats and found that the weight of the leg muscles fell to 22% of normal (Weiss & Edds 1946). They suggested that the decrease in muscle weight associated with denervation was a result of the loss of contractile tissue. However, denervation experiments in the opposum demonstrated that skeletal muscle retained its histological characteristics 485 days after loss of its nerve supply (Sunderland 1978). Bowden and Gutmann found normal fibres in human muscle three years after denervation (Bowden & Gutmann 1944). Gutmann performed denervation experiments on rabbits and found that muscle had degenerated by twenty months but retained the ability to form new end-plates and regenerate on reinnervation (Gutmann 1948).

As muscle degeneration progresses, fibroblasts proliferate and there is a relative increase in the amount of connective tissue with thickening of the perimysium and endomysium. Muscle fibres may be replaced with fibrous tissue which can result in shortening of muscle and the formation of contractures.

Reinnervation of muscle takes place when pioneering axons reach motor end-plates and form new NMJs. However, the reestablishment of muscle function depends on other factors. These include innervation of appropriate target organs and the subsequent maturation of the associated nerve and muscle fibres to allow return of precision and power of motor function. Good return of function has been observed in humans after periods of denervation of a year (Sunderland 1978). Factors leading to a poor outcome in the return of motor function include a reduction in the number of effective axons, fibre mismatching at the suture line resulting in an abnormal pattern of reinnervation, abnormalities of activation at a central level and irreversible changes

in muscle fibres resulting in abnormal function despite appropriate innervation (Sunderland 1978).

10.2 TWITCH TIME

Muscle can contract isotonically or isometrically. During an isotonic contraction muscle shortens as it performs work against a fixed load. The characteristics of the contraction depend both on the size of the load against which it contracts and also the inertia of the load. In an isometric contraction the length of the muscle remains unchanged. In an isometric system the muscle contracts against a constant load (*e.g.* a tension transducer) and only the changes generated by the force of contraction are recorded. Isometric contraction is easier to measure experimentally as both ends of the muscle are fixed. Isometric contraction was therefore used in the work presented in this thesis.

As previously described excitation of muscle results in release of Ca^{2+}ions from the sarcoplasmic reticulum into the sarcoplasm, where they bind to troponin. This results in the release of the contractile mechanism from the inhibitory troponin-tropomyosin complex. In both normal and cross-innervated muscle the intrinsic speed of shortening of sarcomeres is directly proportional to the specific activity of actin-activated ATPase of myosin (Close 1972). Relaxation of the muscle occurs when Ca^{2+} is removed from the troponin-tropomyosin complex and taken up by the sarcoplasmic reticulum.

The capacity of a muscle to generate tension is termed the active state. The duration of the active state which follows a single stimulus is thought to be determined by one of the two following mechanisms. The first of these is that the rate of re-uptake of Ca^{2+} ions by the sarcoplasmic reticulum determines the rate of muscle relaxation. In

vitro studies using fragmented sarcoplasmic reticulum have demonstrated that the rate of uptake of Ca^{2+} in fast muscles is between four to eleven times faster than that for slow muscles (Fiehn & Peter 1971). Furthermore, fast muscles have twice as much sarcoplasmic reticulum as slow muscles. The second proposal is that the process is under an intrinsic control mechanism. One such mechanism may be that Ca^{2+} ions displaced from the contractile material are in a form which prevents them from binding to the contractile mechanism again but allows its uptake by the sarcoplasmic reticulum. The isometric twitch time is three times shorter in fast-twitch muscle than slow-twitch muscle (Close 1964).

Cross-innervation experiments have demonstrated that the speed of muscle contraction is influenced by the type of innervation. Buller *at al* performed cross-innervation experiments in the cat using the nerve to soleus which contains slow motor neurones and the nerve to flexor digitorum longus (FDL) which contains fast motor neurones. They demonstrated that when soleus was cross-innervated with the nerve to FDL it assumed the characteristics of a fast muscle. Conversely, when FDL was cross-innervated with the nerve to soleus it altered its characteristics to those of a slow muscle (Buller, Eccles, & Eccles 1959). Cross performed similar experiments in the rat model. He cross-innervated extensor digitorum longus (EDL) with the nerve to soleus and soleus with the nerve to EDL. He showed that these muscles converted to slow-twitch and fast-twitch types respectively (Close 1965a). Further cross-innervation experiments in the rat demonstrated that a change in the type of innervation resulted in an altered population of muscle fibres (Barany & Close 1970).

Isometric twitch time was measured in this work as it was postulated that it might be increased after nerve injury. The rationale for this was that after nerve transection muscle is reinnervated by thinner, slower axons and as discussed, previous research

has shown that both speed of muscle contraction and muscle-fibre type are influenced by the type of innervation. The isometric twitch time includes both the time for muscle to contract and also the time for muscle to relax. In the present work this was assessed by measurement of the time to the peak (isometric) twitch tension (denoted *time to peak twitch*) and the time for the muscle to relax to half the peak twitch tension (denoted *time to half relaxation*). The time to half-relaxation of the muscle as opposed to full relaxation of the muscle was measured because this point could be more reliably identified (see Section 10.6).

10.3 TWITCH AND TETANIC TENSION

Muscle contains a contractile component and an elastic component. The elastic component consists of non-contractile structures such as connective tissue, sarcolemma, blood vessels and nerves. These structures stretch during muscle contraction. There is no tension in an unstimulated muscle of resting length. However, as muscle is stretched the amount of tension increases owing to the elastic component. This is termed the resting or passive tension. The tension which develops as muscle contracts is termed the active tension.

The maximum isometric tetanic tension is generated when a muscle is stretched to 120% of its resting length, prior to stimulation (Close 1972). According to the sliding filament theory maximum tetanic tension is obtained when there is maximum overlap of thick and thin filaments. If the muscle length is too short the thick filaments are limited because they oppose each other at the Z-bands. Furthermore, the process of activation of the muscle is thought to be less efficient at shorter lengths. Conversely if the muscle is stretched so the length of the sarcomere exceeds the combined length of

the thick and thin filaments *i.e.* there is no overlap; there is a linear decline in tetanic tension (Gordon, Huxley, & Julian 1966a).

The optimal muscle length to generate the maximum isometric twitch tension is 5% to 10% greater than that for isometric tetanic tension. Muscle lengths below the optimal tetanic length do not alter twitch tension however, as the pre-stimulus length of the muscle is increased from the optimal tetanic length to the optimal twitch length the twitch tension generated increases. This is thought to result from the extent of overlap of thick and thin filaments and a length-dependent change in activation (Gordon, Huxley, & Julian 1966b). The optimum length of a sarcomere needed to generate the maximum twitch tension is 2μm (Gordon, Huxley, & Julian 1966b).

Isometric twitch tension is a function of the number of active motor units and the frequency at which these units repetitively contract (Lippold 1952). This may be related to the concentration of Ca^{2+} ions released. Desmedt and Hainaut showed that repetitive stimulation of muscle resulted in an increase of twitch tension to 136% of that initially obtained (Desmedt & Hainaut 1968). The speed of muscle contraction and relaxation was also decreased. These authors attributed this to a greater release of Ca^{2+} ions from an action potential and an increased rate of reuptake of Ca^{2+}ions.

Burke showed that fast motor units generate more tension than slow motor units (Burke 1967). Luff *et al,* also in the cat, found that fast-fatiguable motor units generated higher tensions than fast-non-fatiguable units which in turn generated more tension than slow units (Luff, Hatcher, et al. 1988).

An isometric twitch is produced by the delivery of a single stimulus to the muscle. Hartree and Hill showed that for a single stimulus H/Tl (where H is heat, T is twitch and l is muscle length) had the same value and proposed that isometric twitch tension is the best measure of mechanical response of a muscle (Hartree & Hill 1921).

However, an isometric twitch contraction does not allow adequate time for the contractile mechanism to develop maximum tension. Furthermore, the tension recorded at the muscle tendon is diminished by the passive elastic component which is still stretching (Desmedt & Hainaut 1968).

Individual twitch contractions can add together to increase the overall intensity of muscle contraction. This is termed summation. There are two types of summation, multiple fibre summation and frequency summation. The latter is also known as tetanus. In multiple fibre summation the number of motor units contracting is increased. Low levels of stimulation result in activation of the smallest motor units (Burke 1980). As the signal strength is increases, progressively larger motor units are recruited. This is known as the size principle.

In tetanus (frequency summation) the frequency of motor unit contraction is increased. Low frequency stimulation of muscle results in twitch contractions one after the other. As the frequency of stimulation is increased the next contraction occurs before the previous one has finished. These contractions add together and the strength of muscle contraction is increased. At higher rates of stimulation the contractions fuse together and muscle contraction becomes smooth and continuous. This is tetanus. The force of tetanic contraction can be increased until a point when Ca^{2+} ions remain in the sarcoplasm between action potentials and the contractile state is constantly maintained. Therefore, tetanus allows complete activation of muscle. The ratio of isometric twitch tension to isometric tetanic tension, in adult mammals at 37°C, is 1 to 3-5 (Close 1972).

After nerve injury, muscle is reinnervated with smaller, slower nerve fibres. As previously discussed this may result in a change in muscle fibres to a slower type

which produce less tension. Therefore, after nerve injury, there may be a reduction in both twitch and tetanic tension.

Two other measurements, relating to muscle tension, were also used in this present work. These were *time tension integral* and *time tension index*. *Time tension integral* was the total force generated by the muscle to the arbitrary point of half-relaxation of the twitch contraction (or half-fatigue of the tetanic contraction). The *time tension integral* was equal to the momentum (mass × velocity) produced in a heavy suspended mass, by muscle contraction (Hartree & Hill 1921). It therefore reflected the ability of a muscle to move heavy loads. Hartree and Hill found a linear relationship between the time tension integral and the amount of heat produced by the muscle. The *time tension index* represented the average force generated by the muscle, again to the point of half relaxation. It was calculated by dividing the *time tension integral* by the *time to half relaxation* (or *half fatigue*).

10.4 FACIAL NERVE EXPERIMENTAL SET-UP

The existing incision, previously used to expose the left facial nerve, was extended to reach the snout of the animal. The levator labii maxillaris muscle was identified lying superficially beneath the distal end of the incision. This muscle originated from the maxilla and inserted by means of a single tendon into the snout. Levator labii maxillaris was selected because it was supplied by the facial nerve and had a discrete tendon which could be easily attached to a tension transducer. Previous workers had used mass movement of the snout to assess target muscle physiology however, it was thought that a single muscle would allow more specific measurements to be made. The proximal end of the muscle was left *in situ* and disturbed as little as possible to minimise damage to its innervation and blood supply. The distal tendon was dissected free. The end of the tendon was attached with non-extensible linen thread to the arm of an isometric tension transducer (#52-9503, Harvard Instruments, Edenbridge, UK) which was mounted on a heavy photographic stand. The base of this stand had three adjustable feet, the height of which could be altered to compensate for any uneveness of the floor. The platform of the photographic stand, on which the tension transducer was mounted, could be moved in three planes which enabled optimal positioning of both the tension transducer and the muscle.

The longitudinal orientation of the muscle was maintained as closely as possible to the anatomical position. However, the tendon of the muscle was elevated slightly so that the muscle was not in contact with surrounding structures both at rest and during contraction. This was to stop friction interfering with the subsequent measurements. The platform on the photographic stand was positioned so that the longitudinal orientation of the muscle, and therefore the direction of the tension generated, was at

ninety degrees to the arm of the tension transducer. The muscle was stretched to 120% to 130% of its resting length because as previously discussed muscle length has been shown to affect the force of contraction (Buller, Eccles, & Eccles 1960;Close 1972). The output signal from the tension transducer was connected to an amplifier which in turn was connected to the y-input of an oscilloscope. The amplifier could be set to amplify a 50 or 500g f.s.d. input depending on the amount of tension expected to be generated.

A calibration curve was plotted to convert the output of the tension transducer from volts to newtons. The tension transducer was mounted on the photographic stand so that its arm was parallel to the floor. The DC output from the transducer was connected to the y-input of the oscilloscope. A succession of weights was suspended from the transducer over a range of 5g to 400g. The deflection on the oscilloscope was noted for each weight. The force each weight produced was calculated using the equation

$$F = g \times m$$

Where:

F = force produced in newtons (N)

m = mass in kilograms (kg)

g = acceleration produced by gravity = $9.81 ms^{-2}$

A graph of force against voltage was plotted. Using a mathematical modelling program, Datafit, the best-fit curve was drawn through the points and the equation of the line was calculated. This was found to be linear and its equation was

$$y = 2.593x + 0.037$$

Where:

y = force produced in newtons (N)

x = voltage recorded (V)

Figure 10.1 shows the calibration plot for the tension transducer.

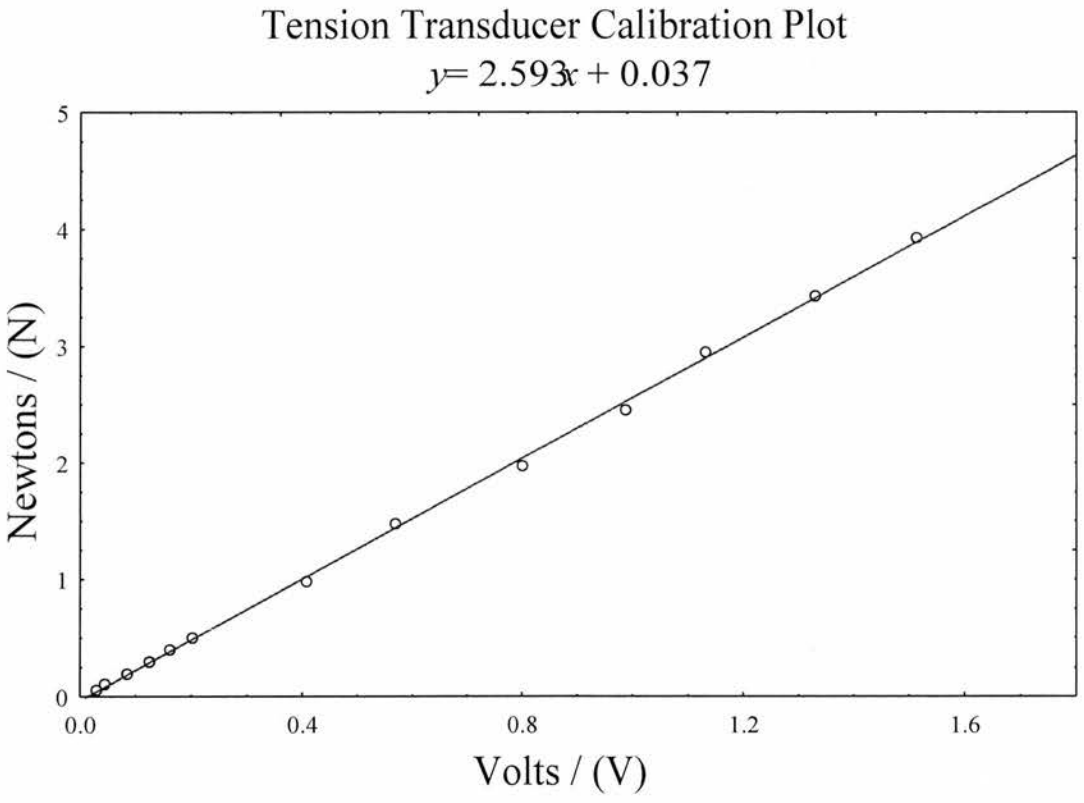

Figure 10.1 shows the calibration graph for the tension transducer.

All recording and stimulating electrodes were removed except for the distal stimulating electrode, S1, which was left in the same position on the facial nerve. The input to S1 was changed from stimulator A on the Medelec to a isolated stimulator, which in turn was connected to the Medelec. The Medelec was also connected to

channel A of the oscilloscope. An isolated stimulator was used because it was not possible to set the Medelec to both stimulate the nerve, and trigger the oscilloscope to record. However, the Medelec could be used to both trigger the signal generator to deliver a stimulus to the nerve and trigger the oscilloscope to record. Furthermore, the Medelec was required to provide the repetitive stimulation required to induce tetanus in the muscle.

The isolated stimulator produced constant current, square wave impulses of 100μs duration. The amplitude of the current was set at the previously determined supramaximal level. A constant current output was selected because as previously discussed this is better than constant voltage for repetitive stimulation of a nerve, where changes in resistance may occur. Figure 10.2 is a diagram which shows the connections between the equipment described above.

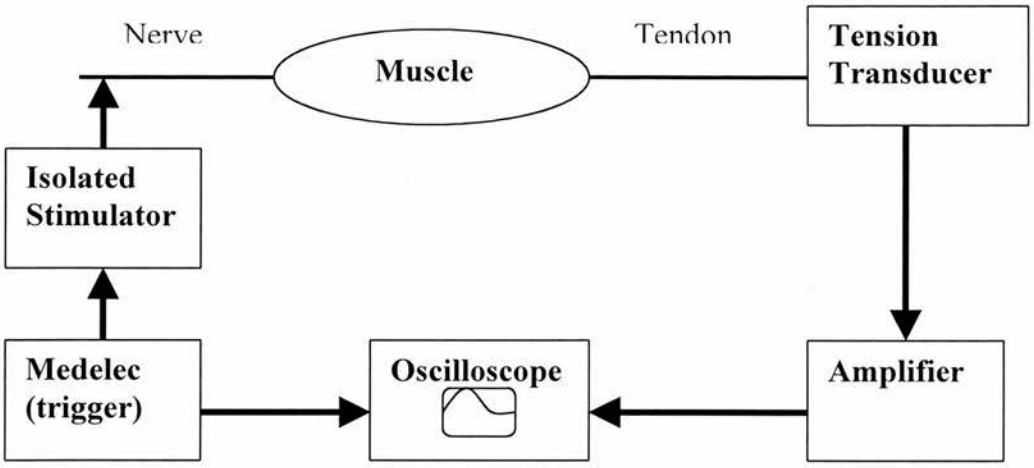

Figure 10.2 This is a diagram to show the electronic set-up required to make the isometric twitch and tetanic measurements.

10.5 MEDIAN NERVE EXPERIMENTAL SET-UP

The existing incision, previously used to expose the median nerve, was extended distally along the volar surface of the sheep's foreleg. This exposed the flexor carpi radialis (FCR) muscle. FCR lay adjacent to the bigger flexor carpi ulnaris (FCU) muscle and on top of flexor digitorum superficialis and flexor digitorum profundus. FCR and FCU were enclosed in a fascial sheath which was incised. The proximal portion of FCR was left intact so as not to disturb its blood supply and innervation. Using a finger, the tendon of FCR was dissected free to its insertion, distal to the elbow, on the radius. The tendon was divided here.

A length of linen was tied around the tendon, 1cm from its distal end. The two free ends of the linen were knotted together to form a loop. The portion of tendon distal to the linen tie was folded back, along the proximal tendon, to form a loop with the linen tie at its apex. The tendon was secured in this position with a second tie. Previous workers had used steel wire to attach the tendon to the tension transducer. However, this had resulted in problems with the wire cutting through the tendon during muscle contraction. The method described above, using linen ties, was found to be a more secure method of attachment of the tendon.

Stimulation of the median nerve resulted in contraction of all its target muscles. It was therefore necessary to secure the forelimb with an opposing and at least equal force to that generated by these muscles. The limb was released from its support which was then detached from the operating table. A hole was drilled through the keratinous portion of the cloven hoof using a 4.5mm power drill. A Steinman pin was then inserted through this tunnel, such that it lay at 90^{o} to the long axis of the forelimb.

A G clamp, with a metal hook soldered on to it, was attached to a nearby bench which itself was securely attached to the wall. A steel cable was attached to the Steinman pin by means of a karabiner. A second karabiner at the other end of the rope was attached to the hook on the G clamp. Tension on the forelimb was increased by rotating the operating table away from the G clamp and also by use of a tensioner on the steel cable.

FCR was attached to the tension transducer using the loop of linen previously tied to it. The muscle was maintained as closely as possible to its anatomical orientation except that the tendon was elevated so that the muscle did not touch surrounding structures. The arm of the tension transducer was adjusted so it lay at 90^{o} to the length of the muscle. FCR was stretched to 120% of its resting length, to maximise the tension subsequently generated.

The proximal stimulating electrode was removed from the median nerve and the distal electrode was left in the same position on the nerve, that had been used for the previous experiments. The input to this electrode was changed from stimulator A on the Medelec, to the isolated stimulator. The connections between the Medelec, signal generator, tension transducer, amplifier and oscilloscope were the same as those previously described for the facial nerve experiments and as shown in Figure 10.2.

10.6 TWITCH TENSION MEASUREMENTS

The twitch tension program was selected from the test menu on the Medelec machine. The Medelec was changed to external stimulator mode. For twitch measurements the y-axis of the oscilloscope was set to 0.5V or 1V per division. This was adjusted depending on the size of the twitch generated. The sweep speed on the oscilloscope was set to 5ms f.s.d. The stimulus button, on the Medelec control panel, was pressed. This triggered the stimulus isolator to deliver a 100μs supramaximal-square wave impulse to the nerve. The Medelec simultaneously triggered the oscilloscope to record. The baseline of the oscilloscope was adjusted so that the datum lines coincided with the take-off point of the twitch trace. The following measurements were made by moving a cursor along the trace and by using the waveform processing facility on the oscilloscope which calculated the area under the twitch trace.

The following measurements were recorded:

(i) ***Amplitude of peak twitch*** (N): This represented the maximum force generated by the twitch contraction. This was the distance on the y-axis from the take-off point of the twitch-tension curve to the point of maximum amplitude.

(ii) ***Time to peak twitch*** (ms): This was the time from the onset of muscle contraction to point of maximum contraction. On the twitch-tension curve this was the distance along the x-axis from the take-off point to the point of maximum amplitude.

(iii) ***Time to half relaxation*** (ms): This was the time from the point of maximum muscle contraction to the point where the muscle had half-relaxed. On the twitch-tension curve this was measured on the x-axis from the point of maximum amplitude to the point on the downslope of the curve which was half the amplitude of the maximum amplitude of the curve. Half relaxation as opposed to full relaxation was

used because oscillations of the trace around the baseline made the latter difficult to identify accurately. Relaxation of muscle is mathematically asymptotic because of the viscoelastic properties of the muscle.

(iv) ***Time tension integral*** (mNs): This represented the total force generated by the twitch contraction to the point of half relaxation of the muscle. This was the area under the twitch tension curve from the take off point to the point on the downslope of the curve which was half the amplitude of the maximum amplitude of the curve.

(v) ***Time tension index*** (N): This represented the average force generated by the muscle to the point of half relaxation. It was calculated by dividing the *time tension integral* by the *time to half relaxation.*

10.7 TETANIC TENSION MEASUREMENTS

For the measurement of tetanic tension the muscle was stimulated at a frequency of 100Hz, using square-wave impulses of 50μs duration, of the same supramaximal amplitude which had been used for the twitch tension measurements. These stimuli induced tetanus in the muscle. The oscilloscope settings were altered to a sweep speed of 20s f.s.d. and the y-axis set at 2V per division. Stimulation of the muscle was stopped when the tetanic contraction had fatigued to half of its maximum force.

The following measurements were recorded by moving a cursor along the tetanic-tension trace and the use of the waveform processing facility on the oscilloscope.

Maximum tetanic tension (N): This was the maximum tetanic force generated by the muscle. This was measured on the y-axis from the baseline to the point of maximum amplitude of the tetanic-tension trace.

Time to half fatigue (s): This was the time from the start of muscle contraction to that point when the muscle had fatigued to half of its maximum force. It was measured on the y-axis from the take-off point to the point where the trace was half of the maximum amplitude. Half fatigue as opposed to complete fatigue was used because oscillations of the trace around the baseline made the latter difficult to accurately identify.

Time tension integral (Ns): This was the area under the tetanic tension curve from the take off point to the point of half fatigue. It represented the total force generated by the muscle, to the point of half-fatigue.

Time tension index (N): This represented the average force generated by the tetanic contraction. This was calculated by dividing the *time tension integral* by the *time to half fatigue.*

10.8 MUSCLE MASS

When the twitch and tetanic measurements were complete the muscle was dissected proximally to its origin on the bone. Both FCR and LLM were easy to remove in their entirety. The wet weights of the muscles were determined using a balance, with an accuracy to two decimal places.

10.9 Facial Nerve Results for Muscle Physiology

There was no asymmetry of the animals' faces and no wasting of the facial muscles on the operated side. Previous workers who had carried out experiments on the facial nerve of the sheep used mass movement of the snout to assess muscle tension. This method was originally developed for the assessment of facial nerve injuries in smaller animals such as rats. However, it was proposed that use of a single muscle would be a more accurate method of assessing target muscle physiology in the sheep. Dissection around the region of the snout revealed levator labii maxillaris. This was a discrete muscle, supplied by the facial nerve, which originated from the maxilla and inserted into the snout by means of a single tendon. This muscle was used in the muscle physiology experiments presented in this work.

There were no problems identifying the levator labii maxillaris muscle and isolating its tendon (as discussed in Chapter 3). However, on one occasion more extensive dissection was performed and it was thought that the nerve supply to the muscle was damaged preventing further assessment. In subsequent experiments the minimum amount of dissection, required to expose the tendon, was performed. There were no incidences of detachment of the tendon from the tension transducer as had been experienced by previous workers assessing larger muscles supplied by the median nerve.

10.9.1 Facial Nerve Twitch Measurements

The raw data for the results of these experiments are shown in Appendix 2. A small number of outliers were excluded using the half normal plot method. The distribution of data was determined using the normal plot method. The variable *time to half relaxation* was normally distributed. All the other variables (*amplitude of peak twitch, time to peak twitch, time twitch-tension integral* and *time twitch-tension index*) were non-parametrically distributed. F tests were then performed to identify between-groups variation. A one-way ANOVA test was used on the normally distributed data and a Kruskal-Wallis test was used on the non-parametric data. There were no significant differences among any the experimental groups for any of the variables. However, the normal group had the highest mean values for *amplitude of peak twitch, time twitch-tension integral* and *time twitch-tension index*. There was no correlation of the severity of nerve injury with the variables *time to peak twitch* and *time to half relaxation*. The mean values for the twitch tension measurements are shown in Table 10.1.

Facial nerve **Mean values twitch tension**						
	Norm	Neura	Axono	Neurot & Suture	Neurot & Wrap	Graft
Amplitude peak (N) [SEM]	2.20 [0.42]	1.72 [0.13]	1.37 [0.11]	1.28 [0.29]	1.80 [0.47]	1.80 [0.53]
Time to peak (ms) [SEM]	31.3 [3.1]	22.3 [1.3]	26.3 [2.3]	29.7 [3.5]	34.1 [3.6]	30.3 [3.6]
Time to ½ relaxation (ms) [SEM]	45.3 [9.3]	18.4 [1.5]	37.3 [8.1]	31.6 [13.8]	39.4 [8.2]	43.6 [13.6]
Time tension integral(mNs) [SEM]	124.4 [36.6]	45.7 [4.6]	60.7 [10.2]	92.4 [42.9]	102.8 [38.0]	68.4 [29.7]
Time tension index (N) [SEM]	1.6 [0.3]	1.1 [0.1]	0.9 [0.1]	1.2 [0.4]	1.3 [0.4]	1.3 [0.4]

Table 10.1 shows the mean values of the twitch tension measurements for the facial nerve.

10.9.2 Facial Nerve Tetanic Measurements

The raw data for the results of these experiments are shown in Appendix 2. A small number of outliers were excluded using the half normal plot method. The distribution of data was determined using the normal plot method. The measurements of *peak tetanus* and *time tetanic-tension index* were normally distributed. The measurements of *time to half fatigue* and *time tetanic-tension integral* were non-parametrically distributed. F tests were then performed to identify between-groups variation. A one-way ANOVA test was used on the normally distributed data and a Kruskal-Wallis test was used on the non-parametric data. There were no significant differences among any of the experimental groups for any of the variables and there was no correlation of the mean values with the severity of nerve injury. The mean values for the tetanic tension measurements are shown in Table 10.2.

Facial nerve Mean values tetanic tension						
	Normal	Neura	Axono	Neurot&Suture	Neurot&Wrap	Graft
Peak tetanus (N) [SEM]	5.9 [1.1]	10.1 [1.1]	5.1 [1.0]	6.4 [1.6]	5.8 [1.2]	5.7 [1.3]
Time to ½ fatigue (s) [SEM]	27.5 [8.4]	17.6 [7.6]	26.7 [7.5]	24.9 [5.0]	20.7 [5.0]	24.0 [7.5]
Time tension integral (Ns) [SEM]	87.8 [25.1]	105.1 [24.8]	82.2 [18.7]	80.9 [29.2]	58.4 [16.5]	76.5 [16.7]
Time tension index (N) [SEM]	3.8 [0.7]	6.3 [0.7]	3.6 [0.6]	3.9 [1.1]	3.5 [0.8]	3.8 [0.8]

Table 10.2 shows the mean values of the tetanic tension measurements for the facial nerve.

10.9.3 Facial Nerve Muscle Mass

The raw data for the results of these experiments are shown in Appendix 2. A small number of outliers were excluded using the half normal plot method. The distribution of data was determined using the normal plot method. Measurements of muscle mass were normally distributed, therefore a one-way ANOVA test was used to detect the presence of between-groups variation. There were no significant differences among the experimental groups and there was no obvious correlation between muscle mass and the severity of nerve injury. The mean values for the mass of levator labii maxillaris are shown in Table 10.3.

Facial nerve Mean values muscle mass						
	Normal	Neura	Axono	Neurot&Suture	Neurot&Wrap	Graft
Mass (g) [SEM]	2.08 [0.23]	2.83 [0.20]	2.49 [0.16]	2.26 [0.22]	2.15 [0.14]	2.01 [0.12]

Table 10.3 shows the mean values of mass for levator labii maxillaris which is supplied by the facial nerve.

10.10 MEDIAN NERVE RESULTS MUSCLE PHYSIOLOGY

Previous workers had used steel wire to attach the tendon of FCR to the tension transducer. However, during muscle contraction the wire had often cut through the tendon, detaching the muscle from the transducer. The method of attachment developed for this work, using linen thread, was found to be a more reliable method of securing the tendon. Furthermore, linen has a lower elasticity than steel wire and therefore was less likely to stretch during muscle contraction (which could alter the tension recorded).

No other technical difficulties were encountered in the assessment of median nerve target muscle physiology.

10.10.1 Median Nerve Twitch Measurements

The raw data for the results of these experiments are shown in Appendix 2. The mean values for the twitch tension measurements are shown in Table 10.4. The variable *time to peak twitch* was normally distributed. All the other measurements of muscle twitch (*amplitude of peak twitch, time to half relaxation, time twitch-tension integral* and *time twitch-tension index*) were non-parametrically distributed. F tests were then performed to identify between-groups variation. A one-way ANOVA test was used on the normally distributed data and a Kruskal-Wallis test was used on the non-parametric data. No significant differences were found among the experimental groups for any of these variables. However, the normal group had the highest mean values for *amplitude of peak twitch, time tension integral* and *time tension index*, whilst the graft group had the lowest mean values. There was no obvious correlation between the severity of nerve injury and *time to peak twitch* and *time to half relaxation.*

Median nerve Mean values twitch tension						
	Normal	Neura	Axono	Neurot & Suture	Neurot & Wrap	Graft
Amplitude peak (N) [SEM]	5.5 [0.9]	3.0 [0.4]	4.8 [1.9]	2.6 [0.9]	4.9 [1.5]	2.1 [0.4]
Time to peak (ms) [SEM]	48.0 [5.0]	43.2 [1.1]	39.2 [5.5]	46.4 [6.8]	41.2 [2.4]	37.3 [4.9]
Time to $\frac{1}{2}$ *relaxation* (ms) [SEM]	61.5 [12.9]	35.3 [7.1]	36.6 [9.4]	40.1 [8.5]	70.6 [13.3]	35.6 [7.0]
Time tension integral (mNs) [SEM]	433.0 [91.5]	163.7 [29.3]	352.4 [120.8]	136.6 [43.6]	280.5 [74.4]	97.6 [20.2]
Time tension index (N) [SEM]	3.8 [0.6]	2.0 [0.2]	3.3 [1.4]	2.2 [0.8]	3.2 [0.8]	1.3 [0.3]

Table 10.4 shows the mean values of the twitch tension measurements for the median nerve.

10.10.2 Median Nerve Tetanic Measurements

The raw data for the results of these experiments are shown in Appendix 2. The mean values for the tetanic tension measurements for the median nerve are shown in Table 10.5. The variables *time to ½ fatigue tetanus* and *time tetanic-tension integral* were normally distributed. The remaining variables, *maximum tetanic force* and *time tetanic-tension index*, were non-parametrically distributed.

One-way ANOVA tests, performed on the normally distributed data, revealed between-groups variation for *time tetanic-tension integral*. However, Scheffé tests performed between pairs of experimental groups showed no significant differences. The non-transection injuries had higher mean values for *time tetanic-tension integral* than the transection injuries, with the nerve graft group having the lowest mean value.

Kruskal-Wallis tests, which were performed on non-parametrically distributed data, revealed between-groups variation for *time tetanic-tension index*. Mann-Whitney-U tests were then performed between each combination of pairs of experimental groups to identify where these differences lay. The results are shown in Table 10.6. The axonotmesis group had the highest mean value (21.80N) and was significantly different from all the other experimental groups except the neurapraxia group. The nerve graft group had the lowest mean value (11.95N). The results for *time tetanic-tension index* are also presented in Figure 10.3 using a box and whisker plot. Power studies showed that *time tetanic-tension index* had a power of 1.

Although not statistically different, the normal group had the highest mean value for the *peak tetanic force* generated and the graft group had the lowest mean value.

Median nerve Mean values tetanic tension						
	Normal	Neura	Axono	Neurot&Suture	Neurot&Wrap	Graft
Peak tetanus (N) [SEM]	22.9 [0.9]	22.2 [0.9]	22.6 [2.0]	17.2 [2.5]	22.7 [0.5]	17.6 [3.2]
Time to ½ fatigue (s) [SEM]	20.5 [1.6]	18.1 [2.6]	21.2 [5.1]	13.8 [3.5]	18.6 [1.3]	13.0 [3.0]
Time tension integral(Ns) [SEM]	392.2 [34.1]	351.7 [61.9]	461.3 [109.5]	197.6 [67.8]	332.4 [26.2]	165.2 [66.3]
Time tension index (N) [SEM]	19.2 [0.8]	19.2 [1.6]	21.8 [0.5]	13.5 [2.5]	17.8 [0.5]	12.0 [2.5]

Table 10.5 shows the mean values of the tetanic tension measurements for the median nerve.

Median Nerve: Mann Whitney U test Time Tension Index / (N)						
	Normal	Neurapraxia	Axonotmesis	Neurotmesis (suture)	Neurotmesis (wrap)	Graft
Normal		0.807	0.022	0.088	0.115	0.023
Neurapraxia			0.110	0.117	0.200	0.050
Axonotmesis				0.014	0.010	0.021
Neurotmesis (suture)					0.200	0.624
Neurotmesis (wrap)						0.087
Graft						
Mean [SEM]	19.2 [0.82]	19.2 [1.57]	21.8 [0.50]	13.5 [2.52]	17.8 [0.51]	12.0 [2.47]

Table 10.6 shows the p values between pairs of experimental groups for the Mann-Whitney U test. Significantly different results ($p<0.05$) are highlighted in red. The mean value ±SEM for each group is shown in the bottom row.

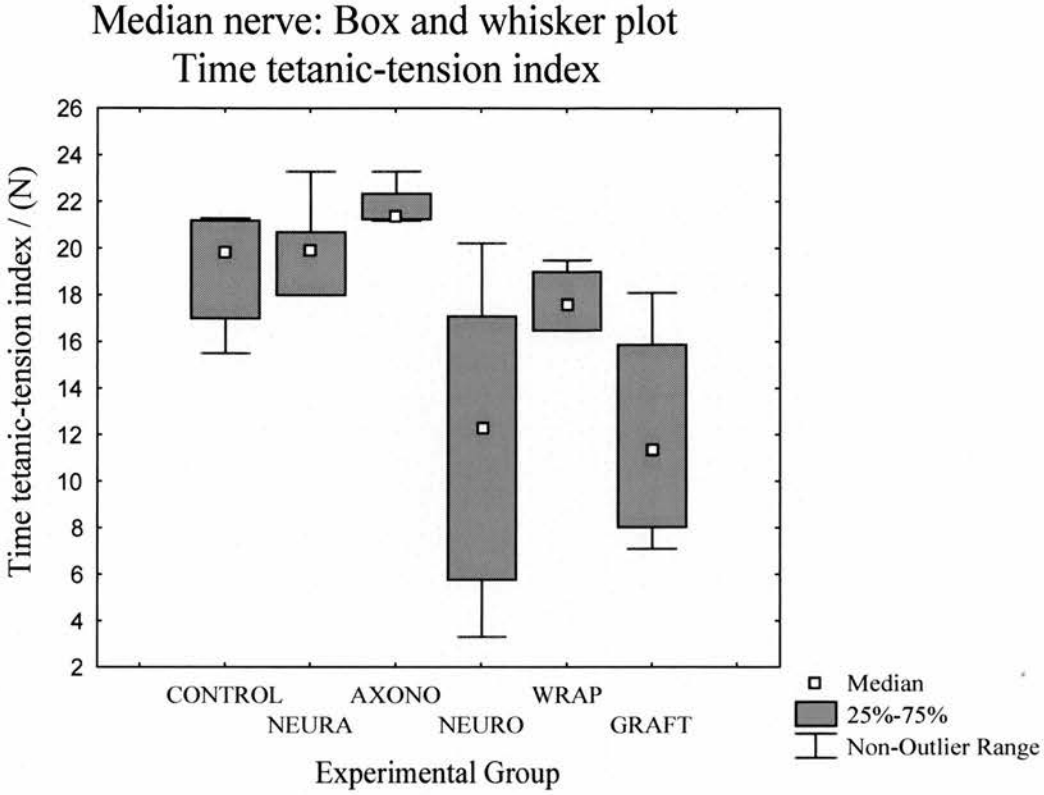

Figure 10.3 is a box and whisker plot showing the time tetanic-tension index results for the median nerve.

10.10.3 Median Nerve Muscle Mass

The raw data for the results of these experiments are shown in Appendix 2. The variable *muscle mass* was normally distributed. A one-way ANOVA test revealed between-groups variation. Scheffé tests performed between pairs of experimental groups showed that there was a significant difference between the normal control group and the neurotmesis and suture repair group ($p=0.004$), the neurotmesis and wrap repair group ($p=0.022$) and the nerve graft group ($p=0.032$). There was also a significant difference between the neurapraxia group and the neurotmesis and suture repair group ($p=0.021$). Table 10.7 shows the p values and the mean values for each experimental group. There is a decline in the mean *muscle mass* for each group from the normal control group to the nerve graft group. The results are presented in a box and whisker plot in Figure 10.4. The plot shows the median value, the boxes indicate the 25^{th} to the 75^{th} percentiles and the whiskers the non-outlier range. Power studies showed that *muscle mass* had a power of 0.9.

Median Nerve: Scheffé test Muscle Mass / (g)						
	Normal	Neurapraxia	Axonotmesis	Neurotmesis (suture)	Neurotmesis (wrap)	Graft
Normal		0.997	0.533	0.004	0.022	0.032
Neurapraxia			0.819	0.021	0.095	0.118
Axonotmesis				0.435	0.800	0.821
Neurotmesis (suture)					0.984	0.988
Neurotmesis (wrap)						1.000
Graft						
Mean [SEM]	9.6 [0.7]	9.0 [0.8]	7.5 [0.2]	5.2 [0.7]	5.9 [0.6]	5.9 [0.8]

Table 10.7 shows the p values between groups for muscle mass using the Scheffé and the mean values ±SEM for muscle mass.

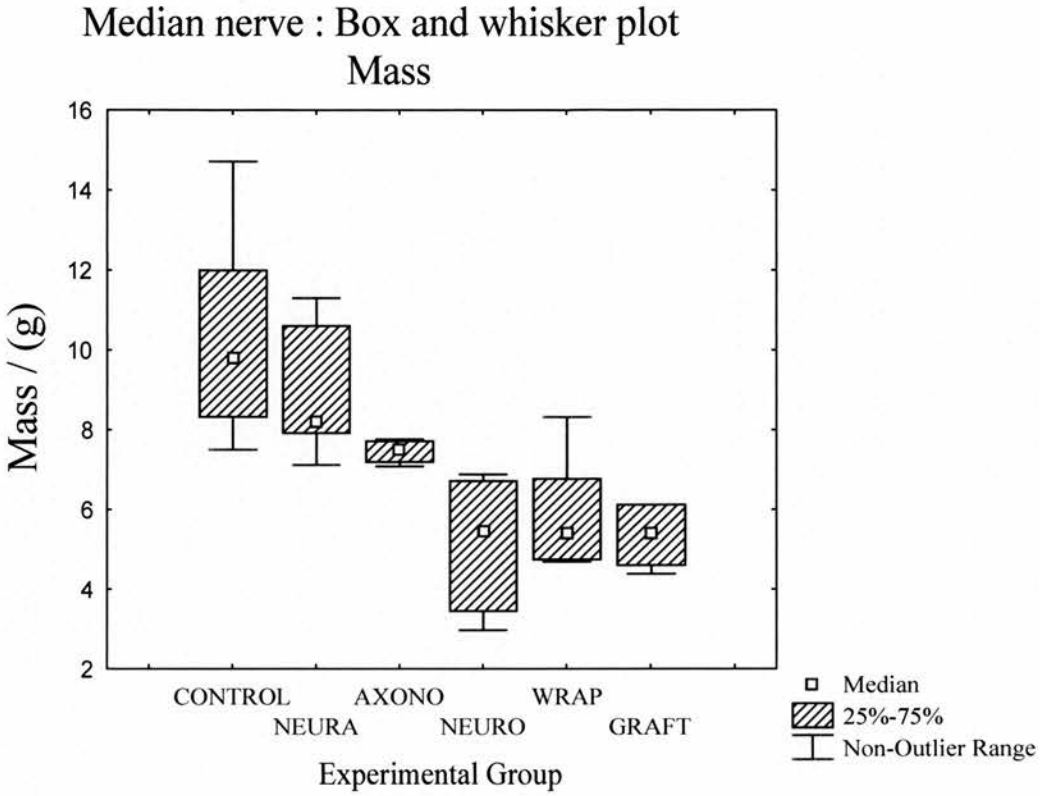

Figure 10.4 is a box and whisker plot showing the muscle mass results for the median nerve.

10.11 DISCUSSION

There were no significant differences among any of the facial nerve experimental groups for any of the measurements of isometric twitch tension and time. However, the normal group had the highest mean value for the amplitude of the twitch contraction, the time tension integral and the time tension index. There was no correlation between the nature and severity of nerve injury and the speed of muscle contraction and relaxation.

There were no significant differences among any of the median nerve experimental groups for any of the measurements of isometric twitch tension and time. However, the normal median nerve group had the highest mean value (and the graft group the lowest mean value) for the amplitude of the twitch contraction, the time tension integral and the time tension index. Again, there was no correlation between the severity of nerve injury and the speed of muscle contraction and relaxation.

Cross-innervation experiments described earlier in this chapter demonstrated that reinnervation of fast muscle with slow motor neurons resulted in an increase in twitch contraction time whilst reinnervation of slow muscle with fast motor neurons resulted in a decrease in twitch contraction time (Buller, Eccles, & Eccles 1959; Close 1965a; Barany & Close 1970). The experiments on maximum conduction velocity (*CVmax*), presented in Chapter 7, showed that *CVmax* decreased with increasing severity of nerve injury. Therefore, it might have been expected that the twitch time would be increased in those models of more severe nerve injury where the muscle was reinnervated by slower fibres. However, previous experiments where the muscle was reinnervated with its original nerve showed this was not necessarily the case.

Gillespie *et al* transected the common nerve to gastrocnemius (fast twitch) and soleus (slow twitch) in the rat, and studied the effect on muscle fibre type after reinnervation of the muscles with the original nerve (Gillespie, Gordon, & Murphy 1985). They found that the proportion of slow fibres increased in the gastrocnemius muscle and the proportion of fast fibres increased in the soleus muscle but overall the proportions of fast and slow fibres remained unchanged. When they studied the twitch times in the reinnervated muscle they found that the rate of contraction of gastrocnemius was normal but the rate of relaxation was increased. However, in soleus the speed of contraction was increased to approach that of gastrocnemius but the rate of relaxation remained the same. These authors concluded that muscle fibres do not show a preference for a specific type of innervation and that the 'force profile' of a muscle is determined by the relative proportions of slow and fast fibres. They also concluded that fast fibres dictate the speed of muscle contraction and slow fibres the rate of relaxation. Close performed cross-innervation experiments and self-reinnervation experiments on the extensor digitorum longus (EDL, fast twitch) and soleus (slow twitch) muscles in the rat (Close 1965b). He found no difference in the speed of contraction between the self-reinnervated muscles and normal muscles. However, in the cross-innervated muscles the speed of contraction of EDL was decreased and of soleus was increased. Barany and Close specifically looked at the properties of myosin (Barany & Close 1970). They showed that myosin in cross-innervated muscles underwent a conformational change whereas the myosin in self-reinnervated muscles did not. Furthermore, they concluded that the ATPase activity of myosin was correlated with the speed of muscle contraction.

Lewis and Chamberlain transected the medial popliteal nerve in the rat and studied the characteristics of soleus (slow twitch) and plantaris (fast twitch) after reinnervation

with the original nerve (Lewis & Chamberlain 1993). They found that both the *time to peak twitch* and *time to half relaxation* remained longer for soleus than plantaris. They stained the muscles for ATPase activity and found that the number of slow fibres in soleus was twice that in plantaris. The proportions of fast and slow fibres in plantaris were consistent with random reinnervation. The authors proposed that the higher proportion of slow fibres in soleus was due to an effect exerted on the motor neurons by the originally slow muscle fibres rather than preferential innervation of soleus by slow muscle fibres. They postulated that the mechanism of influence of muscle fibre type on nerve fibre type could have been due to mismatching of fast motor neurones to slow muscle fibres which prevented restoration of fast motor neurone characteristics, or, that the slow muscle fibres released a neurotrophic substance which was taken up by the motor axon and induced changes within it.

At a single motor unit level, Gordon and Stein found that in self-reinnervated muscle in the cat, the proportions of fast and slow motor unit types were the same as in normal muscle and that the nerve fibres showed no preference for their original muscle fibres (Gordon & Stein 1982). They concluded that fast and slow fibres are equally successful at reinnervation of muscle.

From the papers discussed above it seems reasonable to suggest that the 'force profile' of a muscle is largely determined by its innervation and that unless the relative proportions of different nerve fibre types is altered (or an entirely different nerve is used as in the cross-innervation experiments) then the muscle will retain its original characteristics. However, there is also evidence that muscle has a reciprocal effect on nerve fibres. In the work presented here, the influence of the different types of newly regenerated axons may be similar enough to that of normal axons to allow regeneration of a population of muscle fibres similar to the original one. This could

explain why no differences were observed among any of the experimental groups for the twitch tension contraction and relaxation times.

It is known that reinnervated motor units have an altered configuration such that the muscle fibres of a particular unit are situated more closely to each other. This increase in fibre density results in areas of more intense depolarisation (Kugelberg, Edström, & Abbruzzese 1970); (Wiechers 1990). New motor units may also contain more muscle fibres (Luff, Hatcher, et al. 1988). Luff *et al* transected the L7 ventral root in kittens to produce partial denervation of soleus and flexor digitorum longus (FDL) (Luff, Hatcher, et al. 1988). They found increases in the force generated by new motor units from between two to sixteen times normal. Cross-sections of FDL and soleus revealed minimal fibre hypertrophy but large motor units containing between 3000 to 5000 muscle fibres. These authors attributed the increase in motor-unit force to the increased size of the motor units as opposed to hypertrophy of the muscle fibres. The increased size of motor units in reinnervated muscles may explain why no significant differences were found among both the facial nerve and the median nerve experimental groups for the size of the isometric twitch and tetanic tensions. Luff *et al* showed that only 5% of the original number of nerve fibres were required to generate the original force of a muscle (Luff, Hatcher et el. 1988).

Twitch tension may be a less reliable measurement of muscle function than tetanic tension. This is because during a twitch contraction the muscle does not develop its maximum tension, therefore there is the potential for more variability in this test. Twitch tension may also be affected by prior stimulation of the muscle. Desmedt and Hainaut described a phenomenon, in association with successive twitch contractions, which they called staircase potentiation (Desmedt & Hainaut 1968). They observed that with the first twenty twitch contractions the twitch tension decreased and with

subsequent contractions it progressively increased. They ascribed this to the increased release of Ca^{2+} ions. In both the facial nerve and the median nerve muscle physiology experiments, the target muscles had already been subjected to a variable number of stimulations during the preceding experiments *e.g.* CV_{max}, *DCV, refractory period* and in the case of the median nerve experiments *jitter* (which was also measured in FCR). It was more difficult to obtain adequate CMAPs in the nerve graft groups than the normal or non-transection injury groups, therefore, the muscles in the graft group had probably been subjected to a higher number of stimulations. It is possible that the muscles of different experimental groups were at different stages of potentiation.

There were no significant differences among the facial nerve experimental groups for the measurements of tetanic tension and time and no correlation of the mean values with the severity of nerve injury. There were no significant differences among the median nerve groups for the size of the tetanic force generated, the time tetanic-tension integral and the time to half fatigue. However, the mean values for these variables were generally higher in the non-transection models of nerve injury. The median nerve also showed significant differences among the experimental groups for the variable *time tetanic-tension index*. The axonotmesis group had the highest mean value and was statistically different from all the other experimental groups except the neurapraxia group. The nerve graft group had the lowest mean value. As described above, there were no significant differences in the maximum tetanic tension generated among any of the median groups however, the fact that the *time tetanic-tension index* was higher in the non-transection groups may indicate that these muscles were functioning more efficiently.

In their muscle denervation studies Luff *et al* found there was a limit to the size to which motor units could increase (Luff, Hatcher et el. 1988). They found that in those

muscles which had undergone the most extensive denervation there was histological evidence of denervated fibres and the total force generated by the muscle was decreased. Furthermore, some reinnervated muscles were unable to maintain tetanic contractions at higher frequencies of stimulation. This was attributed to failure of transmission at the NMJ or propagation of the impulses by the terminal motor axon, rather than muscle fatigue, as the muscles were immediately able to respond to stimulation at lower frequencies. Luff *et al* proposed that this was because the reinnervation of muscles was less 'secure' than normal reinnervation. These findings may explain the results of the work presented here. The reason no significant differences were found among the experimental groups for either nerve for the measurements of tetanic tension may be because the new larger motor units could generate an adequate force. However, differences were found among the median nerve experimental groups for *time tetanic-tension index* and this may be because the overall functioning or efficiency of the reinnervated muscles was reduced when compared to normal *e.g.* they had a lower and less sustainable supply of energy and/or a poorer blood supply.

The fact that no differences were found among the facial nerve experimental groups for the tetanic tension measurements may be because the facial nerve is a motor nerve whereas the median nerve is a mixed nerve. Therefore, there is less potential for miss-matching of fibres in the facial nerve as opposed to the median nerve so that reinnervation of the facial muscles may be more 'secure' or similar to the original situation. Most limb and trunk muscles contain all three types of muscle fibres (Burke 1980). It may be that the facial muscles contain a more homogeneous selection of muscle fibres as opposed to the FCR and while it has been documented that

pioneering axons can reinnervate any type of fibre, if the axon-muscle fibre match is the same as the original one this may produce a better functioning unit.

There were no significant differences among the facial nerve experimental groups for the mass of levator labii maxillaris (LLM). All the groups had similar mean values for muscle mass (2.0g to 2.8g) and there was no correlation with the severity of nerve injury. However, in the median nerve, FCR in the normal group was significantly heavier than those groups with transection injuries. The neurapraxia group was also significantly heavier than the neurotmesis and suture repair group. Figure 10.4 shows a progressive decline in the mass of FCR with increasing severity of injury to the median nerve. The different results for the two nerves and their respective muscles may be due to the both the speed or type of reinnervation or the different fibre-type composition of the muscle.

Muscle atrophy should not have occurred in the control and neurapraxia groups as the muscle was not denervated. However, nerves of the axonotmesis and transection injury groups underwent Wallerian degeneration, therefore, the associated muscle would have atrophied until they it was reinnervated. The grafted nerves may have taken the longest to regenerate. In these nerves the pioneering axons had to cross two suture lines, which has been shown to slow the rate of regeneration (Gutmann, Guttmann et al. 1942). Finkelstein *et al* studied the effect on muscle of delayed reinnervation (Finkelstein, Dooley, & Luff 1993). They transected the nerve to medial gastrocnemius in the rat and repaired it after different time intervals (immediate repair and delays of 3 days, 7 days, 3 weeks and 8 weeks). In the immediate repair group they found the muscle regenerated to 75% of the mass of normal muscle. When the transection groups were compared with each other the recovery of muscle mass was decreased in the three week delay group and was significantly less in the eight week

delay group. Therefore, they concluded that the length of time of denervation affects muscle regeneration.

The difference in the mass results between the facial and median nerves and their respective muscles may be due to increased mismatching of nerve and muscle fibres types in the median nerve when compared to the facial nerve, as previously discussed. There may also be increased mismatching of the axons and endoneurial tubes, within the median nerve, with increasing severity of nerve injury. Differences in the relative proportions of muscle fibre types could also have affected the change in mass. LLM is a postural muscle and therefore probably predominantly composed of slow fibres whereas FCR is a phasic muscle and the predominant muscle fibre type is probably fast-fatiguable.

In summary, although many of the measured variables of muscle physiology were not significantly different, the less severe injuries generally performed better. Smaller differences were found among the facial nerve groups than among the median nerve groups and this may have been as a consequence of both the different types of nerve (motor and mixed) and the different types of muscle (fast and slow). However, the differences in muscle physiology among the experimental groups were perhaps less than might have been expected from the severity of some of the nerve injuries, particularly when the poor outcome of peripheral nerve repair in clinical practice is considered. Therefore, whilst muscle physiology goes some way to assess the recovery of function, the return and assessment of other modalities such as proprioception and sensation are probably equally (or more) important in determining the final functional outcome.

11 MORPHOMETRY

11.1 INTRODUCTION

The function of each nerve fibre is determined by both its central and peripheral connections and also by the velocity and frequency with which it conducts impulses (Young 1942). Neurotmesis and axonotmesis result in Wallerian degeneration of the nerve distal to the site of injury. In the distal stump axons and myelin degenerate and are removed by phagocytosis. However, the endoneurial tubes remain and become filled with Schwann cells. They are now referred to as 'bands of Bungner'. Each nerve contains different sizes of endoneurial tube and this size differential is maintained during and after degeneration (Young 1942). The size of the endoneurial tube is important as it can influence fibre diameter.

The proximal nerve stump sends out large numbers of thin, pioneering axons which invade the endoneurial tubes. Initially each tube, particularly the larger ones, contains many of these thin axons. To survive, axons must enter a suitable endoneurial tube and reinnervate an appropriate target organ. Axons which make inappropriate distal connections or fail to reach the target organ will die. Therefore, the number of axons within each endoneurial tube decreases over time. If an axon successfully reinnervates a target organ the fibres then increase in diameter and in the case of motor fibres become medullated (Gutmann & Sanders 1943). This increase in fibre diameter and myelin sheath thickness may be necessary before the axons can conduct impulses which produce effective function (Young 1942). Normal function of a nerve will only return if an adequate number of axons reach endoneurial tubes in the peripheral stump

which allow them to mature properly and also guide them to an appropriate target organ.

CV_{max} is reduced after nerve injury owing to a combination of factors including, a reduction in fibre diameter, reduced myelin sheath thickness and shortened internodal length (Waxman 1980). Several experimental and computer simulation studies (previously discussed in Chapter 7) have demonstrated that conduction velocity is proportional to fibre diameter (Waxman 1980; Hursh 1939; Boyd 1964; Rushton 1951; Goldman & Albus 1968). An increase in fibre diameter should therefore correlate with an increase in conduction velocity. Therefore, measurement of *fibre diameter* is useful in the assessment of nerve regeneration.

Conduction velocity is also affected by myelin sheath thickness, faster fibres have thicker myelin sheaths (Smith & Koles 1970). The ratio of axon diameter to the overall fibre diameter is termed the '*g ratio*'. The *g ratio* may therefore be regarded as an expression of myelin sheath thickness for a given axon diameter. The *g ratio* is particularly useful to assess nerve maturation. Studies of myelin sheath thickness have demonstrated that conduction velocity is optimised at a *g ratio* between 0.6 and 0.7 (Goldman & Albus 1968); (Moore, Joyner et al. 1978); (Rushton 1951); (Smith & Koles 1970). This value is generally observed in normal peripheral nerves (Goldman & Albus 1968). Therefore, measurement of *myelin sheath thickness* and *g ratio* are also useful in the assessment of nerve regeneration.

11.2 MATERIALS AND METHODS

11.2.1 Preparation of Nerve Sections

After the electrophysiology and muscle physiology experiments were completed a 2cm specimen of nerve was harvested, distal to the site of injury. This was laid on a piece of card and placed in a 4% cacodylate-buffered gluteraldehyde solution for one hour at room temperature. This resulted in firming of the nerve such that it was possible to cut the nerve into 1mm transverse sections using a razor blade. This was performed with the aid of a microscope. Sectioning the nerve allowed better penetration of the nerve with gluteraldehyde. The nerve sections were replaced in cacodylate-gluteraldehyde solution and left overnight at room temperature. The next morning the sections were washed three times for twenty minutes in sucrose buffer then immersed in 1% cacodylate-buffered osmium tetroxide for three hours to allow staining of myelin with osmium. The osmium tetroxide stained and fixed the myelin by reacting with its double bonds to form an insoluble ester. Despite being firmer than fresh nerve the fixed specimens were too soft to cut and were therefore embedded in an epoxy resin, Araldite. However, as Araldite was immiscible with water the specimens were dehydrated using alcohol. This was achieved by three thirty minute washes in 10% alcohol then three thirty minute washes in 100% alcohol. As Araldite was also immiscible with alcohol this was followed by one thirty minute wash in propylene oxide (which was miscible with both water and alcohol).

The sections were removed from the propylene oxide, placed in plastic moulds and then immersed in Araldite. These were left overnight at room temperature to allow penetration of the nerve with Araldite. The next morning the specimens were transferred to smaller moulds which were filled with fresh Araldite. One or two

sections were placed in each mould and orientated with a cut edge parallel to one of the sides of the mould, so that the sections would be easier to cut. The moulds were placed in an oven, maintained at a temperature of 60°C, and left for at least forty-eight hours to allow polymerisation of the Araldite.

After the Araldite was set the specimens were removed from the moulds. If the cut end of the nerve had been orientated parallel to the short side of the mould then the specimen could be mounted by itself in the support on the microtome. However, if the cut end was parallel to the long side then excess Araldite was removed with a razor blade and the specimen was mounted on a half-centimetre length of wood dowelling using molten wax. The specimen was viewed under a microscope using $\times 10$ magnification. Further excess Araldite was removed from around the top and sides of the nerve using a razor blade, to minimise blunting of the delicate glass knife. Semithin (1μm) sections of nerve were then cut using a glass knife and microtome. As the sections were cut they were floated onto a water-bath, created with a wax mould, in order to minimise damage. Four or five nerve sections were transferred onto a bleb of water on a glass slide. Wrinkles in the sections were reduced by exposing them to chloroform, on a pipette held above the slides. The sections were then gently dried on a hotplate then stained with 1% toluidine blue in 1% sodium tetraborate. The slide was placed onto the hotplate for twenty to thirty seconds, rinsed under running tap water then replaced onto the hotplate to dry.

11.2.2 Creating the Digitised Image

Each section was viewed using a binocular microscope. The eyepieces had a magnification $\times 10$ and a $\times 40$ objective lens was selected, resulting in $\times 400$ magnification at the observer's eye. The microscope was connected to a camera which enabled each image to be displayed on a monitor screen. The output from the camera

was also connected to an image analysis program (Analytical Imaging Station (AIS), version 3.0, Imaging Research Inc, Canada). When an adequate image was achieved on the monitor screen (by adjusting the position of the slide, the focus and the level of lighting) it was stored, using the AIS program, as a TIFF (Tagged Image File Format) file for subsequent analysis. Four or five images were stored for each nerve. This system required calibration, and the image of a 2mm graticule with 10μm divisions was similarly digitised. The computer program recorded this calibration and this was used for all measurements to be obtained.

11.2.3 Counting

The AIS program was calibrated by placement of a cursor at either side of one of the divisions of the digitised image of the graticule. As the true length of this division was known to be 10μm the ratio of the size of the digitised image to the actual size of the nerve fibres could be calculated. This calibration was used for all subsequent measurements. *Axon diameter* and *fibre diameter* were measured using the AIS program. Measurements were made by placement of a cursor across the smallest diameter of the fibre (and corresponding axon diameter). By convention, the smallest diameter was used (and also to minimise artefact arising if the fibre had been cut obliquely). A total of two hundred measurements from ten different areas were made for each nerve. This method of systematic random sampling had previously been shown to be representative of the whole nerve and had been employed by previous workers within the group (Mayhew 1990). The *axon* and *fibre diameters* were stored in separate files and care was taken to ensure that the corresponding *axon* and *fibre diameters* were at the same position in both files. The results were initially saved as Lotus 1-2-3 files as this program was compatible with the AIS program. They were subsequently exported into Excel spreadsheets where *myelin sheath thickness* and *g-*

ratio were calculated using the program's formula function. *Myelin sheath thickness* was calculated using the formula

$$\frac{\textit{fibre diameter} - \textit{axon diameter}}{2}$$

and *g-ratio* was calculated using the formula

$$\frac{\textit{axon diameter}}{\textit{fibre diameter}}$$

11.3 FACIAL NERVE RESULTS

A small number of outliers were excluded using the half normal plot method. The distribution of data was determined using the normal plot method. All the data (*axon diameter, fibre diameter, myelin sheath thickness* and *g ratio*) were normally distributed. F tests were then performed to identify between-groups variation. As the data were normally distributed a one-way ANOVA test was used. This revealed between-groups variation for *fibre diameter*. None of the other groups showed significant between-groups variation. A Scheffé test was performed on the *fibre diameter* data to identify where these differences lay. It did not reveal any significant difference between individual experimental groups. However, the mean value for *fibre diameter* was greatest for the normal experimental group and decreased as the severity of injury increased. The same pattern was seen for the mean *axon diameter* values. *Myelin sheath thickness* was greatest for the normal and neurapraxia groups but there was no obvious pattern for *g ratio*. The mean value for each experimental group is shown in Table 11.1. Figures 11.1 to 11.6 are combined *axon-diameter* and *fibre-diameter* histograms for the facial nerve models of injury.

Facial nerve morphometry (mean values)				
	Axon diameter (μm)	*Fibre diameter (μm)*	*Myelin thickness* (μm)	*g ratio*
Normal [SD]	6.59 [0.70]	11.63 [1.17]	2.45 [0.37]	0.57 [0.05]
Neurapraxia [SD]	6.28 [0.78]	10.97 [1.37]	2.34 [0.52]	0.59 [0.04]
Axonotmesis [SD]	6.02 [0.46]	9.90 [1.28]	1.94 [0.45]	0.61 [0.04]
Neurotmesis (suture) [SD]	6.06 [0.95]	9.87 [1.45]	1.91 [0.40]	0.61 [0.01]
Neurotmesis (wrap) [SD]	5.78 [0.68]	9.70 [0.69]	1.89 [0.10]	0.58 [0.03]
Graft [SD]	5.65 [0.64]	9.59 [1.00]	1.97 [0.30]	0.58 [0.04]
All groups [SD]	6.06 [0.71]	10.25 [1.32]	2.07 [0.42]	0.59 [0.04]

Table 11.1 shows the mean morphometric results for the each experimental group for the facial nerve.

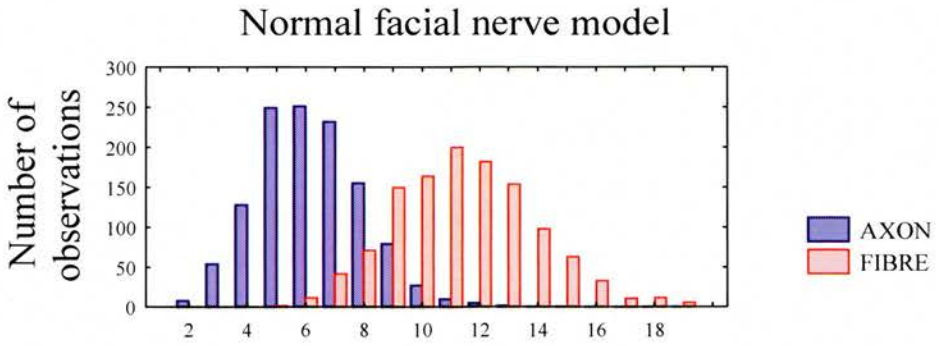

Figure 11.1

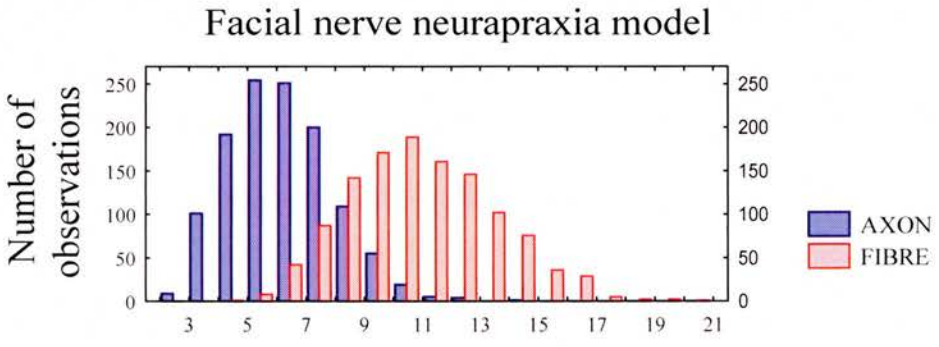

Figure 11.2

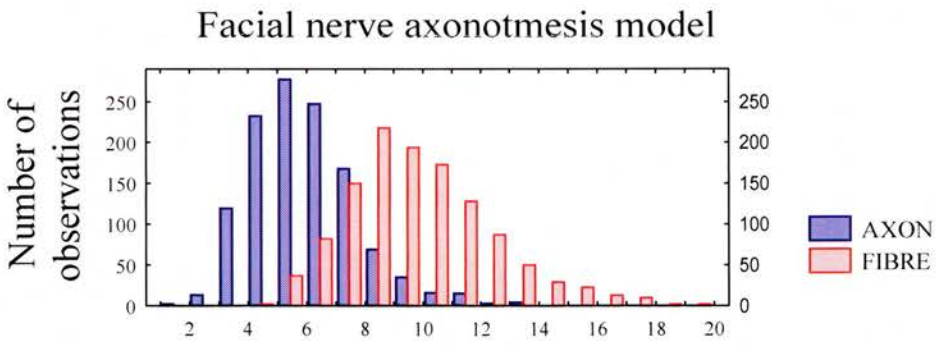

Figure 11.3

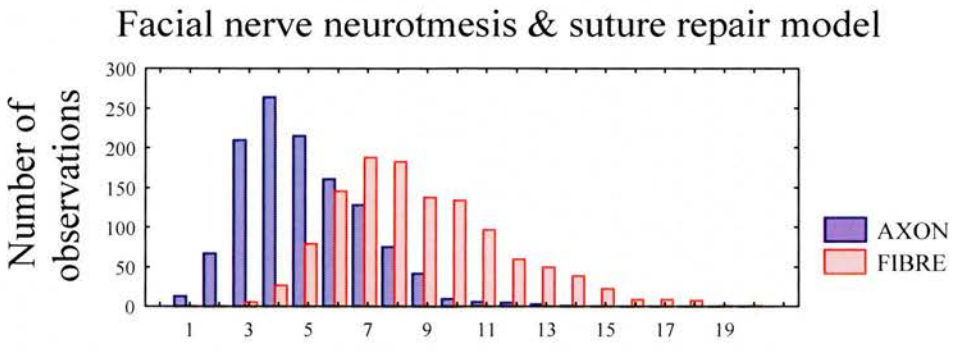

Figure 11.4

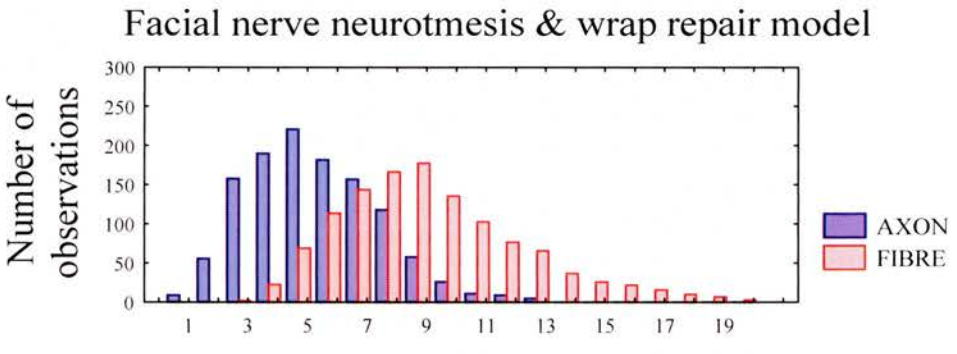

Figure 11.5

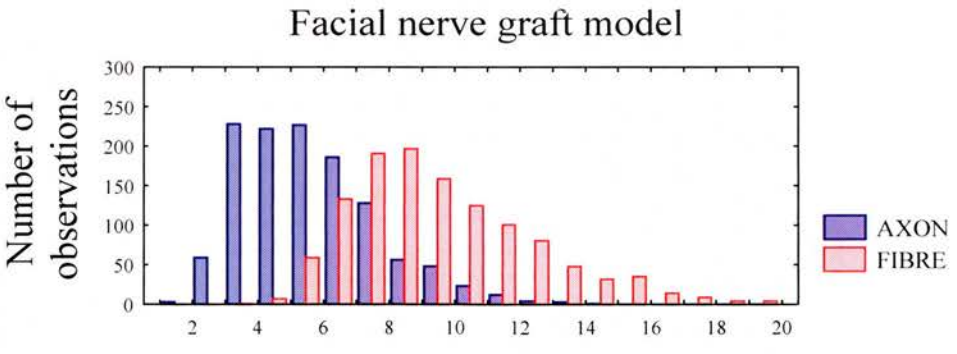

Figure 11.6

11.4 MEDIAN NERVE RESULTS

The Araldite in which the graft segments were immersed failed to polymerise. Expert advice was sought and an attempt was made to extract the Araldite from the nerves and reimmerse them in fresh resin. However, this process resulted in the nerve segments becoming brittle and fragmenting when an attempt was made to cut semithin sections with the glass knife. Therefore, no morphometric analysis was possible for the median nerve graft group.

A small number of outliers were excluded using the half normal plot method. The distribution of data was determined using the normal plot method. All the data (*axon diameter, fibre diameter, myelin sheath thickness* and *g ratio*) were non-parametrically distributed. F tests were then performed to identify between-groups variation. As the data was non-parametrically distributed a Kruskal-Wallis test was used. This revealed between-groups variation for all four groups. The Mann-Whitney-U test was subsequently performed to identify where these differences lay. The results for each test are shown in Table 11.2 to Table 11.5. The mean value for each experimental group is shown at the bottom of each column.

The mean value for *fibre diameter* was greatest for the normal experimental group and decreased as the severity of injury increased. The same pattern was seen for the mean values of *axon diameter*. *Myelin sheath thickness* was greatest for the normal and neurapraxia groups but there was no obvious pattern for *g ratio*. The mean value for all four morphometric variables, for each experimental group is shown in Table 11.6. Figure 11.7 to Figure 11.11 are combined *axon-diameter* and *fibre-diameter* histograms for the median nerve models of injury.

Median Nerve: Mann Whitney U test **p values for the comparison of *axon diameter* / (µm)**					
	Normal	Neurapraxia	Axonotmesis	Neurotmesis (suture)	Neurotmesis (wrap)
Normal		0.03	0.01	0.01	0.01
Neurapraxia			0.25	0.01	0.01
Axonotmesis				0.01	0.01
Neurotmesis (suture)					0.14
Neurotmesis (wrap)					
Mean [SD]	8.99 [0.55]	7.44 [1.07]	6.46 [1.26]	4.75 [0.33]	4.41 [0.42]

Table 11.2 shows the results of the Mann Whitney U test for the variable *axon diameter*. Results were significant at p<0.05. The mean value for each group is shown in the bottom row.

Median Nerve: Mann Whitney U test **p values for the comparison of *fibre diameter* / (µm)**					
	Normal	Neurapraxia	Axonotmesis	Neurotmesis (suture)	Neurotmesis (wrap)
Normal		0.12	0.01	0.01	0.01
Neurapraxia			0.03	0.01	0.01
Axonotmesis				0.01	0.03
Neurotmesis (suture)					1.00
Neurotmesis (wrap)					
Mean [SD]	16.72 [0.64]	15.29 [1.85]	10.82 [2.08]	8.39 [0.35]	8.31 [0.69]

Table 11.3 shows the results of the Mann Whitney U test for the variable *fibre diameter*. Results were significant at p<0.05. The mean value for each group is shown in the bottom row.

Median Nerve: Mann Whitney U test **P values for the comparison of *myelin thickness* / (µm)**					
	Normal	Neurapraxia	Axonotmesis	Neurotmesis (suture)	Neurotmesis (wrap)
Normal		0.58	0.01	0.01	0.01
Neurapraxia			0.01	0.01	0.01
Axonotmesis				0.22	0.60
Neurotmesis (suture)					0.22
Neurotmesis (wrap)					
Mean [SD]	3.87 [0.24]	4.12 [0.74]	2.17 [0.45]	1.82 [0.08]	1.95 [0.26]

Table 11.4 shows the results of the Mann Whitney U test for the variable *myelin sheath thickness.* Results were significant at p<0.05. The mean value for each group is shown in the bottom row.

Median Nerve: Mann Whitney U test **p values for the comparison of *g ratio***					
	Normal	Neurapraxia	Axonotmesis	Neurotmesis (suture)	Neurotmesis (wrap)
Normal		0.05	0.01	0.29	0.86
Neurapraxia			0.01	0.05	0.05
Axonotmesis				0.05	0.02
Neurotmesis (suture)					0.22
Neurotmesis (wrap)					
Mean [SD]	0.54 [0.03]	0.48 [0.04]	0.60 [0.02]	0.56 [0.02]	0.53 [0.04]

Table 11.5 shows the results of the Mann Whitney U test for the variable *g ratio.* Results were significant at p<0.05. The mean value for each group is shown in the bottom row.

Median nerve morphometry (mean values)				
	Axon diameter (μm)	*Fibre diameter (μm)*	*Myelin thickness (μm)*	*g ratio*
Normal [SD]	8.99 [0.55]	16.72 [0.64]	3.87 [0.24]	0.54 [0.03]
Neurapraxia [SD]	7.44 [1.07]	15.29 [1.85]	4.12 [0.74]	0.48 [0.04]
Axonotmesis [SD]	6.46 [1.26]	10.82 [2.08]	2.17 [0.45]	0.60 [0.02]
Neurotmesis (suture) [SD]	4.75 [0.33]	8.39 [0.35]	1.82 [0.08]	0.56 [0.02]
Neurotmesis (wrap) [SD]	4.41 [0.42]	8.31 [0.69]	1.95 [0.26]	0.53 [0.03]
All groups [SD]	6.48 [1.90]	12.05 [3.77]	2.87 [1.09]	0.53 [0.05]

Table 11.6 shows the mean morphometric results for each experimental group for the median nerve.

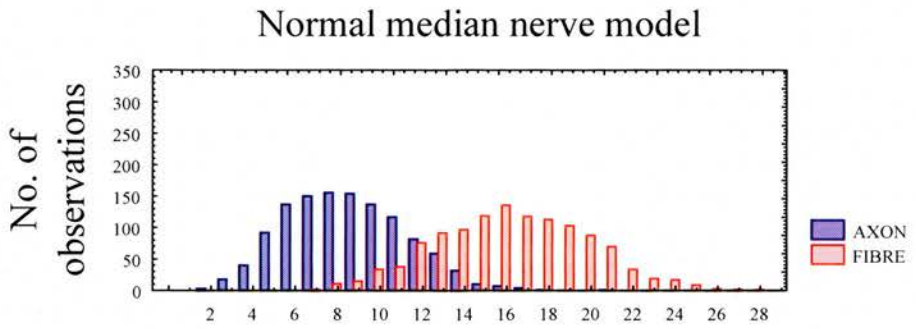

Figure 11.7

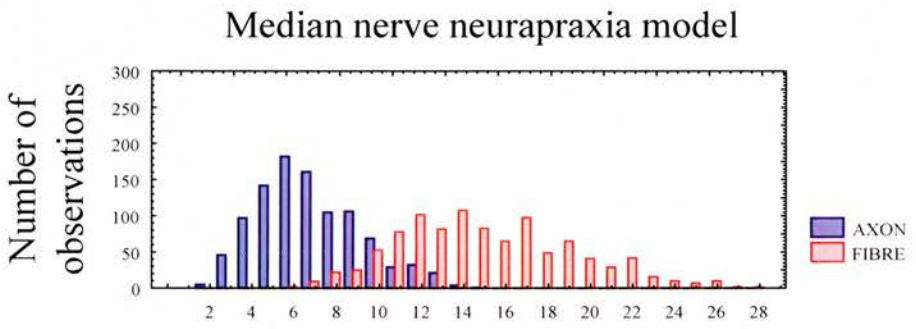

Figure 11.8

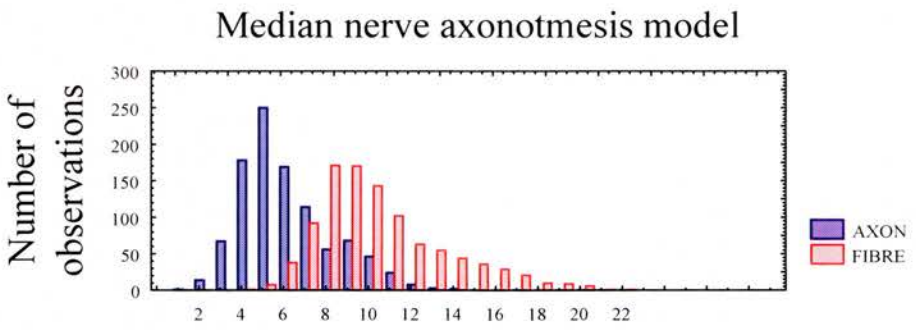

Figure 11.9

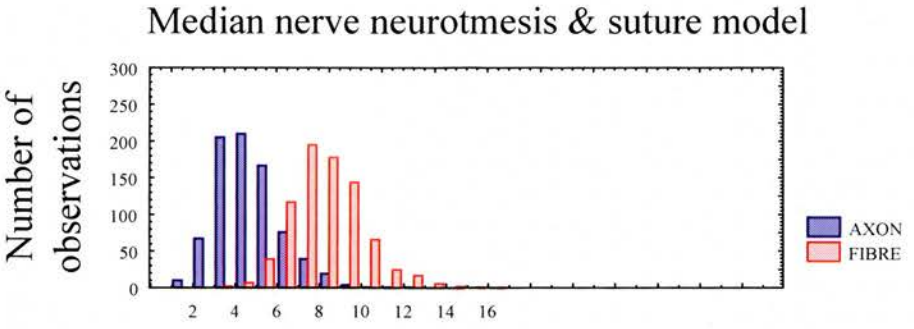

Figure 11.10

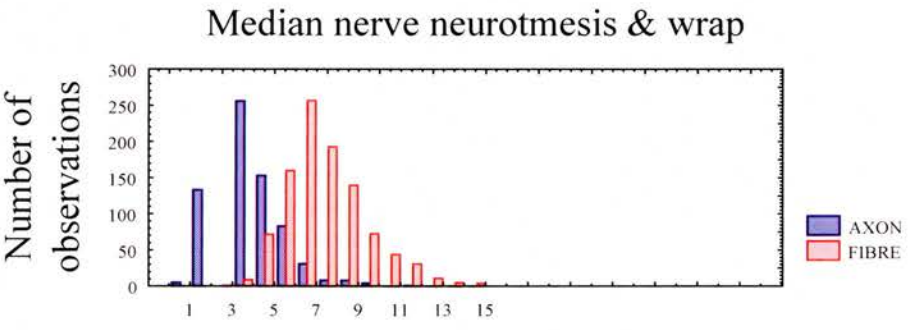

Figure 11.11

11.5 Comparison of Facial Nerve & Median Nerve Morphometric Results

The results for *axon diameter, fibre diameter and myelin sheath thickness* were compared for the facial and median nerves. Data sets of the mean values for both nerves were combined and normality of the data was determined using the Shapiro Wilk test. The combined sets of data for *axon diameter, fibre diameter* and *myelin sheath thickness* were normally distributed. Factorial ANOVA was used (as there were two independent grouping variables) to detect the presence of between-groups variation. Factorial ANOVA confirmed the presence of between-groups variation when both the nerve and the experimental group were considered together. Scheffé tests were then performed to detect where these differences lay. The results of these tests are shown in Table 11.7, Table 11.8 and Table 11.9. For *axon diameter* the normal median nerve group was significantly bigger than the normal facial nerve group but there were no significant differences among the other pairs of experimental groups. For *fibre diameter* and *myelin sheath thickness* both the median nerve normal and neurapraxia groups were significantly bigger than the equivalent facial nerve groups however, there were no significant differences among the models of more severe injury. The mean results for these three variables are shown in Table 11.10 and presented graphically in Figure 11.12. It can be seen that the mean values are higher in the median nerve for the non-transection injuries but higher in the facial nerve for the transection injuries. Table 11.11 shows the mean values for the morphometric variables expressed as a percentage of each normal group. The results for the neurapraxia groups are similar for the two nerves, around 90% for all variables. The facial nerve groups remain between 80% to 90% of normal for the other experimental groups, including the graft group. However, the median nerve axonotmesis group fell

to between 60% and 70% of normal and the transection injuries were only 50% of normal.

Median nerve versus facial nerve: Scheffé test p values for comparison of *axon diameter*					
	Normal	Neurapraxia	Axonotmesis	Neurotmesis (suture)	Neurotmesis (wrap)
Normal	0.01				
Neurapraxia		0.76			
Axonotmesis			0.99		
Neurotmesis (suture)				0.27	
Neurotmesis (wrap)					0.98

Table 11.7 shows the results of the Scheffé test for median nerve versus facial nerve for axon diameter. Results were significant at $p<0.05$.

Median nerve versus facial nerve: Scheffé test p values for comparison of *fibre diameter*					
	Normal	Neurapraxia	Axonotmesis	Neurotmesis (suture)	Neurotmesis (wrap)
Normal	0.00				
Neurapraxia		0.00			
Axonotmesis			1.00		
Neurotmesis (suture)				0.91	
Neurotmesis (wrap)					1.00

Table 11.8 shows the results of the Scheffé test for median nerve versus facial nerve for *fibre diameter*. Results were significant at $p<0.05$.

Median nerve versus facial nerve: Scheffé test p values for comparison of *myelin sheath thickness*					
	Normal	Neurapraxia	Axonotmesis	Neurotmesis (suture)	Neurotmesis (wrap)
Normal	0.00				
Neurapraxia		0.00			
Axonotmesis			1.00		
Neurotmesis (suture)				1.00	
Neurotmesis (wrap)					1.00

Table 11.9 shows the results of the Scheffé test for median nerve versus facial nerve for *myelin sheath thickness*. Results were significant at $p<0.05$.

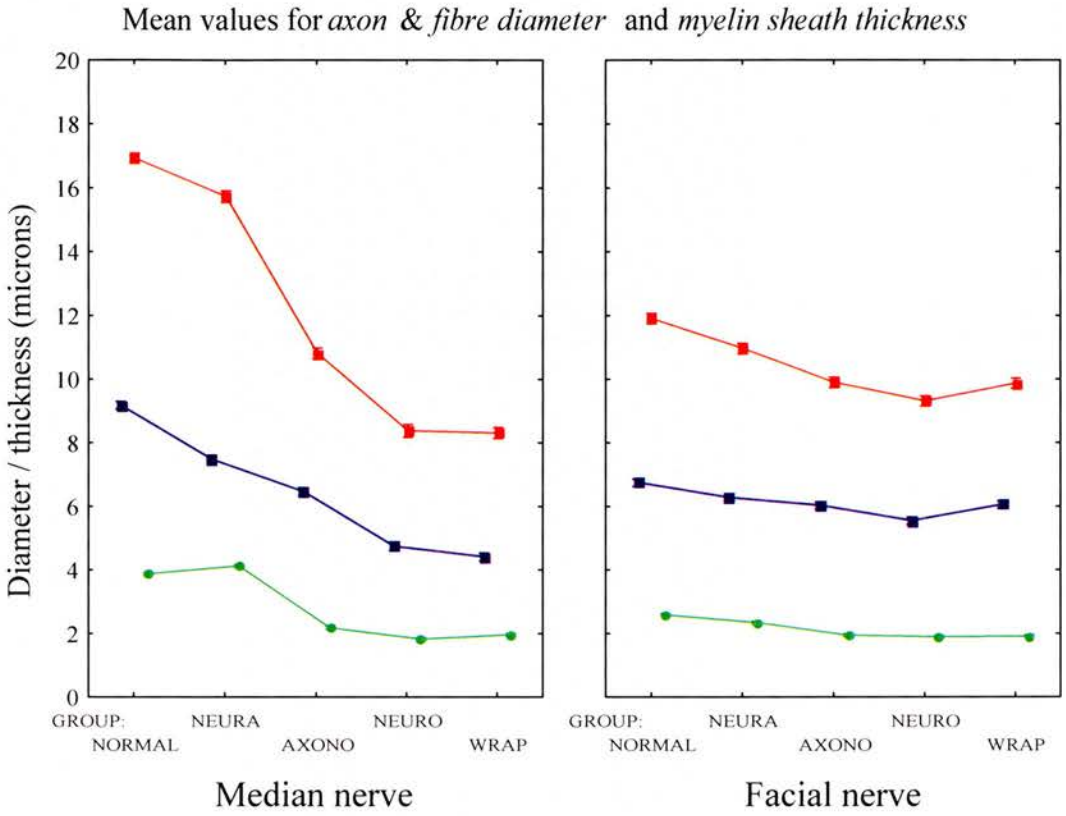

Figure 11.12 shows a comparison of the mean values for axon diameter, fibre diameter and myelin sheath thickness for the median nerve and the facial nerve.
axon **fibre** **myelin sheath**

	Mean values median and facial nerve morphometry					
	Median axon	***Facial axon***	***Median fibre***	***Facial fibre***	***Median myelin sheath***	***Facial myelin sheath***
Normal	8.99	6.59	16.72	11.63	3.87	2.45
Neurapraxia	7.44	6.28	15.29	10.97	4.12	2.34
Axonotmesis	6.46	6.02	10.82	9.90	2.17	1.94
Neurotmesis (suture)	4.75	6.06	8.39	9.87	1.82	1.91
Neurotmesis (wrap)	4.41	5.78	8.31	9.70	1.95	1.89
Graft		5.65		9.59		1.97

Table 11.10 shows the mean morphometric results for each experimental groups for the median nerve and the facial nerve.

Mean facial nerve & median nerve results as expressed as a % of the normal mean value					
	Neurapraxia	**Axonotmesis**	**Neurotmesis (Suture)**	**Neurotmesis (Wrap)**	**Graft**
Facial *axon diameter*	95%	91%	92%	87%	86%
Median *axon diameter*	83%	72%	53%	49%	
Facial *fibre diameter*	94%	85%	85%	83%	82%
Median *fibre diameter*	91%	65%	50%	50%	
Facial *myelin sheath*	96%	79%	78%	77%	82%
Median *myelin sheath*	106%	56%	47%	50%	

Table 11.11 shows the mean morphometric results for each experimental group expressed as a percentage of the normal group for both the median nerve and the facial nerve.

11.6 DISCUSSION

There was no correlation between *g ratio* and the severity of nerve injury for either the facial nerve or the median nerve. *g ratio* is an indicator of the maturity of a nerve fibre. The fact that there was no variation among the experimental groups for this variable indicates that whilst the myelin sheath was thinner in the more severe nerve injuries, it was of an appropriate thickness for those fibres. This indicates that the measured fibres have successfully innervated the target muscle and had matured. Therefore, this validates the comparison of the different models of injury because they were all mature repairs. As mentioned previously suture lines slow the rate of axonal regeneration, therefore, the transection injuries, in particular the graft group, may have taken longer to regenerate (Gutmann, Guttmann et al. 1942).

It has been demonstrated that the optimal *g ratio* for impulse conduction in peripheral nerves is between 0.6 and 0.7 (Goldman & Albus 1968; Moore, Joyner et al. 1978; Rushton 1951; Smith & Koles 1970). This is the ratio generally found in normal peripheral nerves (Goldman & Albus 1968). The *g ratio* was close to this range in all the experimental groups for both the facial nerve and the median nerve. This is further evidence that the repairs had matured and that the myelin sheath had reached the optimal thickness for the size of the fibres.

No significant differences were found among the facial nerve experimental groups for any of the morphometric variables. However, the less severe injuries had higher mean values for *fibre diameter, axon diameter* and *myelin sheath thickness*. The median nerve *axon and fibre diameter* histograms shifted progressively to the left with increasing severity of nerve injury. Unfortunately no morphometric data were

available for the median nerve graft experimental group because of technical problems in the processing of these particular nerve segments. The normal median nerve group had the highest mean value for *axon diameter* and this was significantly higher than all the other experimental groups. The normal group also had the highest mean value for *fibre diameter* and this was significantly higher than all the other experimental groups except neurapraxia. There was a decrease in *axon* and *fibre diameter* with increasing severity of nerve injury and this decrease was particularly marked for the transection injuries. The neurapraxia group had the highest mean value for *myelin sheath thickness*. There was no significant difference between the neurapraxia group and the normal group for this variable but both these groups were significantly higher than the other experimental groups. The non-transection injuries had higher mean values for *myelin sheath thickness* than the transection injuries.

NEURAPRAXIA INJURIES

There were no significant differences between the normal and neurapraxia groups for the variables *axon diameter, fibre diameter* and *myelin sheath thickness* for both the facial nerve and the median nerve (with the exception of *axon diameter* for the median nerve). Furthermore, both groups had similar distributions and profiles of the *axon* and *fibre diameter* histograms. However, the mean values for *axon diameter, fibre diameter* and *myelin sheath thickness* were slightly lower in the neurapraxia groups for both nerves, being around 90% of the normal group.

This work was the first example that an experimental model for neurapraxia had been described. Therefore, there was no previous literature with which to compare these results. Neurapraxia results in localised destruction of myelin but no Wallerian degeneration. Therefore, theoretically, there should be no change in fibre size.

However, there was a small difference between the neurapraxia group and the normal group. This may have been because a few of the fibres were disrupted and did undergo Wallerian degeneration (although the majority of fibres must have remained intact because when the nerve was stimulated distal to the site of injury, during the experiment to validate the neurapraxia model, it was possible to produce a CMAP of normal amplitude). Other possibilities are that there was some disruption of the axonal transport mechanism or that the blood supply to the nerve was damaged either by the ligature or by dissection of the tissues around the nerve.

AXONOTMESIS INJURIES

Gutman and Sanders looked at the effects on fibre number and diameter, in the peroneal nerve in rabbits, after crushing (Gutmann & Sanders 1943). They found that fibre diameter as well as the total number of fibres and the fibre-diameter histogram returned to normal. They also observed a return of the normal toe-spreading reflex. Cragg and Thomas also performed crush experiments on the peroneal nerve in adult rabbits (Cragg & Thomas 1964). However, these workers found a small reduction in *fibre diameter*, a normal *g ratio* and a reduction in *internodal length* of more than 50%. They also measured a reduction in CV_{max} of 25% compared with normal controls.

The results reported in this work show a reduction in the mean values of *axon* and *fibre diameter* and *myelin sheath thickness* for the axonotmesis group when compared to both the normal and the neurapraxia group. This reduction was more marked for the median nerve (60% to 70% of normal) than the facial nerve (80% to 90% of normal). In the facial nerve experiments there were no significant differences among any of the groups but the axonotmesis group had lower mean values for *axon diameter, fibre diameter* and *myelin sheath thickness* than the normal and neurapraxia groups but

higher mean values than the transection injuries. For the median nerve the normal and neurapraxia groups were significantly different from the axonotmesis group for *axon diameter, fibre diameter* and *myelin sheath thickness* (except the neurapraxia group for *axon diameter*) but the axonotmesis group was significantly different from the transection injuries.

Therefore, for both the median nerve and the facial nerve, the axonotmesis group had a poorer outcome than the normal and neurapraxia groups but a better outcome than the transection injuries. Axonotmesis results in Wallerian degeneration distal to the site of injury, then regeneration of fibres from proximal to the site of injury. It may be that damage to the fibres and the process of regeneration does not enable the fibres to return to normal, despite being in the correct endoneurial tubes. The regenerating fibres also have to cross the site of injury which may be affected by scarring. Another possibility is that the method used to produce the axonotmesis injury *i.e.* crushing the nerve with a clamp, disrupted some of the endoneurial tubes. This could also explain why the median nerve had a poorer outcome than the facial nerve. If there was no disruption of the endoneurial tubes then the type of nerve (motor/mixed) should have been irrelevant. However, if some of the endoneurial tubes were damaged this could have resulted in proportionately more mismatching of fibres with inappropriate endoneurial tubes in the median nerve as compared with the facial nerve (this is discussed in more detail in the next section).

NEUROTMESIS INJURIES

In nerve regeneration full function will only return if an adequate number of axons reach endoneurial tubes which are sufficiently appropriate to allow them to mature

and to reach target organs similar to those to which they were formerly connected (Young 1942).

In the work presented here, for both the facial nerve and the median nerve, the normal group and the non-transection injury groups had higher mean values for *axon diameter, fibre diameter* and *myelin sheath thickness*. There are several factors which could contribute to the poor outcome of transection injuries. Like the axonotmesis injuries transected nerves undergo Wallerian degeneration and axonal regeneration from the proximal nerve stump. However, in transection injuries the axons have to regenerate across a suture line (and in the case of grafts two suture lines) which has been shown to impede axonal regeneration. Furthermore, all the endoneurial tubes are also transected and the pioneering axons must locate a new tube through which to regenerate.

The facial nerve transection injuries did much better than the median nerve transection injuries. For the facial nerve, the mean values of the variables *axon diameter, fibre diameter* and *myelin sheath thickness* were 80% to 90% of the mean values of the normal group. However, the same variables for the median nerve were only 50% of the mean values of the normal group. Even the facial nerve graft group was not significantly different from the facial nerve normal group (also being 80% to 90% of the normal group). The poor outcome in the median nerve could have been a result of misdirection of motor fibres into small sensory endoneurial tubes which were not big enough to allow them to adequately increase in diameter and furthermore directed them to an inappropriate target organ. This mismatching of fibres and endoneurial tubes was described by Gutman and Sanders (Gutmann & Sanders 1943). These workers looked at the effects on fibre number and diameter, in the peroneal

nerve in rabbits, after crushing and nerve transection and immediate epineurial suture repair (Gutmann & Sanders 1943). In the end-to-end-suture group both the total number of fibres and the fibre diameter were reduced and the normal toe-spreading reflex was not regained. However, Gutman and Sanders found that sixty days after an axonotmesis injury there was return of the normal toe-spreading reflex despite the fact that the fibres in these nerves were smaller than in the nerves with neurotmesis injuries two hundred days after injury, where the normal toe-spreading reflex had not returned (Gutmann & Sanders 1943). These authors postulated that it was not only fibre size (and by inference conduction velocity) which decided the functional outcome of the regenerative process. They suggested that disruption of fibres at the suture line in the neurotmesis group resulted in fibres attempting to regenerate in inappropriate endoneurial tubes so that they were functionally "lost" or unable to mature to their potential size. In contrast the fibres in the axonotmesis group regenerated along their original tubes to an appropriate target organ. However, it should be noted that these authors described evidence of "pull-out" and/or neuromata formation in some of the sutured repairs which must had a detrimental effect on the functional outcome.

Berry *et al* transected the tibial, peroneal and saphenous nerves of cats and performed immediate epineurial suture repair (Berry, Grundfest, & Hinsy 1944). These authors found both *fibre diameter* and CV_{max} were reduced by more than 20% of the normal value.

Young transected a spinal nerve (containing large medullated fibres) and sutured it either to its own distal stump or to the post-ganglionic trunk of the anterior mesenteric nerve (which contained predominantly small, non-myelinated fibres) (Young 1942). He found that the fibres in the distal stump of the latter group were smaller and

attributed this to the smaller endoneurial tubes. However, he also performed the converse experiment, transecting the anterior mesenteric nerve and suturing its proximal stump to the peripheral stump of the spinal nerve. This repair produced muscle contraction but the distal stump contained fine non-myelinated fibres despite large calibre endoneurial tubes. Therefore, he concluded that both the original fibre type and the size of the endoneurial tubes in the distal stump influence fibre diameter. Holmes and Young performed delayed nerve repairs and found this resulted in smaller fibres in the distal stump which they proposed was due to shrinkage of the endoneurial tubes (Holmes & Young 1942). Thomas attributed this shrinkage to formation of a new layer of collagen between the inner endoneurial sheath and the basement membrane (Thomas 1964).

In the rabbit the tibial and peroneal nerves are mixed nerves in the proximal thigh but distally divide into predominantly motor (large fibres) and sensory (small fibres) branches. Sanders and Young transected these nerves just proximal to the branching point, performed end-to-end suture and studied the sizes of the regenerated fibres in the two branches (Sanders & Young 1944). The reinnervated motor branch contained larger fibres than the sensory branch, although these fibres were smaller than in the normal nerve. They also performed the same procedure after a delay of ten months and again found that the motor branch contained bigger fibres than the sensory branch but these were smaller than those in the immediate repair group. These workers concluded that the size of the endoneurial tubes had an effect on fibre diameter. However, they also concluded that the diameter which a regenerating fibre was capable of reaching was determined by the calibre of fibre from which it arises in the central stump. Gutman and Sanders proposed that there was a greater outflow of

axoplasm from the proximal stump of larger fibres and that this resulted in larger regenerated fibres (Gutmann & Sanders 1943).

There continues to be some debate about whether the matching of axonal sprout to endoneurial tube is a random event or under the influence of neurotropic factors. In the results presented here, the disparity between the facial nerve and the median nerve would support the former. A large number of peripheral nerve injuries were sustained during the First World War. Reports of the outcome of the repair of these injuries showed that repair of the radial nerve (predominantly motor) was much more successful than either repair of the median nerve or the ulnar nerve (which are both mixed) (Platt & Bristow 1924).

Gillespie *et al* transected the common nerve to the rat gastrocnemius (fast twitch) and soleus (slow twitch) muscles, to study whether there was any selective reinnervation of the muscles (Gillespie, Gordon, & Murphy 1985). The results were consistent with random reinnervation. However, Hoh found that the denervated rat extensor digitorum muscle was preferentially reinnervated by its own nerve as opposed to the nerve to soleus (Hoh 1975). Brushart suggested that specificity of fibre-endoneurial tube pairing arose by 'pruning' of inappropriate fibres within the tube rather than by selection of a particular endoneurial tube by an axon (Brushart 1993).

It has been suggested that entubulation of nerves as opposed to end-to-end suture may improve the specificity with which motor axons find their target muscle. Bodine-Fowler *et al* transected the rat sciatic nerve and repaired it with a standard epineurial suture repair or using a silicone conduit leaving a 5mm gap between the nerve ends (Bodine-Fowler et al. 1997). They found no difference in outcome between the two groups. Similarly in the work presented here there was no difference between the

transected nerves repaired by suture or entubulation for either the facial nerve or the median nerve.

For the facial nerve the mean values of *axon diameter, fibre diameter* and *myelin sheath thickness* were lowest in the graft group, although there were no significant differences among the experimental groups (and the graft group was 80% to 90% of the normal group for these variables). As mentioned previously no morphometric data were available for the median nerve graft experimental group because of technical problems in the processing of these nerve segments. The same factors which had a detrimental effect on outcome in the simple transection injuries (disruption at the suture line, mismatching of fibres and endoneurial tubes) would have had a bigger effect on the graft groups because they contained two suture lines. Given this, it would seem reasonable to assume that the median nerve graft group would have had a particularly poor outcome.

Gutman and Sanders performed four graft repairs on the peroneal nerve (Gutmann & Sanders 1943). They found that the fibre diameter was reduced as well as the total number of fibres, and that these fibres were smaller than those after the end-to-end suture of the same nerve. The second peak of the fibre diameter histogram was also lost in the grafted nerves. However, the graft repairs were only assessed up to two hundred days and since the neurotmesis and suture repair group improved between 200 and 364 days it seems likely that the graft repairs were not mature. Interestingly, these workers found higher numbers of fibres within the graft than in the nerve distal to it. They suggested that fibres were lost by further disruption at the second suture line. However, Young ascribed the higher number of fibres in the graft to the fact that it contained more endoneurial tubes than the distal stump (Young 1942).

In summary the variables *axon diameter, fibre diameter* and *myelin sheath thickness* all decreased with increasing severity of nerve injury. The transection injuries had a poorer outcome because of the disruption at the suture line(s) and mismatching of fibres and endoneurial tubes. The median nerve, being a mixed nerve did worse in this regard than the purely motor facial nerve. The apparent influence of the size of endoneurial tubes over fibre diameter raises the question of the use of sensory nerve cable grafts, which contain small endoneurial tubes, in the repair of motor nerves, which contain large fibres.

12 DISCUSSION

12.1 OUTCOME OF DIFFERENT MODELS OF NERVE INJURY

The return of normal function was seen in the neurapraxia groups for both the facial nerve and the median nerve. Therefore, it would appear that the nerves were able to fully recover from this localised demyelination injury. There was a detectable difference between the axonotmesis group and the normal group. However, the axonotmesis injuries had a better functional and morphometric outcome than the transection injuries. In axonotmesis the nerve distal to the site of injury undergoes Wallerian degeneration. Although the regenerating axons regrow along their original endoneurial tubes, it appears that this process of degeneration and regeneration has a small effect on the function of the nerve. Therefore, even in optimal conditions *i.e.* intact endoneurial tubes, the process of regeneration is not able to completely restore the nerve to its former state. This process of regeneration is obviously very different from the initial development of the peripheral nervous system *in utero* and during the early years of life. Hursh demonstrated that in kittens, up until the age of three months, fibre diameter increased as the limbs and peripheral nerves lengthened (Hursh 1939). Furthermore, Lascelles and Thomas demonstrated that the internodal length in peripheral nerves in the limb increased as the limb lengthened (Lascelles & Thomas 1966). They stated that during development, at the time of myelination, internodal length was universally short, that the number of nodes along a particular fibre remained constant and that internodal length was determined by the growth in length of the body part in which the nerve was situated. As injured nerves do not undergo these processes this may explain the thinner fibres and shorter internodal

lengths observed, with consequent effects on conduction velocity. Furthermore, although in axonotmesis injuries axons regenerate along their original tube to reach the original target organ, it is recognised that this type of injury can result in reconfiguration of motor units and this may be another factor which affects the outcome of these injuries. Also, as previously discussed the model of axonotmesis injury used in these experiments may disrupt some of the endoneurial tubes, effectively resulting in a mixed Sunderland Type III and Type IV nerve injury.

In both the facial nerve and the median nerve the transection injuries had a poorer outcome than the non-transection injuries. This difference was not as marked for the facial nerve as for the median nerve (the reasons for this are discussed in the next section). There were no differences in outcome between the end-to-end suture group and the entubulation group for either nerve. This raises the possibility of the use of the 'wrap' method in clinical practice, which would obviate the need for microsurgical technique and an operating microscope. This could be particularly useful in 'field' hospitals during war-time and also in developing countries. Entubulation may also offer a mechanism for the introduction of, for example, growth factors, in the chemical manipulation of nerve regeneration. Furthermore, it has been suggested that entubulation of nerves as opposed to end-to-end suture may improve the specificity with which motor axons find their target muscle. However, Bodine-Fowler *et al* found no evidence of this when they compared entubulation with suture repair (Bodine-Fowler, Meyer et al. 1997) and as discussed later it appears more likely that axon and endoneurial tube pairing is a random event.

The graft models had the poorest outcome for both the facial nerve and the median nerve, and again there was a more profound effect on the median nerve. This indicated that the further disruption of axons and endoneurial tubes at a second suture

line had a cumulatively detrimental effect on the functional outcome of nerve regeneration.

12.2 Comparison of Facial Nerve Results with Median Nerve Results

There were no differences among any of the experimental groups for both the facial nerve and the median nerve for the measurement of *jitter*. This indicated that the new NMJs were mature in both nerves in all the experimental groups. Furthermore, there were no differences in *g ratio* among the experimental groups for both the facial nerve and the median nerve. This indicated that the myelin sheath was an appropriate thickness for the fibre diameter and was further evidence that all the repairs had matured. This validated comparison of the results between the experimental groups and between the two nerves.

A large number of peripheral nerve injuries were sustained during the First World War. Reports of the outcome of the repair of these injuries suggested that repair of the radial nerve (predominantly motor) was much more successful than either repair of the median nerve or the ulnar nerve (both mixed nerves) (Platt & Bristow 1924). One of the aims of this work was to investigate, using standardised models of nerve injury and reliable, objective methods of assessment, whether the type of nerve affected the outcome after injury. It was postulated that a mixed nerve may suffer a higher proportion of inappropriate pairing of fibres and endoneurial tubes at suture lines. It followed from this that a mixed nerve would do relatively worse, when compared with a unimodal nerve, after transection injuries than non-transection injuries. This hypothesis was confirmed by the work presented in this thesis. The facial nerve was selected as a purely motor nerve and the median nerve as the mixed nerve. Both these nerves are commonly injured (due to trauma or surgery) and/or affected by other conditions (Bell's palsy, carpal tunnel syndrome).

In both the facial nerve and the median nerve CV_{max} decreased with increasing severity of nerve injury. The normal, neurapraxia and axonotmesis median nerve groups all conducted faster than the equivalent facial nerve groups. However, in the transection injury groups, both nerves conducted impulses at similar velocities. This indicated that the median nerve had a relatively poorer outcome after transection than the facial nerve. Similar results were found for the *DCV* experiments. In both the facial nerve groups and the median nerve groups the *DCV* profiles shifted to the left with increasing severity of injury. However, this shift was more marked for the median nerve. Furthermore, it was impossible to obtain *DCV* profiles for the median nerve graft group because of the degree of distortion of the CMAP traces.

For both the facial nerve and the median nerve, there were no significant differences among the experimental groups for the measurements of twitch tension and time. This may have been because the regenerated axons were similar enough to the original axons to allow the muscle to regain its former force profile. The 'self-reinnervation' experiments described in Chapter 10 (Muscle Physiology) demonstrated that muscle reinnervated by its original nerve retained its original twitch characteristics (Barany & Close 1970). No significant differences were found among the experimental groups for either nerve for the measurements of tetanic tension. This lack of variation among the groups may be further explained by the fact that only 5% of the original number of axons is required to reinnervate a muscle to enable it to generate the original force.

Significant differences were found among the median nerve groups for the variable *tetanic tension index*, which decreased with the increasing severity of nerve injury. However, this relationship was not observed for the facial nerve injuries. Luff *et al* demonstrated that some reinnervated muscles were unable to maintain tetanus at higher frequencies of stimulation (Luff, Hatcher, et al. 1988). These authors proposed

that reinnervation of muscles was less 'secure' than normal innervation. Therefore, whilst they were able to generate the same amount of tension the overall functioning or efficiency of the reinnervated muscles in the median nerve groups may have been reduced. This could have been a result of a lower and less sustainable supply of energy and/or a poorer blood supply. In this regard, the superior performance of the facial nerve experimental groups is further evidence that the type of nerve affects the functional outcome of nerve repair. As there is less potential for mismatching of fibres in the facial nerve (as opposed to the median nerve) reinnervation of the facial muscles may be more 'secure' or similar to the original situation. Furthermore, most limb and trunk muscles contain all three types of muscle fibres (Burke 1980). It may be that the facial muscles contain a more homogeneous selection of muscle fibres, and, whilst it has been documented that pioneering axons are able to reinnervate any type of fibre if the axon-muscle fibre match is the same as the original this may produce a better functioning unit. Furthermore, there were no significant differences among the facial nerve groups for the measurement of target muscle mass (LLM). However, the median nerve groups showed a progressive decline in target muscle mass (FCR) with the increasing severity of nerve injury.

Nerve transection and repair (by whatever method) means that pioneering axons must find new endoneurial tubes in the distal nerve stump. To survive, axons must enter a suitable endoneurial tube and reinnervate an appropriate target organ. Axons which make inappropriate distal connections or fail to reach the target organ will die. Normal function of a nerve will only return if an adequate number of axons reach endoneurial tubes in the peripheral stump which allow them to mature properly and also guide them to an appropriate target organ (Young 1942).

The work presented here illustrated that this process was more successful in a purely motor nerve (facial nerve) than a mixed nerve (median nerve). It is likely that this was because a higher proportion of the axons in the median nerve attempted to regenerate along the wrong type of endoneurial tube. This mismatching of fibres and endoneurial tubes could have resulted in pairing of motor fibres with small sensory endoneurial tubes which were not big enough to allow them to adequately increase in diameter and furthermore directed them to an inappropriate target organ. However, in the case of the facial nerve, whilst it is unlikely that the axons regenerated along their original tubes, most of the available endoneurial tubes would have guided the axons to a suitable target organ and supported their regeneration and maturation.

There continues to be debate about whether the pairing of pioneering axons and endoneurial tubes is a controlled or random event. Results of work performed by Gillespie *et al* were consistent with random reinnervation, whereas Hoh suggested there was control of this process (Gillespie, Gordon, & Murphy 1985; Hoh 1975). In the work presented here there was a large discrepancy in outcome after transection of the median nerve compared with transection of the facial nerve. Therefore, it seems unlikely that a controlled selection process, analogous to that suggested by Hoh, was occurring to any significant degree. In conclusion, the pairing of pioneering axons and endoneurial tubes would appear to be a random event ultimately resulting in a poorer functional outcome after transection and repair of a mixed nerve when compared to a motor nerve.

12.3 Comparison of Tests and Applicability for Use in Clinical Practice and Research

In motor studies both *jitter* and *g ratio* may be regarded as measurements of the successfulness and maturity of reinnervation of a target muscle. The results for *jitter* and *g ratio* correlated with each other. There were no differences among any of the experimental groups for both the facial and the median nerve for the measurement of *jitter*. This indicates that all the assessed NMJs were mature and functioning. Similarly there were no differences among any of the experimental groups for both the facial nerve and the median nerve for the measurement of *g ratio*. This indicates that all the nerve injuries were mature and that those fibres that were assessed had successfully reinnervated target muscles.

Jitter is a quick, simple test to perform in a clinical setting to assess the maturity of muscle reinnervation. The work of Lenihan *et al* showed that jitter decreased from the time of nerve injury in those nerves that successfully reinnervated muscle and in the work presented here confirmed that the muscle reinnervation had matured (Lenihan et al 1997). Therefore, the use of jitter in a clinical setting may be useful to monitor muscle reinnervation, identify those cases where reinnervation has failed and identify the end-point of reinnervation when the NMJs have matured.

There were no differences in refractory period among the experimental groups for both nerves. Therefore, refractory period cannot be recommended as a useful tool to discriminate between nerve injuries. However, in these experiments refractory period was measured distal to the site of injury. Experience from the *DCV* experiments, where the nerve was repeatedly stimulated proximal to the site of injury, showed that the more severe injuries needed longer to recover between stimulations. Therefore,

measurement of this variable using stimulation proximal to the injury may have revealed longer refractory periods in the more severe injuries.

There was a big range of the refractory period of fibres *within* each nerve, and measurement of this range could increase the accuracy of *DCV*. It is generally accepted that slower fibres have longer refractory periods than faster fibres but there is some debate about the precise nature of the relationship between refractory period and conduction velocity. There is a need to establish whether refractory period has an inverse relationship with conduction velocity (as suggested by Harayama *et al*) or is skewed so that the majority of fibres have a short refractory period (as suggested by Betts *et al*) (Betts, Johnston, & Brown 1976; Harayama, Shinozawa et al. 1990). This would determine whether an inverse relationship should be employed between conduction velocity and refractory period or a single median value. The same set-up of stimulating and recording electrodes is used in the calculation of both refractory period and DCV. Therefore, using the double stimulation technique described by Betts *et al,* the range of refractory period could be quickly determined before the calculation of *DCV* (Betts, Johnston, & Brown 1976). If an inverse relationship existed, then failure to incorporate refractory period into the calculation of *DCV* would result in underestimation of the conduction velocity of slower fibres as the refractory period would constitute a bigger proportion of the latency of the impulse of these fibres. However, as previously discussed, in the work presented here there were no significant differences in refractory period among the experimental groups. Therefore, in this case failure to consider refractory period in the calculation of *DCV* may have had a similar effect on all the experimental groups.

The results for CV_{max} correlated with the *DCV* profiles, that is CV_{max} decreased with increasing severity of nerve injury whilst the *DCV* profiles shifted to the left with

increasing severity of nerve injury. *DCV* is a more comprehensive test than CV_{max} as it enables calculation of the conduction velocities of all fibres within a nerve rather than just the fastest fibres. However, in the assessment of peripheral nerve injuries *DCV* has no clinical advantage over CV_{max}. This is because the extent of these injuries is such that they do not require subtle tests to detect them. Furthermore, larger faster fibres are more susceptible to injury and damage to these fibres would be detected by the measurement of CV_{max}. The work presented here has demonstrated that CV_{max} differentiates between different types of nerve injury and this test must therefore be recommended in the clinical assessment of these injuries.

DCV may have a role in the assessment of more subtle conditions *e.g.* Bell's palsy. The House-Brackman classification is widely used to determine the severity of facial weakness. This depends on subjective grading of the degree of facial weakness on the part of the clinician. Objective electrophysiological tests used in the assessment of this condition are electroneurography (ENOG) and electromyography. In ENOG studies the facial nerve is stimulated at stylomastoid foramen and CMAPs are recorded from facial muscles by placement of a surface electrode over the nasolabial fold. If the amplitude of the CMAP on the affected side is less than 10% of the amplitude of the CMAP on the unaffected side then EMG tests are performed.

Surgical decompression of the facial nerve in the treatment of Bell's palsy remains controversial, with many surgeons questioning the efficacy of the procedure. However, in those centres that do perform facial nerve decompression, failure to detect muscle action potentials on the affected side of the face, is taken as an indication for surgery.

Therefore, there may be a group of patients undergoing unnecessary procedures *i.e.* those who would make a spontaneous recovery and also those in whom recovery is

unlikely regardless of surgery. Furthermore, the procedure itself is not without risk and entails decompression of the nerve along the length of its intratemporal course. *DCV* is a comprehensive test, providing information on the functioning of all fibres within a nerve. It is possible that the addition of *DCV* into the assessment of patients with Bell's palsy may refine the selection process and enable better patient selection for surgery.

For both the facial nerve and the median nerve, assessment of the twitch tension profile (including the twitch tension and time) failed to discriminate between nerve injuries. As discussed earlier, this may have been because the regenerated axons were similar enough to the original axons to allow the muscle to regain its former force profile. However, there is some doubt as to the reliability and/or reproducibility of the measurement of twitch tension. This is because during a twitch contraction the maximum force of the muscle is not generated and also because the magnitude of the twitch tension is affected by the number of previous stimulations of the muscle (and this varied between different nerves and experimental groups) (Desmedt & Hainaut 1968).

Measurements of tetanic tension did not reveal any relationship with the severity of nerve injury for the facial nerve. No significant differences were found among the median nerve groups for the measurement of tetanic tension (although the non-transection injuries had higher mean values). Luff *et al* demonstrated that new motor units contain higher numbers of muscle fibres and can generate forces two to sixteen times that of normal motor units (Luff, Hatcher, et al. 1988). These authors also demonstrated that reinnervation of muscle with only 5% of the original number of nerve fibres was required to generate the original force.

Clearly these objective measurements of individual muscle tension and mass cannot be made in clinical practice. However, muscle strength can be subjectively assessed in clinical practice using the MRC grading for the limbs and the House-Brackman scale for facial nerve function. The usefulness of these measurments in a research setting is debatable. The work presented here shows they are not sensitive discriminators between nerve injuries, none the less, in motor studies they do provide information on target muscle function.

It has been shown that only 5% of the original number of axons are required to restore normal muscle power (Luff, Hatcher, et al. 1988), therefore, in this respect muscle tension does not provide detailed quantitative information on the number of regenerated nerve fibres. Furthermore, it must be considered how much qualitative information it provides on the functional outcome of nerve repairs. The return of power is only a part of the return of function of a mixed nerve (of which it should be remembered is the type of nerve where these tests discriminate between injuries) other modalities such as sensation and proprioception should also be considered. In median nerve injuries the alteration of sensation and proprioception probably contributes more to the poor outcome than a loss of power.

This work has demonstrated that measurement of axon and fibre diameter and myelin sheath thickness can discriminate between different types of nerve injury. Although these tests are inapplicable to clinical practice they remain useful in the laboratory investigation of peripheral nerve injuries. If an axon successfully reinnervates a target organ the fibres then increase in diameter and in the case of motor fibres become medullated (Gutmann & Sanders 1943). This increase in fibre diameter and myelin sheath thickness may be necessary before the axons can conduct impulses which produce effective function (Young 1942). Therefore, the level of regeneration,

maturation and, to an extent, the function of a nerve can be inferred by morphometric analysis. Furthermore, g ratio is useful in the assessment of the maturity of nerve fibres.

In conclusion the measurement *CVmax* would appear to be the most useful test for the objective assessment of nerve injuries in clinical practice. The potential role of *DCV* (with the incorporation of refractory period) has yet to be established. In this work morphometric analysis was demonstrated to discriminate between different nerve injuries and, whilst inapplicable to clinical practice, remains an important investigation in a research setting.

13 REFERENCES

Adour, K., Ruboyianes, J., Von Doersten, P., Byl, F., Trent, C., Quesenberry, C., & Hitchcock, T. 1996, "Bell's palsy treatment with acyclovir and prednisone compared with prednisone alone: a double-blind, randomized, controlled trial.", *Annals of Otology Rhinology and Laryngology*, vol. 105, no. 5, pp. 371-378.

Adrian, E. 1921, "The recovery process of excitable tissues.", *Journal of Physiology*, vol. 55, pp. 193-225.

Barany, M. & Close, R.I., 1970 "The transformation of myosin in cross-innervated rat muscles.", *Journal of Physiology*, vol. 213, pp. 455-474.

Bennett, GJ & Xie YK. 1988, "A peripheral mononeuropathy in rat that produces disorders of pain sensation like those seen in man". *Pain*, vol. 42, pp. 253-255.

Berry, C., Grundfest, H., & Hinsy, J. 1944, "The electrical activity of regenerating nerves in the cat", *Journal of Neurophysiology*, vol. 7, pp. 103-115.

Betts, R., Johnston, D., & Brown, B. 1976, "Nerve fibre velocity and refractory period distributions in nerve trunks.", *Journal of Neurology, Neurosurgery and Psychiatry*, vol. 39, pp. 694-700.

Binnie, C., Cooper, R., Fowler, C., Mauguiere, F., & Prior, P. Clinical Neurophysiology. First. 1995. Butterworth-Heinemann Limited.
Ref Type: Serial (Book,Monograph)

Blair, E.A. & Erlanger, J. 1946, "A comparison of the characteristics of axons through their individual electrical responses.", *American Journal of Physiology*, vol. 106, pp. 524-564.

Bodine-Fowler, S., Meyer, R., Moskovitz, A., Abrams, R., & Botte, M. 1997, "Inaccurate projection of rat soleus motoneurons: A comparison of nerve repair techniques", *Muscle & Nerve*, vol. 20, pp. 29-37.

Borg, J. 1980, "Axonal refractory period of single short toe extensor motor-units in man.", *Journal of Neurology, Neurosurgery and Psychiatry*, vol. 43, pp. 917-924.

Bowden, R.E.M. & Gutmann, E., 1944, "Deinnervation and reinneravtion of human voluntary muscle.", *Brain*, vol. 67, pp. 273-281.

Boyd, I. 1964, "The relation between conduction velocity and diameter for the three groups of efferent fibres in nerves to mammalian skeletal muscle.", *Journal of Physiology*, vol. 175, pp. 33P-35P.

Brill, M. H., Waxman, S. D., Moore, J. W., & Joyner, R. W. 1977, "Conduction velocity and spike configuration in myelinated fibres. Computed dependence on internode length.", *Journal of Neurology, Neurosurgery and Psychiatry*, vol. 40, pp. 769-774.

Brown, M., Martin, J., & Asbury, A. 1974, "Painful diabetic neuropathy: A morphometric study", *Archives of Neurology*, vol. 33, pp. 164-171.

Brushart, T. 1993, "Motor axons preferentially reinnervate motor pathways", *Journal of Neuroscience*, vol. 13, pp. 2730-2738.

Buller, A., Eccles, J., & Eccles, R. 1959, "Inetraction between Motoneurones and Muscles in Respect of the Characteristic Speeds of their Responses.", *Journal of Physiology*, vol. 150, pp. 417-439.

Buller, A., Eccles, J., & Eccles, R. 1960, "Differentitiation of fast and slow muscles in the cat hand limb.", *Journal of Physiology*, vol. 150, no. 417, p. 439.

Burke, R. 1967, "Motor unit types of cat triceps surae muscle", *Journal of Plastic Surgery*, vol. 193, pp. 141-160.

Burke, R. 1980, "Motor unit types: functional specialisations in motor control.", *Trends in Neuroscience*, vol. , pp. 255-258.

Cajal, R. 1928, *Degeneration and regeneration of the nervous system.* Oxford University Press, London.

Clark, W., Trumble, T., Swiontowski, M., & Tencer, A. 1992, "Nerve tension and blood flow in a rat model of immediate and delayed repairs", *The Journal of Hand Surgery*, vol. 17A, pp. 677-687.

Close, R. 1964, "Dynamic Properties of Fast and Slow Skeletal Muscles of the Rat During Development.", *Journal of Physiology*, vol. 173, pp. 74-95.

Close, R. 1965a, "The effects of cross-innervation of motor nerves to fast and slow skeletal muscle.", *Nature*, vol. 206, pp. 831-832.

Close, R. 1965b, "The effects of cross-innervation of motor nerves to fast and slow skeletal muscle.", *Nature*, vol. 206, pp. 831-832.

Close, R. 1972, "Dynamic Properties of Mammalian Skeletal Muscles", *Physiological Reviews*, vol. 52, pp. 129-197.

Coles, A. 2001, "The seventh cranial nerve", *Advances in Clinical Neoroscience and Rehabilitation*, vol. 1, no. 4, pp. 16-17.

Coppin, C. & Jak, J. 1971, "Internodal length and conduction velocity of cat muscle afferent nerve fibres.", *Journal of Physiology*, vol. 222, pp. 91P-93P.

Cragg, B. & Thomas, P. 1964, "The Conduction Velocity of Regenerated Peripheral Nerve Fibres", *Journal of Physiology*, vol. 171, pp. 164-175.

Cross, T., Sheard, C., Garrud, P., Nikolopoulos, T., & O'Donoghue, G. 2000, "Impact of facial paralysis on patients with acoustic neuroma", *Laryngoscope*, vol. 110(9), pp. 1539-1542.

Cummins, K. & Dorfman, L. J. 1981, "Nerve fibre conduction velocity distributions: Studies of normal and diabetic human nerves.", *Annals of Neurology*, vol. 9, pp. 67-74.

Cummins, K., Perkel, D., & Dorfman, L. J. 1978, "Nerve fibre conduction-velocity distributions. I. Estimation based on the single-fibre and compound action potentials.", *Electroencephalography and clinical Neurophysiology*, vol. 46, pp. 634-646.

Cummins, K., Dorfman, L. J., & Perkel, D. 1979, "Nerve fibre conduction-velocity distributions. II. Estimation based on two compound action potentials.", *Electroencephalography and clinical Neurophysiology*, vol. 46, pp. 647-658.

de Jesus, P., Hausmanowa-Petrusewicz, M., & Barchi, R. 1973, "The effect of cold on nerve conduction of human slow and fast nerve fibres.", *Neurology*, vol. 23, pp. 1182-1189.

Desmedt, J. & Hainaut, K. 1968, "Kinetics of Myofilament Activation in Potentiated Contraction: Staircase Phenomenon in Human Skeletal Muscle.", *Nature*, vol. 217, pp. 529-532.

Dorfman, L. J. 1984, "The distribution of conduction velocities (DCV) in peripheral nerves: a review", *Muscle & Nerve* no. 7, pp. 2-11.

Dorfman, L. J., Cummins, K., & Abraham, G. 1982, "Conduction velocity distributions of the human median nerve: Comparison of methods", *Muscle & Nerve*, vol. 5, p. S148-S153.

Drew, S., Fullarton, A., Glasby, M., Mountain, R., & Murray, J. 1995, "Re-innervation of facial nerve territory using a composite hypoglossal nerve-muscle autograft-facial nerve bridge. An experimental model in sheep.", *Clinical Otolarynglogy*, vol. 20, pp. 109-117.

Enver, M. & Hall, S. 1994, "Are Schwann cells essential for axonal regeneration into muscle autografts?", *Neuropathology and Applied Neurobiology*, vol. 20, pp. 587-598.

Erlanger, J. & Schoepfle, G. 1946, "A Study of Nerve Degeneration and Regeneration", *American Journal of Physiology*, vol. 147, pp. 550-581.

Finkelstein, D., Dooley, P., & Luff, A. 1993, "Recovery of muscle after different periods of denervation and treatments", *Muscle & Nerve*, vol. 16, pp. 769-777.

Flores, A., Lavernia, C., & Owens, P. 2000, "Anatomy and Physiology of Peripheral Nerve Injury and Repair.", *The American Journal of Orthopaedics*, vol. 29, no. 3, pp. 167-173.

Fullarton, A. 1994, *An Investigation into the Recovery of Function after Different Types of Nerve Injury and Repair of Peripheral Nerve- A Comparison Between Non-diabetic and STZ Diabetic Rats.*

Fullarton, A.C., Myles, L.M., Lenihan, D.V., Hems, T.E.J. & Glasby, M.A., 2001, "Obstetric bracial plexus palsy: a comparison of the degree of the degree of recovery after repair of a C6 ventral root avulsion in newborn and adult sheep.", *Journal of Plastic Surgery*, vol. 54, pp. 697-704.

Fiehn, W. & Peter, J.B., 1971 "Properties of the fragmented sarcoplasmic reticulum from fast-twitch and slow-twitch muscles.", *Journal of Clinical Investigations*, vol. 50, pp. 570-573.

Gasser, H. & Erlanger, J. 1927, "The role played by the sizes of constituent fibres of a nerve trunk in determining the form of ita action potential wave.", *American Journal of Physiology*, vol. 80, pp. 522-547.

Gasser, H. & Grundfest, H. 1939, "Axon diameters in relation to the spike dimensions and the conduction velocity in mammalian A fibres.", *American Journal of Physiology*, vol. 127, pp. 393-414.

Gilchrist, T., Glasby, M. A., Healy, D. M., Kelly, G., Lenihan, D. V., McDowall, K. L., Miller, I. A., & Myles, L. M. 1998, "In vitro nerve repair - in vivo. The reconstruction of peripheral nerves by entubulation with biodegradable glass tubes - a preliminary report.", *British Journal of Plastic Surgery*, vol. 51, pp. 231-237.

Gillespie, M., Gordon, T., & Murphy, P. 1985, "Reinnervation of the lateral gastrocnemius and soleus muscles in the rat by their common nerve.", *Journal of Physiology*, vol. 372, pp. 485-500.

Gilliatt, R. & Willison, R. 1963, "The refractory and supernormal periods of the human median nerve", *Journal of Neurology, Neurosurgery and Psychiatry*, vol. 26, pp. 136-147.

Glasby, M., Fullarton, A., & Lawson, G. 1997, "Immediate and delayed nerve repair using freeze-thawed muscle autografts in complex nerve injuries. Cavitation, fibrosis and haematoma.", *Journal of Hand Surgery*, vol. 22, pp. 479-485.

Glasby, M., Fullarton, A., & Lawson, G. 1998, "Immediate and delayed nerve repair using freeze-thawed muscle autografts in complex nerve injuries. Associated arterial injuries.", *Journal of Hand Surgery*, vol. 23, pp. 354-359.

Goldman, L. & Albus, J. S. 1968, "Computation of impulse conduction in myelinated fibres; theoretical basis of the velocity-diameter relation", *Biophysical Journal*, vol. 8, pp. 597-607.

Gordon, A., Huxley, A., & Julian, F. 1966a, "Tension Development In Highly Stretched Vertebrate Muscle Fibres.", *Journal of Physiology*, vol. 184, pp. 143-169.

Gordon, A., Huxley, A., & Julian, F. 1966b, "The Variation in Isometric Tension with Sarcomere Length in Vertebrate Muscle Fibres.", *Journal of Physiology*, vol. 184, pp. 170-192.

Gordon, T. & Stein, R. 1982, "Reorganization of motor-unit properties in reinnervated muscles of the cat.", *Journal of Neurophysiology*, vol. 48, pp. 1175-1190.

Grogan, P. & Gronseth, G. 2001, "Practice Parameter: Steroids, acyclovir, and surgery for Bell's palsy (an evidence-based review): report of the Quality Standards Subcommittee of the American Academy of Neurology.", *Neurology*, vol. 56, no. 7, pp. 830-836.

Gutmann, E. 1948, "Effect of delay of innervation on recovery of muscle after nerve lesions", *Journal of Neurophysiology*, vol. 11, pp. 277-293.

Gutmann, E., Guttmann, L., Medawar, P., & Young, J. 1942, "The rate of regeneration of nerve.", *Journal of Experimental Biology*, vol. 19, pp. 14-44.

Gutmann, E. & Sanders, F. 1943, "Recovery of fibre numbers and diameters in the regeneration of peripheral nerves.", *Journal of Physiology*, vol. 101, pp. 489-518.

Guyton, A. 1991, *Textbook of medical physiology*, Eight edn, W.B.Saunders Company, Philadelphia.

Hall, S. 2001, "Nerve Repair: A Neurobiologist's View", *The Journal of Hand Surgery*, vol. 26, pp. 129-136.

Harayama, H., Shinozawa, K., Kondo, H., & Miyatake, T. 1990, "A method to measure the distribution of motor conduction velocity in man.", *Electroencephalography and clinical Neurophysiology*, vol. 81, pp. 323-331.

Hartree, W. & Hill, A. 1921, "The regulation of the supply of energy in muscular contraction.", *Journal of Physiology*, vol. 55, pp. 133-158.

Henneman, E., Clamann, H., Gillies, J., & Skinner, R. 1974, "Rank order of motoneurons within a pool: Law of combination.", *American Journal of Physiology*, vol. 37, pp. 1338-1349.

Hoh, J. 1975, "Selective and non-selective reinnervation of rat skeletal muscle.", *Journal of Physiology*, vol. 251, pp. 791-801.

Holmes, W. & Young, J. 1942, "Nerve regeneration after immediate and delayed suture", *Journal of Anatomy*, vol. 77, pp. 63-92.

Hursh, J. B. 1939, "Conduction velocity and diameter of nerve fibres.", *American Journal of Physiology*, vol. 127, pp. 131-139.

Ingram, D., Davis, G., & Swash, M. 1986, "The double collision technique: a new method for measurement of the motor nerve refractory period distribution in man.", *Electroencephalography and clinical Neurophysiology*, vol. 66, pp. 225-234.

Ingram, D., Davis, G., & Swash, M. 1987, "Motor nerve conduction velocity distributions in man: results of a new computer-based collision technique.", *Electroencephalography and clinical Neurophysiology*, vol. 66, pp. 235-243.

Johnson, E. & Olsen, K. 1960, "Clinical value of motor nerve conduction velocity determination.", *Journal of the American Medical Association*, vol. 172, pp. 2031-2035.

Kelleher, M., Al-Abri, R., Eleutério, M., Myles, L., Lenihan, D., & Glasby, M. 2001, "The use of conventional and invaginated autologous vein grafts for nerve repair by means of entubulation.", *Journal of Plastic Surgery*, vol. 54, pp. 53-57.

Kimura, J. 1976, "A method for estimating the refractory period of motor fibers in the human peripheral nerve.", *Journal of Neurological Science*, vol. 28, pp. 485-490.

Kimura, J. Electrodiagnosis in diseases of nerve and muscle. 1983. Davis,F A. Ref Type: Serial (Book, Monograph)

Kimura, J., Yamada, T., & Rodnitzky, R. 1978, "Refractory period of human motor nerve fibres", *Journal of Neurology, Neurosurgery and Psychiatry*, vol. 41, pp. 784-790.

Kline, D., Hayes, G., & Morse, A. 1964a, "A comparative study of response of species to peripheral-nerve injury. I. Severance", *Journal of Neurosurgery*, vol. 21, pp. 968-979.

Kline, D., Hayes, G., & Morse, A. 1964b, "A comparative study of response of species to peripheral-nerve injury. II. Crush and severance with primary suture.", *Journal of Neurosurgery*, vol. 21, pp. 980-988.

Koles, Z. & Rasminsky, M. 1972, "A computer simulation of conduction in demyelinated nerve fibres.", *Journal of Physiology*, vol. 227, pp. 351-364.

Kopec, J., Delbecke, J., & McComas, A. 1978, "Refractory period studies in a human neuromuscular preparation.", *Journal of Neurology, Neurosurgery and Psychiatry*, vol. 41, pp. 54-64.

Kugelberg, E., Edström, L., & Abbruzzese, M. 1970, "Mapping of motor units in experimentally reinnervated rat muscle.", *Journal of Neurology, Neurosurgery and Psychiatry*, vol. 33, pp. 319-329.

Lascelles, R. & Thomas, P. 1966, "Changes due to age in internodal length in the sural nerve in man", *Journal of Neurology, Neurosurgery and Psychiatry*, vol. 29, pp. 40-44.

Lee, R., Ashby, P., White, D., & Aguayo, A. 1975, "Analysis of motor conduction velocity in the human median nerve by computer simulation of compound muscle action potentials.", *Electroencephalography and clinical Neurophysiology*, vol. 39, pp. 225-237.

Lenihan, D., Sojitra, N., & Glasby, M. 1998, "Stimulated jitter measurement in the assessment of recovery after different methods of peripheral nerve repair", *Journal of Hand Surgery*, vol. 23B, no. 1, pp. 12-16.

Lenihan, D., Sojitra, N., Ikeda, M., Carter, A., & Glasby, M. 1997, "Stimulated jitter measurements in the assessment of recovery after peripheral nerve repair", *Journal of Hand Surgery*, vol. 22B, no. 6, pp. 772-777.

Lewis, D. & Chamberlain, S. 1993, "Differences between contractions *in vitro* of slow and fast rat skeletal muscle persist after random reinnervation.", *Journal of Physiology*, vol. 465, pp. 731-745.

Lippold, O. 1952, "The relation between integrated action potentials in a human muscle and its iosmetric tension.", *Journal of Physiology*, vol. 117, pp. 492-499.

Lowitzsch, K., Gohring, U., Hecking, E., & Kohler, H. 1981, "Refractory period, sensory conduction velocity and visual evoked potentials before and after haemodialysis.", *Journal of Neurology, Neurosurgery and Psychiatry*, vol. 44, pp. 121-128.

Luff, A. R., Hatcher, D. D., & Torkko, K. 1988, "Enlarged motor units resulting from partial denervation of cat hindlimb muscles", *Journal of Neurophysiology*, vol. 59, pp. 1377-1394.

Lundborg, G. 2000, "A 25-Year Perspective of Peripheral Nerve Surgery: Evolving Neuroscientific Concepts and Clinical Significance.", *The Journal of Hand Surgery*, vol. 25, pp. 391-414.

Lundborg, G., Dahlin, L., & Danielson, N. 1991, "Ulnar nerve repair by the silicone chamber technique.", *Scandinavian Journal of Plastic Reconstructive Surgery and Hand Surgery*, vol. 25, pp. 79-82.

Mackinnon, S. & Dellon, A. 1988, *Surgery of the peripheral nerve*, First edn, Thieme Medicall Publishers, New York.

Mayhew, T. 1990, "Efficient and unbiased sampling of nerve fibres for estimating fibre number and size.", *Methods in Neurosciences*, vol. 3, pp. 172-187.

McQuarrie IG & Grafstein, B. 1973, "Axonal outgrowth enhanced by a previous injury.", *Archives of Neurology*, vol. 29, no. 53, p. 55.

Mihelin, M., Trontelj, J., & Stålberg, E. 1991, "Muscle fiber recovery functions studied with double pulse stimulation.", *Muscle & Nerve*, vol. 14, pp. 739-747.

Miller, R. 1987, "Injury to Peripheral Motor Nerves", *Muscle and Nerve*, vol. 10, pp. 698-710.

Moore, J. W., Joyner, R. W., Brill, M. H., Waxman, S. D., & Najar-Joa, M. 1978, "Simulations of conduction in uniform myelinated fibres; Relative sensitivity to changes in nodal and internodal parameters", *Biophysical Journal*, vol. 21, pp. 147-160.

Morita, G., Tu, Y., Okajima, Y., Honda, S., & Tomita, Y. 2002, "Estimation of the conduction velocity distribution of human sensory fibres.", *Journal of Electromyography and Kinesiology*, vol. 12, pp. 37-43.

Nathan, C. 1987, "Secretory products of macrophages.", *Journal of Clinical Investigations*, vol. 79, pp. 319-326.

Norris, A. & Wagman, I. 1953, "Age changes in the maximum conduction velocity of motor fibres of human ulnar nerves.", *Journal of Applied Phsiology*, vol. 5, pp. 589-593.

Platt, H. & Bristow, W. 1924, "The remote results of operations for injuries of the peripheral nerves.", *British Journal of Surgery*, vol. 11, pp. 535-563.

Ramsey, M., DerSimonian, R., Holtel, M., & Burgess, L. 2000, "Corticosteroid treatment for idiopathic facial nerve paralysis meta-analysis.", *Laryngoscope*, vol. 110, pp. 335-341.

Robinson, L. 2000, "Traumatic Injury to Peripheral Nerves", *Muscle & Nerve*, vol. 23, pp. 863-873.

Ruijten, M.W.M.M., Sallé, H.J.A. & Kingma, R. "Comparison of two techniques to measure the motor conduction velocity distribution.", *Electroencephalography and clinical Neurophysiology*, vol. 89, pp. 375-381.

Rushton, W. A. H. 1951, "A theory of the effects of fibre size in medullated nerve", *Journal of Physiology*, vol. 115, pp. 101-121.

Sanders, F. & Whitteridge, D. 1946, "Conduction velocity and myelin sheath thickness in regenerating nerve fibres.", *Journal of Physiology*, vol. 105, pp. 152-174.

Sanders, F. & Young, J. 1944, "The role of the peripheral stump in the control of fibre diameter in regenerating nerves.", *Journal of Physiology*, vol. 103, pp. 119-136.

Seckel, B. 1990, "Enhancement of peripheral nerve regeneration.", *Muscle & Nerve*, vol. 13, pp. 785-800.

Seddon, H. 1972, *Surgical disorders of peripheral nerves.* Churchill Livingstone, Edinburgh.

Shefner, J. & Dawson, D. 1990, "The use of sensory action potentials in the diagnosis of peripheral nerve disease.", *Archives of Neurology*, vol. 47, pp. 341-348.

Sillman, J., Niparko, J., Lee, S., & Kileny, P. 1992, "Prognostic value of evoked and standard electromyography in acute facial paralysis.", *Otolarygology Head and Neck Surgery*, vol. 107, pp. 377-381.

Sittel, C., Sittel, A., Guntinas-Lichius, O., & Eckel, H. 2000, "Bell's palsy: a 10-year experience with anti-phlogistic-rheologic infusion therapy.", *American Journal of Otology*, vol. 21, no. 3, pp. 425-432.

Smith, R. S. & Koles, Z. J. 1970, "Myelinated nerve fibres: computed effect of myelin thickness on conduction velocity", *American Journal of Physiology*, vol. 219, pp. 1256-1257.

Stålberg, E. 1990, "Use of single fibre EMG and macro EMG in study of reinnervation", *Muscle & Nerve*, vol. 13, pp. 804-813.

Stålberg, E. & Trontelj, J. 1994a, "Jitter and impulse blocking," in *Single fibre electromyography. Studies in healthy and diseased muscle.*, Second edition edn, Raven Press, New York, pp. 45-82.

Stålberg, E. & Trontelj, J. Single Fiber Electromyography. Studies in healthy and diseased muscle. Stålberg, E and Trontelj, JV. Second edition. 1994b. New York, Raven Press.
Ref Type: Serial (Book,Monograph)

Stålberg, E., Trontelj, J., & Mihelin, M. 1992, "Electrical microstimulation with single-fibre electromyography: A useful method to study the physiology of the motor unit.", *Journal of Clinical Neurophysiology*, vol. 9, pp. 105-119.

Sunderland, S. Nerves and Nerve Injuries. 2. 1978. Edinburgh, Churchill Livingstone.
Ref Type: Serial (Book,Monograph)

Synergy user mobile manual. 2000. Surrey,UK, Oxford Instruments, Medical Systems Division.

Terenghi G, Calder JS, Birch R, & Hall SM 1998, "A morphological study of Schwann cells and axonal regeneration in chronically transected human peripheral nerves.", *Journal of Hand Surgery*, vol. 23, pp. 583-587.

Thomas, P. 1964, "Changes in the endoneurial sheaths of peripheral myelinated nerve fibres during Wallerian degeneration", *Journal of Anatomy*, vol. 98, pp. 175-182.

Trontelj, J., Mihelin, M., Fernandez, J., & Stålberg, E. 1986, "Axonal stimulation for end-plate jitter studies", *Journal of Neurology, Neurosurgery and Psychiatry*, vol. 49, pp. 677-685.

Trontelj, J. & Stålberg, E. 1992, "Jitter measurement by axonal micro-stimulation. Guidelines and technical notes.", *Electroencephalography and clinical Neurophysiology*, vol. 85, pp. 30-37.

Trontelj, J., Stålberg, E., & Mihelin, M. 1990, "Jitter in the muscle fibre", *Journal of Neurology, Neurosurgery and Psychiatry*, vol. 53, pp. 49-54.

VanSwearingen, J., Cohn, J., & Bajaj-Luthra, A. 1999, "Specific impairment of smiling increases the severity of depressive symptoms in patients with facial neuromuscular disorders", *Aesthetic Plastic Surgery*, vol. 23(6), pp. 416-423.

Wagman, I. & Flick, E. 1951, "Relative refractory period of peripheral nerve and muscle in man", *American Journal of Physiology*, vol. 167, p. 834.

Wagman, I. & Lesse, H. 1952, "Maximum conduction velocities of motor fibres of ulnar nerve in human subjects of various ags and sizes.", *Journal of Neurophysiology*, vol. 115, pp. 235-244.

Waxman, S. G. 1980, "Determinants of conduction velocity in myelinated fibres.", *Muscle & Nerve*, vol. 3, pp. 141-150.

Weisl, H. & Osborne, G.V. 1964, "The pathological changes in rats' nerves subject to moderate compression." *Journal of Bone and Joint Surgery*, vol. 46(B), pp.297-306.

Weiss, P. & Edds, M. 1946, "Spontaneous recovery of muscle following partial denervation.", *American Journal of Physiology*, vol. 145, pp. 587-598.

Wells, M. & Gozani, S. 1999, "A method to improve the estimation of conduction velocity distributions over a short segment of nerve.", *IEEE Transactions on Biomedical Engineering*, vol. 46, no. 9, pp. 1107-1120.

Wiechers, D. 1990, "Single fiber EMG evaluation in denervation and reinnervation", *Muscle & Nerve*, vol. 13, pp. 829-832.

Yanagihara, N., Hato, N., Murakami, S., & Honda, N. 2001, "Transmastoid decompression as a treatment of Bell's palsy", *Otolarygology Head and Neck Surgery*, vol. 124, no. 3, pp. 282-286.

Young, J. 1942, "The functional repair of nervous tissue", *Physiology Reviews*, vol. 22, pp. 318-374.

APPENDIX 1

Recipes for chemicals

0.4M sodium cacodylate

Dissolve 8.5612 g sodium cacodylate in 50 ml of distilled water. Make up to 100 ml with more distilled water.

0.2M sodium cacodylate buffer, pH 7.4

Take 50 ml of 0.4M sodium cacodylate, add 0.2M hydrochloric acid (about 8 ml) to the solution to pH 7.4. Make up to 100 ml with distilled water.

2.5% gluteraldehyde in 0.1M sodium cacodylate buffer

Take 50 ml of 0.2M sodium cacodylate buffer, pH 7.4. Add 10 ml of 25% gluteraldehyde. Make up to 100 ml with distilled water.

0.2M hydrochloric acid

Take 20 ml of 1N hydrochloric acid and make up to 100 ml with distilled water.

5% sucrose buffer solution

Take 50 ml of 0.2M sodium cacodylate buffer and using a magnetic stirrer add 5.0 g of sucrose and make up to 100 ml with distilled water.

0.1% osmium tetroxide in 0.1M sodium cacodylate buffer

Osmium tetroxide is dangerous and must only be handled in a fume cupboard. Take a 0.1 g ampoule of osmium tetroxide and remove its paper label, cleaning the ampoule with absolute alcohol to remove all trace of the paper. Place this in a universal bottle, with the cap tightly screwed closed, and shake to break the ampoule. Add 5 ml of 0.2M sodium cacodylate buffer, pH 7.4 and 5 ml of distilled water and shake to mix. Place the bottle overnight in the refrigerator to allow the crystals to dissolve.

Araldite epoxy resin

Araldite causes skin irritations and should be handled in a fume cupboard. There are four components of the resin which when mixed slowly polymerise:

1. Araldite CY212
2. Dodecenyl succinic anhydrite (hardener)
3. Dibutylphthalate (plasticizer)
4. Benzyldimethylamine (accelerator)

Mix 1 and 2 in equal proportions. Mix 3 and 4 in a 2:1 mix (two measures of dibutylphthalate with one measure of benzyldimethylamine). Fill a universal bottle to its 'shoulder' with the 1 + 2 mixture and add 0.5 ml of the 3 + 4 mixture. Leave overnight on the rotator and store in the refrigerator.

Pyronin B and Toluidine Blue stain

Mix 1 g of di-Sodium tetrahydoborate decahydrate (Borax) in 100 ml of distilled water (1% solution) with a magnetic stirrer for 1 hour). Then mix 1 g of toluidine blue ($C_{15}H_{16}N_3SCl$) and again stir for 1 hour (this makes 1% solution of toluidine blue in 1% borax).

Mix 1 g of Pyronin B in 100 ml of distilled water (1% solution, use magnetic stirrer for 1 hour).

Mix four parts of the 1% solution of toluidine blue in 1% borax with one part of the 1% Pyronin B solution. Filter the combined solution to remove any precipitate.

APPENDIX 2

Raw data for dependent variables.

Jitter (μs)

Raw data for *jitter* results for the facial nerve.					
Normal	**Neura**	**Axono**	**Neurot. & suture**	**Neurot. & wrap**	**Graft**
9.08	8.66	8.30	8.35	9.74	11.26
11.32	9.90	8.80	10.26	7.51	9.83
10.26	8.98	8.32	8.40	8.15	7.08
7.97	10.61	8.04	6.80	7.61	7.81
8.50	10.26	9.72	8.63	10.41	8.57
7.20	9.72	7.54	8.39		8.25

Raw data for *jitter* results for the median nerve.					
Normal	**Neura**	**Axono**	**Neurot. & suture**	**Neurot. & wrap**	**Graft**
10.64	10.14	10.21	10.70	8.35	9.43
8.13	9.04	9.10	10.54	9.73	9.19
7.57	9.23	9.92	9.84	7.76	11.90
7.98	12.40	10.09	10.99	10.24	10.42
8.41	12.88	10.82	10.36	9.72	11.29
9.54		10.43	8.98	11.51	

Maximum conduction velocity (m s^{-1})

Raw data for CV_{max} results for the facial nerve.					
Normal	**Neura**	**Axono**	**Neurot. & suture**	**Neurot. & wrap**	**Graft**
67.7	66.2	46.1	35.9	43.6	34.0
92.3	35.6	30.0	38.0	38.9	26.6
60	57.9	30.6	37.3	25.3	33.2
53	39.7	33.8	37.5	45.7	37.6
81.3	60.7	45.5	36.7	38.2	51.3
77.5	49.1	43.7	27.2	36.3	

Raw data for CV_{max} results for the median nerve.					
Normal	**Neura**	**Axono**	**Neurot. & suture**	**Neurot. & wrap**	**Graft**
92.6	64.2	61.0	54.4	48.6	63.1
89.5	88.0	65.2	32.7	35.6	32.4
68.7	84.5	58.1	39.5	46.9	21.1
77.5	65.9	47.3	37.8	46.7	47.5
62.0	86.4	49.7	38.0	43.1	
90.0			40.0	34.2	

Minimum absolute refractory period (ms)

Raw data for ARP_{min} results for the facial nerve.					
Normal	**Neura**	**Axono**	**Neurot. & suture**	**Neurot. & wrap**	**Graft**
1.1	1.0	1.7	1.2	1.2	0.9
1.1	1.0	0.6	1.1	1.1	1.0
0.6	1.2	1.0	0.9	1.2	0.9
0.6	0.9	1.1	1.3	1.1	0.5
1.1	0.9	1.5	1.3	0.7	1.1
1.0	0.9		1.1	1.1	0.9

Raw data for ARP_{min} results for the median nerve.					
Normal	**Neura**	**Axono**	**Neurot. & suture**	**Neurot. & wrap**	**Graft**
1.0	0.9	1.0	1.1	0.7	0.9
1.1	0.9	0.9	0.8	0.7	1.0
0.9	0.9	0.8	0.6	0.4	0.6
0.8	1.2	0.6	0.8	0.9	0.9
0.9	1.0	1.0	0.9	0.8	0.6
1.1			0.9	0.7	

Maximum absolute refractory period (ms)

Raw data for ARP_{max} results for the facial nerve.					
Normal	**Neura**	**Axono**	**Neurot. & suture**	**Neurot. & wrap**	**Graft**
5.5	6.5	6.5	6.5	6.0	6.0
5.5	7.0	6.5	6.0	5.5	7.5
6.0	6.5	5.5	6.0	6.5	5.0
6.0	6.0	6.0	5.0	6.0	4.0
6.5	6.0	6.0	6.0	6.0	6.0
4.5	6.5	6.5	5.0	6.0	4.5

Raw data for ARP_{max} results for the median nerve.					
Normal	**Neura**	**Axono**	**Neurot. & suture**	**Neurot. & wrap**	**Graft**
6.5	6.5	6.5	7.5	7.0	6.5
7.0	6.5	5.5	6.5	6.5	6.5
5.5	6.5	6.5	4.5	6.0	6.5
5.5	6.5	6.5	6.0	6.5	5.0
6.5	7.0	6.5	5.5	5.5	9.0
5.5				6.5	

Amplitude peak twitch (N)

Raw data for *amplitude peak twitch* results for the facial nerve.					
Normal	**Neura**	**Axono**	**Neurot. & suture**	**Neurot. & wrap**	**Graft**
0.93	1.41	1.35	2.44	1.67	0.90
0.86	1.80	0.95	1.43	3.59	0.64
1.30	1.85	1.74	0.82	0.60	2.08
3.49	2.22	1.29	0.96	2.54	0.58
1.59	1.76	1.53	0.74	0.56	2.99
2.43	1.27			1.82	3.59

Raw data for *amplitude peak twitch* results for the median nerve.					
Normal	**Neura**	**Axono**	**Neurot. & suture**	**Neurot. & wrap**	**Graft**
7.58	3.07	2.03	1.18	2.22	2.03
7.30	3.12	15.6	6.49	3.67	1.22
6.20	3.80	10.02	1.31	12.02	3.25
7.76	1.62	1.76	1.44	1.93	1.75
2.76	3.17	5.35	3.62	4.50	
2.14					

Time to peak twitch (ms)

Raw data for *time to peak twitch* results for the facial nerve.					
Normal	**Neura**	**Axono**	**Neurot. & suture**	**Neurot. & wrap**	**Graft**
34.5	24.5	19.9	19.5	31.0	23.0
23.6	20.0	28.0	32.5	51.5	24.5
21.0	27.0	21.0	27.5	29.0	24.5
49.0	23.0	33.0	44.0	34.0	31.5
27.0	18.0	29.5	23.5	31.0	32.0
29.0	21.0		31.0	28.0	46.5

Raw data for *time to peak twitch* results for the median nerve.					
Normal	**Neura**	**Axono**	**Neurot. & suture**	**Neurot. & wrap**	**Graft**
42.0	46.5	35.5	64.0	49.0	23.0
65.5	40.0	33.5	44.0	43.5	39.0
39.5	42.5	41.5	24.0	94.0	42.0
54.0	42.0	26.5	49.5	35.0	45.0
33.0	45.0	59.0	32.0	37.5	
37.5					

Time to ½ relaxation peak twitch (ms)

Raw data for *time to ½ relaxation peak twitch* results for the facial nerve.					
Normal	**Neura**	**Axono**	**Neurot. & suture**	**Neurot. & wrap**	**Graft**
68.0	42.5	42.2	41.0	59.0	39.0
48.6	40.0	49.0	58.5	102.0	51.0
49.2	45.0	58.0	51.5	51.5	54.3
119.0	42.5	83.5	107.0	84.0	78.5
54.8	34.5	85.5	15.5	86.5	91.0
65.0	39.5		94.0	57.8	129.5

Raw data for *time to ½ relaxation peak twitch* results for the median nerve.					
Normal	**Neura**	**Axono**	**Neurot. & suture**	**Neurot. & wrap**	**Graft**
92.0	92.0	58.5	107.0	91.0	58.0
150.5	71.5	69.0	80.5	164.0	70.5
78.5	95.5	87.0	52.0	131.0	71.0
115.5	56.5	57.5	108.5	78.5	92.0
77.0	77.0	107.0	81.5	87.5	
92.0					

Maximum tetanic tension (N)

Raw data for *maximum tetanic tension* results for the facial nerve.					
Normal	**Neura**	**Axono**	**Neurot. & suture**	**Neurot. & wrap**	**Graft**
10.90	7.95	2.70	12.85	7.04	2.94
7.30	9.84	2.39	5.90	7.76	1.81
4.50	14.12	7.95	3.54	2.22	8.02
6.93	8.02	6.20	8.93	9.40	3.80
6.90	10.75	6.21	3.04	2.22	8.93
7.66			3.90	5.89	8.49

Raw data for *maximum tetanic tension* results for the median nerve.					
Normal	**Neura**	**Axono**	**Neurot. & suture**	**Neurot. & wrap**	**Graft**
18.10	19.60	14.66	8.33	23.27	25.09
24.50	22.18	25.40	22.28	20.47	11.47
25.90	22.73	24.90	21.10	22.73	20.37
22.70	26.50	23.81	15.10	23.60	13.29
23.60	24.1	24.10	19.10	22.73	
23.60					

Time to ½ fatigue tetanus (s)

Raw data for *time to ½ fatigue tetanus* results for the facial nerve.					
Normal	**Neura**	**Axono**	**Neurot. & suture**	**Neurot. & wrap**	**Graft**
27.5	8.0	54.6	42.4	29.0	10.0
73.4	35.8	31.6	20.1	2.6	60.3
9.0	7.0	26.6	9.7	29.9	18.8
15.2	33.0	10.8	35.9	10.6	14.4
17.3	6.2	10.0	24.6	33.5	21.6
26.8	15.8		16.8	18.5	18.6

Raw data for *time to ½ fatigue tetanus* results for the median nerve.					
Normal	**Neura**	**Axono**	**Neurot. & suture**	**Neurot. & wrap**	**Graft**
26.0	15.4	21.8	4.8	17.8	19.8
15.4	46.6	33.0	19.8	13.6	9.0
18.0	22.6	8.0	13.0	19.6	7.0
20.2	12.0	21.8	13.9	18.6	16.0
19.2	22.4		26.2	18.8	
26.6					

Muscle mass (g)

Raw data for *muscle mass* results for the facial nerve.					
Normal	**Neura**	**Axono**	**Neurot. & suture**	**Neurot. & wrap**	**Graft**
1.23	3.07	3.23	3.15	2.41	2.0
3.06	2.84	2.27	1.88	2.70	2.21
2.79	3.50	2.27	1.69	2.05	2.13
2.24	2.50	2.51	2.07	2.02	2.20
1.57	2.26	2.43	2.70	1.57	1.51
2.48		2.22	2.07	2.13	

Raw data for *muscle mass* results for the median nerve.					
Normal	**Neura**	**Axono**	**Neurot. & suture**	**Neurot. & wrap**	**Graft**
14.72	7.12	7.76	5.09	5.57	5.40
7.50	11.30	7.08	6.71	4.69	4.38
11.20	7.92	7.31	3.45	6.77	6.12
8.52	10.61	7.66	2.97	5.26	4.60
12.0	8.20		5.81	4.74	8.90
8.33					

Facial nerve morphometry (μm)
(mean of 200 measurements)

	Axon	Fibre	Myelin
Normal	6.475	11.92	2.722468
	7.03	10.722	1.846098
	7.12	12.557	2.718673
	7.557	12.827	2.635158
	6.89	13.311	3.21026
	5.414	10.119	2.352585
Neurapraxia	6.343	11.39	2.52344
	4.89	8.431	1.77029
	6.49	11.782	2.646138
	7.054	10.691	1.81832
	6.118	12.363	3.122168
	6.797	11.151	2.176785
Axonotmesis	6.249	10.633	2.191808
	6.455	10.547	2.045843
	5.826	9.05	1.612185
	5.222	8.23	1.503983
	6.008	9.238	1.614898
	6.375	11.71	2.667738
Wrap	5.561	9.091	1.764905
	6.116	10.121	2.00259
	5.014	9.035	2.010623
	6.825	10.755	1.964975
	6.66	10.366	1.853148
	6.16	9.888	1.864298
Neurotmesis	6.264	9.151	2.441883
	7.136	12.02	2.238518
	5.68	10.158	1.910015
	5.013	8.8	1.507603
	4.304	7.319	1.78154
	4.814	8.377	1.443733
Graft	5.66	9.287	1.81351
	6.162	11.217	2.527245
	5.271	9.303	2.01568
	5.336	8.677	1.670128
	4.889	8.706	1.908343
	6.623	10.356	1.866648

Median nerve morphometry (μm)
(mean of 200 measurements)

	Axon	Fibre	Myelin
Normal	10.149	17.972	3.911598
	9.477	17.485	4.00381
	8.462	16.541	4.039585
	8.79	15.759	3.484488
	9.66	17.042	3.6912
	8.536	16.772	4.117908
Neurapraxia	7.747	15.356	4.801995
	5.881	12.387	3.253223
	8.696	15.587	3.44581
	6.945	15.588	4.321713
	7.952	17.556	4.801995
Axonotmesis	7.621	13.385	2.881888
	5.188	8.9	1.85598
	5.984	10.094	2.054948
	5.548	9.049	1.750783
	7.994	12.652	2.328673
Neurotmesis	5.088	8.876	1.894248
	4.98	8.401	1.710363
	4.469	8.116	1.823765
	4.45	8.167	1.85872
Wrap	4.686	9.15	2.23189
	3.894	7.723	1.914713
	4.968	8.736	1.884
	4.176	8.491	2.157385
	4.326	7.497	1.58558